

EXHIBIT DX36

TO DECLARATION OF PETER J. GOSS IN
SUPPORT OF DEFENDANTS' MOTION TO
EXCLUDE PLAINTIFFS' ENGINEERING
EXPERTS

**UNITED STATES DISTRICT COURT
DISTRICT OF MINNESOTA**

In re Bair Hugger Forced Air Warming
Products Liability Litigation

MDL No. 15-2666 (JNE/FLN)

This Document Relates to All Actions

**EXPERT REPORT OF
SAID ELGHOBASHI, M.SC., PH.D., D.SC.**

Attached as exhibit 1 is my report, Effect of Heated-Air Blanket on the Dispersion of Squames in an Operating Room, Dated March 23, 2017

Attached as exhibit 2 is a Summary of Opinions.

Attached as exhibit 3 is my professional Resume.

I have not previously testified in trial or deposition.

My hourly charge for professional services is \$800.00

Date: March 29, 2017



Said Elghobashi, M.Sc., Ph.D., D.Sc.

Exhibit 1

Effect of Heated-Air Blanket on the Dispersion of Squames in an Operating Room

Said Elghobashi

Mechanical and Aerospace Engineering
The Henri Samueli School of Engineering
4220 Engineering Gateway
University of California, Irvine
Irvine, CA 92697-3975
Phone: (949) 824-6131
Email: selghoba@uci.edu

March 23, 2017

Contents

1	Introduction	2
2	Operating Room Geometry and CAD Model	7
3	Numerical Simulation	11
3.1	Large-eddy Simulation (LES): Introduction and Need	12
3.2	Governing Equations	18
3.2.1	Gas-phase equations	19
3.2.2	Equations for calculating the trajectories of individual squames	20
3.3	Computational grid	23
3.4	Boundary Conditions	28
3.4.1	Inlet boundary conditions	28
3.4.2	Hot air blower and other heat sources	31
3.5	Numerical solution method	32
3.5.1	Advancing the Lagrangian squames equations	33
3.5.2	Advancing the Eulerian fluid flow equations	34
4	Results	36
4.1	Flow characteristics	37
4.2	Dispersion of squames	42
4.2.1	Initial locations of squames	42
4.2.2	Trajectories and snapshots of squames	47
4.2.3	Number density of squames in the regions of interest	55
5	Summary and Concluding Remarks	60
	Appendices	63
	Appendix A	63
	Bibliography	65

Effect of Heated-Air Blanket on the Dispersion of Squames in an Operating Room

Abstract

A large-eddy simulation (LES) of the interaction between the ventilation air flow and forced hot air from a blower is performed to investigate the effect of hot air on dispersion of squames in a realistic operating room (OR) consisting of an operating table (OT), side tables, surgical lamps, medical staff, and a patient. Two cases with blower-off and blower-on are calculated together with Lagrangian trajectories of 3 million squames initially placed on the floor surrounding the OT. The squames particles are assumed as spheres of size 10 microns and the drag, lift and buoyancy forces are considered in calculating their instantaneous motion. It is shown that with the blower-off, squames are quickly transported by the ventilation air away from the table and towards the exit grilles. However, with the hot air blower turned on, the ventilation air flow above and below the OT is disrupted significantly. The rising thermal plumes from the hot blower air drag the squames above the OT and the side tables and then they are blown downwards toward the surgical site by the ventilation air from the ceiling. Temporal history of number of squames particles reaching four imaginary boxes surrounding the side tables, the OT, and the patient's knee shows that several particles reach these boxes with the blower turned on. The study shows that LES is necessary to accurately capture the mixing and transport in a turbulent flow and predict the dispersion of squames in an OR.

1 Introduction

Microbial skin colonizers, such as *Staphylococcus aureus*, have been known as a major cause of surgical site infections in operating rooms (Noble, 1975; Clark & de Calcina-Goff, 2009; Wood *et al.*, 2014). These bacteria typically colonize on human skin cells or squames which are routinely shed by humans, roughly about 10^7 particles per day (Noble, 1975). The squame particle size ranges over 4–20 μm of equivalent diameter (Noble *et al.*, 1963; Lees & Brighton, 1972).

Reduction of post-operative surgical site infections has been linked to two main factors: (i) ultra-clean ventilation (UCV) systems, and (ii) perioperative patient warming (Ng *et al.*, 2006; Legg *et al.*, 2012; Wood *et al.*, 2014). Ultra-clean ventilation aims to reduce the quantity of airborne bacteria in the operating room (OR) and most importantly near the surgical site. This is typically achieved by the constant delivery of highly filtered ultra-clean air with a downward uniform velocity of 0.3–0.5 m/s (McGovern *et al.*, 2011). The UCV performance depends critically on volumetric airflow, proper temperature gradients, use of uniform downward flowing ventilation air, potentially in the laminar regime (Memarzadeh & Manning, 2002; Pereira & Tribess, 2005). Surgeons and other medical equipment within the operating room (surgical lights, tables, patient, computers, etc.), motion of surgeon's arms and their bending motion (Chow & Wang, 2012) can disrupt this air flow

17 and create wakes, flow unsteadiness, and turbulence, thereby increasing the amount of cfu in the
18 OR.

19 Perioperative patient warming is the other important clinical practice to prevent inadvertent sur-
20 gical hypothermia, wherein the core temperature of the patient drops below 36°C. Preventing in-
21 advertent perioperative hypothermia has several benefits that include reduced operative blood loss,
22 reduced duration of surgery, improved wound healing, reduced wound infections, reduction in post-
23 operative ulcers, reduced duration of hospital stay, and increased survival rates (Wood *et al.*, 2014;
24 Ng *et al.*, 2006; Legg *et al.*, 2012). Monitoring and maintaining body temperature during surgery is
25 therefore an accepted and required practice. Warttig *et al.* (2014) review different methods used to
26 combat inadvertent perioperative hypothermia. These include use of warm cotton blankets, reflective
27 blankets, warmed intravenous and irrigation solutions, circulating warm water mattresses, a reusable
28 electric blanket, an electric heating pad, and forced-air warmers (Kellam *et al.*, 2013; Austin, 2015).
29 Of these, active warming using forced air warming (FAW) devices, and passive warming based on
30 the use of reflective blankets, are the two main techniques used to keep the patient's body warm
31 and prevent hypothermia. Although passive heating techniques may show similar effectiveness as
32 the FAW devices, the latter have been used for over two decades due to their efficacy in maintain-
33 ing patient's core body temperature. These techniques use forced convection to increase the skin
34 temperature and the total body heat content. These devices contain a blower (such as 3M™ Bair
35 Hugger™) that extracts the room temperature air through an air-intake filter heats the air using a
36 heating coil, and vents the air into the sterile field adjacent to the operative site (Albrecht *et al.*,
37 2011; Leaper *et al.*, 2009; Wood *et al.*, 2014). The filtered and warm air flows through a connecting
38 hose into blankets made of plastic and exits the blankets through tiny holes over the patient's skin.
39 However, this forced warm air has the potential to generate and mobilize airborne contamination in
40 the operating room.

41 A number of studies have examined at the safety of forced-air warming, and whether FAWs
42 can affect surgical site infections through mobilized airborne contamination. FAWs can potentially
43 lead to surgical site contamination in two ways: (i) direct contamination of the air from the blowers
44 that reaches the patient's body, and (ii) disruption of the ultra-clean ventilation air by the thermal
45 plumes and turbulence. The former risk can potentially be reduced by using intake filers that are
46 HEPA-rated and show high filtration efficiency. The latter has been studied extensively as reviewed

47 by *Wood et al. (2014)*. It is hypothesized that the temperature gradients and resultant thermal plumes
48 created by the FAW devices could disrupt the benefits of UCV flow, that is designed to be uniform
49 and downwards. The interaction between the FAW and UCV flows may lead to increased surgical
50 site infections (SSI).

51 *McGovern et al. (2011)*; *Legg et al. (2012)* have shown that temperature gradients and excess
52 heat created by FAW devices can transport air from the unsterilized floor level to the surgical site,
53 thus increasing the potential risk of SSIs. *Moretti et al. (2009)* measured an increase in the bacterial
54 load when FAWs were used. Lack of flow visualization is the main drawback of these studies as
55 it does not provide information about whether the particles came from the floor or from the FAW
56 blower. *Legg et al. (2012)*; *Sessler et al. (2011)* used smoke particle visualization to understand the
57 source of these particles near the surgical site comparing cases with no warming, FAW, and radiant
58 warming. Although they found that FAW increased the particle count with blower turned on (almost
59 10-fold increase), they also showed that the uniform, laminar flow from the ultra-clean ventilation
60 reduced the effect of particles by limiting their numbers near the surgical site.

61 It is clear from the available literature that the interaction between the UCV flow and the rising
62 plumes from the forced-air warming devices plays a critical role in deciding whether FAWs indeed
63 can lead to increased number of particles near the surgical site. However, there have not been de-
64 tailed experimental measurements of flow patterns in the OR setting with the FAW blower turned on.
65 Recently, *McNeill et al. (2012, 2013)* conducted particle-image velocimetry (PIV) measurements
66 to understand the flow pattern in an OR with the ultra-clean ventilation system. This study, however,
67 did not investigate the effect of FAW blower. *McNeill et al. (2013)* also made detailed measure-
68 ments of temperature fields on surgeon's and patient's body to be used for computational modeling.
69 Although the above PIV was able to visualize and measure the flow field, it was limited to planar
70 data (2D PIV) and thus a full three-dimensional data are not available for the OR. Nevertheless,
71 some useful information on the flow unsteadiness, turbulence within the room was obtained from
72 the *McNeill et al. (2013)* study.

73 The only other way to characterize the flow field in an OR with and without FAW blowers,
74 is to use computational fluid dynamics (CFD) modeling in three-dimensions. This, however, is
75 a difficult task due to the size and complexity of the domain involving medical equipment, staff,
76 computers, etc. There are only few CFD studies in the literature that used Reynolds-averaged Navier

77 Stokes (RANS) models (Memarzadeh & Manning, 2002; Memarzadeh, 2003; Chow & Wang, 2012),
 78 wherein only the time-averaged velocity field is computed. All information about the turbulence and
 79 velocity fluctuations is completely *modeled*. As is shown later (section 3), RANS approach is not
 80 predictive, since the instantaneous velocity field needed for calculating the trajectories of squames is
 81 not directly computed. Thus, RANS is incapable of accurately predicting the locations of squames at
 82 any time in the OR. Memarzadeh & Manning (2002); Memarzadeh (2003) investigated the effect of
 83 various UCV inlet flow conditions on the transport of squames particles in an OR. They considered
 84 a realistic OR with medical staff, equipment, surgical lamps, etc. and accounted for the thermal
 85 plumes created by heat radiated from various sources. However, they used a RANS model coupled
 86 with a Lagrangian particle-tracking of around 4000 representative particles. Their study did not
 87 include the FAW blower discharge. They showed that use of a uniform inlet flow with laminar
 88 conditions¹ is better for reducing the number of particles near the surgical site. In addition, they
 89 found that the thermal plume created by the hot surface of the surgical site prevented particles from
 90 reaching the site. They showed that roughly 2-5% of particles reach the surgical site, *provided they*
 91 *are originated very close, about 1.3cm above the site*. Particles originating from locations away
 92 from the surgery did not have a statistically significant probability of reaching the surgical site. As
 93 is discussed later in section 3, RANS model cannot compute the instantaneous velocity field needed
 94 to accurately calculate the forces on particles, and particle trajectories.

95 Chow & Wang (2012) investigated the ultra-clean ventilation flow and its effect on bacteria-
 96 carrying particles in an OR using a RANS model as well. They simulated the bacteria particles as
 97 a non-inertial pollutant, wherein an Eulerian transport equation for the concentration of the bacteria
 98 is calculated. In addition, they considered periodic bending movement of one of the surgeons per-
 99 forming the operation. They found that if the surgical staff stands upright (no bending), the UCV
 100 flow keeps the bacteria concentration very low ($< 1 \text{ cfu/m}^3$) near the surgical site. However, with
 101 the surgeon's bending motion included, they showed that this concentration increased to larger than
 102 the recommended value (10 cfu/m^3).

103 All of the above computational studies are based on RANS modeling and did not include the

¹ It should be noted that the literature uses the terminology 'laminar flow' for the ultra-clean ventilation flow. Based on the standard values of air changes per hour (ACH) for an OR (25 per hour), the inlet grille sizes, and properties of air, the flow Reynolds numbers are much larger than 2000, a critical value beyond which turbulence occurs in a duct. The inlet grille flow, thus is not typically laminar. Although the level of turbulence in the inlet flow is not large ($< 10\%$), the flow contains velocity fluctuations and is unsteady.

FAW blower system together with a blanket cover above the patient. In order to assess the interaction between UCV and FAW blower, a systematic, predictive simulation is needed. Large-eddy simulation (LES) is a numerical technique that involves computing the properties of the large, energy-containing eddies of turbulence accurately, without any user adjustable tuning parameters, and models only the more homogeneous, small scales of turbulence (Pope, 2000; Piomelli, 2014). This technique provides the instantaneous three-dimensional velocity, temperature, and pressure fields and has been shown to be far more accurate than the RANS model. Section 3 outlines the differences between LES and RANS in detail. In addition, since the time dependent, three-dimensional velocity field is available in LES, then the forces on particles and their trajectories can be calculated accurately (Apte *et al.*, 2003b; Ham *et al.*, 2003; Apte *et al.*, 2009; Moin & Apte, 2006; Mahesh *et al.*, 2006). The only challenge with this technique is that it is computationally intensive and requires fine grid resolutions and small time-steps to capture the large-scales of turbulence. Recent advances made in algorithmic developments for LES on arbitrary shaped, unstructured grids (Mahesh *et al.*, 2004; Ham *et al.*, 2003; Moin & Apte, 2006; Mahesh *et al.*, 2006; Ham & Iaccarino, 2004) have facilitated application of LES to more realistic problems involving complex geometries and flow conditions. These advances have been successfully applied to turbulent, reacting flows in a gas-turbine combustion chamber and has led the gas-turbine industry to switch from RANS to the predictive LES technique in their design cycle (Moin & Apte, 2006; Mahesh *et al.*, 2006; Apte *et al.*, 2009).

LES applied to operating rooms with medical staff and other instruments is still challenging, owing to the size of the room and the complexity of the geometries involved. At the time of writing this report, only one LES study has been performed for an operating room by Saarinen *et al.* (2015). They studied the escape of air into an isolation room during opening and closing of a door and passage of a human figure. They used passive smoke visualizations to compute the volume flux of air when a door is opened. Although this study had some complex geometry (a human figure), it did not have the intricacies of the OR table, surgeons, patient and other medical equipment, nor it computer the dispersion of squames in the OR. Nevertheless, it showed that LES can accurately predict such flows through validation with experimental observations.

The main goal of the work reported here is to use large-eddy simulation to compute the interaction of the OR ultra-clean ventilation air flow and the flow created by forced air warming

system (such as 3M™ Bair Hugger™) and investigate their impact on the dispersion of squames. Specifically, computations are conducted for the cases with blower-off and blower-on, including the Lagrangian tracking of inertial squame particles, starting from the operating room floor, to prove whether the FAW system and the resultant thermal plumes play a role in transporting squame particles to the surgical site.

The rest of the report is arranged as follows. In section 2, details of the operating room geometry and CAD model are described. This includes the OR dimensions, the surgical lamps, four medical staff, an operating room table, two side tables, the blower, and the patient undergoing knee surgery. The numerical approach is described in section 3. This includes a detailed discussion of LES and RANS, the governing equations used for LES, the computational grid, and the boundary conditions. The numerical algorithm used is briefly summarized in section 3.5. This is followed by detailed description of the results in section 4 on flow field, particle trajectories and particle counts that reach the surgical site and other key regions of interest. Finally, the findings are summarized in section 5.

2 Operating Room Geometry and CAD Model

The operating room CAD (computer aided design) model was created using Ansys® SpaceClaim Direct Modeler™ (ANSYS, Inc., Canonsburg, PA, USA). The CAD model replicated a realistic operating room (OR) depicting a knee surgery being performed on a patient. An original baseline CAD model was obtained from M/E Engineering P.C. (Straub, 2016) and was further modified to incorporate the measured dimensions of the inlet air grilles and the surgical drape as shown below. Figure 1a shows the OR dimensions used to create the CAD model. The length, width and height of the room are 7.32m, 7.01m and 3.18m, respectively. These dimensions are from 3M video at: <https://www.youtube.com/watch?v=QhzeInWlJ54>. Figure 1b shows a close-up view of the surgeon's hands extended over the patient's knee mimicking a real world operating procedure.

The CAD model also includes several objects that are usually present in a real OR. Typically, there can be several combinations of such objects, but for this study the following objects were included in the model. These are shown in a top view in figure 2 and include: (i) OR Table; (ii) OR drape; (iii) patient's body under the drape with knee exposed; (iv) four surgeons (two of the surgeons have extended hands and two have hands down), (v) two side tables, (vi) two surgical lamps, (vi)

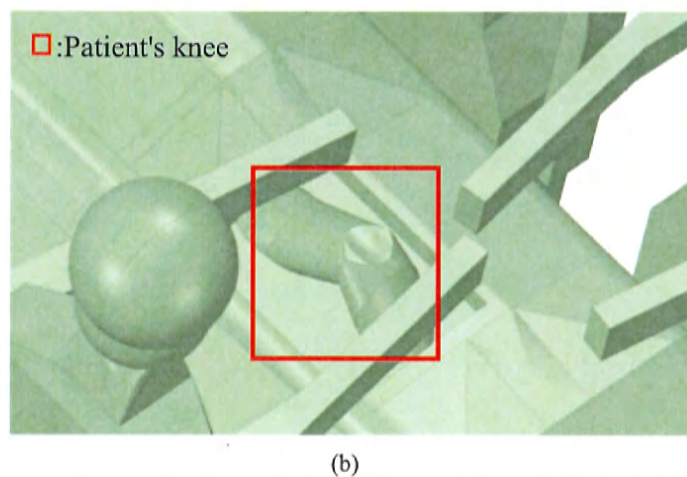
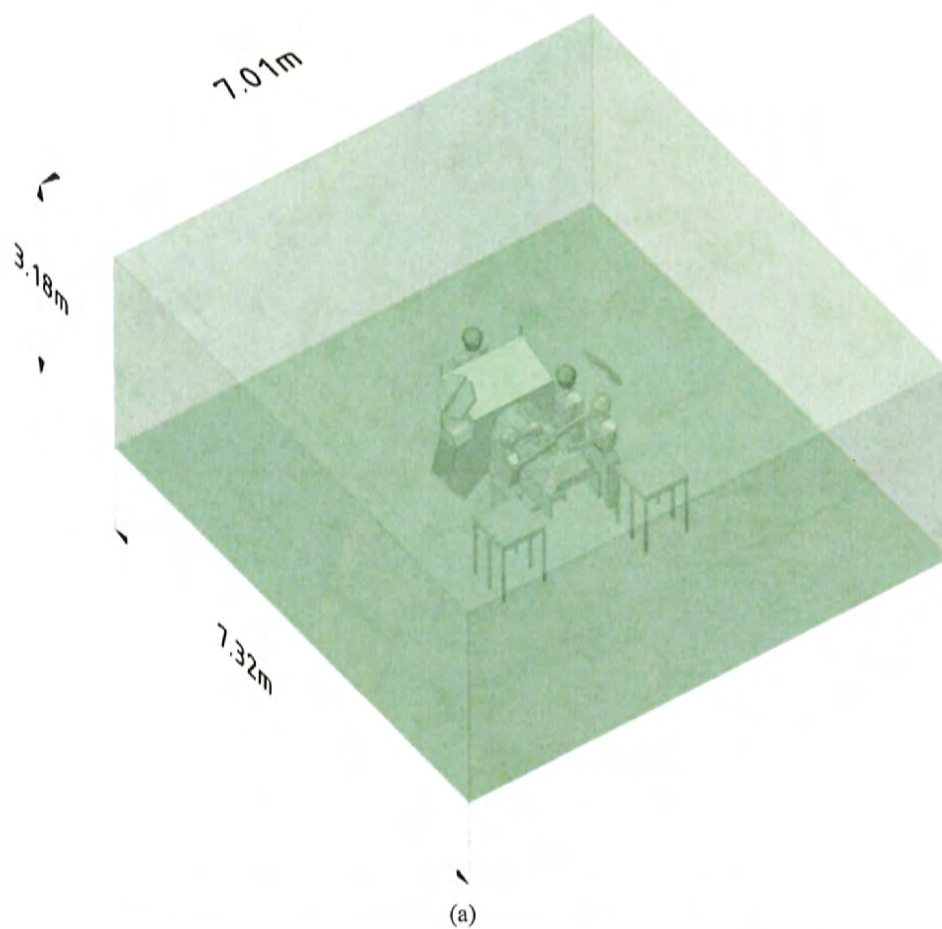


Figure 1: CAD model showing (a) operating room dimensions, and (b) closeup of the patient's knee.

3M™ Bair Hugger™ blower unit (partly visible near the top left corner under the drape).

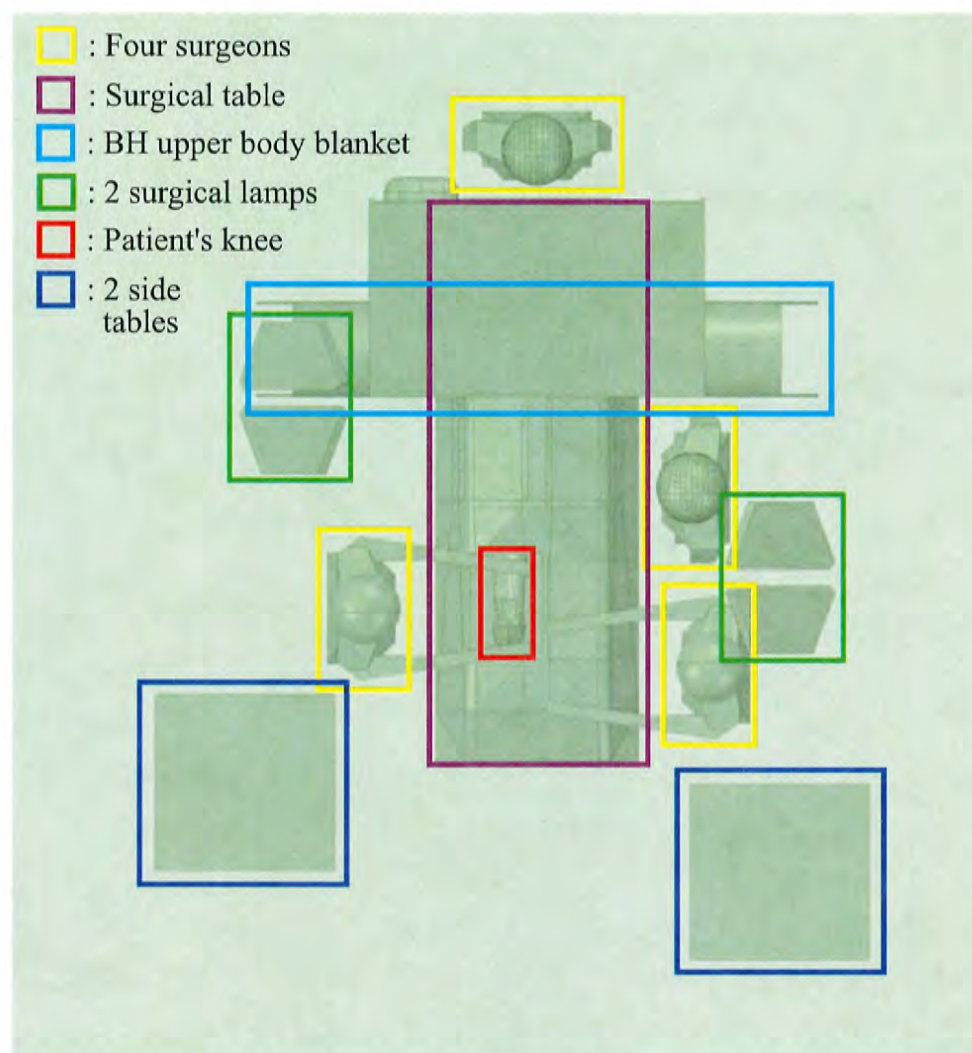


Figure 2: Close-up view of various objects included in the CAD model.

162

163 Figure 3 shows a side view of the OR table together with a few key dimensions. The bottom of
 164 the OR table is 0.94m above the floor of the room. The drape on the OR table covering the patient's
 165 torso is suspended 0.52m above the floor. The 3M™ Bair Hugger™ blower unit is also seen in the
 166 bottom right side of the figure.

167 The drape design from the base CAD model was modified to better represent the drape layout in
 168 a real OR room. The modifications mainly focused on using accurate dimensions and shape of the
 169 drape near the front end based on an actual picture taken in an OR room as shown in figure 4b. A
 170 corresponding CAD model used in the present study is shown in figure 4a. For the CAD model, the

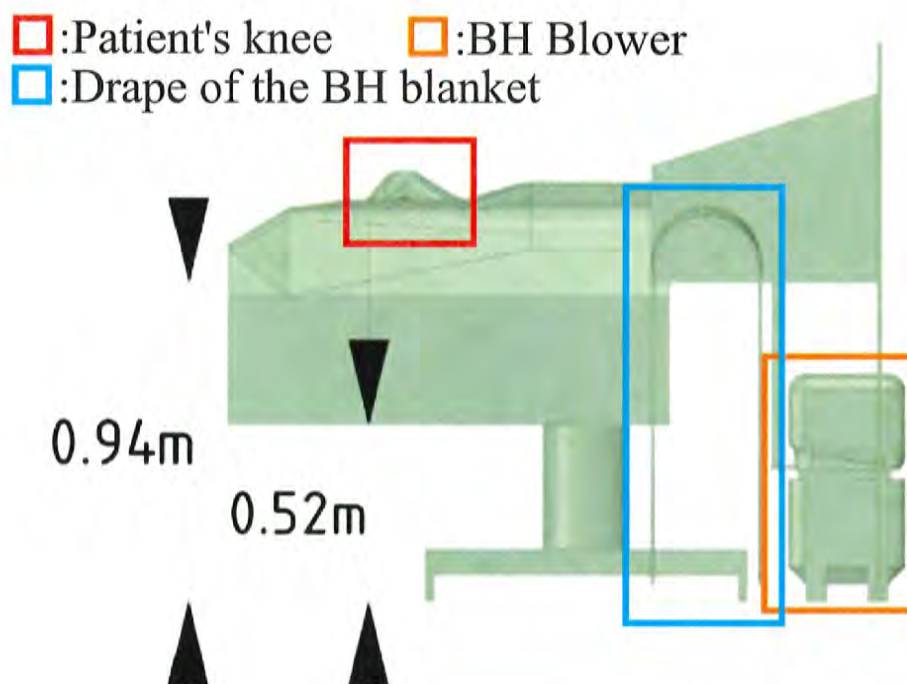


Figure 3: Side view of the OR table with some key dimensions. The 3M™ Bair Hugger™ blower unit is clearly visible on the bottom ride side.

171 front end of the drape was designed to mimic the shape obtained by dimensions A, D, C, E in figure
 172 4a. The dimensions in the CAD model are given in both metric and imperial units (in brackets) in
 173 this figure to facilitate direct comparison with the real picture on the right. The distance between the
 174 vertical bars holding the drape, denoted by dimension F in Figure 4b, was also implemented in the
 175 CAD model.

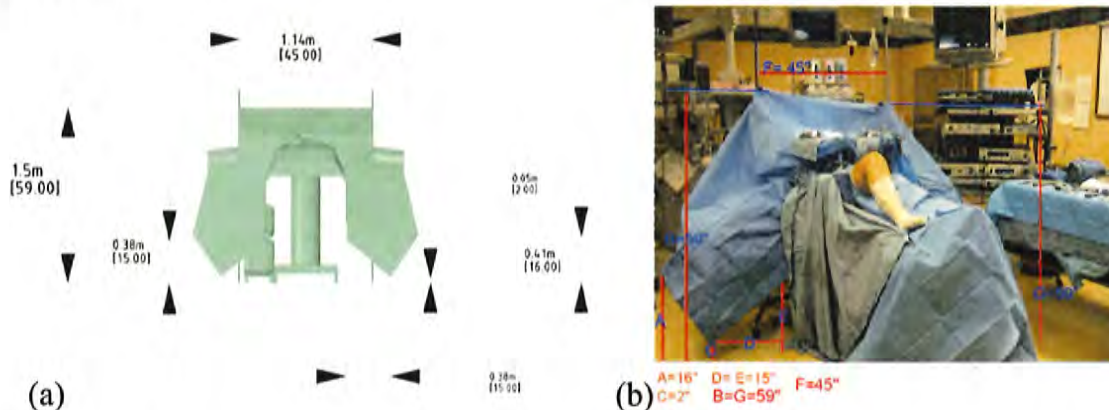


Figure 4: Drapes dimensions and configuration: (a) model developed to match the drape dimensions, (b) actual drape picture in an OR room. The dimensions are shown in both metric and imperial units (in brackets).

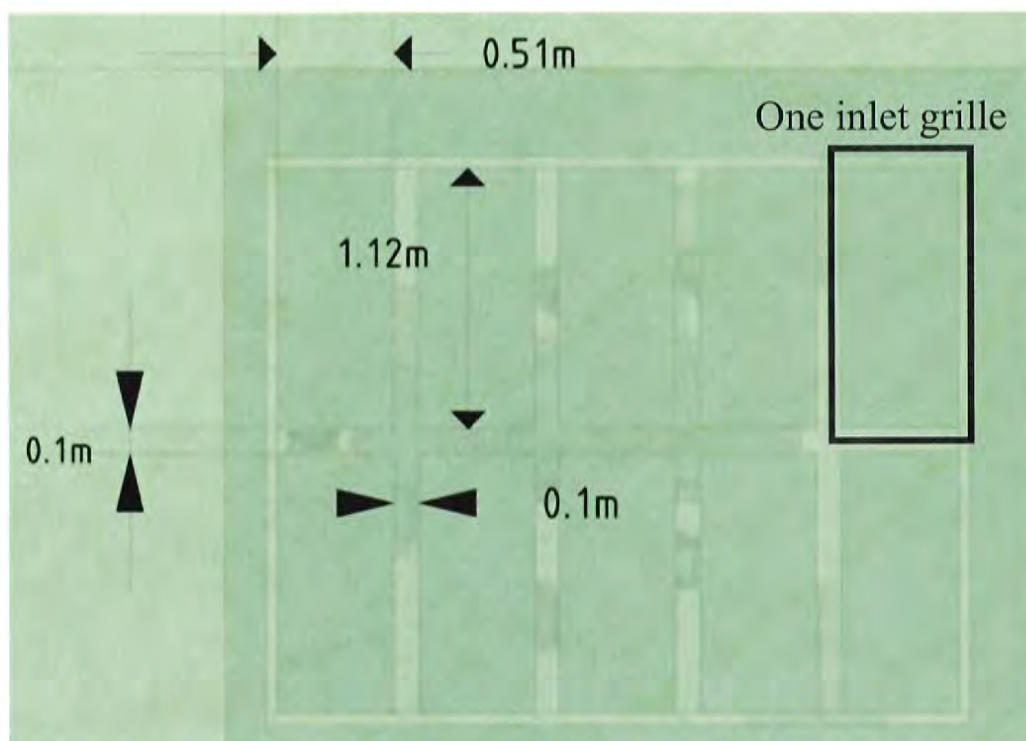


Figure 5: Ten inlet grilles to supply clean filtered air into the OR.

176 The CAD model included ten inlet grilles (figure 5) for supplying clean filtered air to the OR.
 177 Each inlet grille is 0.51m in width and 1.12m in length. All ten grilles are of the same size. There is
 178 a gap of 0.1m between the neighboring grilles at all sides.

179 There are four exhaust (or outlet) vents, two on each side wall. Figure 6 shows two outlet grilles
 180 (with the other two outlets located on the opposite wall). Each outlet grille is 0.71m in width and
 181 0.71m in length.

182 3 Numerical Simulation

183 A state-of-the art, fully parallel, unstructured, co-located grid flow solver based on principles of
 184 kinetic energy conservation for large-eddy simulation (Moin & Apte, 2006) of turbulent flow in
 185 the limit of zero-Mach numbers is used in this study. This solver is MPI-based, uses algebraic
 186 multigrid for the pressure Poisson equation, and third-order WENO-based scheme for transport of
 187 scalar fields such as temperature. It has been thoroughly validated for a number of different particle-
 188 laden turbulent flows (Apte *et al.*, 2003b,a, 2008a, 2009, 2008b) including swirling turbulent flow

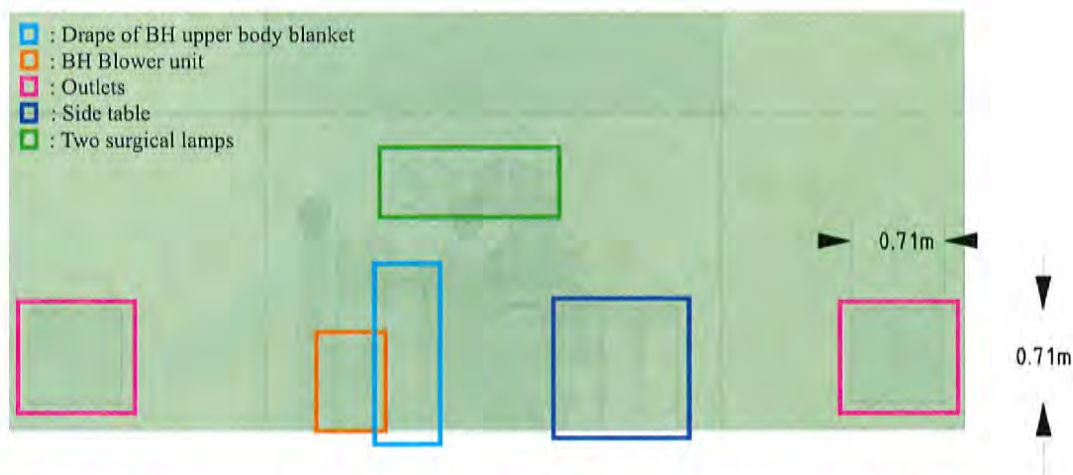


Figure 6: Outlet (exhaust) grilles for air exit from the room. Out of the four outlets in the CAD model, only two are visible in the picture. The other two outlets are on the opposite wall.

189 in a co-axial combustor, turbulent reacting flow, as well as spray combustion in a realistic Pratt and
 190 Whitney gas-turbine combustion chamber (Moin & Apte, 2006; Mahesh *et al.*, 2006).

191 3.1 Large-eddy Simulation (LES): Introduction and Need

192 The physics of turbulent air flow containing heated buoyant plumes and laden with inertial particles
 193 in a real-life operating room is highly complex. Simulating such flows with predictive capability is
 194 difficult as turbulence, by nature, consists of a broad range of length- and time-scales and is inher-
 195 ently three-dimensional. In addition, the geometry of a realistic operating room consists of complex
 196 surfaces involving surgeons, operating table, surgical lights, patient, among other. If a probe mea-
 197 sures the velocity at a certain location in such a flow, the velocity signal will show a broad range of
 198 frequencies and fluctuations around a mean. A typical kinetic energy spectrum obtained via Fourier
 199 transform of turbulent velocity field is shown in figure 7, especially for moderate to large Reynolds
 200 numbers. The spectrum is broad-band with large amount of kinetic energy per wavenumber present
 201 at large scales (small wavenumbers) and small amount of energy present at smaller scales (larger
 202 wavenumbers). There also exists an inertial range, scales in this regime simply transfer the energy
 203 from larger scales to smaller scales through a process commonly known as the energy cascade (Pope,
 204 2000). As the Reynolds number increases, this spectrum is known to broaden. The largest scales
 205 (\mathcal{L}) of motion are typically confined by the size of the domain (for example, size of the inlet jet

or size of the room). However, as the Reynolds number increases, the smallest scales of motion (known as the Kolmogorov scales, η) are reduced until the kinetic energy is dissipated into internal energy by the viscous effects. Owing to this broad range of scales, prediction of turbulent flows at large Reynolds numbers becomes difficult and is only possible if the behavior of all scales of motion is captured properly.

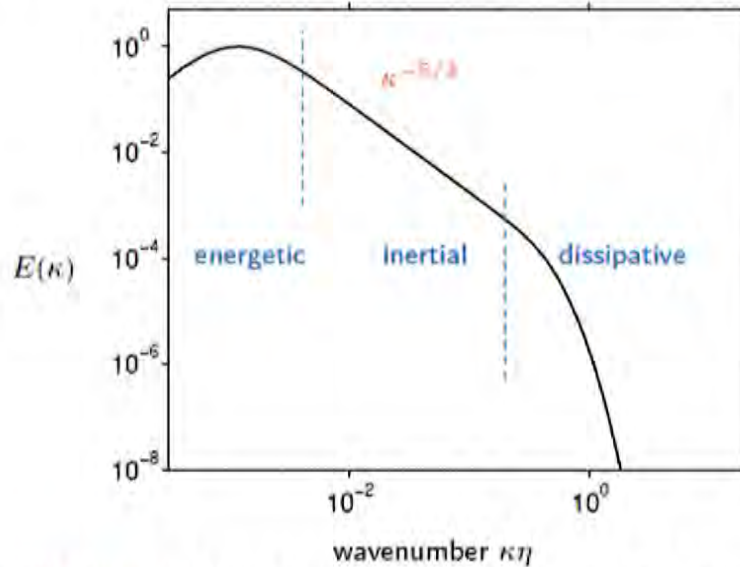


Figure 7: Schematic of a turbulence kinetic energy spectrum showing energy per wavenumber as a function of the wavenumber (Pope, 2000). The inertial range of scales is indicated by the $-5/3$ slope line that separates the energetic large scales and dissipative small scales of turbulence. In DNS, the grid resolution is fine enough to capture all scales, whereas in LES, the grid resolution is coarser (typically 10 times the Kolmogorov length scale), placing the grid cut-off somewhere in the inertial range.

Three basic approaches can be identified for prediction of turbulent flows: (i) direct numerical simulation (DNS), (ii) Reynolds averaged Navier-Stokes (RANS) modeling, and (iii) large-eddy simulation (LES), and are briefly described below.

DNS: In direct numerical simulation (DNS), the Navier-Stokes equations are solved on a computational grid that is fine enough, in space and time, to directly capture *all* the scales associated with the fluid flow motion without requiring any additional models. This means that the computational grid in three-dimensions is small enough to capture the smallest scales of turbulence and the time-step is small enough to capture the smallest time-scale associated with the flow. Using scaling arguments based on the Kolmogorov hypotheses (Tennekes & Lumley, 1972; Pope, 2000) used in the theory of turbulence, it can be shown that for a simple homogeneous, isotropic turbulence in a box, the grid resolution requirement ($\Delta \sim \mathcal{L}/\eta$; where \mathcal{L} is the size of the large, energy-containing

eddy) for DNS varies as $Re_{\mathcal{L}}^{3/4}$, where $Re_{\mathcal{L}}$ is the Reynolds number based on \mathcal{L} and the velocity fluctuations u , in one coordinate. Hence, the total number of mesh points needed in three-dimensions varies as $Re_{\mathcal{L}}^{9/4}$. A simple isotropic turbulence in a box at $Re_{\mathcal{L}} = 2000$, would require computational grid containing about 27M control volumes ($= 300^3$). In addition, based on numerical constraints of a computational solver, for a fluid flow of unit velocity, the grid spacings (Δ) and the time-steps (Δt) are roughly of the same order of magnitude ($CFL = u\Delta t/\Delta \sim 1$) and thus the spatio-temporal resolution will require a computational power that increases as $Re_{\mathcal{L}}^3$. Owing to the grid requirements and associated computational costs, DNS is not practical for realistic engineering applications and is restricted to canonical geometries and flow problems to study the fundamentals of turbulence (Moin & Mahesh, 1998).

RANS: According to the above discussion, the computation of practical turbulent flows relies predominantly on the Reynolds-averaged Navier-Stokes (RANS) equations approach. In RANS, the governing equations are averaged in time to obtain equations for the *time-averaged* velocity field, $\bar{u}(\mathbf{x})$. Thus, in this approach, only the mean velocity field that varies in space is obtained, and all information about the time-dependent fluctuations of the velocity field around the mean flow is lost. Because the momentum equations are non-linear (owing to the inertial, advective terms), a time-average of the non-linear term creates additional quantities that are unknown, giving rise to the classical closure problem of turbulence (Tennekes & Lumley, 1972; Pope, 2000). In order to evaluate these terms, models are introduced wherein the effect of the entire spectrum of turbulence (involving the large, inertial, and small scales shown in Figure 7) is completely modeled. This is usually done by introducing two additional transport equations for the turbulence kinetic energy (k) and the kinetic energy dissipation rate (ε), giving rise to the $k - \varepsilon$ model. It should be noted that the transport equations for k and ε also contain a large number of unknown, unclosed terms which also need to be modeled. The model constants are obtained by fitting the RANS predictions to the experimental data on simple, canonical flows such as wall bounded channel flow, isotropic turbulence, or free-shear flows. Because these models and model constants *are not universal*, using them for a complex flow such as air circulation in an operating room, invariably provides inaccurate results. Experimental data is necessary to adjust the model constants and thus the RANS models are not *predictive*. However, since only the time-averaged velocity field is calculated, the RANS approach is computationally the least expensive because it does not require the spatio-temporal resolution

necessary for the DNS studies. There are modified approaches, wherein the large-time scale variations are captured by solving the RANS equations in an unsteady manner. These unsteady-RANS simulations also suffer from the same hypotheses and models used for the basic RANS and their predictive capability is also poor.

LES: The energy spectrum (figure 7) shows that a substantial portion of the turbulence kinetic energy (TKE) is contained in the large-scales, known as the energy containing scales. In LES, only the contribution of the large, energetic structures to momentum and energy transfer is computed exactly, and the effect of the small scales, also termed as unresolved or subgrid scales, of turbulence is modeled. Since the small scales tend to be more homogeneous, and less affected by the domain boundary conditions as compared to the large eddies, then the subgrid closure models used in LES are universal and can be applied to a range of flows as compared to the RANS closures. Owing to these differences between the LES and RANS approaches, LES has been shown to be far superior to RANS in accurately predicting turbulent mixing of momentum and scalar (Mahesh *et al.*, 2004), pollutant and heat transport, combustion (Pierce, 2001), and particle dispersion (Apte *et al.*, 2003b; Ham *et al.*, 2003).

In LES, the Navier-Stokes (NS) equations are filtered in space (as opposed to time as done in RANS) using a local filter (Gaussian, box, spectral etc.) to obtain a filtered velocity field, $\bar{u}_i(\mathbf{x}, t)$ (Pope, 2000). Using the local grid resolution as a spatial filter, the small, under-resolved scales of turbulence are filtered out. However, applying the filtering operation to the inertial, non-linear terms in the NS equations, gives rise to the closure problem. The resulting additional terms need to be modeled. Most often, the models used to close the unknown terms, known as Reynolds stresses, are based on the same types of assumptions, such as the gradient diffusion hypothesis, as employed in RANS. However, the fact that, in LES, modeling is only applied to capture the effect of unresolved, subgrid scales, which are homogeneous and universal, the closure models work very well in a wide range of problems. A dynamic procedure, typically employed in LES subgrid scale modeling, renders the modeling process completely free of any tuning parameters in contrast to RANS. All constants in the model are obtained directly in the calculations and are not set by the user. As long as the grid resolution is sufficient such that the motion of the energy-containing large eddies is captured correctly, unlike RANS, the LES approach can then be used in a truly predictive manner.

282 In addition, away from the boundaries, a typical LES grid can be 10 times coarser than a DNS
 283 grid in each direction (that is 10 times the Kolmogorov scale), resulting in significant savings in the
 284 computational cost. This makes LES an attractive tool compared to the DNS. However, there are
 285 still several challenges. Just like DNS, the LES computations are inherently three-dimensional and
 286 time-dependent, making the cost of the calculation large as the important large-scale spatio-temporal
 287 variations in the flow must still be resolved. In addition, the computational algorithm must not add
 288 large amounts of numerical dissipation as it has been shown that dissipative numerical approaches
 289 mask the physical dissipation present in turbulent flows and provide inaccurate predictions (Mittal
 290 & Moin, 1997; Kravchenko & Moin, 1997). These restrictions typically limits the use of LES to
 291 simple, canonical geometries and flows (as free-shear flows (jets, wakes, shear layers), wall bounded
 292 channel flows, or flow over backward facing step (Pierce, 2001; Piomelli, 2014)) for which the
 293 underlying algorithms are based on a non-dissipative schemes developed for structured Cartesian
 294 grids.

295 Applying LES to the complex and realistic geometries of engineering applications such as the
 296 the operating room; including the operating table, surgeons, patient and other equipment, or other
 297 applications such as gas-turbine combustors, propellers, among others, requires use of arbitrary
 298 shaped unstructured meshes. In recent years; however, considerable progress has been made in
 299 handling complex configurations and unstructured grids accurately (Piomelli, 2014). Mahesh *et al.*
 300 (2004); Ham *et al.* (2003); Mahesh *et al.* (2006) have developed a numerical algorithm for high-
 301 fidelity simulations of incompressible, variable density flows on unstructured grids. A novelty of
 302 their algorithm is that it is discretely energy-conserving which makes it robust at high Reynolds
 303 numbers *without numerical dissipation*. This makes LES applicable to complex configurations and
 304 it has been successfully used to simulate multiphase, spray combustion processes in a realistic Pratt
 305 and Whitney gas-turbine combustion chamber (Moin & Apte, 2006; Mahesh *et al.*, 2006; Apte
 306 *et al.*, 2009). These simulations are still computationally intensive, often requiring 3–4 weeks of
 307 simulation on parallel supercomputers, however, the detailed data obtained from the simulations are
 308 of significant importance to researchers and engineers since such information could not be obtained
 309 from laboratory experiments. This has led several gas-turbine industries, who generally use RANS
 310 in their design cycle, to switch from RANS-based approaches to LES.

311 Furthermore, turbulent flows laden with dispersed particles (either solid particles, or droplets or

bubbles) involve the complexity of capturing the dynamics of turbulence as well as that of the dispersed phase. The physics of particle-turbulence interactions is complex (Elghobashi, 1994, 2006), and depending upon the magnitudes of the particle relaxation times relative to the Kolmogorov time scales, heavier-than-fluid particles (solid particles, droplets, squames) can exhibit behavior such as preferential clustering on the edges of vortices (Eaton & Fessler, 1994; Rouson & Eaton, 2001; Kulick *et al.*, 2006; Reade & Collins, 2000; Eaton & Segura, 2006), whereas, lighter-than-fluid particles (bubbles) can break the vortical structures (Ferrante & Elghobashi, 2004; Druzhinin & Elghobashi, 1998; Ferrante & Elghobashi, 2007; Sridhar & Katz, 1999).

RANS is not capable of capturing this complex physics of particles interacting with turbulence because only the mean velocity field is computed by RANS, yet it is commonly used owing to its low cost. However, if the objective is to accurately simulate the dispersion of inertial particles in a turbulent flow, then a three-dimensional, instantaneous velocity field is necessary to calculate the forces on the particles. Inertial particle trajectories and dispersion are strongly influenced by the spatio-temporal variations in the velocity fields. Hence, using only the mean velocity field provides inaccurate dispersion characteristics. An improved RANS to capture the transient effects uses a model for particle motion that utilizes the local turbulence kinetic energy and introduces some randomness (typically a Gaussian distribution) in the particle equations (Sommerfeld *et al.*, 1992) is necessary. Recent work on the dispersion of squames in an operating room and the effect of different inlet air flow conditions used RANS together with such a stochastic, Lagrangian particle-tracking algorithm (Memarzadeh & Manning, 2002). Such a model must be tuned by the user to calculate different particle-laden flows and can behave differently in free-shear versus wall-bounded flows. As can be seen from the results presented by Sommerfeld *et al.* (1992); Chen & Pereira (1998), particle dispersion predicted using a RANS approach for turbulent flows in a wide range of applications involving swirling, separated flows do not agree with the experimental data. However, the same flowfields computed using LES (Apte *et al.*, 2003b; Moin & Apte, 2006; Apte *et al.*, 2008b, 2009) show considerably better predictive capability and agree with the experimental data very well. In LES, the resolved instantaneous velocity field, which varies in time and space, at the particle location is used to compute the forces on the particles as opposed to the time-averaged velocity in RANS. Accordingly, the effect of the energetic, turbulence scales (of the order of the grid resolution and larger) are completely captured in LES, thus predicting its impact on particle dispersion directly.

To summarize, it is essential to use LES instead of RANS to accurately predict the air circulation and dispersion of squames in an operating room for the following reasons:

- LES provides a three-dimensional, instantaneous flow field (velocity, pressure, temperature) of the resolved, energetic, large-scales, and only models the effect of the unresolved, subgrid (small) scales of turbulence. The subgrid scales tend to be more homogeneous, and less affected by the domain boundary conditions and thus allow the appropriate use of the eddy-viscosity models to calculate their stresses. RANS, on the other hand, only calculates the time-averaged velocity field and models the effect of all the scales of turbulence on the mean flow, resulting in unrealistic flow predictions.
- The subgrid model constants used in LES can be obtained dynamically, thus making LES truly predictive without any user-defined tuning parameters, whereas RANS model constants are not universal and often require manual tuning.
- LES is considerably more accurate in predicting passive as well as inertial particle dispersion since the instantaneous, three-dimensional resolved velocity field is available for computing the forces on the particles. In RANS, a random perturbation must be added to the mean velocity field to construct an artificial, time-dependent, three-dimensional velocity field needed to calculate the particle motion. This renders the calculation of particle dispersion highly inaccurate.

3.2 Governing Equations

The air flow in an operating room involves temperature variations within the room owing to various sources of heat; such as the operating room lamps, heat radiated from the medical personnel bodies, hot air discharged from a blower system, among others. The local temperature variations change the local air density. However, since the air flow in the room is low-speed (maximum velocity on the order of, $u \sim 0.5$ m/s compared to speed of sound of around, $c \sim 343$ m/s), the Mach number (u/c), that represents the ratio of acoustic to convective time-scales, is small (< 0.01). Small Mach numbers mean that the convective time-scales are much larger than acoustic time-scales, and thus the compressibility effects are negligibly small. Under these conditions, the variable-density equations in the limit of zero-Mach number are valid and the pressure field at any point within the

domain and time can be split into a bulk thermodynamic pressure, P_0 , and the dynamic pressure p that appears in the momentum equation,

$$P(x, t) = P_0(t) + p(x, t). \quad (1)$$

The background thermodynamic pressure (P_0) for the operating room is assumed constant and equal to the atmospheric pressure, $P_0 = 1 \text{ atm.}$ Accordingly, the density of the air (assumed as ideal gas) varies only with the local temperature field according to the equation of state as,

$$\rho = \frac{P_0 R_{\text{universal}} T}{M_{\text{air}}}, \quad (2)$$

361 where $R_{\text{universal}}$ is the universal gas constant, M_{air} is the molecular mass of the air, and T is the
362 absolute temperature. The governing equations for large-eddy simulation of turbulent flows with
363 variable density in the limit of zero Mach number are given below.

364 3.2.1 Gas-phase equations

365 The spatially filtered, Favre averaged, governing equations used for large-eddy simulation of particle-
366 laden, turbulent air flow with heat transfer and buoyancy effects are given as,

$$\frac{\partial \bar{\rho}_g}{\partial t} + \frac{\partial \bar{\rho}_g \tilde{u}_j}{\partial x_j} = 0. \quad (3)$$

$$\frac{\partial \bar{\rho}_g \tilde{u}_i}{\partial t} + \frac{\partial \bar{\rho}_g \tilde{u}_i \tilde{u}_j}{\partial x_j} = -\frac{\partial \bar{p}}{\partial x_i} + \frac{\partial}{\partial x_j} (2\bar{\mu} \tilde{S}_{ij}) - \frac{\partial q_{ij}^r}{\partial x_j} + (\bar{\rho}_g - \rho_0) g_i, \quad (4)$$

$$\frac{\partial \bar{\rho}_g \tilde{h}}{\partial t} + \frac{\partial \bar{\rho}_g \tilde{h} \tilde{u}_j}{\partial x_j} = \frac{\partial}{\partial x_j} \left(\bar{\rho}_g \tilde{\alpha}_h \frac{\partial \tilde{h}}{\partial x_j} \right) - \frac{\partial q_{hj}^r}{\partial x_j}, \quad (5)$$

where

$$\tilde{S}_{ij} = \frac{1}{2} \left(\frac{\partial \tilde{u}_i}{\partial x_j} + \frac{\partial \tilde{u}_j}{\partial x_i} \right) - \frac{1}{3} \delta_{ij} \frac{\partial \tilde{u}_k}{\partial x_k}. \quad (6)$$

Here, $\bar{\rho}_g$ is the filtered density, \tilde{u}_i is the Favre averaged velocity field, \bar{p} is the filtered pressure, μ is the dynamic viscosity, $\alpha_h = k/\bar{\rho}_g C_p$, is the thermal diffusivity (k is the conductivity and C_p the specific heat at constant pressure), g_i is the gravitational acceleration, and \tilde{S}_{ij} is the filtered rate of

strain. In addition, the specific enthalpy, h , is given as,

$$h = \frac{T - T_0}{T_0}, \quad (7)$$

where T is the local temperature. Also, T_0 and ρ_0 are the temperature and density fields corresponding to the air inlet conditions and pressure of P_0 .

The additional terms q'_{ij} and q'_{hj} in the momentum and the enthalpy equations, respectively, represent the subgrid-scale stress and energy flux and are modeled using the dynamic Smagorinsky model by Moin *et al.* (1991) as demonstrated by Pierce & Moin (1998a). The unclosed terms in Eqs. (4-5) are modeled using the gradient-diffusion hypothesis with eddy-viscosity/diffusivity,

$$q'_{ij} = \overline{\rho_g}(\tilde{u}_i\tilde{u}_j - \widetilde{u_iu_j}) = 2\mu_t\tilde{S}_{ij} - \frac{1}{3}\overline{\rho_g}q^2\delta_{ij}, \quad (8)$$

$$q'_{hj} = \overline{\rho_g}(\tilde{h}\tilde{u}_j - \widetilde{hu_j}) = \overline{\rho_g}\alpha_t\frac{\partial\tilde{h}}{\partial x_j}, \quad (9)$$

where the eddy viscosity (μ_t) and eddy thermal diffusivity α_t are modeled as,

$$\mu_t = C_\mu\overline{\rho_g}\Delta^2\sqrt{\widetilde{S_{ij}S_{ij}}}, \quad (10)$$

$$\overline{\rho_g}\alpha_t = C_\alpha\overline{\rho_g}\Delta^2\sqrt{\widetilde{S_{ij}S_{ij}}}. \quad (11)$$

The coefficients C_μ , C_α are calculated dynamically at each time-step and for each grid point using the dynamic procedure as outlined by Germano *et al.* (1991). For the unstructured grids, the filter width Δ is taken as $V_{cv}^{1/3}$ where V_{cv} is the volume of the grid element.

3.2.2 Equations for calculating the trajectories of individual squames

The human skin cells or squames typically are disc-shaped with a diameter ranging from 4–20 μm and a thickness of 3–5 μm with density close to that of liquid water (1000 kg/m^3) (Noble *et al.*, 1963; Noble, 1975; Snyder, 2009). Although the squames shape is more disc-like, in the present work they are considered as non-deformable, spherical in shape. A spherical shape is assumed as the dynamics of the spherical particle is easier to calculate and also the lift and drag forces on small particles of disc or spherical shape are not significantly different. The diameter of the spherical

379 particle is assumed to be 10 microns and matches an average settling velocity of a disc-shaped
 380 particle considering the mean flow normal and parallel to the disc (see Appendix A). Recent work
 381 using RANS model by Memarzadeh & Manning (2002); Memarzadeh (2003) also approximates the
 382 squames particles as spherical with a size of 10 microns.

An Eulerian-Lagrangian approach is used wherein individual squames trajectories will be tracked in a Lagrangian frame. The different forces on the particles will be calculated using standard closure laws. The effect of the particles on the fluid flow will be negligible owing to their small concentration and thus a one-way coupling approach is adopted, wherein the squame motion uses the fluid flow parameters (velocity) to compute the forces, however, the effect of squames on the fluid momentum is neglected (Elghobashi, 1994, 2006). In addition, since the volume fraction of the squames in an operating room is not very large ($\ll 10^{-3}$), collisions amongst the squames are neglected. The squame particle motion equation is that of Maxey & Riley (1983),

$$\frac{d}{dt}(\mathbf{x}_p) = \mathbf{u}_p \quad (12)$$

$$m_p \frac{d}{dt}(\mathbf{u}_p) = \mathbf{F}_g + \mathbf{F}_d + \mathbf{F}_\ell + \mathbf{F}_{am} + \mathbf{F}_p + \mathbf{F}_H, \quad (13)$$

383 where \mathbf{x}_p is the particle (squames) centroid location, m_p is the mass of an individual particle, \mathbf{u}_p is
 384 the particle velocity, \mathbf{F}_g is the gravitational force, \mathbf{F}_d is the drag force, \mathbf{F}_ℓ is the lift force, \mathbf{F}_{am} is the
 385 added mass force, \mathbf{F}_p is the pressure force, and \mathbf{F}_H is the Basset history force.

386 The large ratio of particle density to air density, ρ_p/ρ_g , renders both the Basset history force
 387 and the added mass force negligible compared to the drag force. The ratio of the Saffman lift to
 388 the drag force is given by, $F_\ell/F_{drag} \sim \rho_g d_p^2 (du/dy)^{1/2}/\mu$, and is dependent on the shear rate and
 389 particle diameter. For particles with small diameter and low inertia this force can also be neglected
 390 in comparison to the drag force (Crowe *et al.*, 1996; Saffman, 1965). However, the lift force is in-
 391 corporated in our calculations to account for the saltation of the squame particles from the operating
 392 room floor. The gravity, drag and lift forces are given as,

$$\mathbf{F}_g = (\rho_p - \bar{\rho}_g) \mathcal{V}_p \mathbf{g}; \quad \mathbf{g} = -9.81 \mathbf{m}/s^2 \quad (14)$$

$$\mathbf{F}_d = -\frac{1}{8}C_d\bar{\rho}_g\pi d_p^2|\mathbf{u}_p - \tilde{\mathbf{u}}_{g,p}|(\mathbf{u}_p - \mathbf{u}_{g,b}); \quad C_d = \frac{24}{Re_p}(1 + 0.15Re_p^{0.687}), \quad (15)$$

$$\mathbf{F}_\ell = -C_\ell m_p \frac{\bar{\rho}_g}{\rho_p}(\mathbf{u}_p - \tilde{\mathbf{u}}_{g,p}) \times (\nabla \times \tilde{\mathbf{u}}_g)_p; \quad C_\ell = \frac{1.61 \times 6}{\pi d_p} \sqrt{\frac{\mu}{\bar{\rho}_g}} |(\nabla \times \tilde{\mathbf{u}}_g)_p| \quad (16)$$

where the subscript p represents the squame particle, $\tilde{\mathbf{u}}_{g,p}$ represents the fluid velocity interpolated at the particle center location, \mathcal{V}_p is the particle volume, d_p is the particle diameter, $Re_p = \bar{\rho}_g|\mathbf{u}_p - \tilde{\mathbf{u}}_{g,p}|d_p/\mu$ is the particle Reynolds number, C_d is the drag coefficient, C_ℓ is the lift coefficient.

The gas-phase velocity, $\tilde{\mathbf{u}}_g$, in the particle equations above, is computed at individual particle locations within a control volume using a generalized, tri-linear interpolation scheme for arbitrary shaped elements. Introducing higher order accurate interpolation is straight forward; however, it was found that tri-linear interpolation is sufficient to represent the gas-phase velocity field at particle locations. As mentioned earlier, in LES of particle-laden flows, the particles are presumed to be *subgrid*, and the particle-size is smaller than the filter-width used. The gas-phase velocity field required in equations (12) and (13) is the total (unfiltered) velocity, however, only the filtered velocity field is computed in equations (4). The direct effect of the unresolved (subgrid) velocity fluctuations on particle trajectories depends on the particle relaxation time-scale, and the subgrid kinetic energy. Pozorski & Apte (2009) performed a systematic study of the direct effect of subgrid scale velocity on particle motion for forced isotropic turbulence. It was shown that, in poorly resolved regions, where the subgrid kinetic energy is more than 30%, the effect on particle motion is more pronounced. A stochastic model reconstructing the subgrid-scale velocity in a statistical sense was developed (Pozorski & Apte, 2009). However, in well resolved regions, where the amount of energy in the subgrid scales is small, this direct effect was negligible. In the present work, the direct effect of subgrid scale velocity on the droplet motion is neglected. However, it should be noted that the particles *do feel* the subgrid scale stresses through the subgrid model that affects the resolved velocity field. For well-resolved LES of swirling, separated flows with the subgrid scale energy content much smaller than the resolved scales, the direct effect is shown to be small (Apte *et al.*, 2003b, 2009). This is the main advantage of LES as compared to RANS. In RANS, only the time-average mean velocity is available, and all scales of turbulence affecting the instantaneous fluctuations around the mean

must be modeled. Approximating the effect of turbulent fluctuations on the particle dispersion is thus necessary for RANS, whereas, it is implicitly accounted for in the LES.

Equations (12,13) are integrated using a fourth-order Runge-Kutta time-stepping algorithm. After obtaining the new particle positions, the particles are relocated, particles that cross interprocessor boundaries are duly transferred, boundary conditions on particles crossing boundaries are applied, source terms in the gas-phase equation are computed, and the computation is further advanced. Solving these Lagrangian equations thus requires addressing the following key issues: (i) efficient search and location of particles on an unstructured grid (ii) interpolation of gas-phase properties to the particle location for arbitrarily shaped control volumes (iii) inter-processor particle transfer. The details on efficiently locating the particles on unstructured grids, search algorithms for particles, and interpolation schemes can be found in the work by *Apte et al. (2003b, 2009)*.

In addition, if the squames impact internal boundaries, a simple, perfectly elastic specular reflection is assumed wherein the squames reverse the wall-normal velocity and preserve the wall-tangential velocity. If the squames impact the patient's knee or the inlet (suction port) of the 3M™ Bair Hugger™ blower system, they are assumed to stick to the surface and are no longer advanced in the computations.

3.3 Computational grid

Use of high quality computational mesh is critical in LES for accurate prediction of the turbulent flow, but also having a stable numerical solution. However, to handle complex configurations, use of hybrid elements involving tetrahedrons, pyramids, hexagons and wedges, etc. is common in a typical computational grid. This helps with the grid generation surrounding complex features such as the operating table, the surgeons, the patient and the drape, for example. The transitions from one type of grid element to another; however, can lead to skewed elements. It is thus critical that the numerical algorithm be robust, stable and accurate at high Reynolds numbers on skewed or bad grid elements. A numerical algorithm developed for arbitrary shaped unstructured grids (*Mahesh et al., 2004; Ham et al., 2003; Ham & Iaccarino, 2004; Mahesh et al., 2006*) that is based on kinetic energy conservation principles offers the much needed robustness and accuracy on such grids without resorting to explicit artificial dissipation. As discussed below, we use a research solver based on

446 such an algorithm.

447 For the present study, a computational mesh (figure 8) was generated using the CAD model
 448 described earlier to facilitate predictive large eddy simulations. The mesh was generated using both
 449 tetrahedral and hexahedral cells. The transition of mesh from tetrahedral cells to hexahedral cells
 450 was done using a combination of pyramid and wedge type cells. Care was taken to generate a
 451 computational grid that minimizes the grid skewness as much as possible. As shown below, in the
 452 regions away from the complex OR configuration involving the surgeons, the tables, the patient and
 453 the drape, a mostly hex-dominant mesh is used. As one approaches closer to the operating table, the
 454 computational grid is transitioned to a predominantly tetrahedra-based mesh (see figure 8b). The
 455 total mesh count for the computational domain is about 66 million.

456 Figure 9 shows the grid resolution near the air inlet cross-sections. The grid is appropriately re-
 457 fined to capture the shear layer generated by the inlet flow between the grilles. The mesh surrounding
 458 the OR table, patient, surgeons, side tables, the blower, and surgical lamps is predominantly tetra-
 459 hedral. The tetrahedral mesh was carefully refined to capture surface curvature. Extra refinement
 460 was performed near surfaces which were in close proximity to other surfaces. This enhanced mesh
 461 refinement is to ensure that the effect of surface shapes on the flow and particles going around them
 462 will be captured by the simulation (figure 10a,b.)

463 As is shown in the above figures, a high quality mesh was generated for the present LES inves-
 464 tigation. The minimum tetrahedral cell size (defined as cube root of the cell volume) used near all
 465 key regions such as drape, patient, operating bed, surgeons, etc. was around 1mm. Smallest grid
 466 spacing in proximity regions resolving the gaps between closely placed surfaces is 0.7mm. The
 467 coarsest tetrahedral cell size used away from the key regions is 2.5cm. As mentioned earlier in the
 468 report a fine mesh was used near the inlet regions to resolve the flow entering the operating room.
 469 A uniform hexahedral cell size of 2.5cm was used to resolve the air inlet grille faces with 20 cells
 470 along its width and 44 cells along its length. The gaps between the inlet grilles were resolved us-
 471 ing a finer mesh with each cell size of 0.63cm. To capture the inlet air flow structures properly,
 472 a refined uniform mesh of 0.38cm was used along the flow direction. Finally, a uniform cell size
 473 of 2.5cm was used to resolve each outlet grille with 28 cells along its width and 28 cells along its
 474 length. Various mesh metrics were checked to ensure that the quality of the generated mesh was
 475 good. Figure 11a shows histogram plot of cell skewness in the mesh. The average skewness was

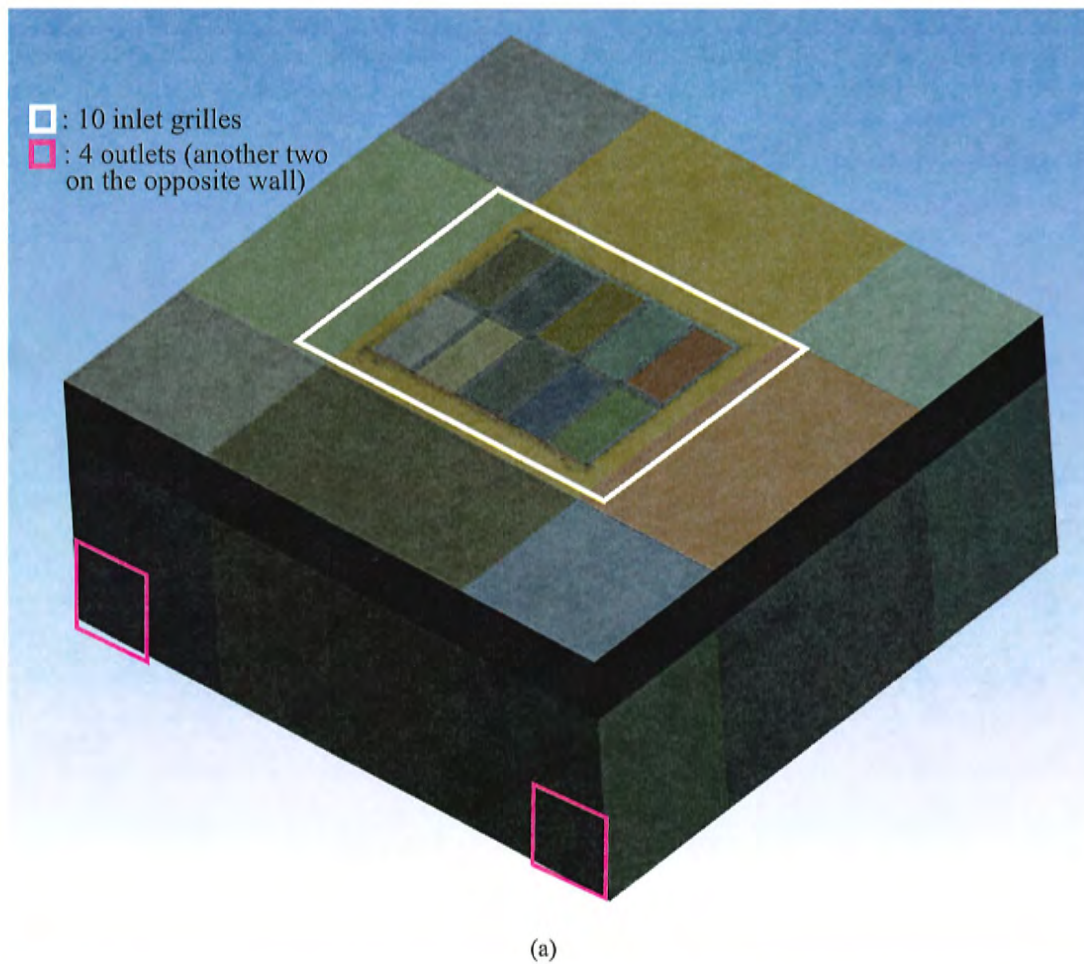
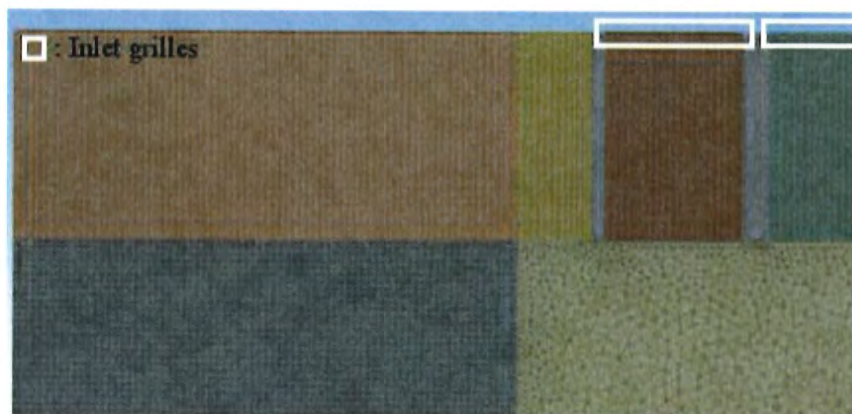


Figure 8: Computational mesh for the operating room model consisting of about 66M hybrid grid elements consisting of hexagons, tetrahedrons, pyramids and wedges: (a) the full 3D mesh, (b) cross-sectional slice showing hex-dominant mesh in the inlet and outlet regions and a tetrahedral mesh near the operating table.

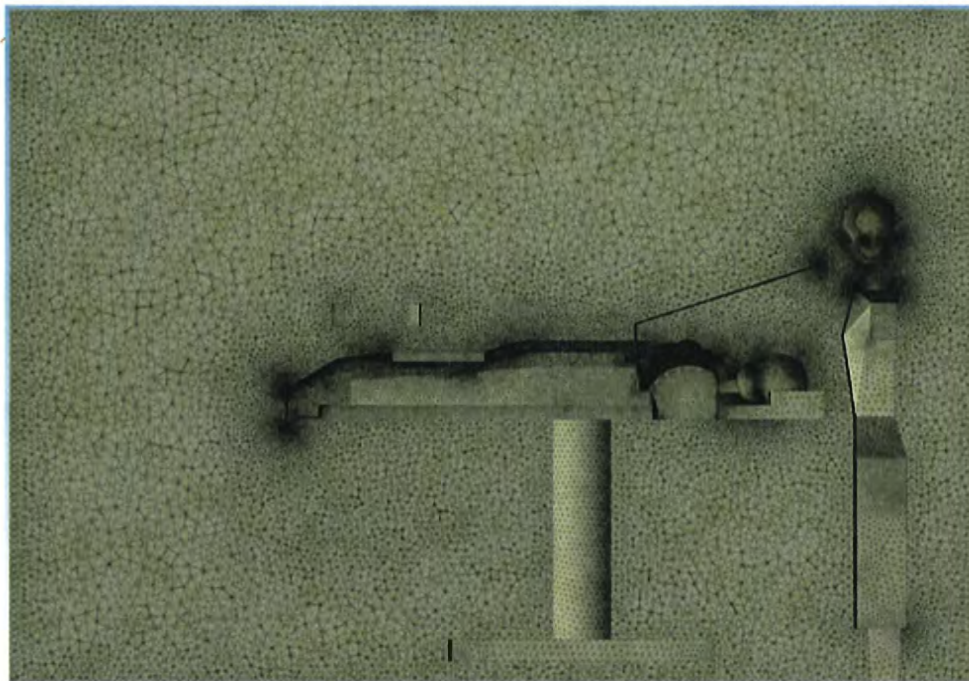


(a)

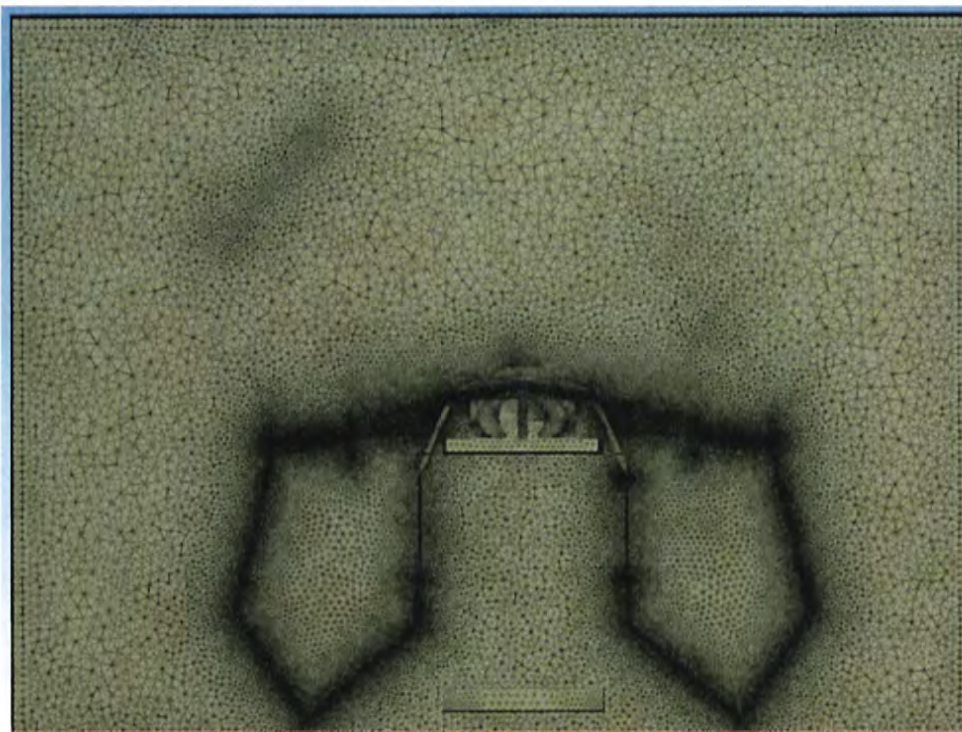


(b)

Figure 9: A cross section cut showing fine mesh near the ceiling of the room: (a) top view zoom-in, (b) top view showing all air inlet grilles.



(a)



(b)

Figure 10: Mesh refinement near curved surfaces and surfaces that are in close proximity to others: (a) side view showing the entire operating table, (b) side view showing drapes.

0.14 and with maximum skewness was 0.91. Only 0.018% of cells had total skewness greater than 0.8 indicating the high quality of cells in the mesh. Another mesh metric that was checked was the aspect ratio of cells. The maximum aspect ratio was 16.2 and the average cell aspect ratio was 2.9, which indicate that a majority of cells in the mesh were mostly uniform (see figure 11b).

3.4 Boundary Conditions

This subsection provides details of all boundary conditions used in the calculation, starting with operating room (OR) air inlet conditions, heat sources, BH hot air blower inflow (suction) and outflow, and OR air outlet conditions.

3.4.1 Inlet boundary conditions

The dimensions of the operating room are shown in Table 1. As shown, there are 10 inlet grilles supplying air. The net supply air volumetric flow rate, \dot{V} , is 1.10436 m³/s (0.39 ft³/s). Using the inlet flow rates, the air changes per hour (ACH) of the room is calculated as follows,

$$ACH = \dot{V} \times 3600 / (LWH) = 24.45 \text{ per hour}, \quad (17)$$

where L , W and H are the room length (in x), width (in y) and height (in z) directions. The ACH is according to the ASHRAE handbook [Memarzadeh & Manning \(2002\)](#), which suggests the ACH to be about 25 per hour for an operating room with recirculating air system.

The inlet boundary conditions are imposed at the 10 grilles on the ceiling of the operating room to model the inlet part of the forced ventilation system. The average inlet velocity, \bar{U}_{in} , is found to be 0.1933m/s based on,

$$\bar{U}_{in} = \dot{V} / (10 \times A_{grill}), \quad (18)$$

where A_{grill} is the area of the cross-section ($1.12 \times 0.51 = 0.5712\text{m}^2$) and $\dot{V} = 1.1044\text{m}^3/\text{s}$ ($39\text{ft}^3/\text{s}$) is the net inlet volumetric flow rate. The air temperature of the inlet flow, T_{in} , is set to 59°F (15°C).

Based on Reynolds number for the inlet grilles, $Re_{in} = 9226.54$ (Table 1), the inlet flow is turbulent. In order to have completely predictive numerical simulation and to minimize the effect of boundary conditions, it is necessary to impose a proper, fully developed turbulent flow field at the in-

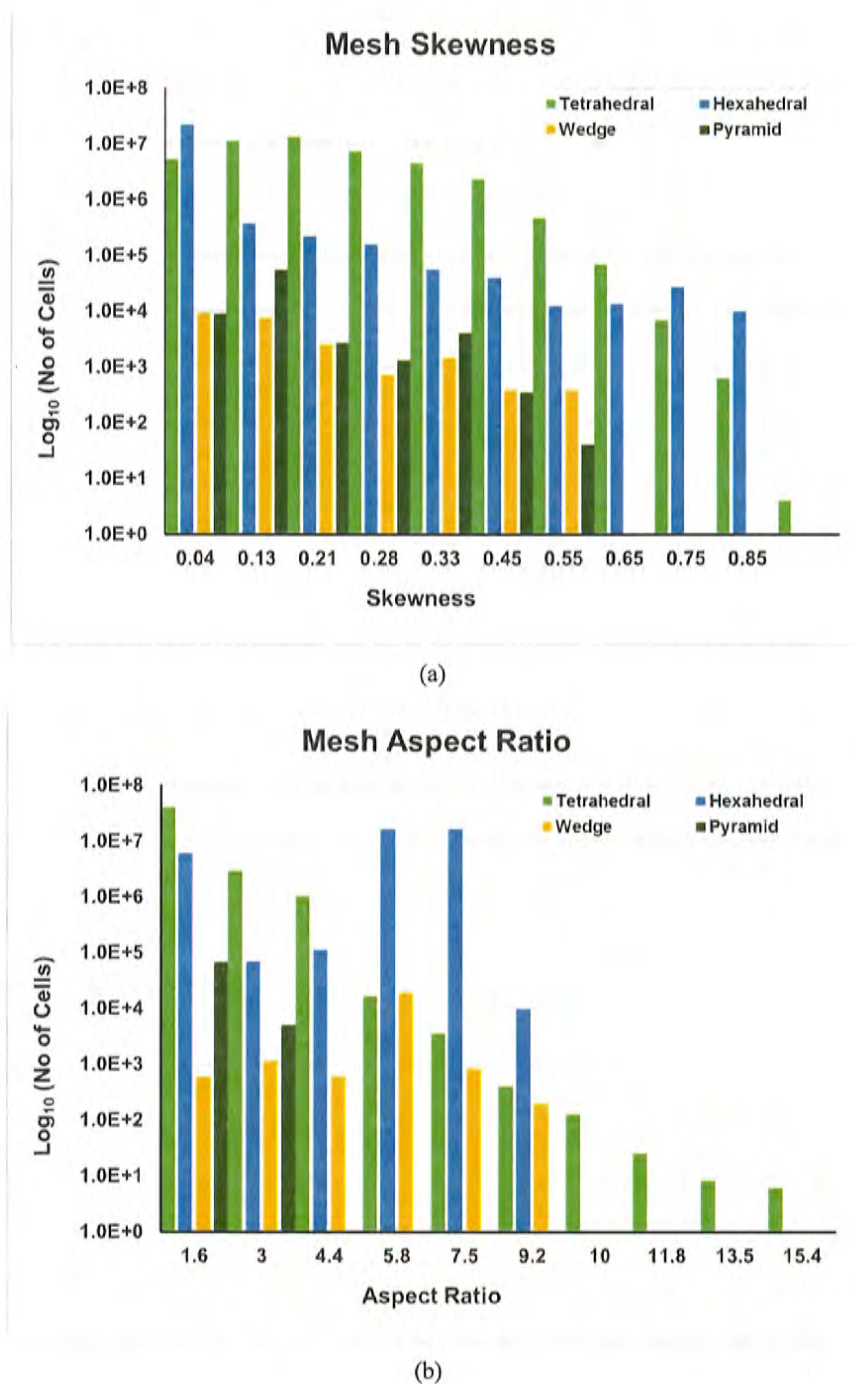


Figure 11: Statistics histograms of the quality of mesh used in the computation: (a) skewness, (b) aspect ratio.

Table 1: Operating room characteristics

Parameter	Value
Room dimensions [m], L, W, H	$7.315 \times 7.00 \times 3.175$
Supply air flow rate [m^3/s], \dot{V}	1.10436
ACH [1/hr]	24.45
Room air temperature [$^{\circ}\text{C}$]	15
Inlet air density [kg/m^3], ρ_{in}	1.225
Supply air temperature [$^{\circ}\text{C}$]	15
Room air pressure [Pa]	1.0131×10^5
Grille dimensions [m]	1.12×0.51
Grille Area [m^2]	0.5712
Grille hydraulic diameter [m], D_h	0.7
Mean inlet velocity [m/s], \bar{U}_{in}	0.1933
Inlet Reynolds number, $Re_{in} = \frac{\rho_{in} \bar{U}_{in} D_h}{\mu}$	9226.54

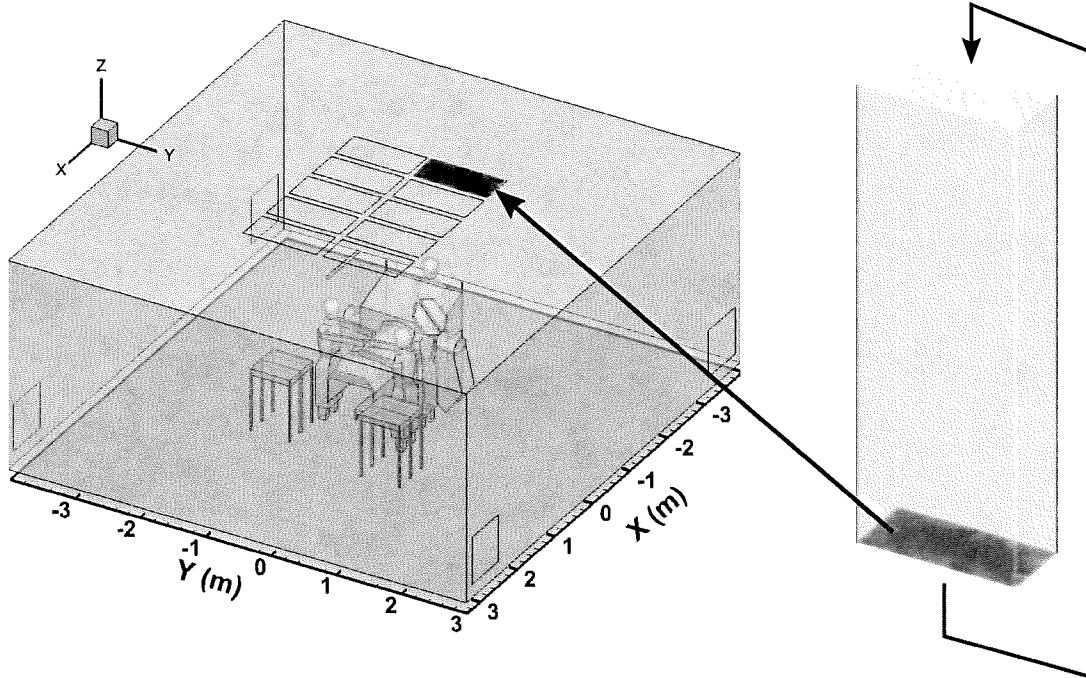


Figure 12: Schematic of the periodic duct used to generate inlet flow data.

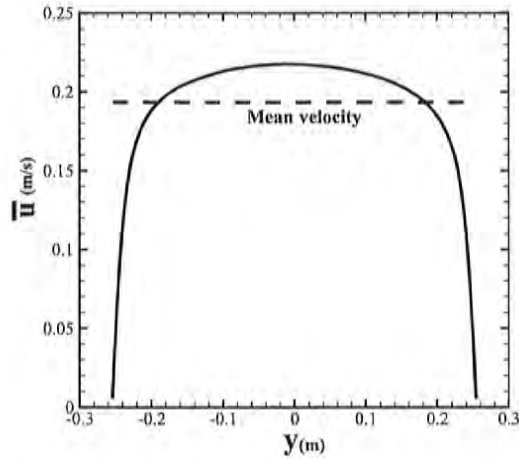


Figure 13: Mean velocity profile generated by a periodic duct flow for the inlet grilles.

493 let. Thus, a periodic turbulent duct flow was computed (figure 12) to produce a target mean flow rate
 494 equal to that prescribed ($\dot{V} = 1.10436 \text{ m}^3/\text{s}$) using a body force technique of [Pierce & Moin \(1998b\)](#).
 495 This also generates turbulence fluctuations at the inlet plane that satisfy the continuity equation. The
 496 cross-sectional area of the periodic duct used is the same as that of each grille ($1.12 \text{ m} \times 0.51 \text{ m}$), and
 497 the length is about 4.5 times the hydraulic diameter of the cross-section. The velocity field data at
 498 the inlet cross-section was recorded in time series for almost 400 seconds of physical time. Figure 13
 499 shows the time-averaged velocity field in the center plane of the duct obtained from the periodic duct
 500 simulation. The turbulence intensity ($I = \sqrt{\frac{1}{3}(u_{rms}^2 + v_{rms}^2 + w_{rms}^2)}/\bar{U}_{in}$) at the inlet cross-section is
 501 5-6% of the mean inlet velocity (\bar{U}_{in}), and is in agreement with the experimental measurements con-
 502 ducted by [McNeill et al. \(2012, 2013\)](#). Here, u_{rms} , v_{rms} and w_{rms} are the root-mean square velocity
 503 components in the x , y and z directions, respectively.

504 3.4.2 Hot air blower and other heat sources

A 3MTM Bair HuggerTM 750 blower draws air from the floor of the operating room, heats it and
 blows it into the blanket (3MTM Bair HuggerTM Model 522) that covers the torso region of the
 patient. The blanket is covered with a plastic drape. The maximum flow rate of the blower is
 $\dot{V}_{blower} = 0.021 \text{ m}^3/\text{s}$. The hot air moves along the surface of the drape that faces the patient and
 then it is discharged into the room along the drape edges. In the present calculation, the bottom
 surface (facing the floor) of the 3MTM Bair HuggerTM blower is considered as a suction surface with

surface area ($A_{\text{extraction}} = 0.03796\text{m}^2$). A Dirichlet boundary condition is applied at this surface that prescribes the extraction velocity $\bar{U}_{\text{extraction}}$ as

$$\bar{U}_{\text{extraction}} = \frac{\dot{V}_{\text{blower}}}{A_{\text{extraction}}}, \quad (19)$$

505 giving an extraction velocity of 0.5532m/s. To model the hot air discharged along the edges of the
506 drape. The total area of this edge of the drape is measured to be $A_{\text{drape}} = 0.07794\text{m}^2$. A Dirichlet
507 boundary condition is applied such that the air is injected into the room perpendicular to the edges
508 of the drape with velocity, \bar{U}_{drape} , calculated as,

$$\bar{U}_{\text{drape}} = \frac{\dot{V}_{\text{blower}}}{A_{\text{drape}}}, \quad (20)$$

509 giving an average injection velocity along the drape edge as 0.2694 m/s. The temperature of the
510 hot air at the BH blower outlet is prescribed equal to 109°F (42.77°C) and the temperature of the air
511 leaving the drape edge is set equal to 106°F (41.11°C) according to 3M video at:

512 <https://www.youtube.com/watch?v=QhzeInWlj54>. The flow rates at the inlet grilles and for the
513 blower are summarized in Table 3.4.2.

514 Other heat sources in the surgical room are mainly the surgeons, patient, surgical lamps, and
515 exposed surface of the patient's knee. These heat sources can cause warming of the air in contact
516 with the surfaces and result in a rising thermal plume. For these surfaces, a Dirichlet condition was
517 used for temperature based on the experimentally measured values. In their work, McNeill *et al.*
518 (2012) conducted detailed measurements of detailed surface temperatures that may lead to buoyant
519 plumes specifically to be used in CFD calculations. The values are summarized in Table 3.4.2,
520 among which, the temperatures of surgeons and patient's heads as well as the surgical lamps are
521 based on the work of McNeill *et al.* (2012) and the rest are from the 3M video. For all other other
522 solid surfaces, a no heat flux Neumann condition was specified, $\frac{\partial T}{\partial n} = 0$.

523 3.5 Numerical solution method

524 The computational approach is based on a co-located, finite-volume, energy-conserving numerical
525 scheme on unstructured grids (Moin & Apte, 2006; Mahesh *et al.*, 2006) and solves the variable

Table 2: Flow and temperature conditions

Parameter	Value
Inlet volume flow rate \dot{V} , [m ³ /s]	1.1044
Temperature of inlet grille air, [°C]	15
Mean inlet velocity [m/s], \bar{U}_{in}	0.1933
BH blower volume flow rate \dot{V}_{blower} , [m ³ /s]	0.021
Temperature of hot air leaving the drape edge, [°C]	41.11
Heads of the surgeons and patient, [°C]	31.44
The patient's knee, [°C]	37.78
Two surgical lamps, [°C]	93.92

density gas-phase flow equations in the limit of zero-Mach number. In this co-located scheme, the velocity and pressure fields are stored and solved at the centroids of the control volumes. Numerical solution of the governing equations of the continuum fluid phase and particle phase (squames) are staggered in time to maintain time-centered, second-order advection of the fluid equations. Denoting the time level by a superscript index, the velocities are located at time level t^n and t^{n+1} , and pressure, density, viscosity, and the scalar fields at time levels $t^{n+3/2}$ and $t^{n+1/2}$. Squames position and velocity are advanced explicitly from $t^{n+1/2}$ to $t^{n+3/2}$ using fluid quantities at time-centered position of t^{n+1} .

3.5.1 Advancing the Lagrangian squames equations

The squames (particles) equations are advanced using a fourth-order Runge-Kutta scheme. Owing to the disparities in the flow field time-scale (τ_f) and the squames relaxation time (τ_p) sub-cycling of the squames equations may become necessary. Accordingly, the time-step for squames equation advancement (Δt_p) is chosen as the minimum of τ_p and the time-step for the flow solver (Δt). For the present simulations, the squames relaxation time, τ_p , based on the drag force, was found to be always larger than the time-step, Δt , used for solving the fluid flow equations in LES. Thus, the temporal evolution of the squames was well resolved by the flow time step, and subcycling of the particle equations was not necessary.

After obtaining their new positions, the squames are relocated, and the squames that cross inter-processor boundaries are duly transferred. Boundary conditions for squames crossing boundaries are applied and the computation is further advanced. Solving these Lagrangian equations thus requires

addressing the following key issues: (i) efficient search for locations of squames on an unstructured grid, (ii) interpolation of gas-phase properties to the squames location for arbitrarily shaped control volumes, (iii) inter-processor transfer of the squames.

Locating the squames particles in a generalized-coordinate structured code is straightforward since the physical coordinates can be transformed into a uniform computational space. This is not the case for unstructured grids used in the present simulations (Apte *et al.*, 2003b,a, 2009). The approach used here, projects the squames location onto the faces of the control volume and compares these vectors with outward face-normals for all faces. If the particle lies within the cell, the projected vectors point the same way as the outward face-normals. This technique is found to be very accurate even for highly skewed elements. A search algorithm is then required to efficiently select the control volume to which the criterion should be applied. An efficient technique termed as ‘the known vicinity algorithm’ was used to identify the control volume number in which the particle lies. Given the previous particle location, the known-vicinity algorithm identifies neighboring grid cells by traversing the direction the particle has moved. In LES, the time steps used are typically small in order to resolve the temporal scales of the fluid motion. Knowing the initial and final location of the particle, this algorithm searches in the direction of the particle motion until it is relocated. The neighbor-to-neighbor search is extremely efficient if the particle is located within 5-10 attempts, which is usually the case for 98% of the squames in the present simulation. Once this cell is identified, the fluid parameters are interpolated to the particle location using a generalized, tri-linear interpolation scheme for arbitrary shaped elements. Introducing higher order accurate interpolation is straight forward; however, it was found that tri-linear interpolation is sufficient to represent the gas-phase velocity field at particle locations. In the present case, particles are distributed over several processors used in the computation, and the load-imbalance was not significant. Details of the algorithm can be found in Apte *et al.* (2003b, 2009). The overall increase in computational cost due to addition of about 3 million particles was about 25% per time-step.

3.5.2 Advancing the Eulerian fluid flow equations

The scalar field (enthalpy or non-dimensional temperature; equation 5) is advanced using the old time-level velocity field. A second-order WENO scheme is used for scalar advective terms and centered differencing for the diffusive terms. All terms, except the source terms due to buoyancy

effect, are treated implicitly using Crank-Nicholson for temporal discretization. Once the scalar field is computed, the density and temperature fields are obtained from constitutive relations (equation 7) and the ideal gas law (equation 2). The cell-centered velocities are advanced in a predictor step such that the kinetic energy is conserved. The predicted velocities are interpolated to the faces and then projected. Projection yields the pressure at the cell-centers, and its gradient is used to correct the cell and face-normal velocities. The steps involved in solving the projection-correction approach for velocity field are briefly described below, Details of this algorithm may be found in Moin & Apte (2006); Mahesh *et al.* (2006); Apte *et al.* (2008b).

- Advance the fluid momentum equations using the fractional step algorithm. The density field is available at intermediate time level is obtained from arithmetic average at the two time steps $t^{n+3/2}$ and $t^{n+1/2}$.

$$\frac{\rho u_i^* - \rho u_i^n}{\Delta t} + \frac{1}{2V_{cv}} \sum_{\text{faces of cv}} \left[u_{i,f}^n + u_{i,f}^* \right] g_N^{n+1/2} A_f = \quad (21)$$

$$\frac{1}{2V_{cv}} \sum_{\text{faces of cv}} \mu_f \left(\frac{\partial u_{i,f}^*}{\partial x_j} + \frac{\partial u_{i,f}^n}{\partial x_j} \right) A_f + (\rho - \rho_0) g_i$$

where f represents the face values, N the face-normal component, $g_N = \rho u_N$, and A_f is the face area. The superscript ‘*’ represents the predicted velocity field, and $g_N^{n+1/2} = 0.5(g_N^n + g_N^{n+1})$.

- Interpolate the velocity fields to the faces of the control volumes and solve the Poisson equation for pressure:

$$\nabla^2(p\Delta t) = \frac{1}{V_{cv}} \sum_{\text{faces of cv}} \rho_f u_{i,f}^* A_f + \frac{\rho^{n+3/2} - \rho^{n+1/2}}{\Delta t} \quad (22)$$

- Reconstruct the pressure gradient, compute new face-based velocities, and update the cv-velocities using the least-squares interpolation used by Mahesh *et al.* (2004); Ham *et al.* (2003); Mahesh *et al.* (2006),

$$\frac{\rho (u_i^{n+1} - u_i^*)}{\Delta t} = -\frac{\delta p}{\delta x_i} \quad (23)$$

4 Results

The numerical simulation was initiated with stagnant air (zero velocity) in the operating room and proper boundary conditions. A simulation was carried out with the blower off and all surfaces at room temperature for about 67s of physical time, which corresponds to about 4 flow through times based on the average inlet air velocity and the height of the room. After the initial transients, the thermal boundary conditions were applied at the surgeons heads, the patient's knee, the surgical lights. A calculation was performed for another 54s to establish a stationary flow with the thermal plumes created by the surfaces with higher-than-ambient temperatures. At this time, calculation of statistics for time-averaged mean velocity field and turbulence intensity were initiated and also 3 million squame particles were placed at the floor in three different regions surrounding the operating table as described below. With the blower-off the time-step used in the calculation was $\Delta t = 6 \times 10^{-5}$ s giving a CFL number of about 0.75. This time step was able to resolve the important time-scales of turbulence and particle motion accurately. The flow statistics were collected for a total of 80s after a stationary flow field was established and the squames trajectories were calculated for about 21s.

After the above calculation was completed, the remaining squames particles in the computational domain were removed, and the blower was turned on. With the blower discharging a hot air at higher speeds, the time-step was reduced by a factor of 2.5 to $\Delta t = 2.4 \times 10^{-5}$ s maintaining the CFL number about 0.6. The reduction in time step is related to both the explicit treatment of the gravitational source term in the momentum equation as well as increased velocity at the blower discharge location. A calculation was performed for about 30s to obtain a developed plume from the hot air discharged by the blower. Flow statistics and the initial location of 3 million squames particles were initiated. With the blower-on, the flow statistics were collected for about 37s and particle trajectories were calculated for about 30s.

All calculations were performed on a parallel computer and used 1600 processors. The computational domain was decomposed such that each processor contains roughly the same number of control volumes. The overall calculation (including initial transient, the case with blower-off and the case with blower-on including particle trajectories for both cases) took about 2M CPU-hrs. For the case of blower-off, about 20s of physical time would cost roughly 100,000 CPU-hours, whereas

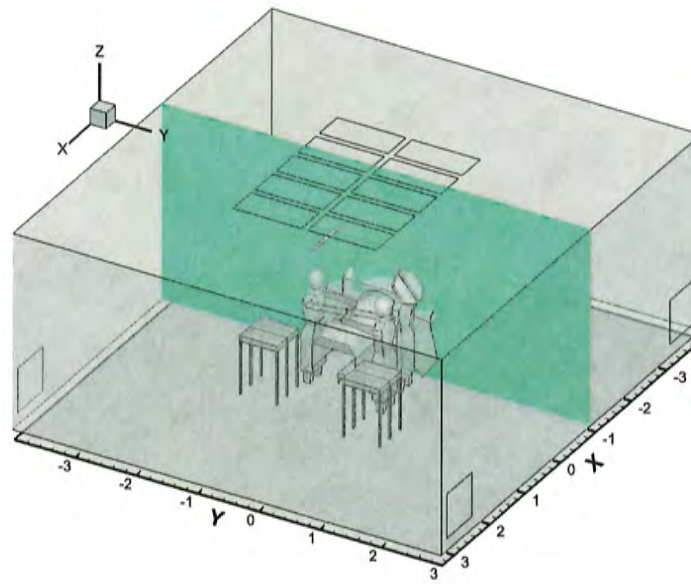
the same calculation with blower-on would cost roughly 220,000 CPU-hours. For each case, tracking 3 million trajectories of squames would add about 20-30% additional computing cost. This is because, initially the 3 million squames are clustered in a small region near the floor causing load imbalance as the particles were present on only a few processor domains. The flow statistics and particle trajectories are discussed below.

4.1 Flow characteristics

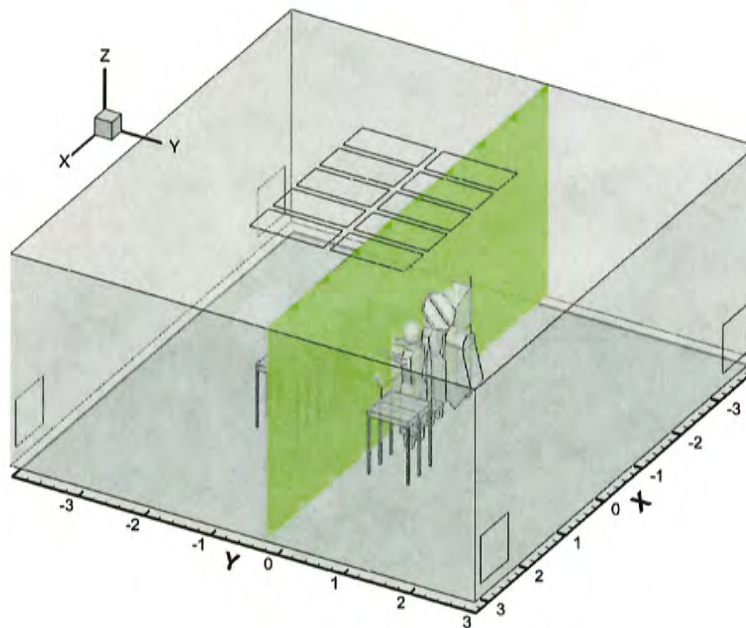
Figures 14a and 14b show the locations of two slices through the three-dimensional computational domain at $x = -0.88\text{m}$ and $y = -0.162\text{m}$ for which the mean velocity magnitude, turbulence intensity, and instantaneous temperature contours are plotted. The $x = -0.88\text{m}$ slice shows a planar cut that includes the surgical lamp and the operating table (OT). The $y = -0.162\text{m}$ slice shows a side view and contains 2 medical staff, a side table, the surgical lamp, and part of the inverted U-shaped drape. For these two slices, the flow characteristics with blower-off and blower-on are compared.

Figures 15, 16, and 17 show the contours of mean velocity magnitude, turbulence intensity, and instantaneous temperature, respectively, for the two cases of blower-off and blower-on. For the case of blower-off, figure 15a shows that the ventilation air from the ceiling inlet grilles moves downwards, gets deflected by the surgical lights and the table, impinges on the floor farther away from the table, and finally exits through the outlet grilles. Large recirculation regions are created on both sides of the table. The flow is not symmetric owing to asymmetries in the configuration itself. In comparison, with the blower turned on, the flow underneath and around the table is considerably modified as can be seen from the large velocity magnitudes under the table (figure 15b). The recirculation region is also disrupted by the rising air from the hot blower discharge. This difference is clearly visible from the turbulence intensity contours shown in figure 16a,b. With the blower-off, the maximum turbulence intensity level is about 30% in the high shear regions between the inlet air streams, as well as near the warm surgical lights due to the buoyant plume. With the blower-on, the turbulence intensity level is as high as 60% in regions affected by the rising thermal plumes from the blower hot air. The instantaneous temperature contours shown in figure 17a,b confirm that the increased turbulence level is mainly because of the thermal plumes from the hot blower air as can be seen by the high temperature regions under the OT.

Figures 18, 19, and 20 show the contours of mean velocity magnitude, turbulence intensity, and



(a)



(b)

Figure 14: Locations of the planes for which contour plots of mean velocity magnitude, turbulence intensity and instantaneous temperature are presented to compare the effect of the blower discharge on the flowfield: (a) $x = -0.88\text{m}$ (b) $y = -0.162\text{m}$.

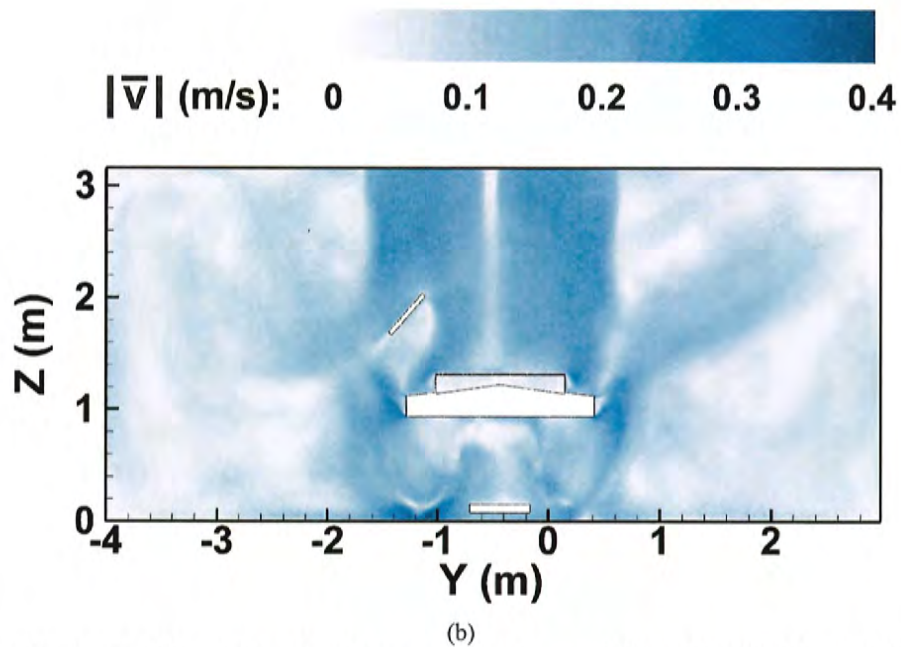
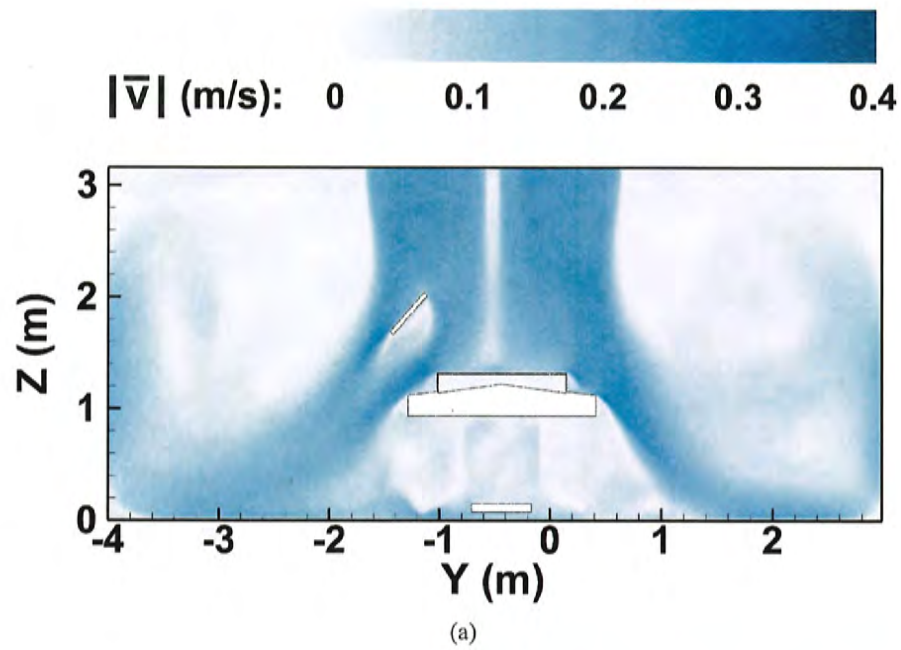


Figure 15: Contours of the mean velocity magnitude at $x = -0.88\text{m}$ (a) with blower-off and (b) with blower-on. The time average is taken over a physical time of 80s (no blower) and 37s (with blower) after establishing a stationary state.

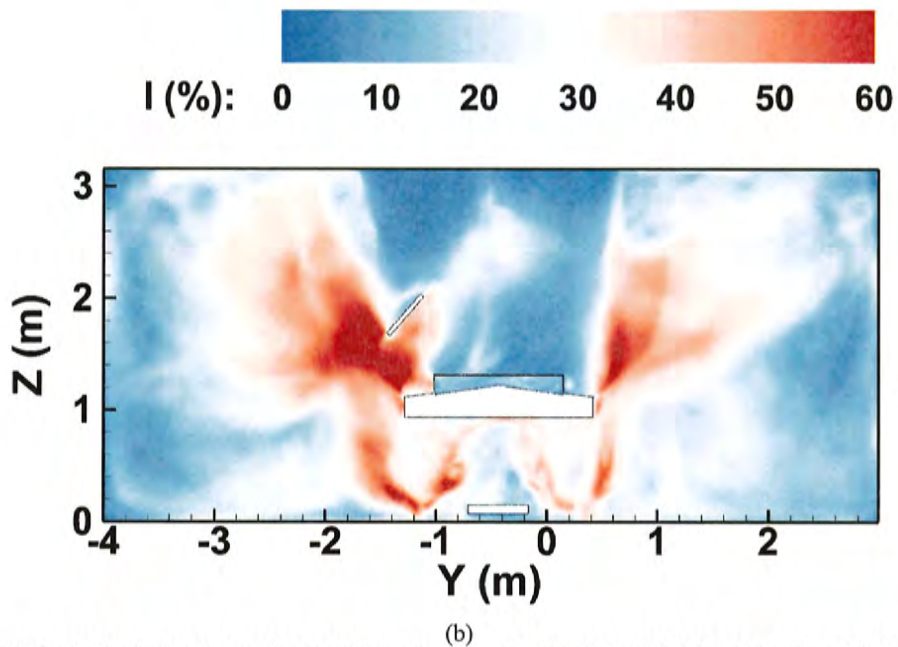
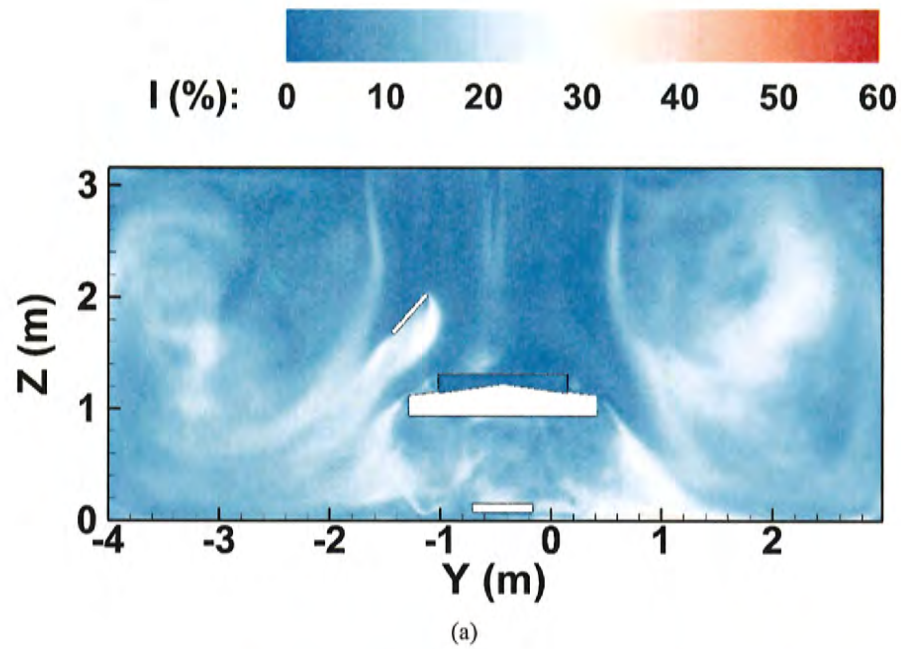


Figure 16: The turbulence intensity contours at $x = -0.88\text{m}$ (a) with blower-off and (b) with blower-on. The time average is taken over a physical time of 80s (no blower) and 37s (with blower) after establishing a stationary state.

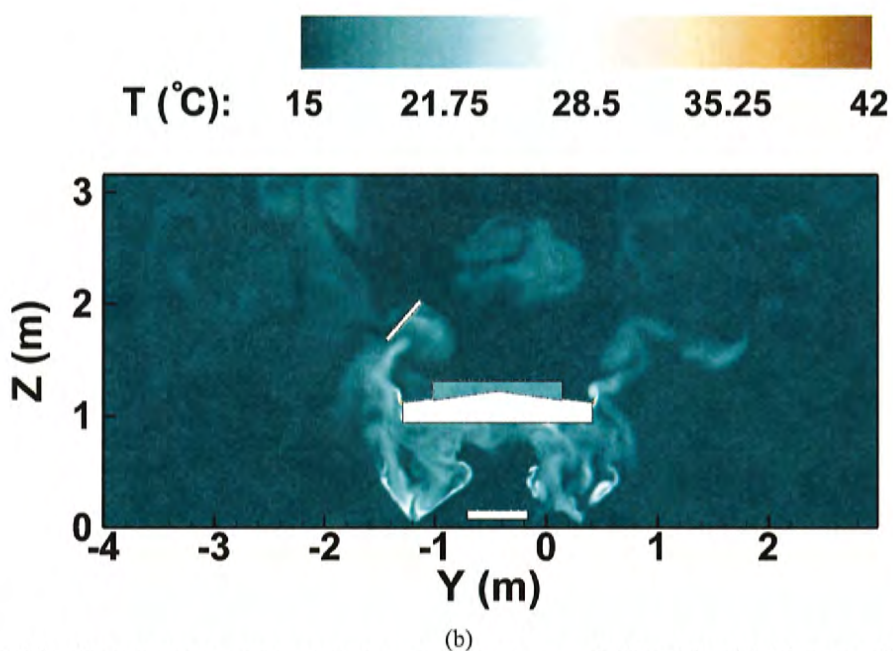
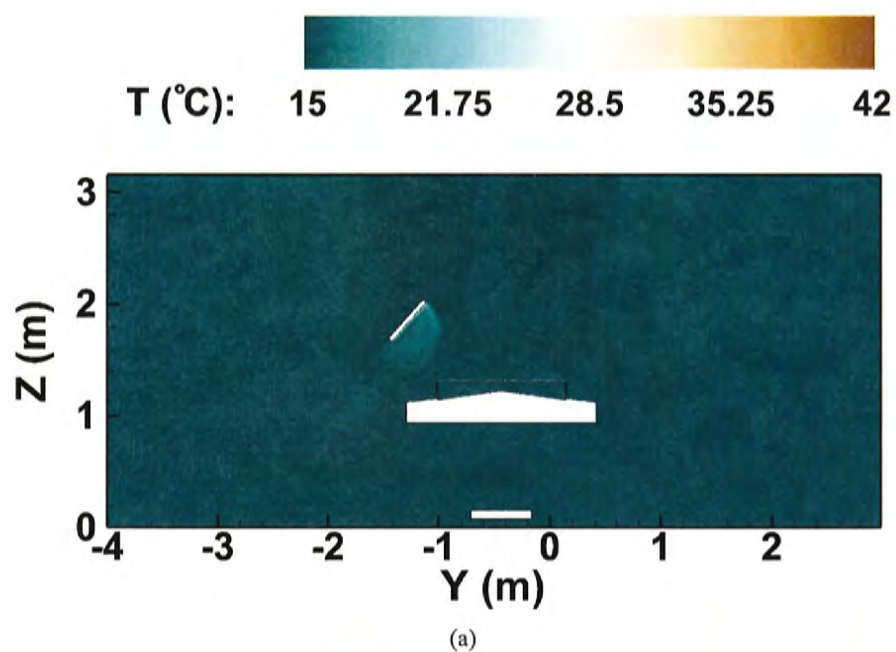


Figure 17: The instantaneous temperature contours at $x = -0.88$ m (a) with blower-off and (b) with blower-on. These snapshots are at about 35s after a stationary flow field was obtained and calculation for flow statistics was initiated.

instantaneous temperature, respectively, for the cases of blower-off and blower-on at $y = -0.162\text{m}$. Similar trends as described before are observed. The hot blower air and the rising thermal plumes disrupt the downward ventilation air flow. The high temperatures and turbulence intensity under the inverted U-shaped drape are clearly visible. The flow is also highly asymmetric with the blower turned on owing to the orientation and location of the drape. It is also seen from figure 20b that the rising thermal plumes may reach the ceiling in some regions. With the blower off, however, the plumes from warm surfaces of surgical lights, surgeons heads, and patient's knee are weak and are not significant enough to disrupt the downward ventilation air flow.

4.2 Dispersion of squames

This section provides details of the initial locations of the squames, their trajectories, and statistics of sampling the particles in regions of interest with high potential of reaching the surgical site.

4.2.1 Initial locations of squames

In order to provide a worst-case (or least probable) scenario for the squames to be carried to the surgical site by the air convection, all 3 million squames were initially placed on the floor and randomly distributed in a small region surrounding the operating table within a height of about 1 cm above the floor of the OR. If these squames are lifted by the turbulent air and moved to the surgical site, other effects such as motion of medical equipment and staff, additional squames shed from the heads and faces of medical staff, surgical garments, etc. will have an even higher probability to reach the surgical site.

Table 3: Coordinates of color-coded regions for initial positions of squames as shown in figure 21.

Color-coded initial position	$(x, y, z)_{\min}$ [m]	$(x, y, z)_{\max}$ [m]
Red	(-1.40, -0.025, 0.0)	(0.70, 0.40, 0.01)
Green	(-1.80, -1.35, 0.0)	(-1.4, 0.4, 0.01)
Yellow	(-1.40, -1.35, 0.0)	(0.70, -0.855, 0.01)

Three million particles with a diameter of 10 micron are placed within a 1 cm thick layer above the floor of the OR. The region where the particles are located is around the OT, surrounding the feet of four surgeons present in the CAD model. To better visualize the trajectories the squames

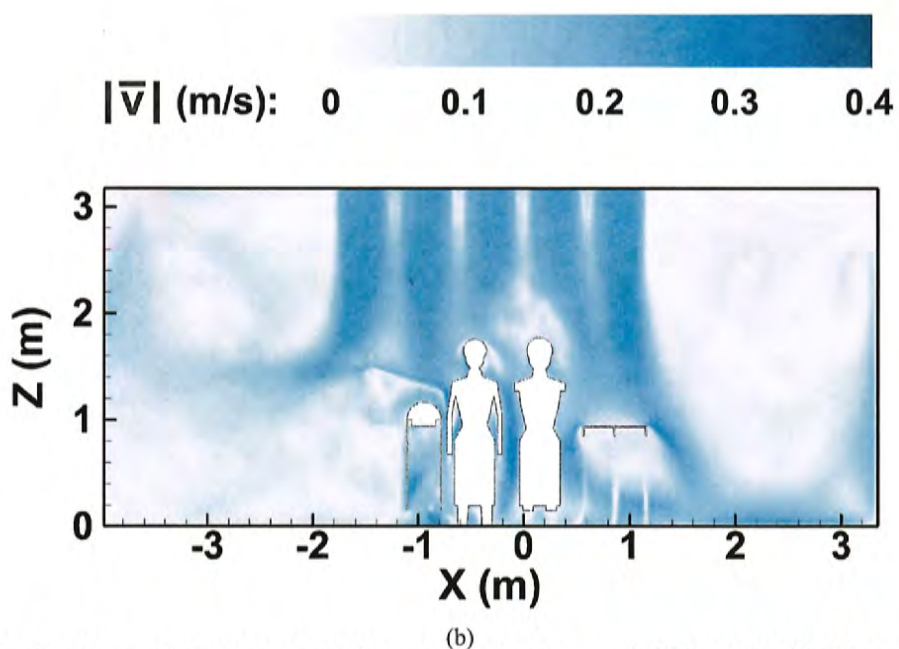
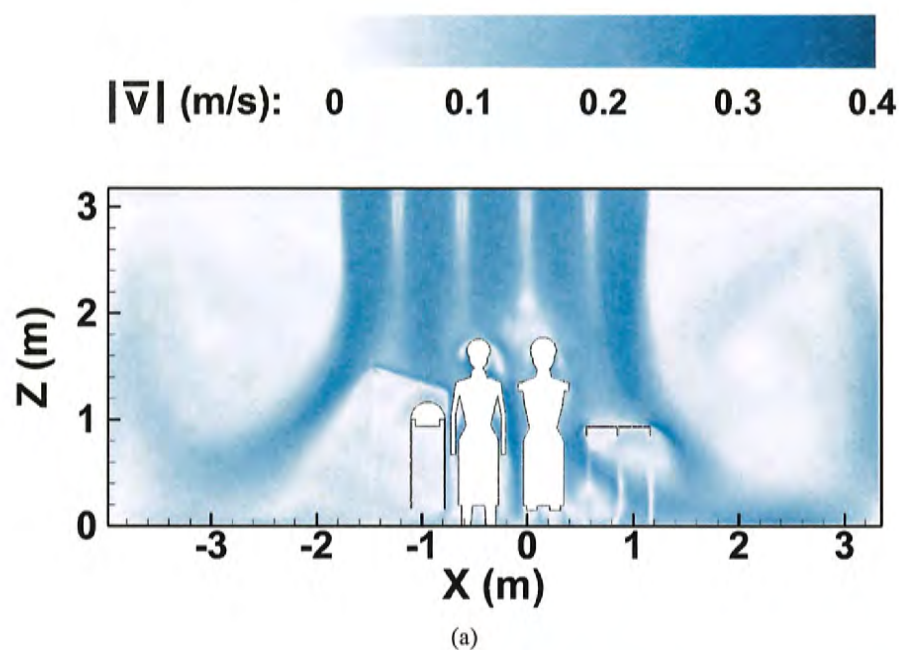


Figure 18: Contours of the mean velocity magnitude at $y = -0.162\text{m}$ (a) with blower-off and (b) with blower-on. The time average is taken over a physical time of 80s (no blower) and 37s (with blower) after establishing a stationary state.

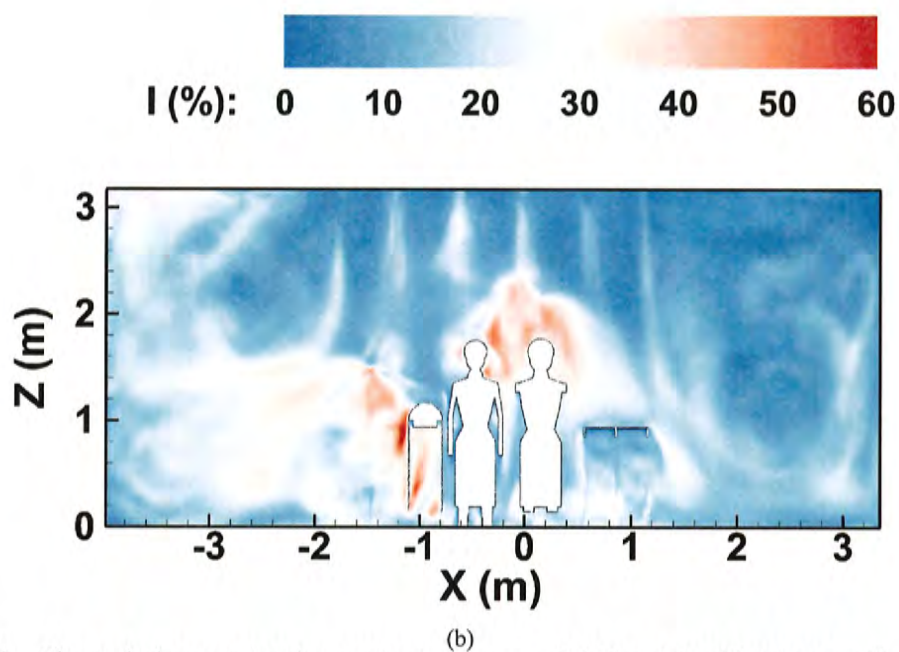
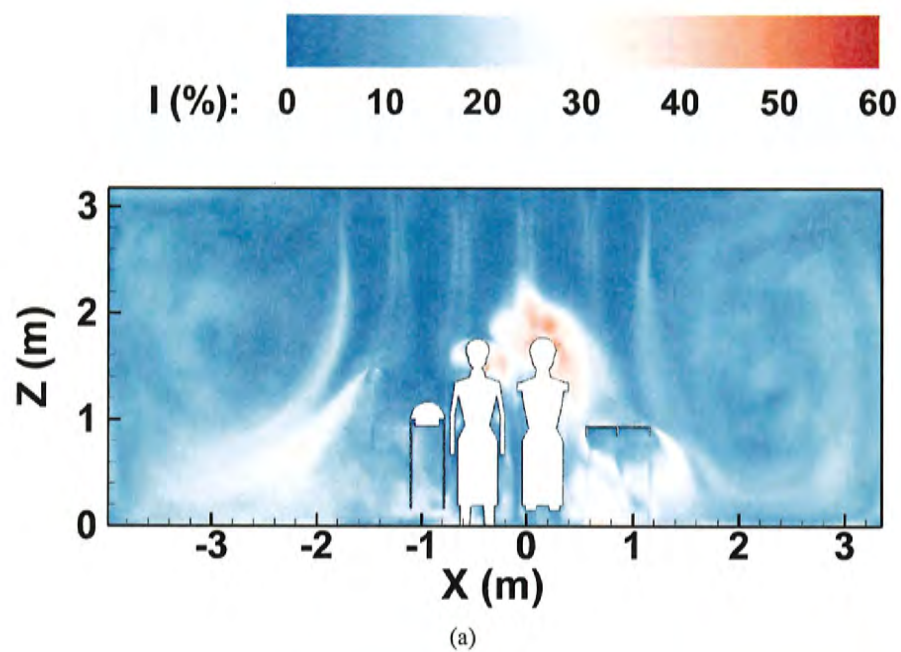


Figure 19: The turbulence intensity contours at $y = -0.162\text{m}$ (a) with blower-off and (b) with blower-on. The time average is taken over a physical time of 80s (no blower) and 37s (with blower) after establishing a stationary state.

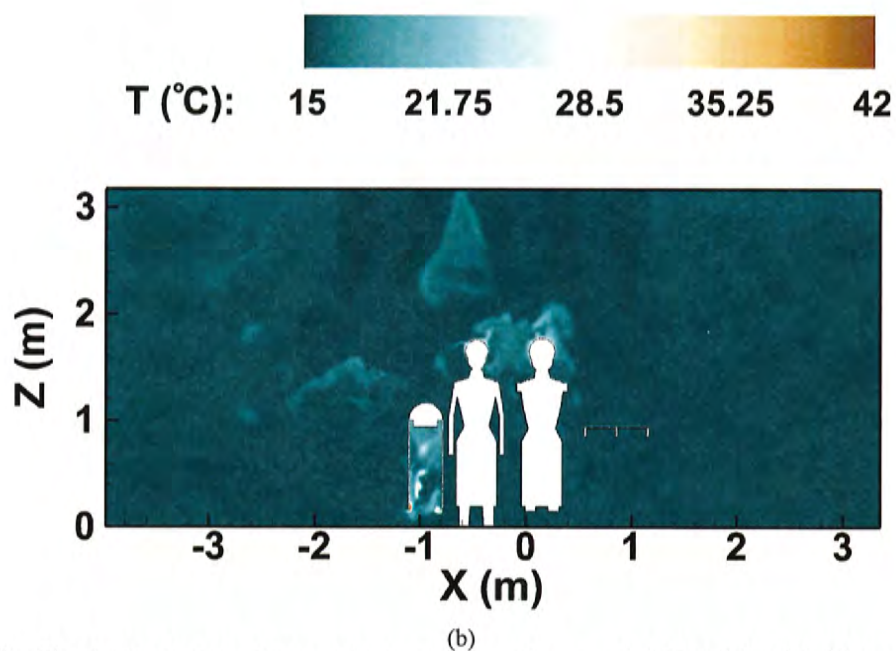
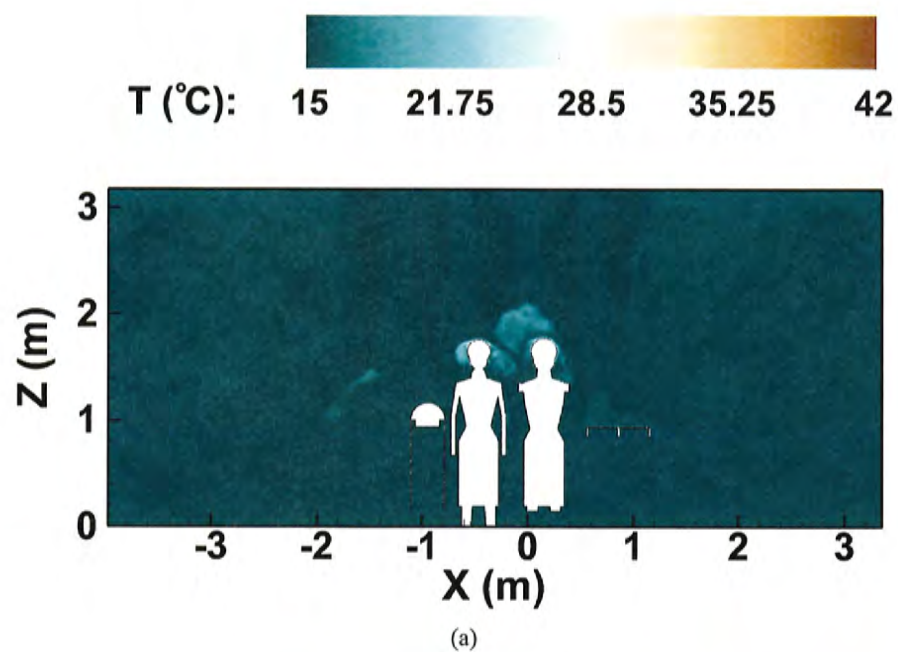


Figure 20: The instantaneous temperature contours at $y = -0.162\text{m}$ (a) with blower-off and (b) with blower-on. These snapshots are at about 35s after a stationary flow field was obtained and calculation for flow statistics was initiated.

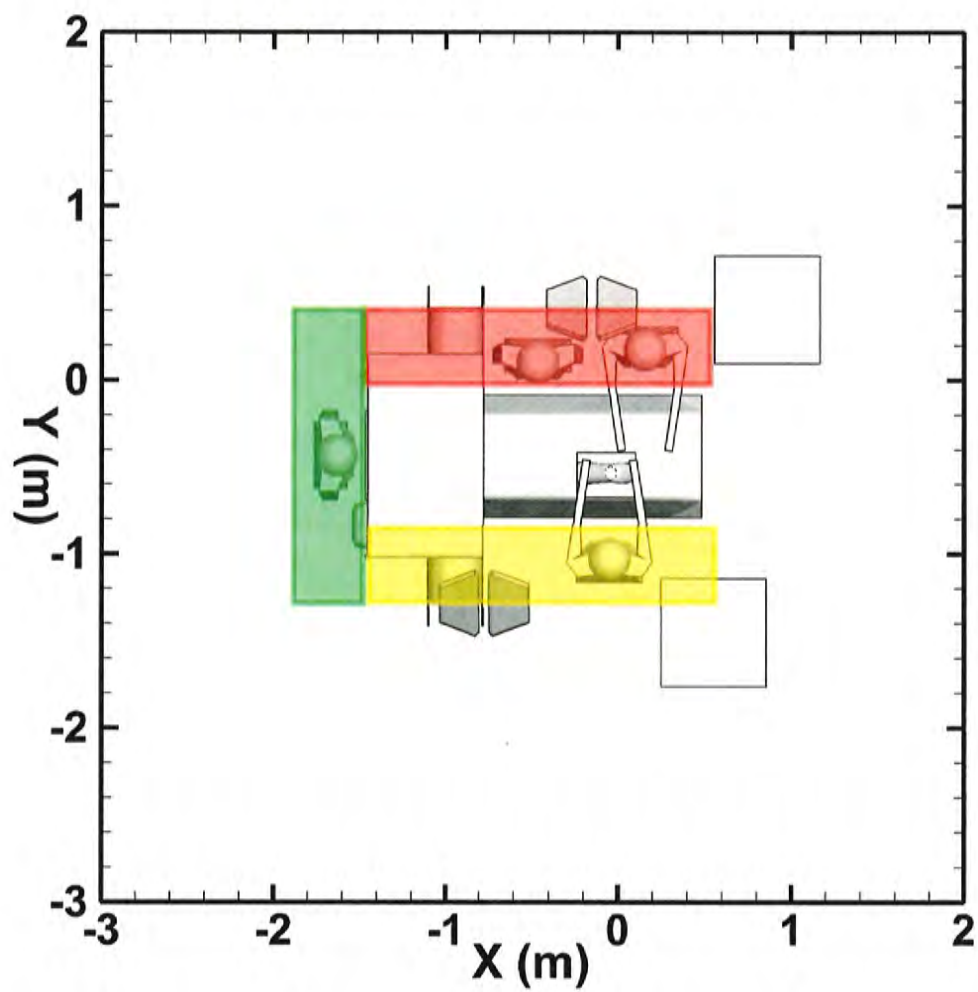


Figure 21: Three color-coded regions where the 3 million squames were initially distributed within a 1 cm height from the floor.

from different initial locations, the U-shaped region is divided into three rectangular sections color-coded as (i) red, (ii) green and (iii) yellow as shown in figure 21. One million squames are placed in each of the three sections at the same time, providing equal probability for the statistical analysis of motion of squames. The position of an individual squame particle in a section is chosen randomly using a uniform distribution. The squames of each section are tagged with distinct IDs. The actual coordinates of the three sections are given in Table 3.

4.2.2 Trajectories and snapshots of squames

In order to visualize the effect of the hot blower air on the trajectory of squames, instantaneous scatter plots of squames are displayed at 10s and 20s after their initiation with blower-off and blower-on in figures 22a,b and 23a,b, respectively. The squames are also color-coded based on their region of origin as highlighted in figure 21. Drastic differences between the blower-off and blower-on cases are observed. It is clear from figures 23a that the majority of the squames are dispersed by the ventilation air flow towards the outlet grilles when the blower is off. None of the squames actually rise to the level of the side tables or the OT. In contrast, in the case of blower-on, a large number of squames are lifted upwards by the rising thermal plumes. Some of the squames (mostly red-colored and some yellow-colored) are lifted above the surgeons heads and are blown towards the OT by the incoming ventilation air. Large number of squames are seen to be above the OT, several are surrounding the surgeons hands, above the side tables, and some are very close to the patient's knee and the surgical site. This is better visualized by the zoom-in view shown in figures 24a,b.

Figures 25, 26, and 27 show a different view angle for the squames at the same time instances as in the above discussion. It is again seen that with the blower-on several particles are lifted upwards by the thermal plumes and rise above the operating table and then are blown downwards by the incoming ventilation air.

Finally, figure 28 shows an instantaneous snapshot of squames very close to the patient's knee. It is seen that several of the red-coded particles are near the bottom of the knee, whereas some yellow-coded particles are in the very close vicinity of the surgical site. Several particles are still suspended above the OT and are being transported downwards by the ventilation air and may potentially reach close to the surgical site.

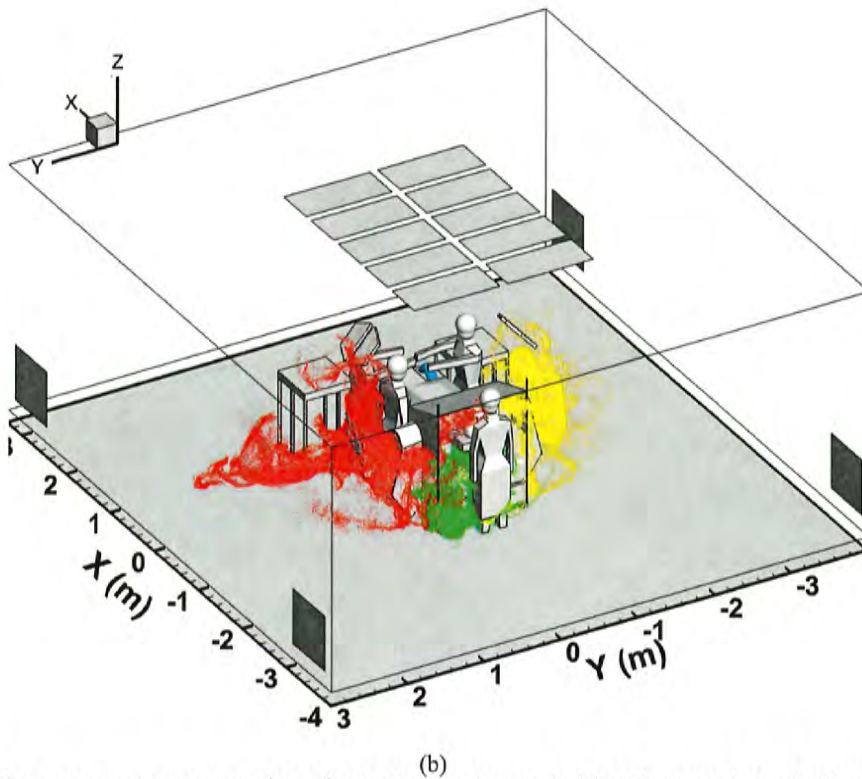
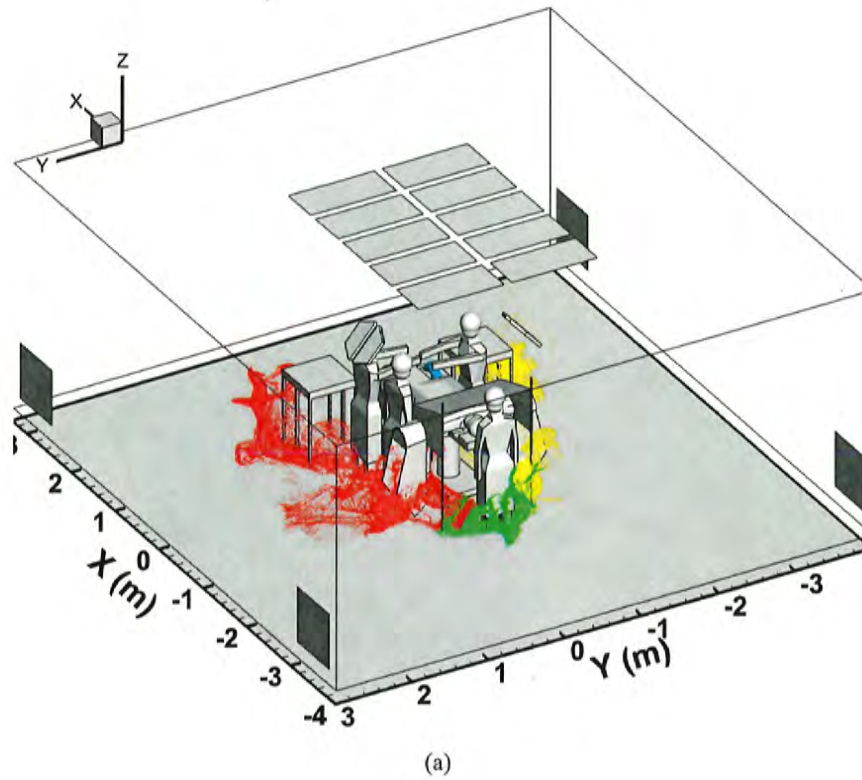


Figure 22: Instantaneous scatter plot of squames color-coded by their region of origin at 10s after initiation: (a) blower-off, (b) blower-on.

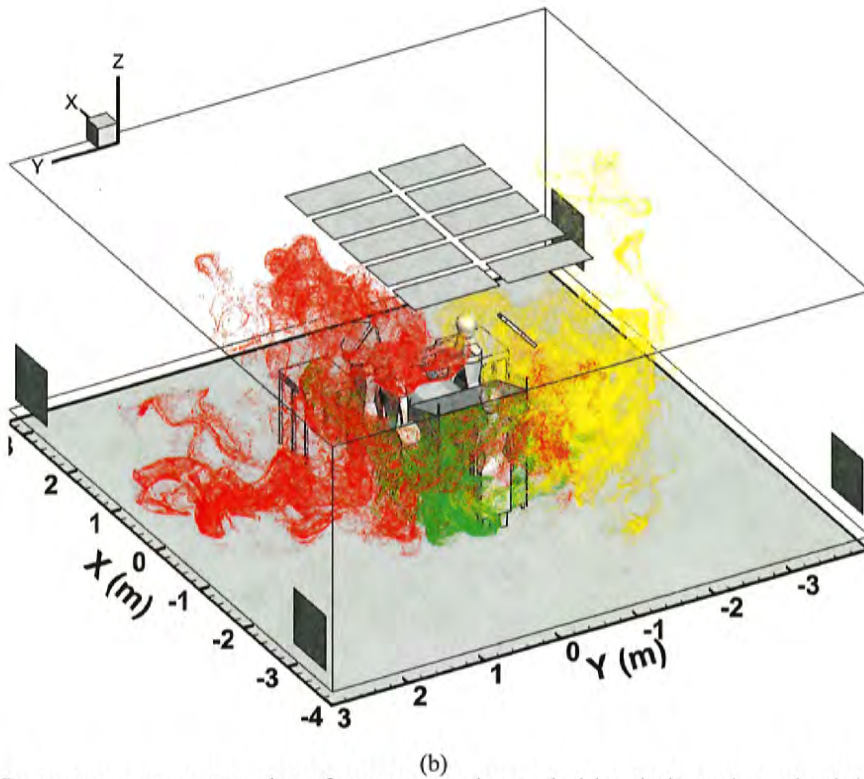
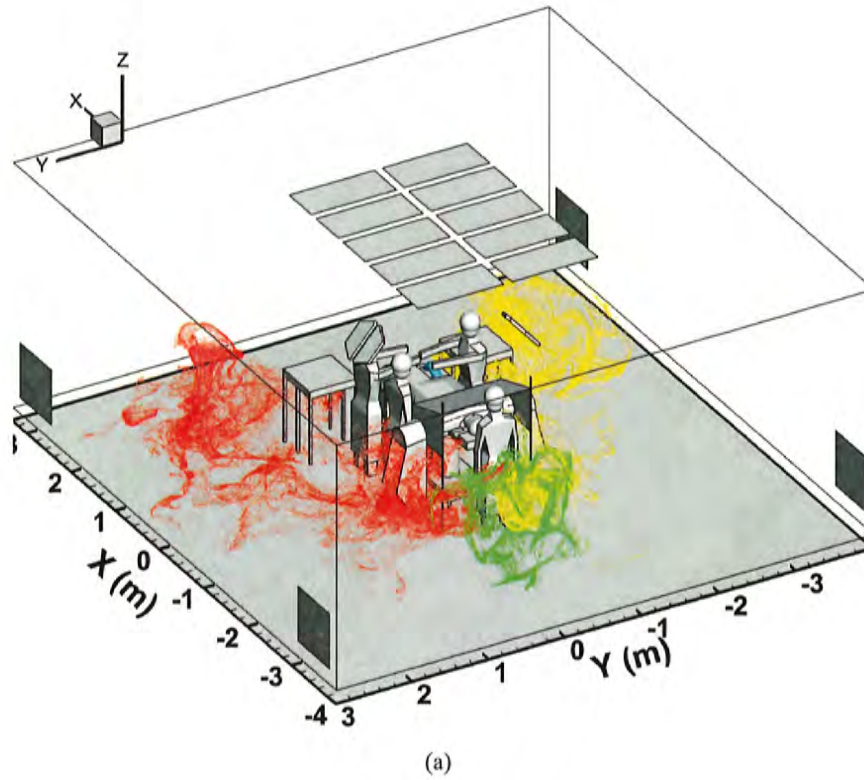
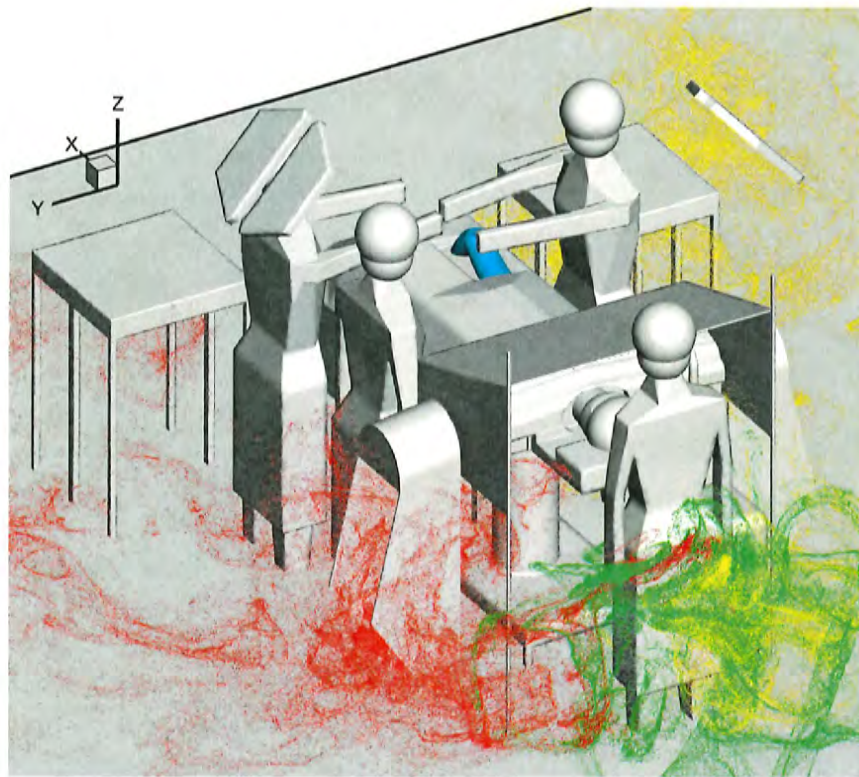
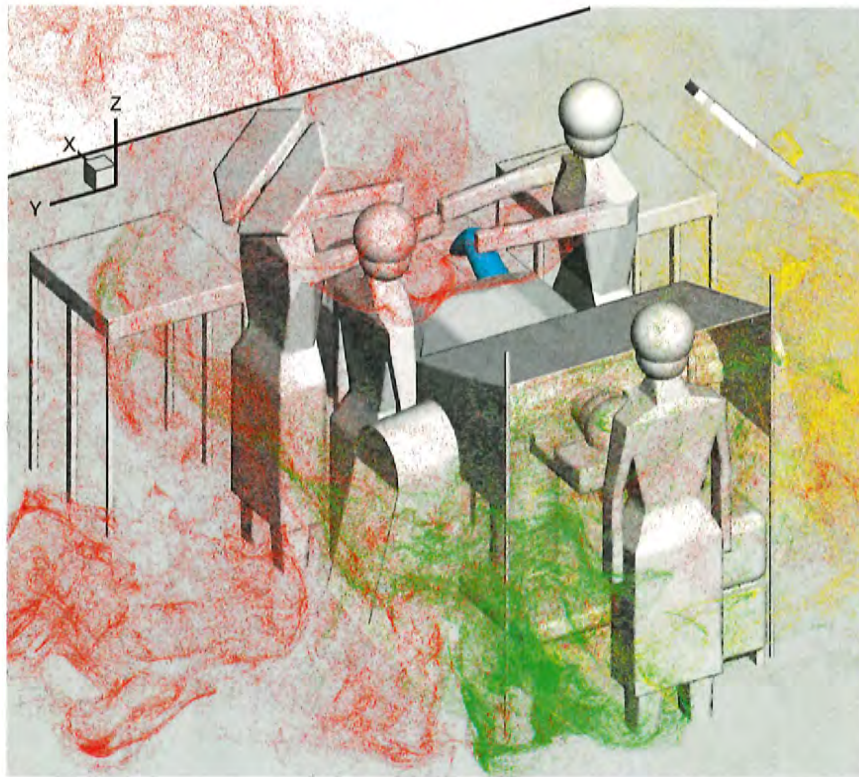


Figure 23: Instantaneous scatter plot of squames color-coded by their region of origin at 20s after initiation: (a) blower-off, (b) blower-on.



(a)



(b)

Figure 24: Zoom-in of the instantaneous scatter plot of squames color-coded by their region of origin at 20s after initiation: (a) blower-off, (b) blower-on.

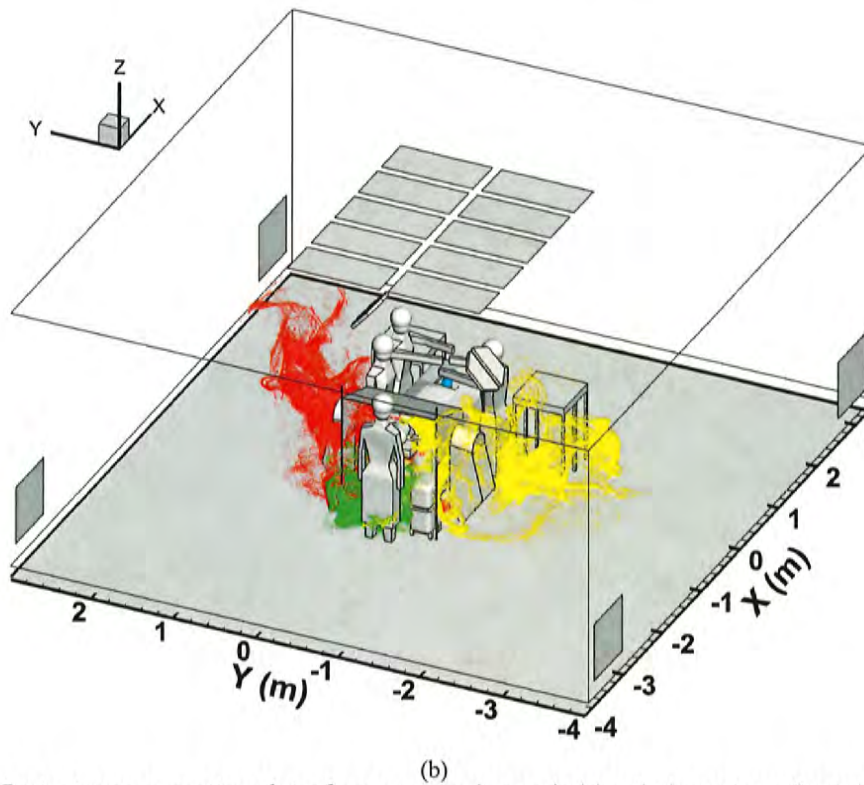
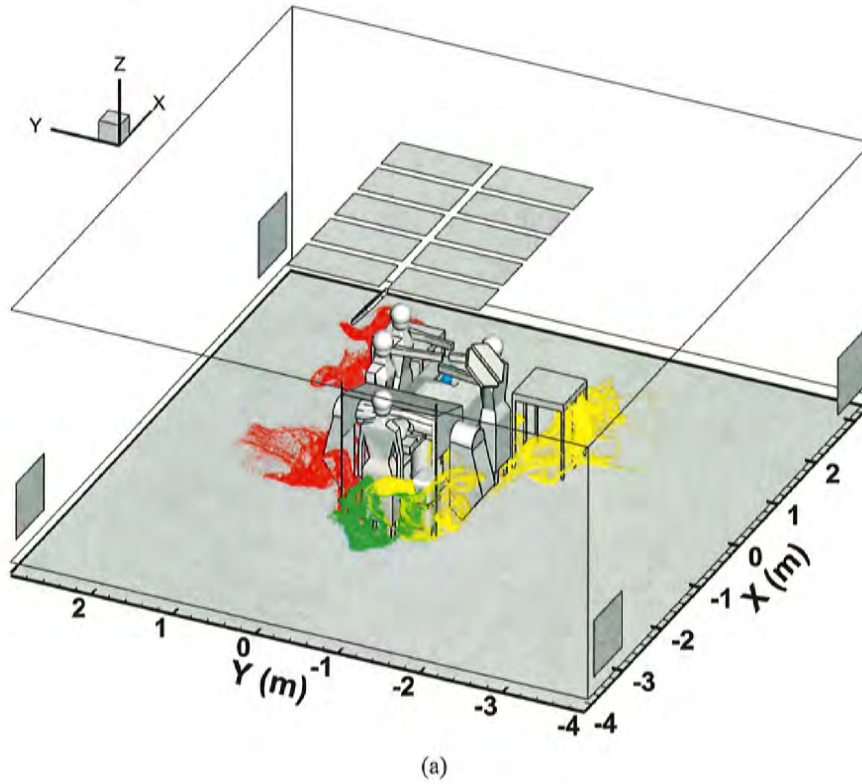


Figure 25: Instantaneous scatter plot of squames color-coded by their region of origin at 10s after initiation: (a) blower-off, (b) blower-on.

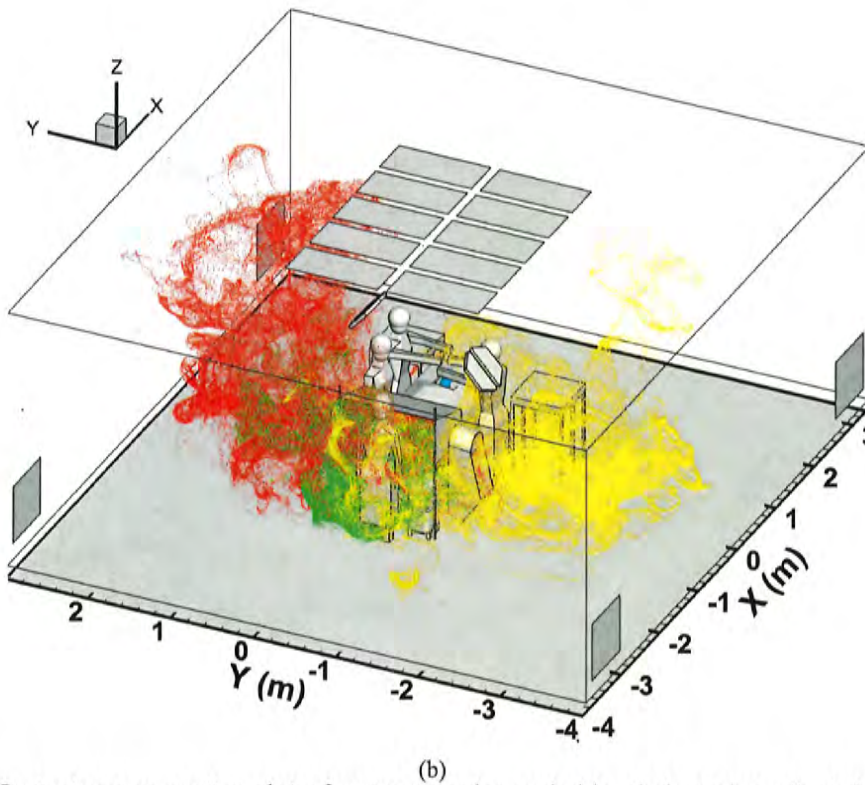
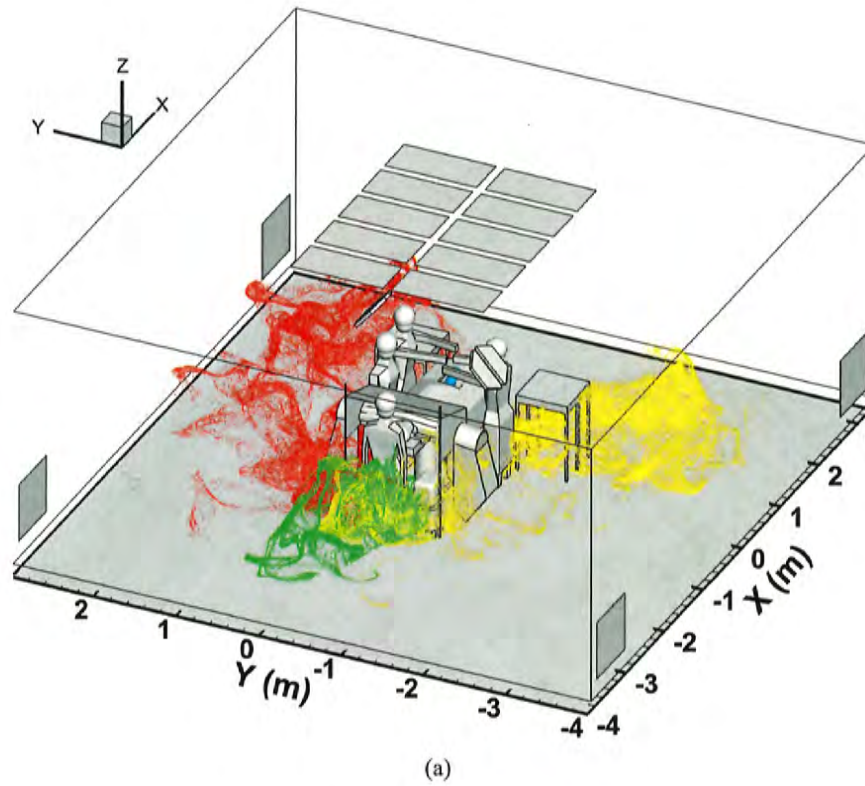
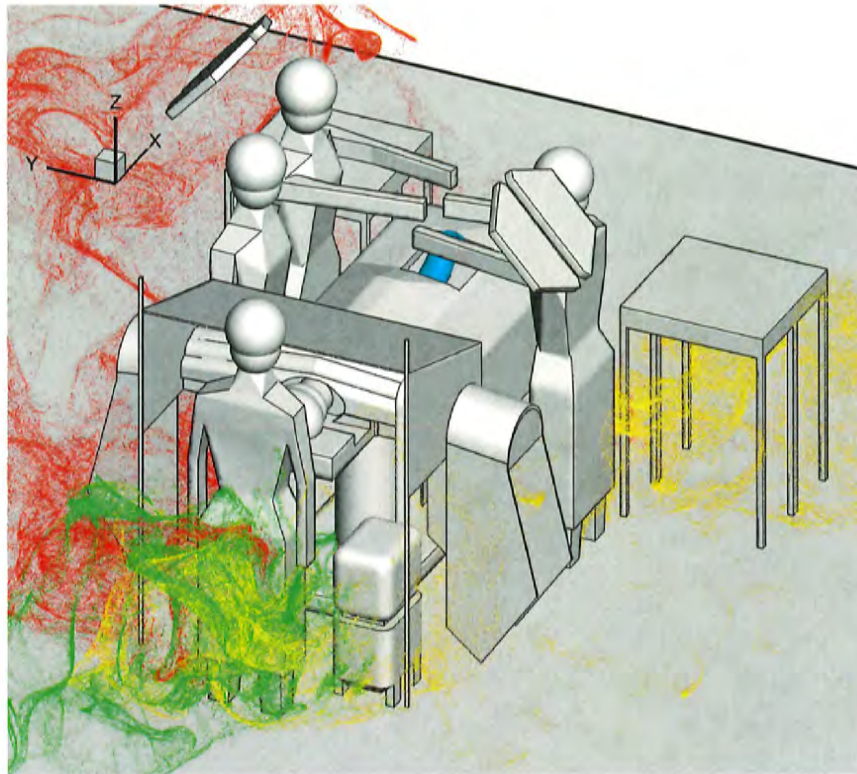
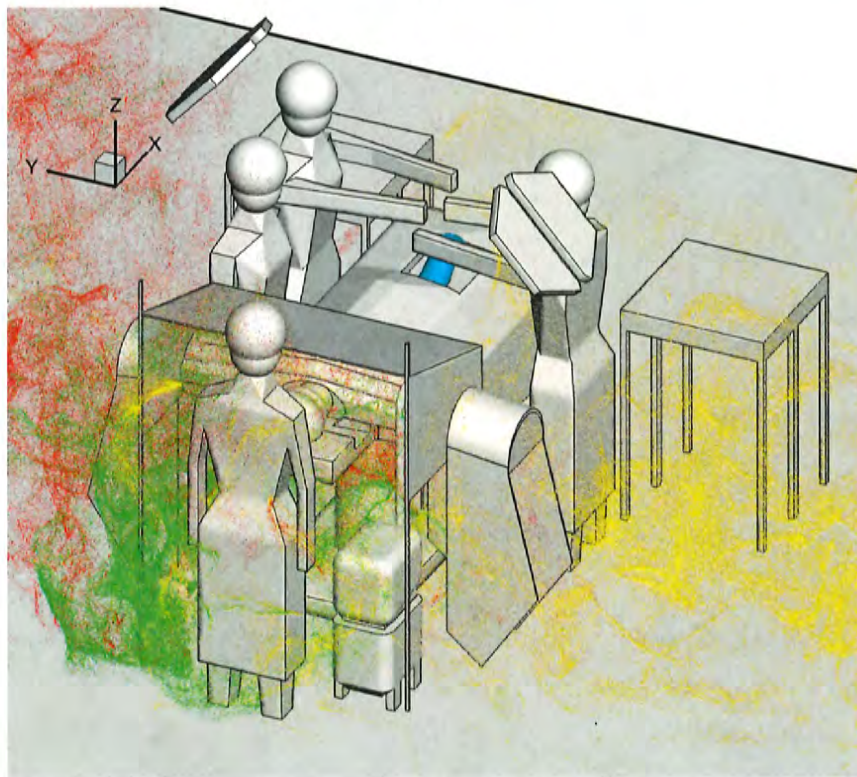


Figure 26: Instantaneous scatter plot of squames color-coded by their region of origin at 20s after initiation: (a) blower-off, (b) blower-on.



(a)



(b)

Figure 27: Zoom-in of the instantaneous scatter plot of squames color-coded by their region of origin at 20s after initiation: (a) blower-off, (b) blower-on.

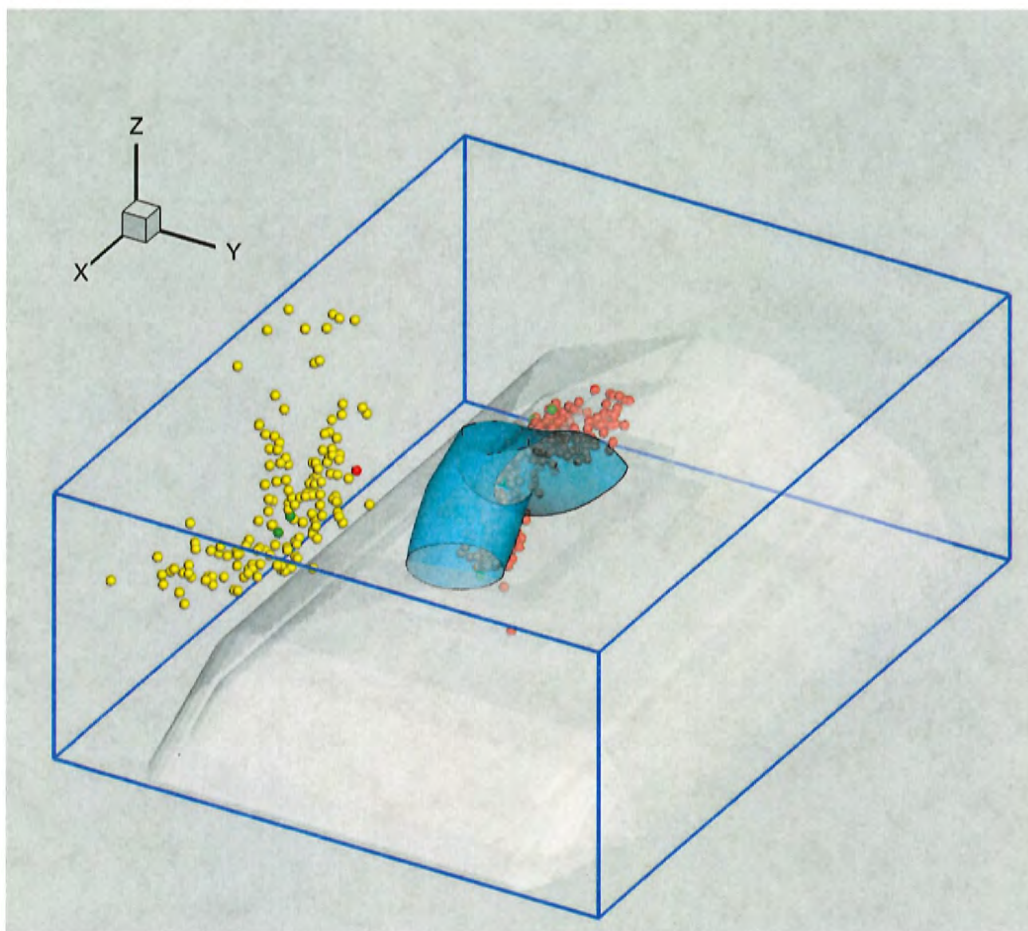


Figure 28: Zoom-in showing the instantaneous snapshot of squames near the surgical site at $t = 27s$.

4.2.3 Number density of squames in the regions of interest

To assess the probability of squames reaching the surgical site, four imaginary boxes were located as follows: two boxes covering the two side tables, a box around the OT, and a box around the patient's knee area. The surgeons and medical assistants are bound to use surgical instruments placed on the side tables. The possibility of squames reaching the surgical site is then dependent on the number density of squames within these four imaginary boxes (see figure 29). The number of squame particles inside the four boxes are recorded in time. A blue box (figure 29 (a) and (c)) is covering the whole OT. The top of this box is about 30 cm high, including the patient's whole body and the surgeons hands. An orange box (figure 29 (b) and (d)) is placed above the OT, just covering the patient's knee and part of the surgeon's hands; and the top of the box is only 2 cm above the surgeon's hands. One purple box (figure 29 (a) - (d)) is placed on each of the two side tables. The height of these boxes is about 1 cm, so that any surgical instrument placed on the side tables would be within the box.

Two computations of the trajectories of squames were performed after a statistically stationary flow field has been reached for the cases of blower-off and blower-on. Based on the average inlet air velocity and the height of the room, it takes 15 – 20s for a fluid particle to travel from the ceiling grille to the floor. First, the blower is turned off and only the ventilation air from the inlet grilles and thermal plumes created by the warm surfaces including surgical lights, surgeons' heads, patient's head, and patient's knee are responsible for the dispersion of squames. It was found that all the squames initiated in all three sections (red, green and yellow) are basically transported by the air flow reaching the floor and quickly dispersed to the for outlet grilles. After a calculation of about 25s of physical time, some squame particles do rise to the underside of the side tables, but none of the squames was found to enter the four imaginary boxes representing the regions of interest. It was concluded that without the hot air discharged from the blower, the ventilation air circulation alone cannot disperse the squames to the surgical site. The thermal plumes from various warm surfaces only slightly affect the air coming from the inlet grilles and do not affect the motion of the squames.

With the blower turned on, computations were carried out for about 30s of physical time to obtain a flow field with well established thermal plumes created by the hot air discharged from the blower. After reaching a stationary state, the squames were initiated in the same color-coded sections and the

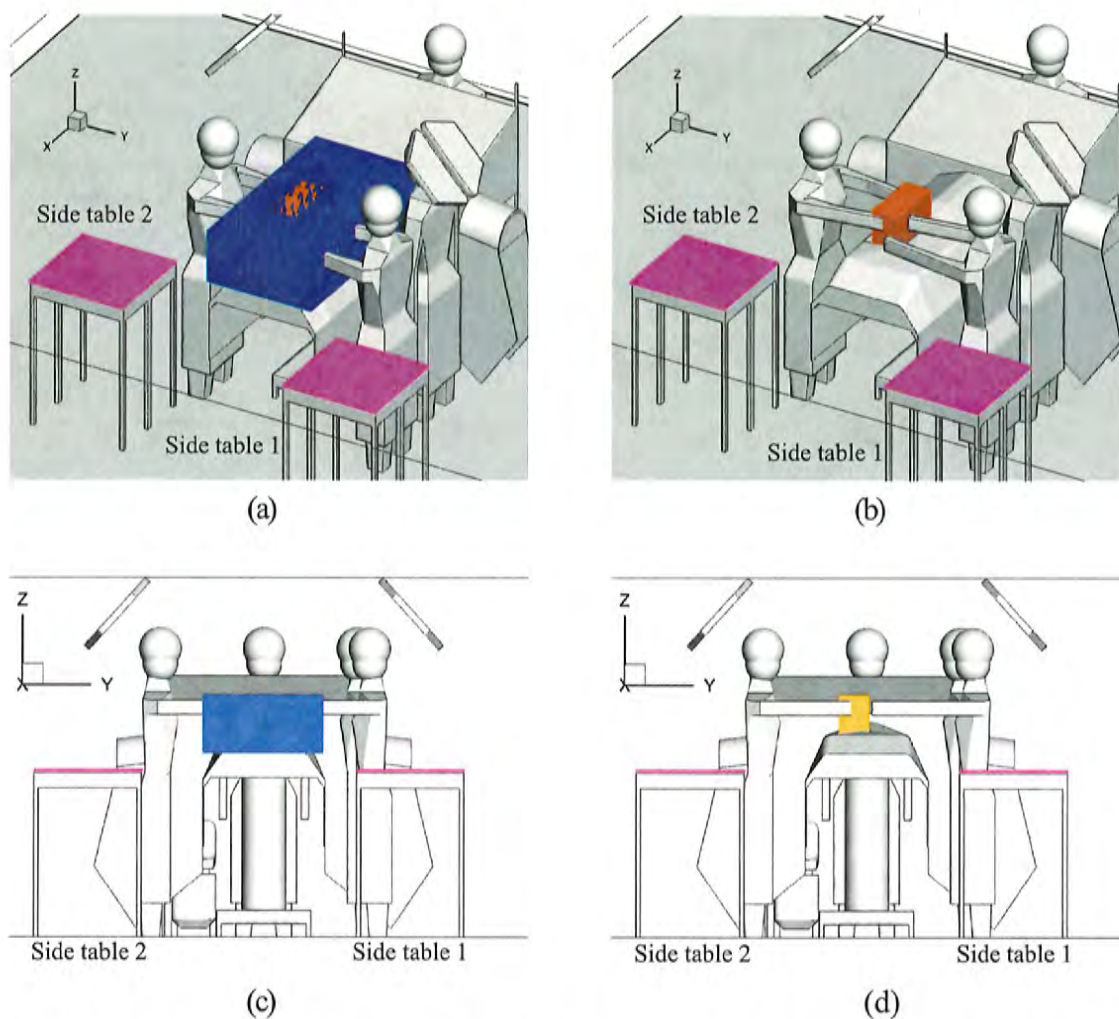
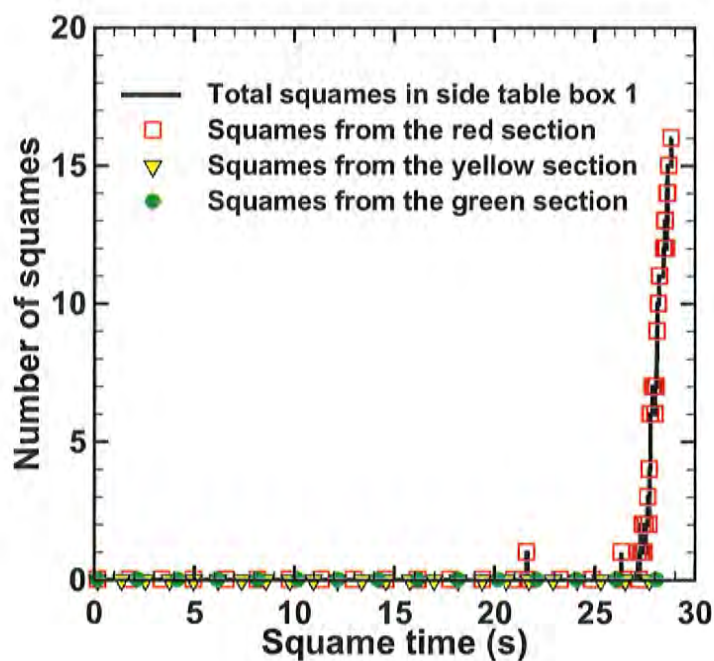


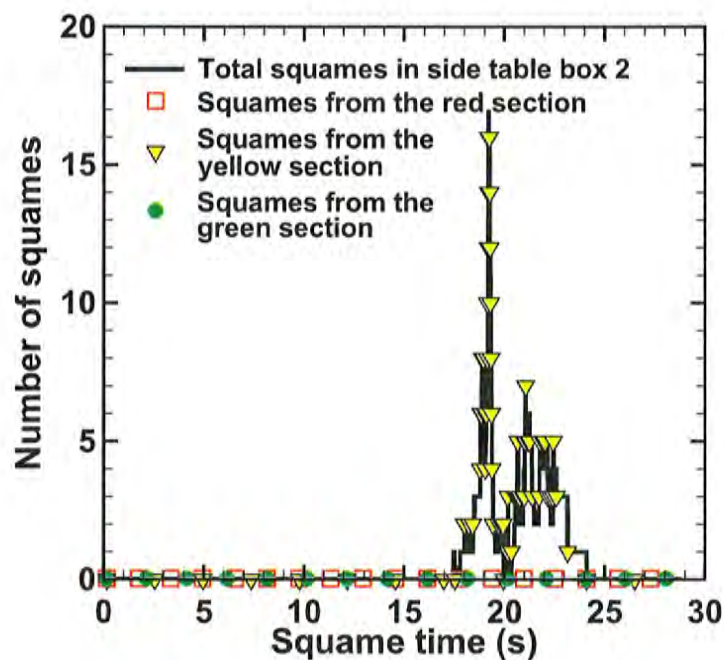
Figure 29: Four color-coded regions of interest, for recording the temporal history of the number of squames reaching them, shown in different views (a–d). The regions of interest include the zones above the two side tables, above the OT, and above the patient’s knee.

computation continued for another 30s. With the blower on, hot air is discharged through the sides covering the patient's arms into the ambient air and strong thermal plumes rise under the operating table. Some of the edges of the drape are very close to the floor (see figure 4b) and the hot air plume drags squames with it making them rise upwards faster than in the case when the blower was off. A majority of the squame particles are transported away from the table towards the outlet grilles. However, a statistically significant number of particles are lifted above the operating table with some even reaching the height of the surgeons. The particles rise due to buoyancy and then get flushed down onto the operating table by the incoming ventilation air from the inlet grilles. The particles then do enter the imaginary boxes of interest, specifically above the operating table and the patient's knee.

Figures 30 and 31 show the number of squame particles as a function of time entering the four imaginary boxes of interest (above the side tables, above the operating table, and patient's knee). It can be seen from Figure 31b that no particles are found inside these boxes for the first 17s, which is about the time needed for the ventilation air to travel from the ceiling to the floor. After this time, the number of squame particles in the box above the OT increases almost in a linear fashion. Within 30s of physical time, the number of squame particles within the OT box are about 2500 and increasing. Figure 31a shows that at about 23s, some of the particles above the OT start to enter the box above the knee, which is a very narrow zone surrounding the patient's knee. The number of these particles increases linearly to about 600. Note that some of these particles do get trapped at the knee, some are carried away by the air flow and hence the number appears to be decreasing after about 25s. From the instantaneous snapshot of the squames shown in figures 24b and 27b, it can be seen that several particles are still above the OT and moving downward due to the air from the inlet grilles. It is thus expected that more particles will enter the box above the patient's knee, potentially raising the probability of infection. It is also interesting to note that the squame particles entering the box above the OT and above the knee are mainly the red-colored particles initiated from the side of the table with two surgeons. Owing to the asymmetry in the CAD model geometry, the flow pattern around each side of the table is different and the recirculation region created by the incoming air from the inlet grilles is also asymmetric. The rise and eventual trapping of the squames within the knee box is thus also related to which side of the table it originated from. The boxes above the side tables also entrain about 15 squame particles as can be seen from figures 30a,b. This suggests that

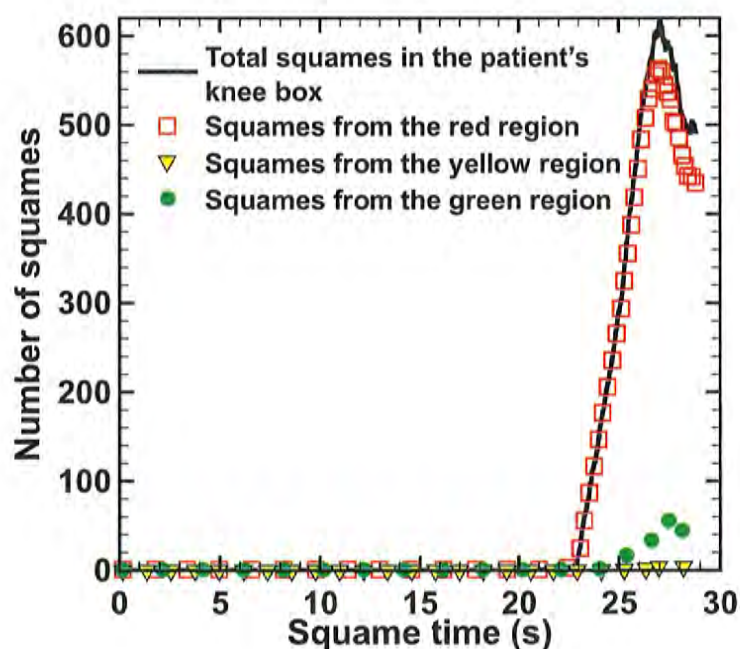


(a)

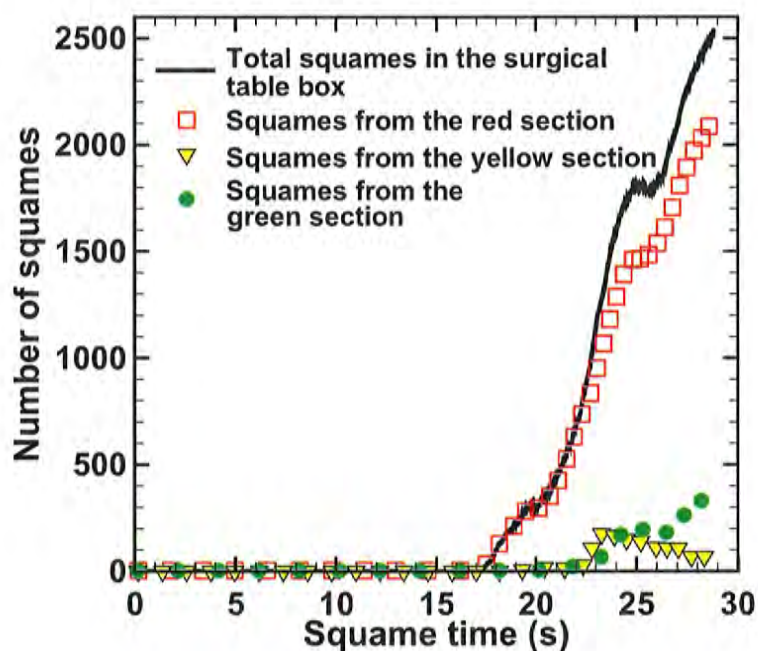


(b)

Figure 30: Temporal history of the total number of squames (shown by black color) entering four different regions of interest: (a) side table box 1, and (b) side table box 2. Also shown in color is the number of color-coded squame particles entering from the red, green and yellow regions of the figure 21.



(a)



(b)

Figure 31: Temporal history of the total number of squames (shown by black color) entering four different regions of interest: (a) the patient's knee area, and (b) the OT box. Also shown in color is the number of color-coded squame particles entering from the red, green and yellow regions of the figure 21.

753 the surgical instruments on the side tables also have a small probability of carrying squames to the
754 surgical site.

755 **5 Summary and Concluding Remarks**

756 A high-fidelity, large-eddy simulation (LES) was performed to study the interaction of the operat-
757 ing room (OR) ultra-clean ventilation air flow and the flow created by a forced air warming system
758 (3MTM Bair HuggerTM blower) and its impact on the dispersion of squames particles. A full three-
759 dimensional design of an OR with operating table (OT), surgical lamps, medical staff, side tables,
760 a blower, and a patient undergoing knee surgery was constructed. Unstructured grid elements in-
761 volving hexahedra, tetrahedra, pyramids and wedges were used to capture the complex geometry of
762 the OR. An arbitrary shaped, unstructured grid flow solver for LES based on governing equations
763 for variable density in the limit of zero-Mach number was used. Ultraclean ventilation air enters the
764 OR through 10 ceiling grilles with air changes per hour (ACH) of 24.45 and flow Reynolds num-
765 ber, based on the air inlet grille size and mean air inlet velocity, of 9226. The air inlet flow was
766 developed from a periodic duct flow with the required target mass flow rate for each grille. No-slip
767 conditions were applied for all solid surfaces and convective outflow condition was used at the four
768 outlet grilles. Temperature values were specified at the surfaces of inlet grilles, the surgical lamps,
769 heads of the medical staff, patient's head, and patient's knee and all other boundary surfaces were
770 assumed adiabatic. Computations were performed on 1600 processors in parallel and flow statistics
771 involving the time-averaged mean velocity field, turbulence intensity, and temperature distribution
772 were computed.

773 Two computations were performed with the blower-off and blower-on to calculate a three-
774 dimensional, time-dependent flow within the OR. Rising thermal plumes from the warm surfaces
775 of surgeons heads, the patient's knee, patient's head, and the surgical lamp were calculated. With
776 the blower on, air was drawn from the floor of the OR, heated, and blown into a blanket that covers
777 the torso region of the patient. The blanket was covered with a plastic drape. The blower hot air
778 generated forced convective currents and strong thermal plumes that interacted with the ultra-clean
779 ventilation air. For both cases, trajectories of 3 million squames, placed initially on the floor in a
780 small region surrounding the OT and surgeons, were calculated and contrasted to quantify the effect

of the hot air blower. The squames particles were assumed to be spherical in shape with 10 micron diameter and density of liquid water. The particle trajectories were tracked in a Lagrangian frame by computing the drag, lift, and buoyancy forces. The temporal variations of the number of squames particles within four imaginary boxes placed strategically above the two side tables, over the OT, and one surrounding the patient's knee were calculated and contrasted between the blower-off and blower-on cases. The following main conclusions can be drawn from these predictive computations:

1. For the case of blower-off, the ventilation air from the ceiling inlet grilles moves downwards, then is deflected by the surgical lights and the table, impinges on the floor farther away from the OT, and finally exits through the outlet grilles. Large recirculation regions are created on both sides of the table. The flow is not symmetric owing to asymmetries in the configuration of the OR contents. The maximum turbulence intensity level is about 30% in the high shear regions between the inlet air streams and the initial stagnant air in the OR, as well as near the warm surgical lights due to the buoyant plume. It is observed that the buoyant plumes from the patient's knee and other warm surfaces are relatively weak, and do not significantly alter the mean ventilation air flow.
2. For the case of blower-on, the mean flow underneath and around the OT is significantly modified and large levels of turbulence intensity are observed under the OT. The turbulence intensity levels are as high as 60% in regions affected by the rising thermal plumes from the blower. The instantaneous temperature contours confirm that the increased turbulence level is mainly because of the thermal plumes from the hot blower air causing higher temperature regions under the OT in comparison with the blower-off case. The flow is also highly asymmetric owing to the orientation and location of the drape. The rising thermal plumes are even observed to reach the ceiling in some regions and the downward ventilation flow from the inlet grilles was modified above the OT which also affected the recirculation region.
3. Drastic differences in the trajectories of the squames are observed between the blower-off and blower-on cases. With the blower-off, the majority of the squames are dispersed by the ventilation air flow towards the outlet grilles. None of the squames actually rise to the level of the side tables or the OT. In contrast, with the blower-on, a large number of squames are lifted upwards by the rising thermal plumes. Some of the squames are lifted above the surgeons

heads and are blown towards the OT by the downward moving ventilation air. Large number of squames are seen to be above the OT, several are surrounding the surgeons hands, above the side tables, and some are very close to the patient's knee and the surgical site. Majority of the squames that come close to the surgical site were found to have originated from the sides parallel to the length of the OT.

4. With the blower off, none of the squames particles were found to enter the four imaginary boxes placed above the side tables, OT, and a region surrounding the patient's knee. Some particles are lifted from the floor over time, but none rise close to the level of the imaginary boxes as the downward flow due to the ventilation air keeps the particles closer to the floor. With the blower turned on, hot air discharged from the edges of the drape and the resultant thermal plumes drag the squames, making them rise upwards. Some of the squames rise above the surgeons heads in the recirculation region on the sides of the OT. These particles are then flushed down onto the OT by the ventilation air from the inlet grilles. Statistically significant particles do enter the imaginary boxes of interest above the operating table and the patient's knee. Few particles are also observed above the side tables.

Starting with the worst-case scenario of having squames on the floor, it was shown that the hot air from the blower and the resultant thermal plumes are capable of lifting the particles and transporting them to the side tables, above the operating table, and the surgical site. It should be emphasized that if we also include the repetitive motion of the surgeons, the motion of medical assistants to fetch the surgical instruments placed on the side tables, and the resulting suspended squames shed by all staff in the OR, then the probability of dispersing the squames to the surgical site will be increased even further.

Although computationally intensive, large-eddy simulation of convective ventilation air flow and hot air from the blower in an OR is necessary to provide reliable predictions of the turbulent flow and dispersion of squames.

Appendix A

The aerodynamic behavior of squames suspended in a fluid is in general dependent upon the size and shape of the squames, their density, relative velocity with respect to the fluid motion, and density of the fluid. In the present study, the squames are suspended in air at room temperature (density ρ_g). The human skin cells or squames typically are disc-shaped with a diameter ranging from 4–20 μm and a thickness of 3–5 μm with density close to that of liquid water ($\rho_p = 1000 \text{ kg/m}^3$) (Noble *et al.*, 1963; Noble, 1975; Snyder, 2009).

Settling of a squame particle depends on its weight, the drag and buoyancy force on the particle, and its orientation relative to the flow direction. Owing to the changes in orientation and also resultant rotation and torque on disc particles, computing large number of trajectories in a Lagrangian frame is complicated. It is thus easier to assume these particles of spherical shape with an equivalent diameter such that their aerodynamic characteristics are matched. An equivalent diameter of the spherical particle should be calculated by matching the settling velocities for the two shapes.

Since $\rho_p/\rho_g = 1000$, the buoyancy force is much smaller compared to the weight of the particle. Then the settling velocity can be obtained from the balance of drag and gravitational forces,

$$F_d = F_g. \quad (24)$$

The drag and gravitational forces on a disc-shaped particle are given as,

$$F_d = C_{d,\text{disc}} \frac{1}{2} \rho_g U_{\text{disc}}^2 A_p, \quad (25)$$

$$F_g = (A_p h_{\text{disc}}) \rho_p g; \quad A_p = \frac{\pi}{4} D_{p,\text{disc}}^2 \quad (26)$$

where U_{disc} is the settling velocity of the disc, $C_{d,\text{disc}}$ is the drag coefficient, A_p is the frontal area of the circular disc, g is the gravitational acceleration, $D_{p,\text{disc}}$ is the diameter, and h_{disc} is the thickness of the disc. Equating the drag force to the weight of the disc to obtain the settling velocity as,

$$U_{\text{disc}} = \sqrt{2g \left(\frac{\rho_p}{\rho_g} \right) \left(\frac{h_{\text{disc}}}{C_{d,\text{disc}}} \right)}. \quad (27)$$

Following similar procedure, the settling velocity of a sphere of diameter $D_{p,\text{sphere}}$ can be ob-

tained as,

$$U_{\text{sphere}} = \sqrt{\frac{4}{3}g \left(\frac{\rho_p}{\rho_g} \right) \left(\frac{D_{p,\text{sphere}}}{C_{d,\text{sphere}}} \right)}, \quad (28)$$

853 where $C_{d,\text{sphere}}$ is the drag coefficient on a spherical particle.

854 In order to match the aerodynamic performance of the two shapes, the two settling velocities
855 should be the same. Equating U_{disc} and U_{sphere} we get,

$$D_{p,\text{sphere}} = \frac{3}{2}h_{\text{disc}} \left(\frac{C_{d,\text{sphere}}}{C_{d,\text{disc}}} \right). \quad (29)$$

For Stokes flow ($Re \leq 1$), the drag coefficients are given as (Munson *et al.*, 1990),

$$C_{d,\text{sphere}} = \frac{24}{Re} \quad (30)$$

$$C_{d,\text{disc}} = \frac{20.4}{Re}, \quad \text{flow normal to circular disc} \quad (31)$$

$$= \frac{13.6}{Re}, \quad \text{flow parallel to circular disc.} \quad (32)$$

856 Using a disc thickness of $h_{\text{disc}} = 5\mu\text{m}$, and using the drag coefficients for the disc and the sphere,
857 equation (29) gives an equivalent spherical diameter in the range of $D_{p,\text{sphere}} = 8.78$ and $13.2\mu\text{m}$.
858 Thus, an assumption of 10 micron spherical particle is reasonable to obtain similar dispersion be-
859 havior on an average as that of the disc-shaped squames particles.

References

- ALBRECHT, MARK, GAUTHIER, ROBERT L, BELANI, KUMAR, LITCHY, MARK & LEAPER, DAVID 2011 Forced-air warming blowers: An evaluation of filtration adequacy and airborne contamination emissions in the operating room. *American journal of infection control* **39** (4), 321–328.
- APTE, SV, GOROKHOVSKI, M. & MOIN, P. 2003a LES of atomizing spray with stochastic modeling of secondary breakup. *International Journal of Multiphase Flow* **29** (9), 1503–1522.
- APTE, SV, MAHESH, K. & LUNDGREN, T. 2008a Accounting for finite-size effects in simulations of disperse particle-laden flows. *International Journal of Multiphase Flow* **34** (3), 260–271.
- APTE, SV, MAHESH, K. & MOIN, P. 2008b Large-eddy simulation of evaporating spray in a coaxial combustor. *Proceedings of the Combustion Institute* **32**, accepted for publication.
- APTE, SV, MAHESH, K., MOIN, P. & OEFELEIN, JC 2003b Large-eddy simulation of swirling particle-laden flows in a coaxial-jet combustor. *International Journal of Multiphase Flow* **29** (8), 1311–1331.
- APTE, SOURABH V, MAHESH, KRISHNAN, GOROKHOVSKI, MICHAEL & MOIN, PARVIZ 2009 Stochastic modeling of atomizing spray in a complex swirl injector using large eddy simulation. *Proceedings of the Combustion Institute* **32** (2), 2257–2266.
- AUSTIN, PAUL N 2015 Guest editorial. *AANA journal* **83** (4), 237.
- CHEN, X-Q & PEREIRA, JCF 1998 Computation of particle dispersion in turbulent liquid flows using an efficient lagrangian trajectory model. *International journal for numerical methods in fluids* **26** (3), 345–364.
- CHOW, TIN-TAI & WANG, JINLIANG 2012 Dynamic simulation on impact of surgeon bending movement on bacteria-carrying particles distribution in operating theatre. *Building and Environment* **57**, 68–80.
- CLARK, RAYMOND P. & DE CALCINA-GOFF, MERVYN L. 2009 Some aspects of the airborne transmission of infection. *Journal of The Royal Society Interface* **6** (Suppl 6), S767–S782.

- 886 CROWE, CT, TROUTT, TR & CHUNG, JN 1996 Numerical models for two-phase turbulent flows.
887 *Annual Review of Fluid Mechanics* **28** (1), 11–43.
- 888 DRUZHININ, OA & ELGHOBASHI, S. 1998 Direct numerical simulations of bubble-laden turbulent
889 flows using the two-fluid formulation. *Physics of Fluids* **10**, 685.
- 890 EATON, JK & FESSLER, JR 1994 Preferential concentration of particles by turbulence. *Interna-
891 tional Journal of Multiphase Flow* **20**, 169–209.
- 892 EATON, J.K. & SEGURA, J.C. 2006 On momentum coupling methods for calculation of turbulence
893 attenuation in dilute particle-laden gas flows. *Fluid Mechanics and its Applications* **81**, 39.
- 894 ELGHOBASHI, S. 1994 On predicting particle-laden turbulent flows. *Flow, Turbulence and Com-
895 bustion* **52** (4), 309–329.
- 896 ELGHOBASHI, S. 2006 An updated classification map of particle-laden turbulent flows. *Fluid Me-
897 chanics and Its Applications* **81**, 3–10.
- 898 FERRANTE, A. & ELGHOBASHI, S. 2004 On the physical mechanisms of drag reduction in a spa-
899 tially developing turbulent boundary layer laden with microbubbles. *Journal of Fluid Mechanics*
900 **503**, 345–355.
- 901 FERRANTE, A. & ELGHOBASHI, S. 2007 On the accuracy of the two-fluid formulation in direct
902 numerical simulation of bubble-laden turbulent boundary layers. *Physics of Fluids* **19**, 045105.
- 903 GERMANO, MASSIMO, PIOMELLI, UGO, MOIN, PARVIZ & CABOT, WILLIAM H 1991 A dynamic
904 subgrid-scale eddy viscosity model. *Physics of Fluids A: Fluid Dynamics (1989-1993)* **3** (7),
905 1760–1765.
- 906 HAM, F., APTE, S., IACCARINO, G., WU, X., HERRMANN, M., CONSTANTINESCU, G., MA-
907 HESH, K. & MOIN, P. 2003 Unstructured LES of reacting multiphase flows in realistic gas turbine
908 combustors. Annual Research Briefs 2003. *Center for Turbulence Research, NASA Ames/Stanford*
909 *Univ* pp. 139–160.
- 910 HAM, FRANK & IACCARINO, GIANLUCA 2004 Energy conservation in collocated discretization
911 schemes on unstructured meshes. *Annual Research Briefs* **2004**, 3–14.

- 912 KELLAM, MELISSA D, DIECKMANN, LORAIN S & AUSTIN, PAUL N 2013 Forced-air warming
913 devices and the risk of surgical site infections. *AORN journal* **98** (4), 353–369.
- 914 KRAVCHENKO, AG & MOIN, PARVIZ 1997 On the effect of numerical errors in large eddy simu-
915 lations of turbulent flows. *Journal of Computational Physics* **131** (2), 310–322.
- 916 KULICK, JD, FESSLER, JR & EATON, JK 2006 Particle response and turbulence modification in
917 fully developed channel flow. *Journal of Fluid Mechanics Digital Archive* **277**, 109–134.
- 918 LEAPER, DAVID, ALBRECHT, MARK & GAUTHIER, ROBERT 2009 Forced-air warming: a source
919 of airborne contamination in the operating room? *Orthopedic reviews* **1** (2), 28.
- 920 LEES, JULIENNE & BRIGHTON, WD 1972 Simulated human skin scales. *Journal of Hygiene*
921 **70** (03), 557–565.
- 922 LEGG, AJ, CANNON, T & HAMER, AJ 2012 Do forced air patient-warming devices disrupt unidi-
923 rectional downward airflow? *J Bone Joint Surg Br* **94** (2), 254–256.
- 924 MAHESH, K., CONSTANTINESCU, G., APTE, S., IACCARINO, G., HAM, F. & MOIN, P. 2006
925 Large-eddy simulation of reacting turbulent flows in complex geometries. *Journal of Applied*
926 *Mechanics* **73**, 374.
- 927 MAHESH, K., CONSTANTINESCU, G. & MOIN, P. 2004 A numerical method for large-eddy sim-
928 ulation in complex geometries. *Journal of Computational Physics* **197** (1), 215–240.
- 929 MAXEY, MARTIN R & RILEY, JAMES J 1983 Equation of motion for a small rigid sphere in a
930 nonuniform flow. *Physics of Fluids (1958-1988)* **26** (4), 883–889.
- 931 MCGOVERN, PD, ALBRECHT, M, BELANI, KG, NACHTSHEIM, C, PARTINGTON, PF, CAR-
932 LUKE, I & REED, MR 2011 Forced-air warming and ultra-clean ventilation do not mix. *J Bone*
933 *Joint Surg Br* **93** (11), 1537–1544.
- 934 MCNEILL, JAMES, HERTZBERG, JEAN & ZHAI, ZHIQIANG JOHN 2013 Experimental investiga-
935 tion of operating room air distribution in a full-scale laboratory chamber using particle image
936 velocimetry and flow visualization .

- 937 MCNEILL, JAMES S *et al.* 2012 Field measurements of thermal conditions during surgical proce-
 938 dures for the development of cfd boundary conditions. *ASHRAE Transactions* **118**, 596.
- 939 MEMARZADEH, FARHAD 2003 Reducing risks of surgery. *ASHRAE journal* **45** (2), 28.
- 940 MEMARZADEH, FARHAD & MANNING, ANDREW P 2002 Comparison of operating room ventila-
 941 tion systems in the protection of the surgical site/discussion. *ASHRAE transactions* **108**, 3.
- 942 MITTAL, RAJAT & MOIN, PARVIZ 1997 Suitability of upwind-biased finite difference schemes for
 943 large-eddy simulation of turbulent flows. *AIAA journal* **35** (8), 1415–1417.
- 944 MOIN, P. & APTE, SV 2006 Large-eddy simulation of realistic gas turbine combustors. *AIAA Jour-
 945 nal* **44** (4), 698–708.
- 946 MOIN, P. & MAHESH, K. 1998 Direct numerical simulation: A tool in turbulence research. *Annual
 947 Reviews in Fluid Mechanics* **30** (1), 539–578.
- 948 MOIN, P., SQUIRES, K., CABOT, W. & LEE, S. 1991 A dynamic subgrid model for compressible
 949 turbulence and scalar transport. *Physics of Fluids A*, **3**, 2746–2757.
- 950 MORETTI, B, LAROCCA, AMV, NAPOLI, C, MARTINELLI, D, PAOLILLO, L, CASSANO, M,
 951 NOTARNICOLA, A, MORETTI, L & PESCE, V 2009 Active warming systems to maintain pe-
 952 rioroperative normothermia in hip replacement surgery: a therapeutic aid or a vector of infection?
 953 *Journal of Hospital Infection* **73** (1), 58–63.
- 954 MUNSON, BRUCE ROY, YOUNG, DONALD F & OKIISHI, THEODORE H 1990 Fundamentals of
 955 fluid mechanics. *New York* **3** (4).
- 956 NG, V, LAI, A & HO, V 2006 Comparison of forced-air warming and electric heating pad for
 957 maintenance of body temperature during total knee replacement. *Anaesthesia* **61** (11), 1100–1104.
- 958 NOBLE, WC 1975 Dispersal of skin microorganisms. *British Journal of Dermatology* **93** (4), 477–
 959 485.
- 960 NOBLE, WC, LIDWELL, OM, KINGSTON, D *et al.* 1963 The size distribution of airborne particles
 961 carrying micro-organisms. *J Hyg (Lond)* **61** (385), e391.

- 962 PEREIRA, MARCELO LUIZ & TRIBESS, ARLINDO 2005 A review of air distribution patterns in
 963 surgery rooms under infection control focus. *Revista de Engenharia Térmica* **4** (2).
- 964 PIERCE, C.D. & MOIN, P. 1998a Turbulent flow over three-dimensional dunes: 2. Fluid and bed
 965 stresses. *Physics of Fluids* **10**, 3041–3044.
- 966 PIERCE, CHARLES DAVID 2001 Progress-variable approach for large-eddy simulation of turbulent
 967 combustion. PhD thesis, Citeseer.
- 968 PIERCE, CHARLES D & MOIN, PARVIZ 1998b Large eddy simulation of a confined coaxial jet with
 969 swirl and heat release. *AIAA paper* **2892**.
- 970 PIOMELLI, U 2014 Large eddy simulations in 2030 and beyond. *Philosophical Transactions of*
 971 *the Royal Society of London A: Mathematical, Physical and Engineering Sciences* **372** (2022),
 972 20130320.
- 973 POPE, SB 2000 *Turbulent Flows*. Cambridge University Press.
- 974 POZORSKI, JACEK & APTE, SOURABH V 2009 Filtered particle tracking in isotropic turbulence
 975 and stochastic modeling of subgrid-scale dispersion. *International Journal of Multiphase Flow*
 976 **35** (2), 118–128.
- 977 READE, W.C. & COLLINS, L.R. 2000 Effect of preferential concentration on turbulent collision
 978 rates. *Physics of Fluids* **12**, 2530.
- 979 ROUSON, D.W.I. & EATON, J.K. 2001 On the preferential concentration of solid particles in tur-
 980 bulent channel flow. *Journal of Fluid Mechanics* **428**, 149–169.
- 981 SAARINEN, PEKKA E, KALLIOMÄKI, PETRI, TANG, JULIAN W & KOSKELA, HANNU 2015
 982 Large eddy simulation of air escape through a hospital isolation room single hinged doorwayval-
 983 idation by using tracer gases and simulated smoke videos. *PloS one* **10** (7), e0130667.
- 984 SAFFMAN, PGT 1965 The lift on a small sphere in a slow shear flow. *Journal of fluid mechanics*
 985 **22** (02), 385–400.

- 986 SESSLER, DANIEL I, OLMSTED, RUSSELL N & KUELPMANN, RUEDIGER 2011 Forced-air warm-
987 ing does not worsen air quality in laminar flow operating rooms. *Anesthesia & Analgesia* **113** (6),
988 1416–1421.
- 989 SNYDER, OP 2009 A ‘Safe Hands’ hand wash program for retail food operations: a technical
990 review. *Yeast* **55** (18.5), 14–8.
- 991 SOMMERFELD, M, ANDO, A & WENNERBERG, D 1992 Swirling, particle-laden flows through a
992 pipe expansion. *Journal of fluids engineering* **114** (4), 648–656.
- 993 SRIDHAR, G. & KATZ, J. 1999 Effect of entrained bubbles on the structure of vortex rings. *J. Fluid*
994 *Mech.* **397** (-1), 171–202.
- 995 STRAUB, A. 2016 *Bentley Microstation Design V8i, M/E Engineering, P.C.*. 150 North Chestnut
996 Street, Rochester, NY 14604, www.meengineering.com.
- 997 TENNEKES, HENDRIK & LUMLEY, JOHN LEASK 1972 *A first course in turbulence*. MIT press.
- 998 WARTTIG, SHERYL, ALDERSON, PHIL, CAMPBELL, GILLIAN & SMITH, ANDREW F 2014 Inter-
999 ventions for treating inadvertent postoperative hypothermia. *The Cochrane Library* .
- 1000 WOOD, AM, MOSS, C, KEENAN, A, REED, MR & LEAPER, DAVID J 2014 Infection control
1001 hazards associated with the use of forced-air warming in operating theatres. *Journal of Hospital*
1002 *Infection* **88** (3), 132–140.

Exhibit 2

Summary of Opinions

I have conducted a computation fluid dynamic simulation of a typical operating room and knee implant surgery procedure. In creating the three-dimensional model of the operating room and its setup, many assumptions were made to reduce the effects of the Bair Hugger patient warming system on disrupting the ventilation air flow. For example, the HVAC system modeled is superior to many, if not all, the HVAC systems used in operating rooms. Similarly, the assumptions made for draping, particle count, position of lights, etc. are all in favor of reducing the disruption caused by the Bair Hugger patient warming system.

Based upon my education, training, experience, and the computation fluid dynamics analysis discussed in Exhibit A, I will offer the following general causation opinions within a reasonable degree of engineering certainty:

1. The use of a Bair Hugger Model 750 Blower with the Bair Hugger Upper Body blanket disrupts the turbulent airflow around the operating table.
2. The use of a Bair Hugger Model 750 Blower with the Bair Hugger Upper Body blanket significantly increases the particle count over the surgical site, operating table, and side tables.
3. The use of a Bair Hugger Model 750 Blower with the Bair Hugger Upper Body blanket significantly reduces the effect of the operating room's HVAC system in protecting the surgical site from contaminants.
4. The use of a Bair Hugger Model 505 Blower with the Bair Hugger Upper Body blanket will have the same effects as stated in items 1 through 3 above, but at a reduced temporal rate, i.e. it would take longer time to observe the same effects of BH Model 750.
5. The Bair Hugger patient warming system significantly increases the number of contaminants reaching the operating table.

Name : S. E. Elghobashi
Nationality : U.S.A.

June 2016

Education :

Degree	Year	Institution
M.Sc. (Mechanical Engineering)	1971	Univ. of Southern California, Los Angeles, USA.
Ph.D. (Mechanical Engineering)	1974	Imperial College, University of London, England.
D.Sc. (Mechanical Engineering)	1999	Imperial College, University of London, England.

Professional Activities (partial list)

Member of the National Academy of Engineering.

Fellow of the American Physical Society.

Fellow of the American Association for the Advancement of Science.

Fellow of the American Society of Mechanical Engineers.

Visiting Fellow of Cambridge University, Wolfson College, England, 1999.

Senior Award of International Conference on Multiphase Flow, Florence, Italy, May 25, 2016.

Chair of the Nominating Committee of American Physical Society, Div. Fluid Dynamics (2014-2015).

Member of Fellowship Committee of American Physical Society, Div. Fluid Dynamics (2009-11).

Member of Science and Engineering Advisory Committee (SETAC) of Blue Waters supercomputer project(2016-2017). <https://bluewaters.ncsa.illinois.edu/setac>

Senior member of the American Institute of Aeronautics and Astronautics(AIAA).

Member of the Combustion Institute.

Member of EuroMech.

Member of the Editorial Advisory Board of International J. of Multiphase Flow(2010-present).

Guest Editor of International J. of Multiphase Flow, Special Issue on Point-particle model for disperse turbulent flows, vol. 35, 2009.

DIC: Diploma of Membership of Imperial College in Mech. Engineering, 1974.

British Science Research Council (SRC) Scholarship (1971-1974).

Major Research Interests

Direct numerical simulation of turbulent flows, including multiphase and chemically-reacting flows, and biomedical flows.

Research and Professional Experience

March 2015 -Present **UC Distinguished Professor**, Mechanical and Aerospace Engineering Department, University of California, Irvine.

July 1985 - Feb. 2014 **Professor**, Mechanical and Aerospace Engineering Department, University of California, Irvine.

July 1997 - June 2002 **Chairman**, Mechanical and Aerospace Engineering Department,
University of California, Irvine.

Aug. 1984 - July 1985 **Visiting Scientist**, DFVLR, German Aerospace
Research Establishment, Institute of Atmospheric Physics,
Oberpfaffenhofen, West Germany (Sabbatical Year).

July 1983 - July 1984 **Vice Chairman** , Mechanical Engineering Department,
University of California, Irvine.

July 1982 - June 1985 **Associate Professor**, Mechanical Engineering Department,
University of California, Irvine.

July 1978 - June 1982 **Assistant Professor**, Mechanical Engineering Department,
University of California, Irvine.

Jan. 1978 - June 1978 **Staff Research Engineer**, Acurex Corporation,
Aerotherm Division, Mountain View, California.

Oct. 1974 - Dec. 1977 **Group Leader**, CHAM, (Concentration, Heat and Momentum),
London, England and Huntsville, Alabama.

Reviewer for:

Journal of Fluid Mechanics
Physics of Fluids
Nature
Science
Physical review Letters
International Journal of Multiphase Flow
Journal of Combustion Science and Technology
Combustion and Flame
Journal of American Institute of Aeronautics and Astronautics
Journal of Fluids Engineering
Journal of Heat Transfer
International Journal of Numerical Heat Transfer
International Journal of Heat and Mass Transfer
International Journal of Heat and Fluid Flow
Progress in Energy and Combustion Science
Journal of Applied Mathematical Modeling
National Science Foundation
NASA
Department of Energy
University of California Energy Research Group
McGraw Hill Book Co.
John Wiley Book Co. and Wiley Interscience Europe.

Consulting

1974 - 1978

NASA- Lewis, NASA- Langley, NASA- Marshall, AFOSR, ARO, ONR

Westinghouse, General Electric, Airesearch
 ALCAN, ALCOA, Corning, Phillip Morris
 Ballistic Missile Advance Technology Center
 Rolls-Royce, England
 Rheinmetall, Germany
 Societe National des Poudres et Explosifs, France
 Spectron Development Labs.

1981 - 1996

Jet Propulsion Laboratory
 Ballistic Missile Advance Technology Center
 R&D Associates
 Physical Research Inc.
 P D A Engineering

1978 - 2000

Science Applications Inc.

Invited Keynote and Distinguished Lectures since 2000

L1. Elghobashi, S. " On the two-fluid and trajectory approaches for DNS of turbulent particle-laden flows", Part 1: DNS of bubble-laden flows via the two-fluid approach, [**Invited Lecture**] Von Karman Institute for Fluid Dynamics, Rhode-Saint-Genese, **Belgium**, April 3-7, 2000.

L2. Elghobashi, S. " On the two-fluid and trajectory approaches for DNS of turbulent particle-laden flows", Part 2: On the approximation of the two-way coupling terms in the trajectory approach, [**Invited Lecture**] Von Karman Institute for Fluid Dynamics, Rhode-Saint-Genese, **Belgium**, April 3-7, 2000.

L3. Elghobashi, S. " On the point-force approximation in DNS of prticle-laden turbulent flows with two-way coupling", [**Invited lecture**] ERCOFTAC Conference on Dynamics of Particle-Laden Flows, Zurich, **Switzerland**, July 3-5, 2000.

L4. L4. Elghobashi, S. "Recent Advance in DNS of Particle-Laden Turbulent Flows" [**Invited Plenary lecture**], XI Congress on Numerical Methods and their Applications, ENIEF 2000 , San Carlos de Bariloche, **Argentina**, November 20-24, 2000.

L5. L5. Elghobashi, S. "The physical mechanisms of modifying the structure of turbulent homogeneous flows by dispersed particles ", [**Invited Plenary Lecture**], ERCOFTAC Conference on Small Particles in Turbulence , Seville, **Spain**, March 11-13, 2002.

L6. S. Elghobashi "On the physical mechanisms of drag reduction in a mirobubble-laden turbulent boundary layer" [**Keynote Lecture**] at **The 5th International Con-**

ference of Multiphase Flow (ICMF 2004), Yokohama, Japan, May 31 - June 3, 2004.

L7. S. Elghobashi “On the drag reduction in a microbubble-laden spatially-developing turbulent boundary layer”, **IUTAM Symposium** on Recent advances in disperse multiphase flow simulation- **[Invited Lecture]**- Chicago-October 2004.

L8. S. Elghobashi “ Reynolds number effect on drag reduction in a microbubble-laden spatially-developing turb. boundary layer”, **Euromech Conference on Hydrodynamics of bubbly flows-** **[Invited Lecture]**- Lorentz Center, Leiden, the Netherlands, June 6-8, 2005.

L9. S. Elghobashi “On drag reduction in a microbubble-laden spatially-developing turbulent boundary layer”, **European Science Foundation- Challenging Turbulent Lagrangian Dynamics**, **[Invited Lecture]**- Castel Gandolfo, Italy, Sept. 1-4, 2005.

L10. S. Elghobashi “On drag reduction in a microbubble-laden spatially-developing turbulent boundary layer”, **Thirteen IUTAM Advanced School & Workshop, Particle Dispersion in Turbulent Flows**, **[Invited Lecture I]** - CISM, Udine, Italy, September 12-16, 2005.

L11. S. Elghobashi “ Reynolds number effect on drag reduction in a microbubble-laden spatially-developing turb. boundary layer”, **Thirteen IUTAM Advanced School & Workshop, Particle Dispersion in Turbulent Flows**, **[Invited Lecture II]**- CISM, Udine, Italy, September 12-16, 2005.

L12. S. Elghobashi, “ Direct simulation of turbulent flows laden with particles or bubbles”, **CIEMAT : Research Centre for Energy, Environment and Technology**, **[Invited Lecture]**, Madrid, Spain, June 21, 2006.

L13. S. Elghobashi, “ DNS of the two-way interactions between dispersed solid particles and turbulent flows”, **Workshop on multiphase turbulence: Dust storms, erosion, hurricanes and tornadoes**, **[Invited Lecture]**, Xian, China, July 16-18, 2007.

L14. S. Elghobashi, “ On the two-way interactions between dispersed solid particles and turbulent flows”, **European Workshop on Direct and Large-Eddy Simulation**, **[Keynote Lecture]**, Trieste, Italy, Sept. 8-10, 2008.

L15. S. Elghobashi “ On the two-way interactions between dispersed particles and turbulent flows ” , **March 2009 Meeting of American Physical Society** Pittsburgh, PA . Bulletin of APS, Vol. 54, 209, **[Invited Lecture]**, March 18, 2009.

- L16.** S. Elghobashi “ The physical mechanisms of two-way interactions between dispersed particles and turbulent flows”, **Workshop on Clouds and Turbulence Institute for Mathematical Sciences**, Imperial College, **[Invited Lecture]**, London, England, March 23-25, 2009.
- L17.** S. Elghobashi “ How do inertial particles modify isotropic turbulence ?” **International Workshop- Solving the Riddle of Turbulence: What, Why, and How?** Max Planck Institute for Dynamics and Self-Organization, **[Invited Lecture]**, Göttingen, Germany, May 6 - May 9, 2009.
- L18.** S. Elghobashi “How do inertial particles modify isotropic turbulence ?” **International Symposium on Turbulence**, **[Invited Lecture]**, Peking University, Beijing, China, Sept. 21-25, 2009.
- L19.** S. Elghobashi “How do inertial particles modify isotropic turbulence ?” **4th Latin-American Workshop on CFD ”**, **[Keynote Lecture]**, Rio de Janiero, Brazil, July 11-14, 2010.
- L20.** S. Elghobashi “On turbulence modulation by dispersed inertial particles” **13th European Turbulence Conference, ETC 13**, **[Keynote Lecture]** University of Warsaw, Poland, September 12-15, 2011.
- L21.** F. Lucci, V.S. Lvov, A. Ferrante and S. Elghobashi, “Eulerian-Lagrangian bridge for the energy and dissipation spectra in homogeneous turbulence”, **[Invited Lecture]**, International Workshop on “Lagrange versus Euler for turbulent flows”, **Wolfgang Pauli Institute, Vienna, Austria**, May 7-12, 2012.
- L22.** S. Elghobashi “On the multi-way interactions between turbulent flows and suspended sediment”
International symposium on two-phase modeling for sediment dynamics in geophysical flows(THESIS-2013) **[Keynote Lecture]** Chatou, Paris, France, June 10-12, 2013.
- L23.** S. Elghobashi “On the multi-way interactions between turbulent flows and suspended particles”
Fluid-Mediated Particle Transport in Geophysical Flows (GEOFLOWS13), Kavli Institute for Theoretical Physics **[Invited Lecture]** UCSB, Santa Barbara, California, December 10, 2013.
- L24.** S. Elghobashi “ Modulation of isotropic turbulence by dispersed particles,” **Huazhong University of Science and Technology, Wuhan, China**, June 9, 2014. **[Plenary Lecture]**.
- L25.** S. Elghobashi “Homogeneous shear turbulence modulation by dispersed small

particles,” **Huazhong University of Science and Technology, Wuhan, China**, June 10, 2014. [keynote Lecture].

L26. S. Elghobashi “Modulation of isotropic turbulence by finite-size particles,” **Huazhong University of Science and Technology, Wuhan, China**, June 11, 2014. [keynote Lecture].

L27. S. Elghobashi “How do dispersed inertial particles modify turbulent flows,” Department of Mechanics and Engineering Science, **Peking University, China**, June 17, 2014 . [Distinguished lecture].

L28. S. Elghobashi “How do dispersed inertial particles modify turbulent flows,” Center for Turbulence Research, **Stanford University**, July 25, 2014. [Distinguished lecture].

L29. S. Elghobashi “How do dispersed inertial particles modify turbulent flows,” Computational and Applied Mathematics, **Pennsylvania State University**, October 10, 2014. [Distinguished lecture].

L30. S. Elghobashi “How do dispersed inertial particles modify turbulent flows,” Aerospace Engineering department, **University of Minnesota**, April 21, 2015. [Distinguished lecture].

L31. S. Elghobashi “How do dispersed inertial particles modify turbulent flows,” Mechanical Engineering department, **Northwestern University**, February 1, 2016. [Distinguished lecture].

L32. S. Elghobashi “How do dispersed inertial particles modify turbulent flows,” Mechanical Engineering department, **MIT**, February 3, 2016. [Distinguished lecture].

Publications

Articles in Books

B1 Elghobashi, S.E., "Studies in the Prediction of Turbulent Diffusion Flames", **Studies in Convection**, Vol. 2, B.E. Launder, ed., Academic Press, London, (1977).

B2 Elghobashi, S. E., and Nomura, K.N., "Direct Simulation of a Passive Diffusion Flame in Sheared and Unsheared Homogeneous Turbulence", **Turbulent Shear Flows 7**, pp. 313-329, W.C. Reynolds, ed., Springer-Verlag, (1991).

B3 Elghobashi, S. E. "Direct Simulation of turbulent flows laden with dispersed particles", **Handbook on Multiphase Flow**, pp. 13-34:13-60, C. Crowe, ed., CRC, (2005).

B4 Elghobashi, S. E. "An updated classification map of particle-laden turbulent flows", **Proceedings of IUTAM Symposium on Computational approaches to multiphase flow**, Springer pp. 3-10, , (2006).

B5 Loy, A.C., Jing, J., Zhang, J., Wang., Y., Elghobashi, S., Chen, Z. and Wong, B.J.F. "Anatomic optical coherence tomography of upper airways", **Optical Coherence Tomography: Technology and Applications**, Ed. W. Drexler and J. Fujimoto, Springer, Chapter 75, pp. 1145-2262, (2015).

Guest Editor

Elghobashi, S.E. "Point-Particle Models for Disperse Turbulent Flows", **International Journal of Multiphase Flow, Special Issue**, Volume 35, Issue 9, Pages 791-878, (September 2009).

Journal Papers

J1 Elghobashi, S.E., Pun, W.M. and Spalding, D.B., "Concentration Fluctuations in Isothermal Turbulent Confined Coaxial Jets", **Chem. Eng. Sci.**, Vol. 32, pp. 161-166 (1977).

J2 Elghobashi, S.E. and Wassel, A.T., "The Effect of Turbulent Heat Transfer on the Propagation of an Optical Beam Across Supersonic Boundary and Free Shear Layers", **Int. J. Heat and Mass Transfer**, Vol. 23, pp. 1229-1241 (1980).

J3 Elghobashi, S.E., Samuelsen, G.S., Wuerer, J.E., and LaRue, J.C., "Prediction and Measurement of Mass, Heat and Momentum Transport in a Nonreacting Turbulent Flow of a Jet in an Opposing Stream", **J. Fluids Engineering**, Vol. 103, pp. 127-132 (1981).

J4 Megahed, I.E.A. and Elghobashi, S.E., "On the Numerical Solution of Indeterminate Steady Elliptic Flows",
Computer Methods in Applied Mechanics and Engineering, Vol. 26, pp. 225-240 (1981).

J5 Elghobashi, S.E. and Megahed, I.E.A., "Mass and Momentum Transport in a Laminar Isothermal Two-Phase Round Jet",
Int. J. Numerical Heat Transfer, Vol. 4, pp. 317-329 (1981).

J6 Elghobashi, S.E. and Abou Arab, T.W., "A Two-Equation Turbulence Model for Two-Phase Flows",
Physics of Fluids, Vol. 26, pp.931-938 (1983).

J7 Elghobashi, S.E. and Launder, B.E., "Turbulent Time Scales and the Dissipation Rate of Temperature Variance in the Thermal Mixing",
Physics of Fluids, Vol. 26, pp. 2415-2419 (1983).

J8 Modarress, D., Tan, H. and Elghobashi, S.E., "Two-Component LDA Measurement in a Two-Phase Turbulent Jet",
AIAA J. Vol. 22, pp. 624-630 (1984).

J9 Modarress, D., Wuerer, J. and Elghobashi, S.E., "An Experimental Study of a Turbulent Round Two-Phase Jet",
Chemical Engineering Communications, Vol. 28, pp. 341-354 (1984).

J10 Wassel, A.T. and Elghobashi, S.E., "Mathematical Simulation of Ocean Thermal Energy Conversion Sea Water Systems",
J. Solar Energy Engineering Vol. 106, pp. 198-205 (1984).

J11 Mostafa A.A. and Elghobashi, S.E., "A Study of the Motion of Vaporizing Droplets in a Turbulent Flow",
AIAA Progress in Astronautics and Aeronautics, Vol. 10, pp. 513-539, Oppenheim and Soloukhin (editors) (1984).

J12 Elghobashi, S.E., Abou-Arab, T., Rizk, M. and Mostafa, A., "Prediction of the Particle-Laden Jet with a Two-Equation Turbulence Model",
Int. J. of Multiphase Flow, Vol. 10, pp. 697-710 (1984).

J13 Bellan J., and Elghobashi, S.E., "Fuel Composition Effects on High Temperature Corrosion in Boiler and Furnaces",
J. of Engineering for Power, Vol. 107, pp. 744-757 (1985).

J14 Rizk, M., and Elghobashi, S.E., "Wall Effects on the Motion of a Spherical Particle Suspended in a Turbulent Flow",
Physics of Fluids, Vol. 28, pp. 806-817 (1985).

J15 Mostafa, A.A. and Elghobashi, S.E., "A Two-Equation Turbulence Model for Jet Flows Laden with Vaporizing Droplets",
Int. J. of Multiphase Flow, Vol. 11, pp. 515-533 (1985).

J16 Schumann, U., Elghobashi, S.E., and Gerz, T., "Direct Simulation of Stably Stratified Turbulent Homogeneous Shear Flows",
Notes on Numerical Fluid Mechanics, Vol. 15, pp. 245-264 (1986).

J17 Prud'homme, M., and Elghobashi, S.E., "Turbulent Heat Transfer Near the Reattachment of Flow Downstream of a Sudden Pipe Expansion",
Int. J. Numerical Heat Transfer, Vol. 10, pp. 349-368 (1986).

J18 Conner, J. and Elghobashi, S.E., "Numerical Solution of Laminar Flow Past a Sphere with Surface Mass Transfer",
Int. J. Numerical Heat Transfer, Vol. 12, pp. 57-82 (1987).

J19 Rizk, M. and Elghobashi, S.E., "A Two-Equation Turbulence Model for Dispersed Dilute Two-Phase Confined Flows",
Int. J. of Multiphase Flow, Vol. 15, pp. 119-133 (1989).

J20 Gerz, T., Schumann, U. and Elghobashi, S., "Direct Simulation of Stably Stratified Homogeneous Turbulent Shear Flows",
J. Fluid Mechanics, Vol. 200, pp. 563-594 (1989).

J21 Tsau, F., Elghobashi, S. E., and Sirignano, W. "Effects of G- Jitter on a Thermally Buoyant Flow",
J. Thermophysics and Heat Transfer, vol. 6, pp. 246-254 (1992).

J22 Elghobashi, S. E., "Particle-Laden Turbulent Flows : Direct Simulation and Closure Models",
J. Applied Scientific Research, vol.48, pp. 301-314 (1991).

J23 Elghobashi, S. E., and Truesdell, G.C., "Direct Simulation of Particle Dispersion in a Decaying Isotropic Turbulence",
J. Fluid Mechanics, vol. 242, pp. 655-700 (1992).

J24 Nomura, K.N., and Elghobashi, S. E. "Mixing characteristics of an inhomoge-

neous scalar in isotropic and homogeneous sheared turbulence”,
Physics of Fluids, vol. 4, pp. 606-625 (1992).

J25 Kim, I., Elghobashi, S. E., and Sirignano, W. ” Three- dimensional flow over two spheres placed side by side”,
J. Fluid Mechanics, vol. 246, pp. 465-488 (1993).

J26 Nomura, K.N.,and Elghobashi, S. E. ” The structure of inhomogeneous turbulence in variable density nonpremixed flames”,
Theoretical and Computational Fluid Dynamics, vol. 5, pp. 153-176 (1993).

J27 Elghobashi, S. E., and Truesdell, G.C., ” On the two-way interaction between homogeneous turbulence and dispersed solid particles ; Part 1 : turbulence modification”,
Physics of Fluids, vol. A5, pp. 1790-1801 (1993).

J28 Elghobashi, S. E., ’On Predicting Particle-Laden Turbulent Flows’ ,
J. Applied Scientific Research, Vol. 52, 4, pp. 309-329 (1994).

J29 Truesdell, G.C., and Elghobashi, S. E.” On the two-way interaction between homogeneous turbulence and dispersed solid particles ; Part 2 : particle dispersion”,
Physics of Fluids, Vol. 6, pp. 1405-1407 (1994).

J30 Kim, I., Elghobashi, S. E., and Sirignano, W. ” Unsteady flow interactions between an advected cylindrical vortex tube and a spherical particle”,
J. Fluid Mechanics, Vol. 288, pp. 123-155 (1995).

J31 Boratav, O., Elghobashi, S. E., and Zhong, R. ” On the alignment of the α -strain and vorticity in turbulent nonpremixed flames”,
Physics of Fluids, Vol. 8, pp. 2251-2253 (1996).

J32 Kim, I., Elghobashi, S. E., and Sirignano, W. ” Unsteady flow interactions between a pair of advected vortex tubes and a rigid sphere”,
International J. Multiphase Flow, Vol. 23, pp. 1-23 (1997).

J33 Druzhinin, O. and Elghobashi, S., ‘ DNS of bubble-laden turbulent flows using the two-fluid formulation’,
Physics of Fluids, Vol. 10, pp. 685-697 (1998).

J34 Kim, I., Elghobashi, S. E., and Sirignano, W. ‘ On the equation for spherical particle motion : effects of Reynolds and acceleration numbers’,
J. Fluid Mechanics, Vol. 367, pp. 221-253 (1998).

J35 Boratav, O., Elghobashi, S. E., and Zhong, R. ‘ On the alignment of strain,

vorticity and scalar gradient in turbulent, buoyant, nonpremixed flames',
Physics of Fluids, Vol. 10, pp. 2260-2267 (1998).

J36 Druzhinin, O. and Elghobashi, S., 'On the decay rate of isotropic turbulence laden with microparticles',
Physics of Fluids, Vol. 11, pp. 602-610 (1999).

J37 Druzhinin, O. and Elghobashi, S., ' A Lagrangian-Eulerian mapping solver for direct numerical simulation of a bubble-laden homogeneous turbulent shear flow using the two-fluid formulation ',
J. Computational Physics, Vol. 154, pp.174-196 (1999).

J38 Elghobashi, S. E., Zhong, R. and Boratav, O. ' Effects of gravity on turbulent nonpremixed flames',
Physics of Fluids, Vol. 11 , pp. 3123-3135 (1999).

J39 Zhong, R. , Elghobashi, S. E., Boratav, O. ' Surface topology of a buoyant turbulent nonpremixed flame',
Physics of Fluids, Vol. 12, pp. 2091-2100 (2000).

J40 Ahmed, A.M. and Elghobashi, S. E. On the mechanisms of modifying the structure of turbulent homogeneous shear flows by dispersed particles,
Physics of Fluids, Vol. 12, pp. 2906-2930 (2000).

J41 Druzhinin, O. and Elghobashi, S., ' Direct numerical simulation of a three-dimensional spatially-developing bubble-laden mixing layer with two-way coupling',
J. Fluid Mechanics, Vol. 429, pp. 23-61 (2001).

J42 Ahmed, A.M. and Elghobashi, S. E. Direct numerical simulation of particle dispersion in homogeneous turbulent shear flows ,
Physics of Fluids, Vol. 13, pp. 3346-3364 (2001).

J43 Ferrante, A. and Elghobashi, S. E. On the physical mechanisms of two-way coupling in particle-laden isotropic turbulence ,
Physics of Fluids, Vol. 15, pp. 315-329 (2003).

J44 Ferrante, A. and Elghobashi, S. E., ' A robust method for generating inflow conditions for direct simulations of spatially-developing turbulent boundary layers',
J. Computational Physics, Vol. 198, pp. 372-387 (2004).

J45 Latz, M. I., Juhl, A. R., Ahmed, A.M., Elghobashi, S. and Rohr, J. ' Hydrodynamic stimulation of dinoflagellate bioluminescence: A computational and experimental study',
J. Experimental Biology, Vol. 207, pp. 1941-1951(2004).

- J46** Ferrante, A. and Elghobashi, S. E., ‘ On the physical mechanisms of drag reduction in a spatially-developing turbulent boundary layer laden with microbubbles’, **J. Fluid Mechanics**, Vol. 503, pp. 345-355. (2004).
- J47** Ferrante, A. and Elghobashi, S. E., Adams P., Valenciano M. and Longmire D. ‘ Evolution of quasi-streamwise vortex tubes and wall-streaks in a microbubble-laden turbulent boundary layer over a flat plate’, **Physics of Fluids**, Vol. 16(9), pp. S2 (2004).
- J48** Ferrante, A. and Elghobashi, S. E., ‘ Reynolds number effect on drag reduction in a microbubble-laden spatially-developing turbulent boundary layer’, **J. Fluid Mechanics**, Vol. 543, pp. 93-106 (2005).
- J49** Ferrante, A. and Elghobashi, S. E., ‘ On the effects of microbubbles on the Taylor-Green vortex flow’, **J. Fluid Mechanics**, Vol. 572 , pp. 145 - 177 (2007).
- J50** Ferrante, A. and Elghobashi, S. E., ‘ On the accuracy of the two-fluid formulation in DNS of bubble-laden turbulent boundary layers’, **Physics of Fluids**, Vol. 19, 045105, pp.1-8 (2007).
- J51** L’vov, V.S., Pomyalov, A., Ferrante, A. and Elghobashi, S. E., ‘ Analytical model of the time Developing turbulent boundary layer’, **J. Exp. Theor. Phys.**, Vol. 86, issue 2, pp. 111-116 (2007).
- J52** Lucci, F., Ferrante, A. and Elghobashi, S. E., ‘ Modulation of isotropic turbulence by particles of Taylor-lengthscale size’, **J. Fluid Mechanics**, Vol. 650, pp. 5-55 (2010).
- J53** Lucci, F., Ferrante, A. and Elghobashi, S. ‘ Is Stokes number an appropriate indicator of turbulence modulation by large particles ?’ **Physics of Fluids**, Vol. 23, pp. 25101-1-7 (2011).
- J54** Cleckler, J., Elghobashi, S. and Liu, F. ‘On the motion of inertial particles by sound waves’ **Physics of Fluids**, Vol. 24, 033301 (2012).
- J55** Lucci, F., L’Vov, V., Ferrante, A., Rosso, M. and Elghobashi, S. , ‘ Eulerian-Lagrangian bridge for the energy and dissipation spectra in isotropic turbulence ’, **Theoretical and Computational Fluid Dynamics**, DOI: 10.1007/s00162-013-0310-5(2013).
- J56** Wang, Y. and Elghobashi, S. , ‘ On locating the obstruction in the upper

airway via numerical simulation ',

J. Respiratory Physiology & Neurobiology, Vol. 193, pp.1-10 (2014).

J57 Mylavarapu, G., Wang, Y., Elghobashi, S. and Gutmark, E. 'PIV measurements and numerical simulations of the flow in a human upper airway phantom', **Biomechanics and Modeling in Mechanobiology**, submitted (2016).

Archival Conference Papers

- C1 Elghobashi, S.E. and Pun, W.M., "A Theoretical and Experimental Study of Turbulent Diffusion Flames in Cylindrical Furnaces", **Proceedings of Fifteenth Symposium (International) on Combustion**, (1974).
- C2 Elghobashi, S.E., Pratt, D.T., Spalding, D.B. and Srivatsa, S.K., "Unsteady Combustion of Fuel Spray in Jet Engine Afterburners", **Proceedings of Third International Symposium on Air Breathing Engines**, Munich (1976).
- C3 Elghobashi, S.E. and Launder, B.E., "Modeling the Dissipation Rate of Scalar Fluctuations in a Thermal Mixing Layer", **Proceedings of Third Symposium on Turbulent Shear Flows**, (1981).
- C4 Elghobashi, S.E. and Abou Arab, T.W., "A Second Order Turbulence Model for Two-Phase Flows", **Proceedings of Seventh International Heat Transfer Conference**, Munich (1982).
- C5 Elghobashi, S.E. and Prud'homme, M., "On the Accuracy and Stability of Quadratic Upstream Differencing in Laminar Elliptic Flows", **Numerical Methods in Laminar and Turbulent Flow**, ed. Taylor, C., Johnson, J., and Smith, W., Pineridge Press, U.K., pp. 317-327 (1983).
- C6 Mostafa A.A. and Elghobashi, S.E., "A Study of the Motion of Vaporizing Droplets in a Turbulent Flow", **Proceedings of Ninth International Colloquium and Dynamics of Explosions and Reactive Systems**, Poitiers, France, July (1983).
- C7 Elghobashi, S.E., Abou Arab, T.W., Rizk, M. and Mostafa, A., "A Mathematical Model of the Turbulent Two-Phase Round Jet", **Proceedings of Fourth International Symposium on Turbulent Shear Flows**, Karlsruhe, Germany, Sept. (1983).
- C8 Elghobashi, S.E., Rizk, M. and Mostafa, A., "A Mathematical Model of the Two-Phase Turbulent Axisymmetric Jet", **Proceedings of the Third Multi-Phase Flow and Heat Transfer Symposium**, Miami, Florida, April (1983).
- C9 Prud'homme, M. and Elghobashi, S.E., "Prediction of Wall-Bounded Turbulent Flows with an Improved Version of a Reynolds-Stress Model", **Proceedings of Fourth International Symposium on Turbulent Shear Flows**, Karlsruhe, Germany, Sept. (1983).
- C10 Elghobashi, S.E. and J.C. LaRue, "The Effect of Mechanical Strain on the Dissipation Rate of a Scalar Variance", **Proceedings of Fourth International Sym-**

posium on Turbulent Shear Flows, Karlsruhe, Germany, Sept. (1983).

C11 Rizk, M. and Elghobashi, S.E., "A Mathematical Model for a Turbulent Gas-Solid Suspension Flow in a Vertical Pipe", **Proceedings of Fifth International Symposium on Turbulent Shear Flows**, Cornell Univ., August (1985).

C12 Elghobashi, S.E., Gerz, T. and Schumann, U., "Direct Simulation of Turbulent Homogeneous Shear Flow with Buoyancy", **Proceedings of Fifth International Symposium on Turbulent Shear Flows**, Cornell Univ., August (1985).

C13 Elghobashi, S.E., Gerz, T. and Schumann, U., "Direct Simulation of the Initial Development and the Homogeneous Limit of the Thermal Mixing Layer", **Proceedings of Sixth International Symposium on Turbulent Shear Flows**, Toulouse, France, (1987).

C14 Elghobashi, S. E., and Nomura, K.N., "Direct Simulation of a Fast Chemical Reaction in a Homogeneous Turbulent Shear Flow", **Proceedings of Seventh Symposium on Turbulent Shear Flows**, Stanford, pp. 711-716 (1989).

C15 Elghobashi, S. E., and Truesdell, G.C., "Direct Simulation of Particle Dispersion in a Decaying Grid Turbulence", **Proceedings of Seventh Symposium on Turbulent Shear Flows**, Poster Session, Stanford (1989).

C16 Tsau, F., Elghobashi, S. E., and Sirignano, W. "Effects of G- Jitter on a Thermal Buoyant Flow", Paper no 90-653, **AIAA 28th Aerospace Science Meeting**, Reno, Nevada, January (1990).

C17 Tsau, F., Elghobashi, S. E., and Sirignano, W. "Prediction of a Liquid Jet in a Gaseous Crossflow", Paper no 90-2067, **AIAA 26th Joint Propulsion Conference**, Orlando, Florida, July (1990).

C18 Nomura, K.N., and Elghobashi, S. E. "Direct Simulation of an Isothermal Nonpremixed Flame in a Homogeneous Turbulent Shear Flow", Paper no 90-148, **AIAA 28th Aerospace Science Meeting**, Reno, Nevada, January (1990).

C19 Kim, I., Elghobashi, S. E., and Sirignano, W. "Three- dimensional droplet interactions in dense sprays", Paper no 91-0073, **AIAA 30th Aerospace Science Meeting**, Reno, Nevada, January (1991).

C20 Truesdell, G.C., and Elghobashi, S. E. "Direct numerical simulation of a particle-laden homogeneous turbulent flow ", **Proceedings of First ASME-JSME Fluids Engineering Conference**, Portland, Oregon, ASME-FED, Vol. 121, pp. 11-17, June

(1991).

C21 Elghobashi, S. E., and Truesdell, G.C., "On the interaction between solid particles and decaying turbulence ", **Proceedings of Eighth Symposium on Turbulent Shear Flows**, Munich, Germany , September (1991).

C22 Sirignano, W.A., Chiang, C.H., Kim, I. and Elghobashi, S. E. " Aerodynamic interactions amongst neighboring droplets", **4th International Symposium on Computational Fluid Dynamics**, Davis, Calif., September (1991).

C23 Kim, I. , Elghobashi, S. E., and Sirignano, W. " Three- dimensional flow computation for two interacting, moving droplets", Paper no 92-0343, **AIAA 30th Aerospace Science Meeting**, Reno, Nevada, January (1992).

C24 Nomura, K.N., and Elghobashi, S. E. " The structure of inhomogeneous turbulence in variable density nonpremixed flames", **Proceedings of IUTAM Symposium on Eddy Structure and Identification in Free Turbulent Shear Flows**, Poitiers, France, October (1992).

C25 Elghobashi, S. E. and Truesdell, G.C., " On the two-way interaction between homogeneous turbulence and dispersed solid particles", Paper AIAA 93-1875, **AIAA /ASME 29th Joint Propulsion Conference**, Monterey, CA (1993).

C26 Elghobashi, S. E." On Predicting particle-laden turbulent flows ", **Proceedings of Seventh Workshop on Two-Phase Flows**, Erlangen, Germany, pp 211-219, April 11 (1994). [**Invited Lecture**]

C27 Elghobashi, S. E." Effects of the two-way coupling on particle dispersion ", **Proceedings of Seventh Workshop on Two-Phase Flows**, Erlangen, Germany, pp 224-230, April 13 (1994). [**Invited Lecture**]

C28 Kim, I. , Elghobashi, S. E., and Sirignano, W. " Unsteady flow interactions between a pair of advected cylindrical vortex tube and a rigid sphere", Paper no 95-0105, **AIAA 33th Aerospace Science Meeting**, Reno, Nevada, January (1995).

C29 Elghobashi, S. E., Lee, Y.Y. and Zhong, R. " Effects of gravity on sheared and nonsheared turbulent nonpremixed flame", **Third International Microgravity Combustion Workshop, NASA Lewis**, Cleveland, Ohio, April 11-13 (1995).

C30 Kim, I. , Elghobashi, S. E., and Sirignano, W. " " The motion of a spherical particle in unsteady flows at moderate Reynolds numbers", **AIAA, 34th Aerospace Sciences Meeting**, Reno, NV, January (1996).

C31 Elghobashi, S. "Direct simulation of dispersed dilute two-phase turbulent flows",

Part 1: Decaying Turbulence, **Proceedings of the 1996 Lecture series programme, Von Karman Institute for Fluid Dynamics**, Rhode-Saint-Genese, Belgium, January 29-February 2, 1996. [**Invited Lecture**]

C32 Elghobashi, S. "Direct simulation of dispersed dilute two-phase turbulent flows", Part 2 : Homogeneous shear, **Proceedings of the 1996 Lecture series programme, Von Karman Institute for Fluid Dynamics**, Rhode-Saint-Genese, Belgium, January 29-February 2, 1996. [**Invited Lecture**]

C33 Elghobashi, S. and Lasheras, J. " Effects of gravity on sheared turbulence laden with bubbles or droplets", **Third Microgravity Fluid Physics Conference, NASA Lewis**, Cleveland, OH, June 13-15, 1996.

C34 Elghobashi, S., Boratav, O. and Zhong, R. " Effects of gravity on sheared and nonsheared turbulent nonpremixed flames", **Fourth International Microgravity Combustion Conference, NASA Lewis**, Cleveland, OH, May 19-21, 1997.

C35 Elghobashi, S. and Ahmed, A.M. ' DNS of turbulent homogeneous shear flow laden with particles: Two-way coupling', **Japan Society of Mechanical Engineers, Centennial Grand Congress**, Tokyo, Japan, July 18-19, 1997. [**Invited Lecture**]

C36 Druzhinin, O. and Elghobashi, S. 'DNS of bubble-laden turbulent flows using a two-fluid formulation', **Third International Conference on Multiphase Flow**, Lyon, France, June 8-12, 1998.

C37 Elghobashi, S. and Lasheras, J. 'Effects of gravity on sheared turbulence laden with bubbles or droplets' **Fourth Microgravity Fluid Physics and Transport Phenomena Conference, NASA-Lewis**, Cleveland, Ohio, August 12-14, 1998.

C38 Elghobashi, S. and Zhong, R. 'Effects of gravity on sheared turbulent non-premixed flames' **Fifth International Microgravity Combustion Conference, NASA-Lewis**, Cleveland, Ohio, May 18-20, 1999.

C39 Elghobashi, S. " On the two-fluid and trajectory approaches for DNS of turbulent particle-laden flows", Part 1: DNS of bubble-laden flows via the two-fluid approach, **Proceedings of the 2000 Lecture series programme, Von Karman Institute for Fluid Dynamics**, Rhode-Saint-Genese, Belgium, April 3-7, 2000. [**Invited Lecture**]

C40 Elghobashi, S. " On the two-fluid and trajectory approaches for DNS of turbulent particle-laden flows", Part 2: On the approximation of the two-way coupling terms in the trajectory approach, **Proceedings of the 2000 Lecture series programme, Von Karman Institute for Fluid Dynamics**, Rhode-Saint-Genese, Belgium, April 3-7, 2000. [**Invited Lecture**]

C41 Ferrante, A. and Elghobashi, S. ‘Effects of Reynolds number on drag reduction in a microbubble-laden spatially-developing turbulent boundary layer’ **Second International Symposium on Seawater Drag Reduction**, Busan, Korea, May 23-26, 2005.

C42 Ferrante, A. and Elghobashi, S. ‘ On the accuracy of the two-fluid formulation in DNS of a microbubble-laden turbulent boundary layer 26th **Symposium on Naval Hydrodynamics**, Rome, Italy, 17-22 September 2006.

C43 Ferrante, A. and Elghobashi, S. ‘ On the effects of finite-size particles on decaying isotropic turbulence’ **International Conference on Multiphase Flow, ICMF 2007**, Leipzig, Germany, July 9 – 13, 2007.

C44 Lucci, F., Ferrante, A. and Elghobashi, S. ‘ Turbulence modulation by particles of the Taylor-lengthscale size: is Stokes number an appropriate indicator ?’ **International Conference on Multiphase Flow, ICMF 2010**, Tampa, Florida, May 30- June 4, 2010.

Abstracts of Papers Presented at Conferences

A1 Mostafa A.A. and Elghobashi, S.E., "Prediction of a Turbulent Round Gaseous Jet Laden with Vaporizing Droplets", Western States/The Combustion Institute, UCLA, October (1983).

A2 Bellan J. and Elghobashi, S.E., "Impact of Fuel Composition on Deposits and on High-Temperature Corrosion in Industrial Furnaces", Western States Meeting, The Combustion Institute, UCLA, October (1983).

A3 Rizk, M. and Elghobashi, S.E., "Turbulent Fluid and Particle Interaction Near a Plane Wall", **Bull. Am. Phys. Soc.**, Vol. 28, pp. 1378 (1983).

A4 Rizk, M. and Elghobashi, S.E., "The Motion of a Spherical Particle Suspended in a Turbulent Flow Near a Plane Wall", **Proceedings of International Symposium on Two-Phase Annular and Dispersed Flows**, Pisa, Italy, June (1984).

A5 Elghobashi, S. E., and Truesdell, G.C., "Direct Simulation of Particle Dispersion in a Homogeneous Turbulent Shear Flow", Paper no. 73 f, **AIChE Annual Meeting**, San Francisco, November (1989).

A6 Elghobashi, S. E. "Direct numerical simulation and modelling of particle-laden turbulent flows", **Shell Conference on Computational Fluid Dynamics**, Apeldoorn, The Netherlands, December 11, 1989.

A7 Elghobashi, S. E., and Truesdell, G.C., "Direct Simulation of Particle Dispersion in Grid Turbulence and Homogeneous Shear Flows", **Bull. Am. Phys. Soc.**, Vol. 34, pp. 2311 (1989).

A8 Elghobashi, S. E., and Truesdell, G.C., "Direct Numerical Simulation of Particle-Laden Decaying Isotropic Turbulence", **21st Annual Meeting of The Fine Particle Society**, San Diego, Calif., August (1990).

A9 Kim, I., Elghobashi, S. E., and Sirignano, W. "Three-dimensional flow interactions between two neighboring spheres", **Bull. Am. Phys. Soc.**, Vol. 36, pp. 2622 (1991).

A10 Elghobashi, S. E., and Truesdell, G.C., "On the modification of the energy spectrum of homogeneous turbulence by dispersed solid particles", **Proceedings of Sixth Workshop on Two-Phase Flows**, Erlangen, Germany, pp 211-219, March 30 (1992). [**Invited Lecture**]

A11 Elghobashi, S. E., "On predicting particle-laden turbulent flows", **Workshop**

on turbulence in particulate multiphase flow, Fluid Dynamics Laboratory, Battelle Pacific Northwest Laboratory, Richland, WA, March 22, 1993. [**Invited Lecture**]

A12 Elghobashi, S. E., " Direct numerical simulation of particle dispersion and turbulence modulation in homogeneous turbulence", **NATO Advanced Research Workshop on Chaotic Advection, Tracer Dynamics, and Turbulent Dispersion**, Alessandria, Italy, May 24-28, 1993. [**Invited Lecture**]

A13

Elghobashi, S. E." One of the unresolved questions in predicting particle-laden turbulent flows ", **International Symposium on Numerical Methods for Multiphase Flows**, Lake Tahoe, NV, June 19-24 (1994). [**Invited Lecture**]

A14 Elghobashi, S. E." Mathematical models of particle-laden turbulent flows ", **Proceedings of 2nd International Workshop on Mathematical Modeling of Turbulent Flows**, Tokyo, Japan, July 29 (1994). [**Invited Lecture**]

A15 Elghobashi, S. E." Direct numerical simulation of particle-laden homogeneous turbulence ", **Proceedings of of 2nd International Workshop on Mathematical Modeling of Turbulent Flows**, Tokyo, Japan, July 30 (1994). [**Invited Lecture**]

A16 Nomura, K.N., and Elghobashi, S. E. "Interaction of chemical energy release and small-scale turbulence in a nonpremixed reacting flow", **47th Annual Meeting of the American Physical Society**, Div. of Fluid Dynamics, Atlanta, GA, (1994).

A17 Elghobashi, S. E." DNS of bubble dispersion in homogeneous turbulent shear flows ", **ONR bubbly flow workshop**, UC San Diego, February 23-24 (1995).

A18 Elghobashi, S. E. "Direct simulation of particle dispersion in a homogeneous turbulent shear flow", Presented at the **Annual ASME/JSME Fluids Engineering Conference**, Hilton Head, S.C., August 13-18, (1995). [Invited lecture]

A19 Elghobashi, S., Boratav, O. and Zhong, R. 'Buoyancy effects on the structure of turbulence in nonpremixed flames', **48th Annual Meeting of American Physical Society**, Div. Fluid Dynamics, Irvine, CA, November 1995.

A20 Elghobashi, S. and Ahmed, A. " Bubble dispersion and turbulence modification in a homogeneous shear flow", **ONR workshop on Bubbly Flows**, UCSD, La Jolla, February 22-23, 1996.

A21 Elghobashi, S., Boratav, O. and Zhong, R. "Effects of buoyancy on turbulent nonpremixed flames', Presented at the '**International Conference on Turbulent Heat Transfer**', San Diego, CA, March 10-15, 1996. [Invited lecture]

A22 Boratav, O. Elghobashi, S. and Zhong, R. 'Buoyancy effects on the struc-

ture of turbulence in nonpremixed flames', **SIAM - 6th International Conference on Numerical Combustion**, New Orleans, March 4-6, 1996.

A23 Elghobashi, S. and Ahmed, A. "On the two-way interactions between a turbulent homogeneous shear flow and dispersed particles", **Eighth Workshop on Turbulent Two-Phase Flows**, Merseburg, Germany, March 25-29, 1996.[Invited lecture]

A24 Elghobashi, S. " How do particles modify the turbulence energy of homogeneous shear flows ?", **ASME Fluids Engineering Conference**, San Diego, CA, July 8-11, 1996. [Invited Lecture]

A25 Elghobashi, S. and Ahmed, A. " How do particles modify the turbulence energy of homogeneous shear flows ?", **49th Annual Meeting of American Physical Society**, Div. Fluid Dynamics, Syracuse, NY, November 1996.

A26 Elghobashi, S., Zhong, R. and Boratav, O. " Evolution of flame surface in buoyant and nonbuoyant turbulent nonpremixed reactions", **49th Annual Meeting of American Physical Society**, Div. Fluid Dynamics, Syracuse, NY, November 1996.

A27 Latz, M., Juhl, A., Elghobashi, S., Ahmed, A. and Rohr, J. "Response of di-noflagellates in well-characterized laminar and turbulent flows: differentiating the effect of shear and acceleration", **Annual meeting of the American Society of Limnology and Oceanography (ASLO)**, Santa Fe, New Mexico, February 1997.

A28 Druzhinin, O. and Elghobashi, S. " A closure model for bubble-laden turbulent flows" **ONR workshop on Dynamics of Bubbly Flows**, UCSD, February 19-21, 1997.

A29 Elghobashi, S. " Modification of a homogeneous turbulent shear flow by dispersed particles" **Workshop on Turbulence Transport and Numerical Modeling**, **Center for Nonlinear Studies**, Los Alamos National Laboratory, June 3-7, 1997.[Invited Lecture]

A30 Elghobashi, S. and Druzhinin, O. " DNS of bubble-laden turbulent flows using the two-fluid formulation" **50th Annual Meeting of American Physical Society**, Div. Fluid Dynamics, San Francisco, CA, November 1997.

A31 Boratav, O., Elghobashi, S. and Zhong, R. " Persistence of strain in buoyant and nonbuoyant turbulent nonpremixed flames" **50th Annual Meeting of American Physical Society**, Div. Fluid Dynamics, San Francisco, CA, November 1997.

A32 Elghobashi, S. and Druzhinin, O. " DNS of bubble-laden turbulent flows using the two-fluid formulation" **ONR workshop on Dynamics of Bubbly Flows**, Caltech, February 25-27, 1998.

A33 Druzhinin, O. and Elghobashi, S. " A Lagrangian-Eulerian mapping solver for DNS of a bubble-laden homogeneous turbulent shear flow using the two-fluid formulation" **51st Annual Meeting of American Physical Society, Div. Fluid Dynamics, Philadelphia, PA**, November 22-24, 1998. Published in **Bulletin of APS, Vo. 43, 1965-2144, 1998.**

A34 Druzhinin, O. and Elghobashi, S. " A bubble-laden turbulent mixing layer: DNS and Closure model" **ONR workshop on Dynamics of Bubbly Flows, UCSD**, February 24-26, 1999.

A35 Druzhinin, O. and Elghobashi, S. " On the point-force approximation in DNS of particle-laden flows with two-way coupling " **51st Annual Meeting of American Physical Society, Div. Fluid Dynamics, New Orleans, LA** November 21-23, 1999. Published in **Bulletin of APS, Vol. 44, 15-194, 1999**

A36 Druzhinin, O. and Elghobashi, S. " DNS and Closure model for a bubble-laden turbulent mixing layer." **ONR workshop on Dynamics of Bubbly Flows, CALTECH**, March 1-3, 2000. *

A37 Druzhinin, O. and Elghobashi, S. " On the point-force approximation in DNS of particle-laden turbulent flows with two-way coupling", **ERCOFTAC Conference on Dynamics of Particle-Laden Flows, Zurich, Switzerland**, July 3-5, 2000.

A38 Elghobashi, S. " Recent Advance in DNS of Particle-Laden Turbulent Flows" [Invited Plenary lecture], **XI Congress on Numerical Methods and their Applications, ENIEF 2000** ,San Carlos de Bariloche, Argentina, November 2000.

A39 Druzhinin, O. and Elghobashi, S. " The properties of a spatially-developing bubble-laden mixing layer with two-way coupling" **53rd Annual Meeting of American Physical Society, Div. Fluid Dynamics, Washington D.C.**, November 2000.

A40 Ahmed, A. and Elghobashi, S. " On the physical mechanisms of modifying the structure of turbulent homogeneous shear flows by dispersed particles " **53rd Annual Meeting of American Physical Society, Div. Fluid Dynamics, Washington D.C.**, November 2000.

A41 Elghobashi, S. E." DNS of bubble-laden turbulent shear flows ", **ONR bubbly flow workshop, CALTECH, Pasadena**, April 17-19, 2001.

A42 Druzhinin, O. and Elghobashi, S. 'Direct numerical simulation of a three-dimensional spatially-developing bubble-laden mixing layer with two-way coupling', **4th International Conference on Multiphase Flow-ICMF 2001**, New Orleans, May 26-31, 2001.

A43 Elghobashi, S. “ The physical mechanisms of modifying the structure of turbulent homogeneous shear flows by dispersed particles ”, **Euromech Colloquium 421: Strongly-Coupled Dispersed Two-Phase Flows** , LEGI, Grenoble, France, September 10-12, 2001.

A44 Elghobashi, S. “ The physical mechanisms of modifying the structure of turbulent homogeneous flows by dispersed particles ”, [Invited Plenary Lecture], **ERCOTAC Conference on Small Particles in Turbulence** , Seville, Spain, March 11-13, 2002.

A45 Elghobashi, S. and Ferrante, A. “ DNS of bubble-laden spatially-developing turbulent boundary layer with one-way coupling” **ONR workshop on Dynamics of Bubbly Flows**, UCSD, La Jolla, Calif., April 3-4, 2002.

A46 Ferrante, A. and Elghobashi, S. “ Dispersion of bubbles in a spatially-developing turbulent boundary layer” **55th Annual Meeting of American Physical Society**, Div. Fluid Dynamics, Dallas, Texas, November 2002.

A47 Elghobashi, S. and Ferrante, A. “ DNS of bubble-laden spatially-developing turbulent boundary layer with two-way coupling” **ONR workshop on Waves and Dynamics of Bubbly Flows**, Caltech, Pasadena, Calif., February 19-20, 2003.

A48 Elghobashi, S. and Ferrante, A. “ DNS of bubble-laden spatially-developing turbulent boundary layer” **5th Euromech Fluid Mechanics Conference**, Toulouse, France, August 24-28, 2003.

A49 Ferrante, A. and Elghobashi, S. “ Drag reduction in a spatially-developing turbulent boundary layer laden with microbubbles,” **ERCOTAC Multiphase Flow Conference**, ETH, Zurich, Switzerland, November, 2003.

A50 Elghobashi, S. and Ferrante, A. “ Drag reduction in a bubble-laden spatially-developing turbulent boundary layer over a flat plate”, **56th Annual Meeting of American Physical Society**, Div. Fluid Dynamics, East Rutherford, New Jersey, November 2003. Published in **Bulletin of APS**, Vol. 48, p.116, 2003.

A51 Ferrante, A. and Elghobashi, S. “ A method for generating inflow conditions for direct simulations of spatially-developing turbulent boundary layers” **56th Annual Meeting of American Physical Society**, Div. Fluid Dynamics, East Rutherford, New Jersey, November 2003. Published in **Bulletin of APS**, Vol. 48, p.119, 2003.

A52 Elghobashi, S. and Ferrante, A. “ The physical mechanisms of drag reduction in a microbubble-laden turbulent boundary layer with one-way coupling” **ONR workshop on Dynamics of Bubbly Flows**, UCSD, La Jolla, Calif., March 24-25, 2004.

- A53** Elghobashi, S. "On the physical mechanisms of drag reduction in a microbubble-laden turbulent boundary layer" **Keynote Lecture at The 5th International Conference of Multiphase Flow (ICMF 2004)**, Yokohama, Japan, May 31 - June 3, 2004.
- A54** Elghobashi, S. "On the drag reduction in a microbubble-laden spatially-developing turbulent boundary layer", IUTAM Symposium on Recent advances in disperse multi-phase flow simulation- **[Invited Lecture]**- Chicago-October 2004.
- A55** Ferrante, A. and Elghobashi, S. "Effects of bubble diameter on drag reduction in a spatially developing turbulent boundary layer over a flat plate", **57th Annual Meeting of American Physical Society**, Div. Fluid Dynamics, Seattle, Washington, November 2004. Published in **Bulletin of APS**, Vol. 49, p.129, 2004.
- A56** Elghobashi, S. "On the drag reduction in a microbubble-laden spatially-developing turbulent boundary layer", **ONR workshop on Dynamics of Bubbly Flows**, Reston, VA, April 4-5, 2005.
- A57** Elghobashi, S. "Reynolds number effect on drag reduction in a microbubble-laden spatially-developing turb. boundary layer", **Euromech Conference on Hydrodynamics of bubbly flows- [Invited Lecture]**- Lorentz Center, Leiden, the Netherlands, June 6-8, 2005.
- A58** Elghobashi, S. "On drag reduction in a microbubble-laden spatially-developing turbulent boundary layer", **European Science Foundation- Challenging Turbulent Lagrangian Dynamics**, **[Invited Lecture]**- Castel Gandolfo, Italy, Sept. 1-4, 2005.
- A59** Elghobashi, S. "On drag reduction in a microbubble-laden spatially-developing turbulent boundary layer", **Thirteen IUTAM Advanced School & Workshop, Particle Dispersion in Turbulent Flows**, **[Invited Lecture I]**- CISM, Udine, Italy, September 12-16, 2005.
- A60** Elghobashi, S. "Reynolds number effect on drag reduction in a microbubble-laden spatially-developing turb. boundary layer", **Thirteen IUTAM Advanced School & Workshop, Particle Dispersion in Turbulent Flows**, **[Invited Lecture II]**- CISM, Udine, Italy, September 12-16, 2005.
- A61** Ferrante, A. and Elghobashi, S. "Effects of microbubbles on the Taylor-Green vortex flow", **58th Annual Meeting of American Physical Society**, Div. Fluid Dynamics, Chicago, IL, November 2005. Published in **Bulletin of APS**, Vol. 50, p.130, 2005.
- A62** Elghobashi, S. and Ferrante, A. "Reynolds number effect on drag reduction

in a microbubble-laden spatially-developing turbulent boundary layer ” , **58th Annual Meeting of American Physical Society**, Div. Fluid Dynamics, Chicago, IL, November 2005. Published in **Bulletin of APS**, Vol. 50, p.132, 2005.

A63 Elghobashi, S. “ On the accuracy of the two- fluid formulation in DNS of a microbubble-laden turbulent boundary layer”, **ONR 2006 Ship Wave-breaking and Bubble Wake Review**, Caltech, Pasadena, CA, March 29-30, 2006.

A64 Ferrante, A. and Elghobashi, S. “ On the accuracy of the two-fluid formulation in DNS of bubble-laden turbulent boundary layers” , **59th Annual Meeting of American Physical Society**, Div. Fluid Dynamics, Tampa, FL, November 2006. Published in **Bulletin of APS**, Vol. 51, 2006.

A65 Elghobashi, S. “ DNS of the two-way interactions between dispersed solid particles and turbulent flows”, **Workshop on multiphase turbulence: Dust storms, erosion, hurricanes and tornadoes**, [Invited Lecture], Xian, China, July 16-18, 2007.

A66 Ferrante, A. and Elghobashi, S. “ Fully resolved DNS of freely moving finite-size particles in decaying isotropic turbulence” , **60th Annual Meeting of American Physical Society**, Div. Fluid Dynamics, Salt Lake City, UT, November 2007. Published in **Bulletin of APS**, Vol. 52, 2007.

A67 Cleckler, J., Liu, F. and Elghobashi, S. “ Aerosol particle motion induced by non-linear sound waves” , **61th Annual Meeting of American Physical Society**, Div. Fluid Dynamics, San Antonio, Texas, November 2008. Published in **Bulletin of APS**, Vol. 53, 2008.

A68 Elghobashi, S. “On the two-way interactions between dispersed solid particles and turbulent flows”, **European Workshop on Direct and Large-Eddy Simulation, Keynote Lecture**, Trieste, Italy, Sept. 8-10, 2008.

A69 Lucci, F., Ferrante, A. and Elghobashi, S. “ DNS of fully resolved spherical particles dispersed in isotropic turbulence ” , **61th Annual Meeting of American Physical Society**, Div. Fluid Dynamics, San Antonio, Texas, November 2008. Published in **Bulletin of APS**, Vol. 53, 2008.

A70 Elghobashi, S. “ On the two-way interactions between dispersed particles and turbulent flows ”, [Invited Lecture], **March 2009 Meeting of American Physical Society** Pittsburgh, PA . Published in **Bulletin of APS**, Vol. 54, 209, March 18, 2009.

A71 Elghobashi, S. “ The physical mechanisms of two-way interactions between dispersed particles and turbulent flows” , **Workshop on Clouds and Turbulence Institute for Mathematical Sciences**, Imperial College, [Invited Lecture], London, England,

March 23-25, 2009.

A72 Elghobashi, S. “ How do inertial particles modify isotropic turbulence ?” **International Workshop- Solving the Riddle of Turbulence: What, Why, and How?** Max Planck Institute for Dynamics and Self-Organization, [Invited Lecture], Göttingen, Germany, May 6-9, 2009.

A73 Elghobashi, S. “How do inertial particles modify isotropic turbulence ?” **International Symposium on Turbulence**, [Invited Lecture], Peking University, Beijing, China, Sept. 21-25, 2009.

A74 Lucci, F., Ferrante, A. and Elghobashi, S. “ On the effects of Taylor-lengthscale size particles on isotropic turbulence ”, **62nd Annual Meeting of American Physical Society, Div. Fluid Dynamics**, Minneapolis, Minnesota. Published in Bulletin of APS, Vol. 54, No. 19, p. 159, November 20-23, 2009.

A75 Lucci, F., Ferrante, A. and Elghobashi, S. “ Is Stokes number an appropriate indicator for turbulence modulation by particles of Taylor-length-scale size? ”, **63rd Annual Meeting of American Physical Society, Div. Fluid Dynamics**, Long Beach, California. Published in Bulletin of APS, Vol. 55, No. 16, p. 150, November 20-23, 2010.

A76 Cleckler, J., Liu, F. and Elghobashi, S. “ Numerical simulation of particle dispersion in an acoustic field ”, **63rd Annual Meeting of American Physical Society, Div. Fluid Dynamics**, Long Beach, California. Published in Bulletin of APS, Vol. 55, No. 16, p. 319, November 23, 2010.

A77 Lucci, F., L’Vov, V., Ferrante, A. and Elghobashi, S. “ On the Lagrangian Power Spectrum of Turbulence Energy in Isotropic Turbulence ”, **64th Annual Meeting of American Physical Society, Div. Fluid Dynamics**, Baltimore, MD , Published in Bulletin of APS, Vol. 56, No. 18, p. 80, November 20-22, 2011.

A78 Wang, Y. and Elghobashi, S. “ Direct numerical simulation of the flow in the pediatric upper airway ”, **34th Annual Int. Conf. of the IEEE Engineering in Medicine & Biology (EMB) Society**, San Diego, CA, August 28-September 1, 2012.

A79 Wang, Y. and Elghobashi, S. “ Direct numerical simulation of the flow in the human upper airway ”, **65th Annual Meeting of American Physical Society, Div. Fluid Dynamics**, San Diego, CA , Published in Bulletin of APS, Vol. 57, No. 17, p. 333, November 18-20, 2012.

A80 Wang, Y. and Elghobashi, S. “ On locating the obstruction in the human upper airway, Direct numerical simulation ”, **66th Annual Meeting of American Physical Society, Div. Fluid Dynamics**, Pittsburgh, PA, November 24-26, 2013.

A81 Y. Wang, L. Oren, E. Gutmark a and S. Elghobashi, “ DNS and PIV measurements of the flow in a model of the human upper airway”, **67th Annual Meeting of American Physical Society, Div. Fluid Dynamics**, San Francisco, CA, November 23-25, 2014.

Technical Reports

Yeh, G.C.K. and Elghobashi, S.E., "A Two-Equation Turbulence Model for a Dispersed Two-Phase Flow with Variable Density Fluid and Constant Density Particles", Defense Nuclear Agency Report DNA-TR-86-42, 1986.

Elghobashi, S.E. and Rizk, M.A., "The Effect of Solid Particles on the Turbulent Flow of a Round Gaseous Jet: A Mathematical and Experimental Study", DOE/PC,30303-5, December (1983).

Wassel, A.T., Elghobashi, S.E., and Wenger, R.S., "Analysis of the Sea Water Systems of Ocean Thermal Energy Conversion Pilot Plants", SAI Report No. 82R-018-LA, October (1982).

Bellam, J. and Elghobashi, S.E., "Present and Projected Status of Computer Modeling in Furnace and Boiler Technology", US DOE, Jet Propulsion Lab. Report, Nov. (1982).

Elghobashi, S.E., Lockwood, F.C. and Naguib, A.S., "The Calculation of Combustion Processes", Imperial College Mech. Engr. Dept., HTS/74/8, (1974).

Elghobashi, S.E., Pun, W.M., "A Theoretical and Experimental Study of Turbulent Diffusion Flames in Cylindrical Chambers", Imperial College, Mech. Engr. Dept., HTS/74/3, (1974).

Elghobashi, S.E., "Concentration Fluctuations in Isothermal Turbulent Confined Jets", Imperial College, Mech. Engr., HTS/75/23, (1975).

Elghobashi, S.E., "Prediction of the Three Dimensional Flow and Radiation Heat Transfer Inside a Cylindrical Glass Furnace", for Corning, (1977).

Elghobashi, S.E., "Prediction of the Three Dimensional Flow Inside a Liquid- Metal Fast-Breeder Reactor Steam Generator", for Westinghouse, (1978).

Elghobashi, S.E., "Prediction of the Flow and the Concentration of CO and NO_x inside a Burning Cigarette", for Philip Morris, (1977).

Elghobashi, S.E., "Prediction of the Flow Around the Earth and the Influence of Temperature Gradients on Both Hemispheres", for NASA Marshall, (1977).

Elghobashi, S.E., "Prediction of the Flow Inside a Crystal-Growth Device at Near-Zero Gravity", for NASA Marshall, (1978).

Elghobashi, S.E., "Prediction of the Effects of Low Gravity and Heat Transfer on the Trajectories of Blood Cells in an Electrophoresis Chamber", for NASA Marshall, (1978).

Elghobashi, S.E., "Prediction of the Flow and Electrical Properties of a Rocket Exhaust Plume", for US Air Force, (1978).

Elghobashi, S.E., Spalding, D.B. and Thyagraja, A., "Prediction of Three Dimensional Supersonic Flow of a Conical Body Interacting with a Plane Blast Wave", prepared for Ballistic Missile Defense Advance Technology Center, Huntsville, (1976).

Elghobashi, S.E., "Prediction of Transient Flow and Heat Transfer in 155 MM Gun Barrel and its Exhauster", prepared for Rheinmetall, West Germany (1976).

Elghobashi, S.E., "Prediction of Three Dimensional flow and Chemical Reaction in a Can Combustor with Fuel Spray", prepared for Airesearch Co. of Arizona (1976).

Elghobashi, S.E., Spalding, D.B. and Srivatsa, S.K. "Prediction of Three Dimensional Flow in a Hall-Cell Aluminum Smelter", prepared for ALCOA (1975).

Elghobashi, S.E., Moulton, A. and Spalding, D.B., "Prediction of Compressible Flow in the Combustion Chamber of a Solid-Propellant Rocket" prepared for Societe National des Poudres et Explosifs, France (1975).

Elghobashi, S., Rosten, H. and Spalding, D.B., "Effects of gravity on Methane-air combustion", **NASA-CR 2671**, (1974).

Elghobashi, S., Pratt, D.T., Runchal, A.K., Spalding, D.B. and Srivatsa, S.K. "Unsteady combustion of fuel spray in jet engine afterburners, The CID4 computer program," CHAM 551/1, (1975).

Elghobashi, S., Spalding, D.B. and Srivatsa, S.K., "Prediction of hydrodynamics and chemistry of confined turbulent methane-air flames with attention to formation of oxides of nitrogen," **NASA CR-135179**, (1977).

Elghobashi, S. and Spalding, D.B., "Equilibrium chemical reaction of supersonic hydrogen-air jets (The ALMA computer program)", **NASA CR-2725**, (1977).

Invited Research Presentations (1983- Present)

“How do dispersed inertial particles modify turbulent flows ?” **École Polytechnique, The Hydrodynamics Laboratory (LadHyX), Palaiseau, France**, June 14, 2013.

“How do dispersed inertial particles modify turbulent flows ?” **University of California, San Diego**, Mechanical and Aerospace Engineering Dept., June 3, 2013.

“Direct numerical simulation of the flow in the upper airway via lattice Boltzmann method” **National Institute of Health**, Bethesda, MD, April 29, 2013.

“On the physical mechanisms of drag reduction in a spatially-developing turbulent boundary layer laden with microbubbles ” **École Normal Supérieure, Paris, France**, March 17, 2011.

“Direct numerical simulation of the flow in the upper airway via lattice Boltzmann method” **National Institute of Health**, Bethesda, MD, Feb. 24, 2011.

“Turbulence modulation by dispersed inertial particles” Mech. Eng. Dept., **Univ. of California, Berkeley**, February 11, 2011.

“ On the two-way interactions between dispersed particles and turbulent flows” **School of Engineering and Mathematical Sciences, City University, London, England**, March 26, 2009.

“On the effects of finite-size solid particles on decaying isotropic turbulence”, **Institut de Mécanique des Fluides de Toulouse, IMFT, Toulouse, France**, June 28, 2007.

“On the physical mechanisms of drag reduction in a spatially-developing turbulent boundary layer laden with microbubbles ” **Ecole Polytechnique, The Hydrodynamics Laboratory (LadHyX), Palaiseau, France**, June 26, 2007.

“Turbulence modification in flows laden with particles or bubbles” **The Johns Hopkins University**, Mechanical Engineering Department, February 15, 2007.

“ Direct simulation of turbulent flows laden with particles or bubbles”, **Invited Lecture, CIEMAT : Research Centre for Energy, Environment and Technology, Madrid, Spain**, June 21, 2006.

”On drag reduction in a spatially-developing turbulent boundary layer laden with microbubbles”, **Department of Mechanics and Aeronautics, University of Rome ”La Sapienza”, Rome,, Italy**, September 5, 2005.

“On the drag reduction in a microbubble-laden spatially-developing turbulent boundary

layer,” **School of Mechanical and Aerospace Engineering, Center for Turbulence and Flow Control Research, Seoul National University, Seoul, South Korea, May 27, 2005.**

“On the physical mechanisms of drag reduction in a microbubble-laden turbulent boundary layer”, **Department of Mechanical Engineering, University of Tokyo, Japan, June 7, 2004.**

“On the physical mechanisms of drag reduction in a spatially-developing turbulent boundary layer laden with microbubbles”, **Mech. Eng. Dept., Univ. California, Santa Barbara, California, February 14, 2004.**

“Recent advances in DNS of particle-laden turbulent flows ”, **Institute for Scientific Computing Research, Lawrence Livermore Research Laboratory, Livermore, California , August 7, 2003.**

“DNS of turbulent flows laden with particles ”, **Institute for Scientific Computing Research, Lawrence Livermore Research Laboratory, Livermore, California , March 27, 2003.**

“ On the physical mechanisms of modifying the structure of turbulent homogeneous shear flows by dispersed particles”, **Mechanical Engineering Dept., Stanford University, Stanford, California, October 30, 2001.**

“Recent Advances in DNS of Turbulent Flows Laden with Particles, Droplets or Bubbles”, **Universite Pierre et Marie Curie, Paris, France, September 19, 2001.**

“Recent advances in direct numerical simulations (DNS) of turbulent shear flows laden with particles ”, **Institute for Scientific Computing Research, Lawrence Livermore Research Laboratory, Livermore, California , May 4, 2001.**

“Recent Advances in DNS of Turbulent Flows Laden with Particles, Droplets or Bubbles”, **The Aerospace Corporation, Los Angeles, California, April 17, 2001.**

“Recent advances in direct numerical simulations (DNS) of turbulent shear flows laden with particles ”, **Institute for Scientific Computing Research, Lawrence Livermore Research Laboratory, Livermore, California , May 4, 2001.**

“ On the physical mechanisms of modifying the structure of turbulent homogeneous shear flows by dispersed particles ”, **ETH, Zürich, Switzerland, October 4, 2000.**

“ Recent advances in direct numerical simulations (DNS) of turbulent shear flows laden with particles ”, **Paul Scherer Institute, Villigen, Switzerland, October 3, 2000.**

" Recent advances in direct numerical simulations (DNS) of turbulent shear flows laden with particles and bubbles", **Mechanical Engineering Department, Imperial College, London**, April 6, 2000.

" Recent advances in direct numerical simulations (DNS) of turbulent shear flows laden with particles and bubbles", **Mechanical and Aerospace Engineering Department, Univ. California, San Diego**, March 15, 2000.

" Direct numerical simulation of particle-laden flows: the trajectory and two-fluid approaches", **Dept. of Mechanical Engineering, Univ. of Illinois, Urbana-Champaign**, November 9, 1999.

" Evolution of flame surface in buoyant and nonbuoyant turbulent nonpremixed reactions", **Graduate Aeronautical Laboratories, California Institute of Technology**, January 16, 1998.

" How do particles modify the turbulence energy in a homogeneous shear flow ?", **Department of Chemical Engineering, Univ. of California, Santa Barbara**, April 16, 1997.

" Direct numerical simulation of particle-laden homogeneous turbulent shear flows", **CEA : Atomic Energy Commission - Military Applications Division**, Bordeaux, France, April 2, 1997.

" Mathematical models of particle-laden flows", **CEA : Atomic Energy Commission - Military Applications Division**, Bordeaux, France, April 2, 1997.

" DNS of surface topology of turbulent nonpremixed flames ", **CEA : Atomic Energy Commission - Military Applications Division**, Bordeaux, France, April 2, 1997.

"Effects of buoyancy on turbulent diffusion flames", Dept. of Mechanical Engineering, **Yale University**, June 10, 1996.

"Particle dispersion and turbulence modification in a homogeneous shear flow", Dept. of Mechanical Engineering, **California Institute of Technology**, April 23, 1996.

" Particle dispersion and turbulence modulation in a homogeneous shear flow", Aerospace Engineering Dept., **University of Southern California**, October 4, (1995).

" DNS of particle dispersion in homogeneous shear turbulence" **Institut de Mecanique des Fluides de Toulouse, Toulouse, France**, September 12, (1995).

" DNS of a turbulent diffusion flame under different gravity conditions" **Institut de Mecanique des Fluides de Toulouse, Toulouse, France**, September 12, (1995).

" DNS of particle dispersion in homogeneous shear turbulence" **Technical University of Delft, Delft, Netherlands**, September 7, (1995).

" DNS of a turbulent diffusion flame under different gravity conditions" **Technical University of Delft, Delft, Netherlands**, September 7, (1995).

" On the two-way interaction between homogeneous turbulence and dispersed solid particles", **Naval Command, Control and Ocean Surveillance Center, San Diego, CA**, Oct. 19, 1993.

" On the two-way interaction between homogeneous turbulence and dispersed solid particles", **Arizona State University, Tempe, Arizona**, Oct. 8, 1993.

" Direct numerical simulation of particle dispersion and turbulence modulation in homogeneous turbulence", **NATO Advanced Research Workshop on Chaotic Advection, Tracer Dynamics, and Turbulent Dispersion, Alessandria, Italy**, May 24-28, 1993.

" On predicting particle-laden turbulent flows", Workshop on turbulence in particulate multiphase flow, **Fluid Dynamics Laboratory, Battelle Pacific Northwest Laboratory, Richland, WA**, March 22, 1993.

" On the two-way interaction between homogeneous turbulence and dispersed solid particles", **AMES Dept. Univ. of California, San Diego**, February 5, 1993.

" On the two-way interaction between homogeneous turbulence and dispersed solid particles", **NASA Langley Research Center**, December 14, 1992.

" On the modification of energy spectrum of homogeneous turbulence by dispersed solid particles", **Department of Mathematics, UCI**, May 21, 1992.

" The two-way coupling between solid particles and homogeneous decaying turbulence", **Mechanical and Aerospace Engineering Department, Princeton University**, August 23, 1991.

" Direct simulation of particle-laden homogeneous turbulence", **Los Alamos National Laboratory**, May 25, 1991.

"The effect of turbulence on the propagation of an electromagnetic wave in a compressible turbulent boundary layer", Workshop on Aerothermal Technology Development, **U.S. Strategic Defense Command , Huntsville, Alabama**, June 13, 1991.

"Direct numerical simulation and closure modelling of particle-laden turbulent flows", Workshop on Turbulence Simulation and Modelling , **NASA-Marshall, Huntsville**,

Alabama, April 14-15, 1991.

"Direct numerical simulation of particle dispersion in sheared and unsheared homogeneous turbulence", **Mechanical Engineering Department, University of Southern California**, March 1, 1990.

"Direct numerical simulation and modelling of particle-laden turbulent flows", **German Aerospace Organization (DLR), Munich, Germany**, December 4, 1989.

"Direct numerical simulation of particle dispersion in homogeneous turbulent flows", **University of Kaiserslautern , West Germany**, December 5, 1989.

"Direct numerical simulation of particle dispersion in isotropic and sheared turbulent flows", **Institut de Mecanique des Fluides, Toulouse, France**, December 6, 1989.

"Direct numerical simulation of particle dispersion in homogeneous turbulent flows", **University of Rouen, France**, December 7, 1989.

"Direct numerical simulation and modelling of particle-laden turbulent flows", **Shell Conference on Computational Fluid Dynamics, Apeldoorn, The Netherlands**, December 11, 1989.

"Direct numerical simulation of particle dispersion in homogeneous turbulent flows", **Norway Institute of Technology, Trondheim, Norway**, December 15, 1989.

"Direct numerical simulation of particle dispersion in grid-generated turbulence", **Workshop on droplets and sprays, AFOSR and ONR Contractors Meeting, Ann Arbor, Michigan**, June 21, 1989.

"Direct numerical simulation of particle dispersion and chemical reaction in turbulent flows", **G.M. Research Laboratory, Thermal Science Department, Warren, Michigan**, June 22, 1989.

"Direct numerical simulation of stratified turbulent homogeneous shear flow", **Idaho National Engineering Laboratory, Idaho Falls**, September 8, 1988.

"Direct numerical simulation of stratified turbulent homogeneous shear flow", **Center for Microgravity and Materials Research, University of Alabama, Huntsville**, August 5, 1988.

"Direct simulation of stable stratified turbulent homogeneous shear flows", **Third International Symposium on Stratified Flows, California Institute of Technology**, February 3-5, 1987.

"Direct simulation of the passive-scalar mixing layer", **Institut de Mecanique des Fluides, Toulouse, France**, September 11, 1987.

"Direct simulation of stratified homogeneous turbulent shear flow", **Department of Aerospace Engineering, University of Southern California**, October 8, 1986.

"Direct simulation of stratified homogeneous turbulent shear flow", **Institut de Mecanique Statistique de la Turbulence, Marseille, France**, October 22, 1986.

"Direct simulation of homogeneous turbulent shear flow", **Mechanical Engineering Department, University of California, Irvine**, July 22, 1986.

"Direct simulation of stratified homogeneous turbulent shear flow", **AMES Department, University of California, San Diego**, February 3, 1986.

"Direct simulation of turbulent shear flow with buoyancy", **Jet Propulsion Laboratory, California Institute of Technology**, May 30, 1986.

"Direct numerical simulation of a turbulent homogeneous shear flow with buoyancy", **Mechanical Engineering Dept., University of California, Irvine**, October 18, 1985.

"Direct simulation of turbulent homogeneous shear flow", **DFVLR, Institute of Atmospheric Physics, Oberpfaffenhofen, West Germany**, June 21, 1985.

"Prediction of the turbulent jet laden with vaporizing droplets" **Dept. of Fluid Mechanics, University of Erlangen, West Germany**, May 22, 1985.

"Experimental study of the turbulent jet laden with particles", **University of the German Armed Forces, Aerospace Department, Munich, West Germany**, February 7, 1985.

"Measurement and prediction of the turbulent two-phase jet", **University of Karlsruhe, Mechanical Engineering Dept.**, December 13, 1984.

"Prediction of the turbulent jet laden with solid spherical particles", **DFVLR, Institute of Atmospheric Physics, Oberpfaffenhofen, West Germany**, December 5, 1984.

"Recent developments in mathematical modeling of dispersed two-phase flows", presented at the **Mechanical Engineering Dept., Technical University of Munich, West Germany**, November 27, 1984.

"Recent developments in mathematical modeling of dispersed two- phase flows", presented at the **Mechanical Engineering Dept., University of California, Berkeley**, March 20, 1984.

"Effects of dispersed two-phase flows on turbulence structure", **Office National d'Etudes et de Recherches Aeronautiques (ONERA), Paris, France**, September 19, 1983.

"Turbulence modulation in a turbulent two-phase jet : theory and experiment", **Mechanical Engineering Department, University of Kaiserslautern, West Germany**, September 16, 1983.

"Passive-scalar time-scales in turbulent flows", **DFVLR, Institute of Atmospheric Physics, Oberpfaffenhofen, West Germany**, September 15, 1983.

"Mathematical models of temperature variance and time-scales for the thermal mixing layer ", **Institut de Mecanique Statistique de la Turbulence, Marseille, France**, July 8, 1983.

"Experimental and theoretical study of dispersed two-phase turbulent jets", **Institut de Mecanique des Fluides, Toulouse, France**, July 6, 1983.

EXHIBIT DX37

TO DECLARATION OF PETER J. GOSS IN
SUPPORT OF DEFENDANTS' MOTION TO
EXCLUDE PLAINTIFFS' ENGINEERING
EXPERTS

**UNITED STATES DISTRICT COURT
DISTRICT OF MINNESOTA**

In re Bair Hugger Forced Air Warming
Products Liability Litigation

MDL No. 15-2666 (JNE/FLN)

This Document Relates to All Actions

**EXPERT REPORT OF
MICHAEL W. BUCK**

I. SUMMARY OF QUALIFICATIONS & EXPERIENCE

A. Education and Training

My education and training have been focused on biology. I received a Bachelor of Arts in Biology, with Concentrations in Physical Science, Chemistry, Economics, and Psychology from Minot State University in 1989. I nearly completed a Master's Degree in Public Health in Industrial Hygiene at the University of Minnesota (39 graduate credits completed).

I have two recent publications: *Chapter 5: Air Monitoring for Quality Evaluation in Healthcare*, APIC 2015 INFECTION PREVENTION MANUAL FOR CONSTRUCTION AND RENOVATION, and DISPLACEMENT VENTILATION AS A VIABLE AIR SOLUTION FOR HOSPITAL PATIENT ROOMS (2010). Since 2003, I have provided presentations at various conferences on issues relating to industrial hygiene in the healthcare setting.

I have the following current certifications: Asbestos Contractor Supervisor Training certified by the Minnesota Department of Health (MDH); Recognition of Indoor Air Quality Issues from the Midwest Center for Occupational Health and Safety; Introduction to Food and Air-Borne Fungi certification from the Centraal bureau voor Schimmelcultures Institute of the Royal Academy of Arts and Sciences at the University of Ottawa; Applied Thermographer – Infrared Technology certification from Restoration Consultants; NIOSH 582 – Asbestos Air Analysis certification from Delta Environmental Consultants; Building Inspector Hazardous

Materials; Asbestos Abatement Site Supervisor. In the past I have been certified as an OSHA 501 Certified Trainer; an Asbestos Project Designer; a Lead Risk Assessor, and a Lead Inspector. A copy of my Curriculum Vitae is attached as Exhibit A.

B. Experience

For over 25 years, I have worked in the Department of Environmental Health and Safety at the University of Minnesota. For over seventeen years, I have been an Environmental Health and Safety Compliance Specialist in the Department of Environmental Health and Safety at the University of Minnesota. In this capacity I have been responsible for conducting indoor air quality investigations, and have coordinated remediation activities. I am responsible for coordinating sample collection from the University Hospital's anesthetic gas employee exposure program, I manage the Departments' Micro Lab (including sample tracking and analysis), and I repair and maintain the Department air quality sampling equipment. Part of my current duties include review of various construction plans and evaluation of IAQ concerns. In addition, I audit the Facilities Management Hazardous Material Program, and work with outside contractors on abatement projects. From 1991 – 2000, I was a Principal Safety Technician in the Department of Environmental Health and Safety at the University of Minnesota, where my principal responsibilities included conducting building hazard assessments, as well as identifying and supervising asbestos identification and abatement projects.

C. Medical/Legal Work Experience

Over the past ten years, I have been retained as an expert consultant on issues relating to hospital certification of critical care environments, including the BMT (Bone Marrow Transplant), ICU (Intensive Care Unit), NICU (Neonatal Intensive Care Unit), and OR (Operating Room), ventilation systems, and air and surface sampling. In my capacity as a consultant I have provided training on HVAC mechanics, as well as water infiltration remediation measures to various building managers. I have also provided consulting on industrial hygiene issues to real estate property management companies. As a consultant, my time is billed at \$200/hour, \$3,000 per day for deposition testimony, and \$6,000 per day for trial testimony. I have provided no testimony by way of deposition and/or trial over the past four years.

II. QUESTION PRESENTED

I was retained to evaluate whether or not the Bair Hugger Forced Air Warming System generates and/or omits particles.

III. METHODOLOGY & METHODS

A. Methodology and Approach to Test for Potential Particles

Healthcare professionals and facilities care deeply about particles, as particles can transmit pathogens. Particles themselves can be extremely small. By way of example, Figure 1, below, shows the size of various pathogens, including

bacteria. As illustrated in Figure 1, the vast majority of bacteria range in size from .3 to 1.2 microns. To provide additional context, Figure 2 illustrates how “big” a micron is, by showing a grain of salt (60 μm), dust mite waste (20 μm), and staphylococcus aureus (0.9 μm), each placed upon a cross section of a human hair (which has a diameter of 100 μm) to show scale.

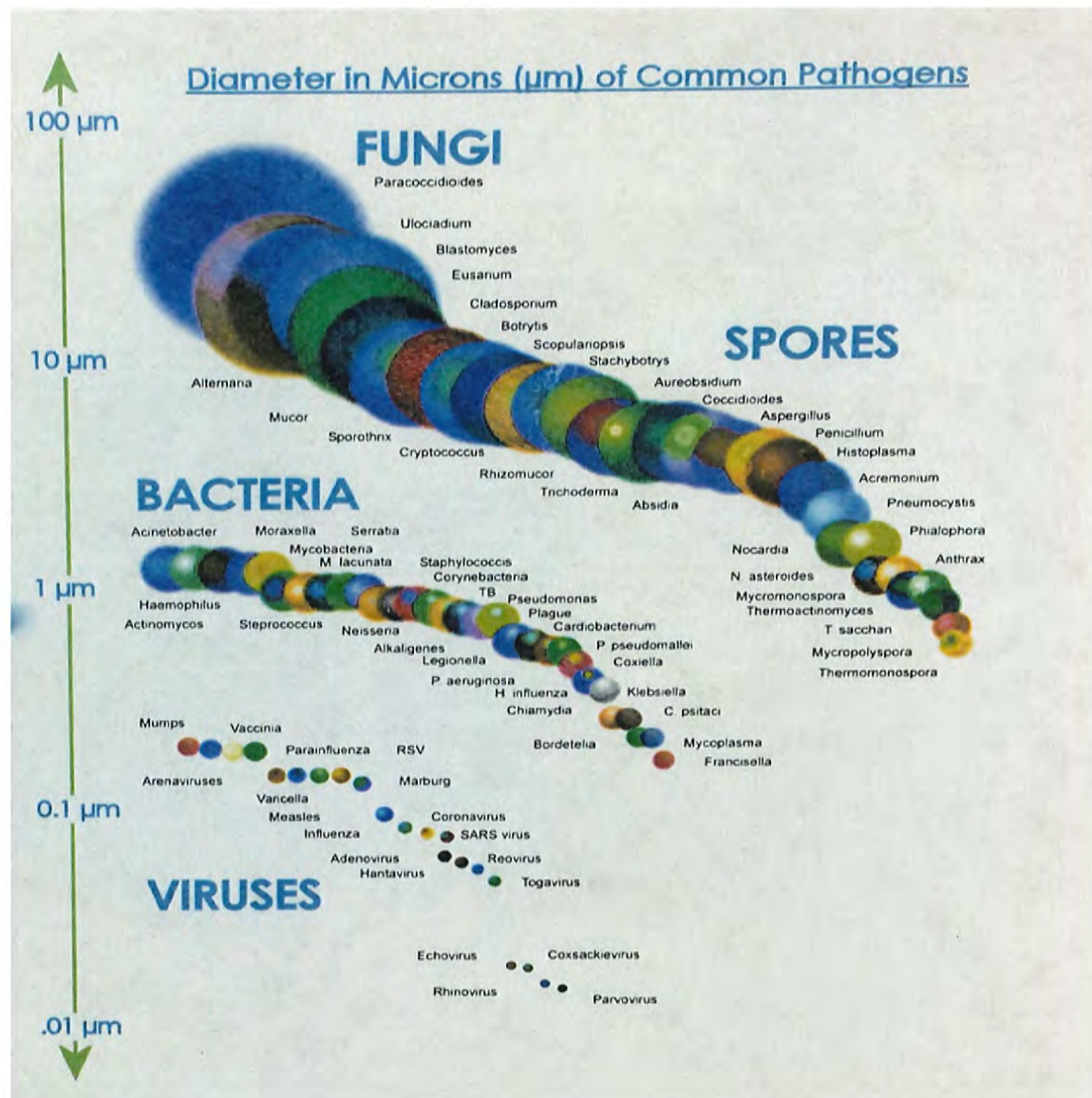


Figure 1

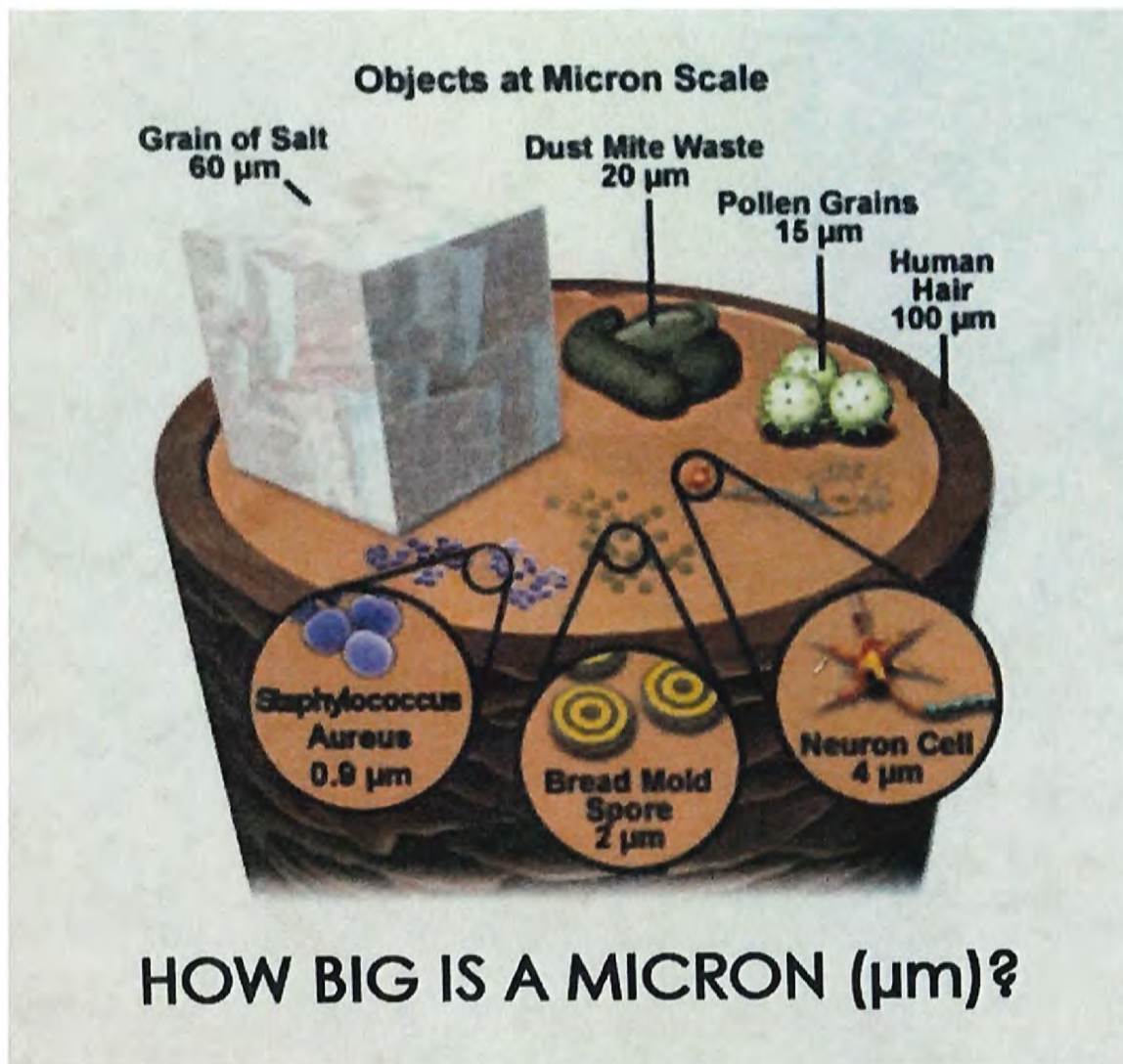


Figure 2

Because these particles are so small, specialized instrumentation is required to identify, measure and quantify them. The experiments discussed in this report were conducted in a cleanroom, using a particle counter.

A **cleanroom** or **clean room** is an environment, typically used in manufacturing, including of pharmaceutical products or scientific research. The cleanroom can be used to evaluate the source of particles. For example, a device such as a bubbling humidifier can be placed in the room and with manipulation of

airflow create an environment of droplet nuclei when saline is aerosolized. A comparison between particles generated by bubbling versus evaporation changed the way we deliver humidified air to patients. A filtered device that blows air can and should be evaluated in a clean room environment in the same manner to determine the difference – if any – with the applicable filter in place and with the applicable filter removed. This is considered an assessment of the *efficiency* of the filter.

A **particle counter** is a portable instrument that measures and reports air contamination. The particles can be differentiated into respective particle sizes using laser and optics to count sizes per unit volume of air. When the investigation includes air quality analysis, comparison data is useful to determine particle generation differences in mode of operation, location of filtration or difference in controls. For example what percentage reduction is observed from breathing zone particle sizes before and after using filtration for supplying air to a device. The experiments outlined below used a Fluke model 983 particle counter.

B. Material and Methods for Testing Bair Hugger Devices

1. Tests on the Machines

The Bair Hugger model units (1 used 750 series and 1 new 775 series) and its component parts (including the blower, filter, hose, and disposable blanket) were studied and evaluated to determine the number and size of any particles generated by the unit itself through normal operating procedures. This evaluation

was completed with a used Bair Hugger Model 750, and new Bair Hugger Model 775.¹ The filter efficiency was also evaluated by removing filter media and comparing and contrasting the number and size of particles recorded with the filter in-line versus when the filter was removed and the machine run without the filter in place.

The first evaluation was carried out in a HEPA filtered (99.97% for $.3\mu\text{m}$ sized particles) clean room using a laser optical particle counter that recorded differential particle sizes ranging from 0.3μ up to greater than 10μ in size. The particle counter isokinetic probe was mounted inside the Bair Hugger air supply hose with the Bair Hugger blower placed on the floor of the clean room.

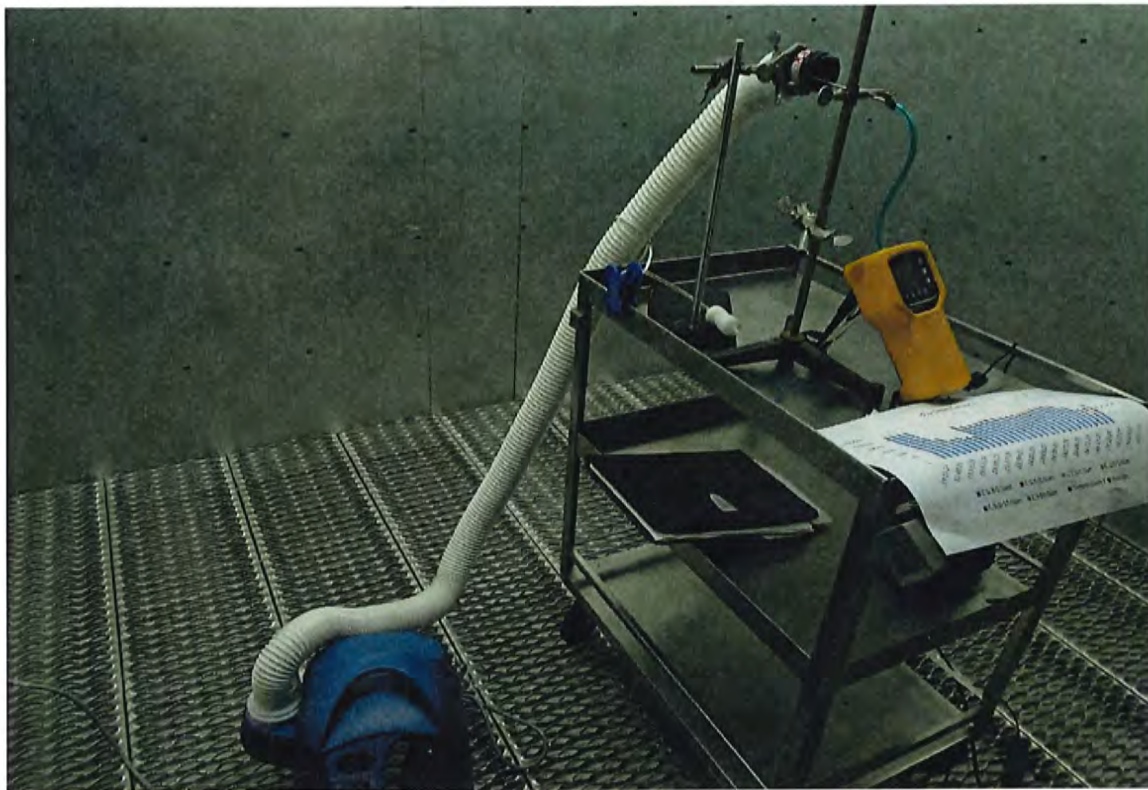


The Bair Hugger was evaluated using normal operating modes (ambient

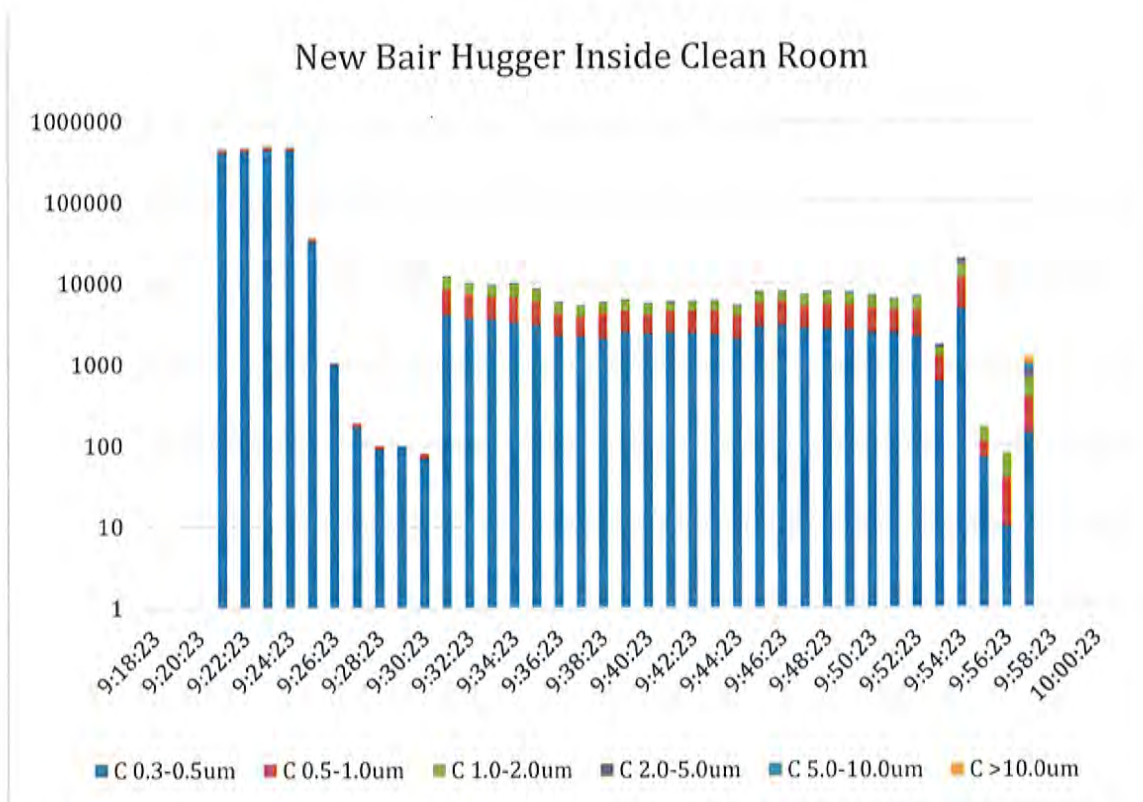
¹ Both Bair Hugger devices were Model 750, provided by MDL Plaintiffs' Counsel.

23°C, 38°C, 43°C, and blower unit on its side) to establish the initial discharge of air (particles) from the end of the air supply hose.



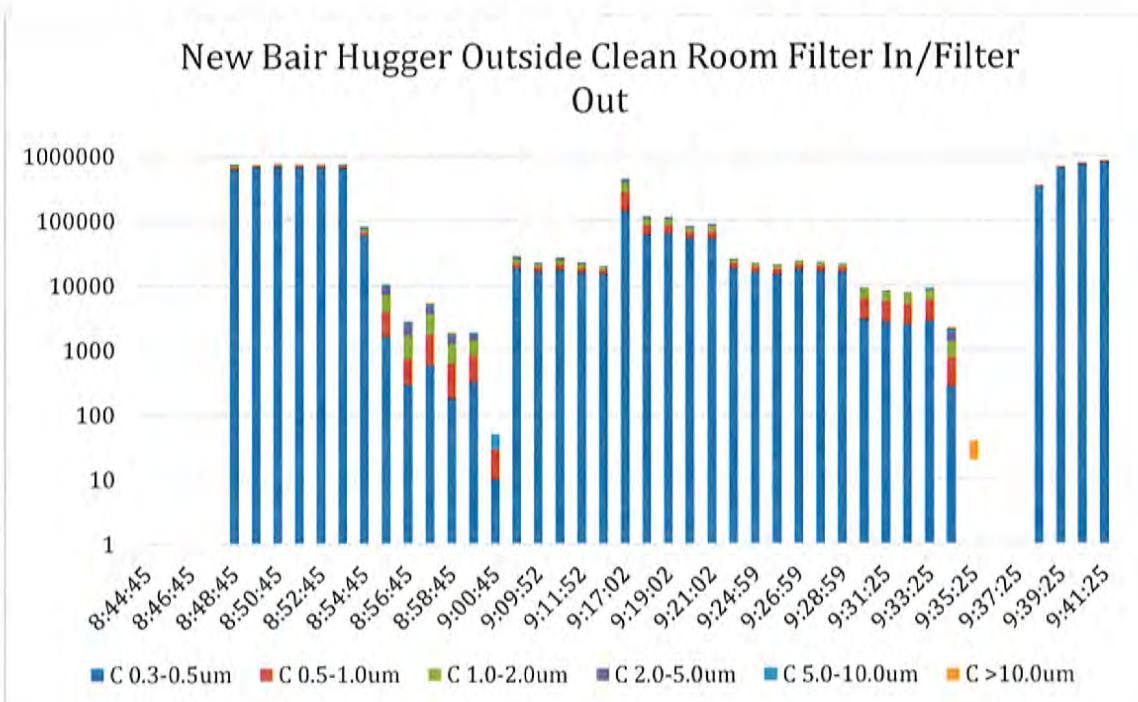
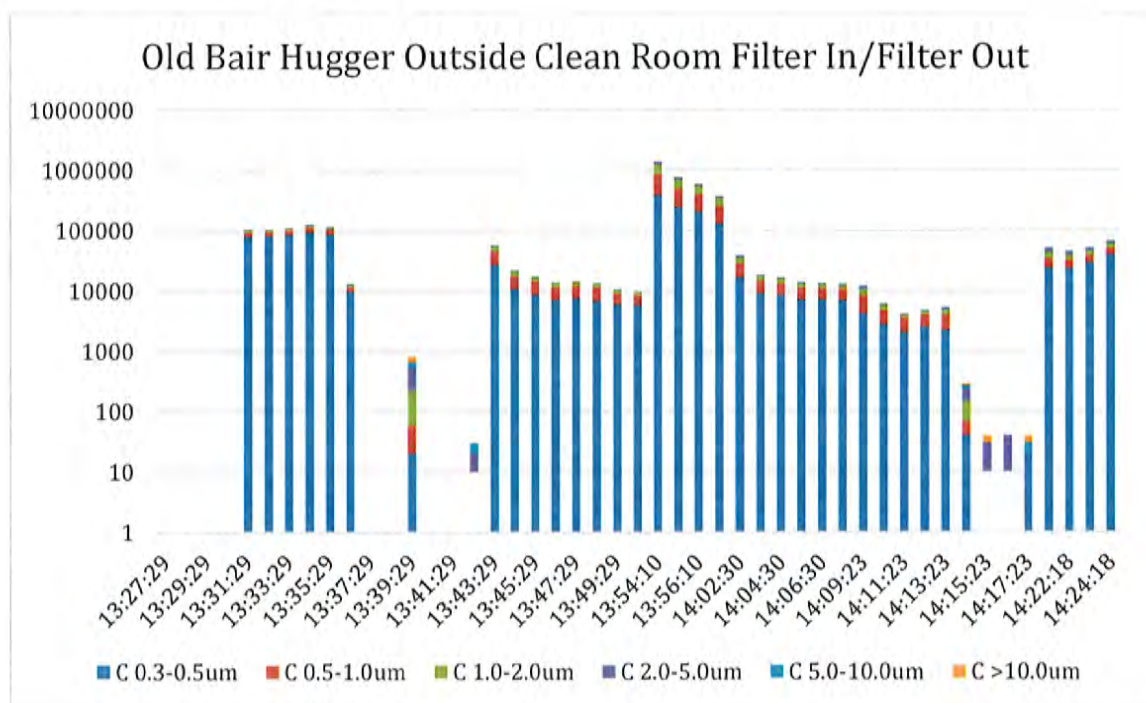


The evaluation of the air discharge was carried out through each operational mode and particle counts were collected at one minute intervals continuously through the end of the evaluation to validate air quality content of the Bair Hugger tested. This evaluation was completed with both a used Bair Hugger 750 and unused Bair Hugger model 775. These evaluations showed particles coming out of both the new and the used Bair Hugger devices.



A second evaluation was also carried out in a HEPA filtered (99.97% for .3 μ m sized particles) clean room using a particle counter that recorded differential particle sizes ranging from .3 μ m up to greater than 10 μ m in size. The particle counter isokinetic probe was mounted inside the Bair Hugger air supply hose which was placed inside the clean room to discharge. The Bair Hugger blower was placed outside the clean room on the floor. The Bair Hugger was evaluated using normal operating modes (ambient 23°C, 38°C, filter out, and filter in) to establish the initial discharge of air (particles) from the end of the air supply hose. The evaluation of the air discharge was carried out through each operational mode and particle counts were collected at one minute continuous intervals to validate air quality content and filter efficiency of the Bair Hugger tested. This evaluation was

also completed with both a used Bair Hugger Model 750 and new Bair Hugger model 775. Again, these evaluations showed particles coming out of both the new and the used Bair Hugger devices.



2. Tests on the Bair Hugger Machine with Blankets

A third evaluation was carried out in a HEPA filtered (99.97% for $.3\mu\text{m}$ sized particles) a simulated operating room using a laser optical particle counters that recorded differential particle sizes ranging from $.02\mu$ up to greater than 10μ in size. The particle counter isokinetic probe was mounted inside a container where the Bair Hugger air supply hose discharged with the Bair Hugger blower placed on the floor of the operating room.



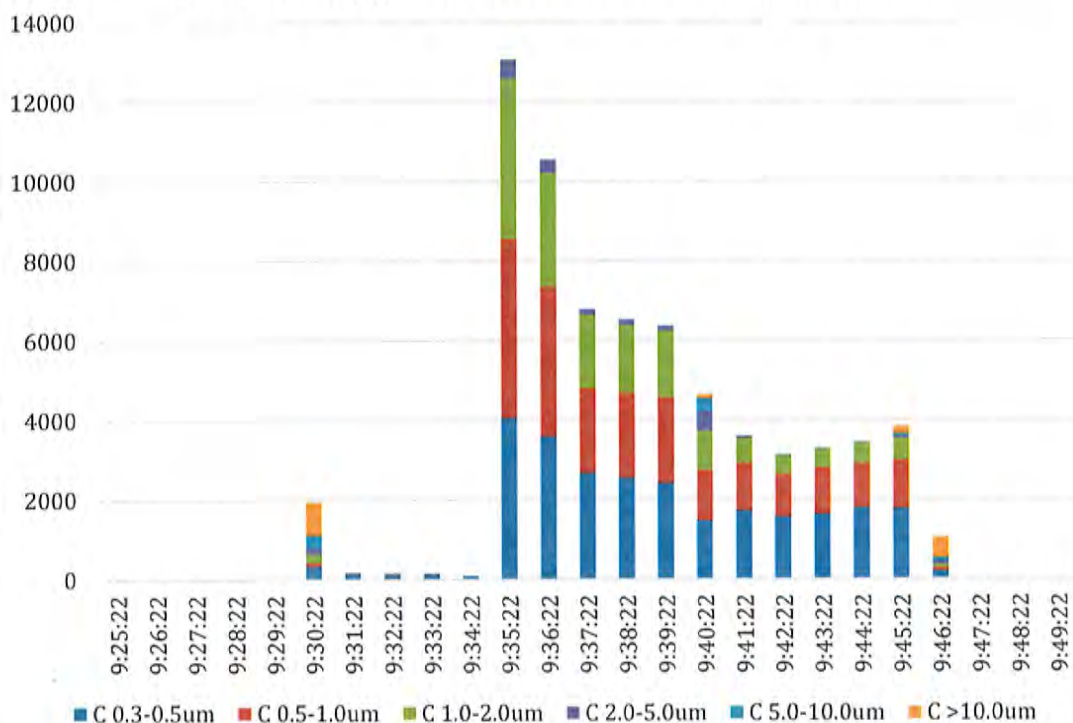


The Bair Hugger was evaluated using normal operating modes (43°C, and blanket paper side down) to establish the initial discharge of air (particles) from the end of the air supply hose. In addition, a new upper body blanket (Model 52200) was attached to the air supply hose inside the box and particles that were released from the blanket were measured.

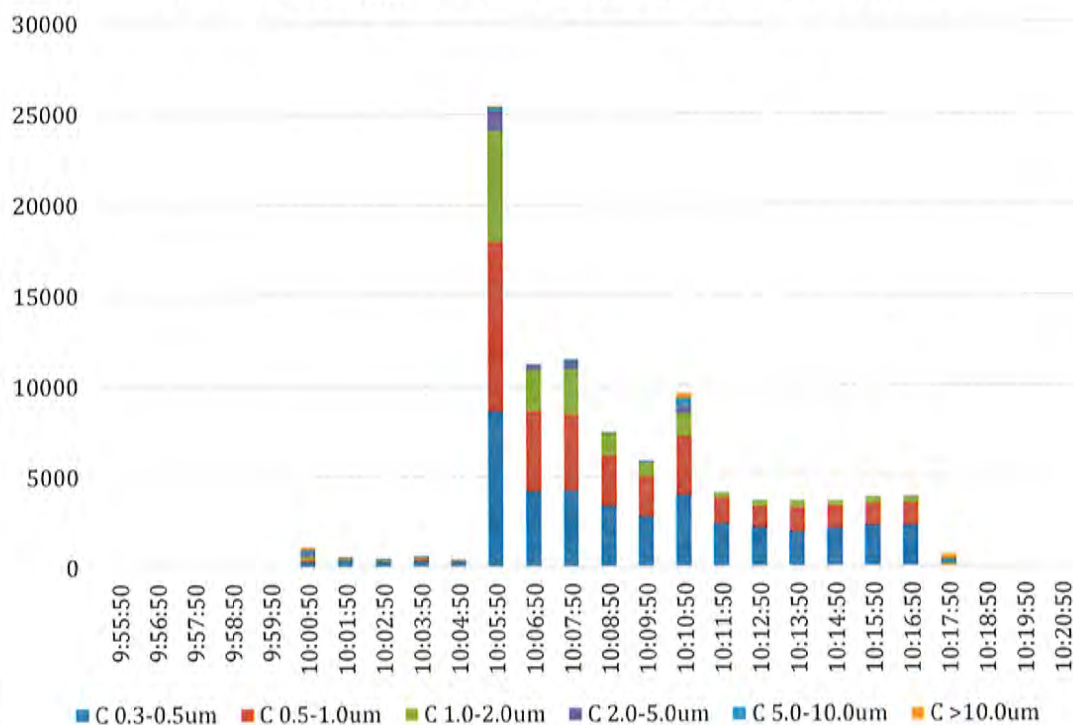


The evaluation of the air discharge was carried out through each operational mode and particle counts were collected at one minute continuous intervals to validate air quality content of the Bair Hugger and blanket. Again, this experiment confirmed particles coming out of both the new and used Bair Hugger machines when connected to new disposable upper body Bair Hugger blankets.

Old Bair Hugger Blanket Test Inside Clean Room




New Bair Hugger Blanket Test Inside Clean Room



A complete copy of the log graphs reflecting data obtained from each of these evaluations is attached at Exhibit B.

IV. CONCLUSIONS/SUMMARY OF OPINIONS

The evaluations showed clearly the Bair Huggers - through all operational modes - demonstrated increased production of particles from internal and/or external sources. This was true for both new and "used" machines, both with the filter in place and without the filter in place, as well as when connected to the disposable upper body blanket. These findings are consistent with both published literature and internal Arizant and 3M Company documents. It is my professional opinion that the Bair Hugger causes an increase in the number of particles in the operating room, and in particular, in close proximity to the surgical site. I reserve the right to amend the opinions in this report if further information becomes available to me.


MICHAEL W. BUCK
HEALTH CARE AND ENVIRONMENTAL
CONSULTING, INC.
13065 Isanti Street NE
Blaine, Minnesota 55449-4943

**EXHIBIT A –
CIRRICULUM VITAE**

MICHAEL W. BUCK

13065 Isanti Street NE
Blaine, Minnesota 55449-4943
763/355-7612

Curriculum Vitae

Areas of Interest – Hospital Environment Consulting.

EDUCATION:

University of Minnesota Minneapolis, Minnesota
School of Public Health - completed most course work (39 graduate credits) for a master's of
Public Health in Industrial Hygiene.

Minot State University Minot, North Dakota
Bachelor of Arts, Biology, February 27, 1989
Concentrations: Physical Science, Chemistry, Economics, Psychology

Experience:

President – Mike Buck, Health Care and Environmental Consulting,
Incorporated 2007

- Provide national consulting for hospital certification of critical care environments (i.e. BMT, ICU, NICU, and OR) ventilation systems and air and surface sampling
- Provide Training to HVAC mechanics and building managers on water infiltration remediation techniques and construction related activities relating to infection control procedures
- Provide industrial hygiene consulting to real estate property management companies

Environmental Health and Safety Compliance Specialist 2000 - Present

Environmental Health and Safety – U of MN Minneapolis, Minnesota

- Conduct indoor air quality investigations and coordinate remediation activities
- Coordinate sample collection of University Hospital's anesthetic gas employee exposure program
- Manage Department's Micro Lab including sample tracking and analysis
- Repair and maintain Department's air quality sampling equipment
- Audit Facilities Management Hazardous Material Program and outside contractor abatement projects and address concerns
- Review construction plans and provide comments on IAQ concerns and hazardous materials
- Participate in the University's After Hours Emergency Response (AHERPS) program requiring fundamental knowledge of hazardous, radioactive and biological spill response techniques

Principal Safety Technician 1991 - 2000

Environmental Health and Safety – U of MN Minneapolis, Minnesota

- Conduct building hazard assessments and communicate results
- Supervise asbestos abatement projects including contractor coordination and building communication; including project tracing and invoicing

Industrial Hygiene Technician 1989 - 1991

Delta Environmental Consultants St. Paul, Minnesota

- Project manager for asbestos site surveys and abatement projects

IAQ Investigations:

2017 - Woman's Hospital OR's Baton Rouge, Louisiana
2016-2017 Plaintiffs Retained Consultant, MDL #2666: *In re: Bair Hugger Products Liability Litigation* (Minneapolis, MN)
2017 - Ann and Robert H. Lurie Children's Hospital of Chicago, Northbrook, IL
2016 - Shriners Hospital for Children, First/Second Floors OSHA Investigation, Minneapolis,
2016 - University of Michigan Medical Center, Ann Arbor, MI
2016 - AI Nemours DuPont Hospital for Children, Wilmington, DE
2016 - Shriners Hospital for Children Kitchen flood, Minneapolis, MN
2016 - Shriners Hospital for Children First Floor Renovation, Minneapolis, MN
2016 - UPMC - University of Pittsburgh Medical Center
2015 - UPMC - University of Pittsburgh Medical Center
2015 - Shriners Hospital for Children, Minneapolis, MN
2015 - HCMC - Hennepin County Medical Center Burn Unit
2015 - Children's National BMT, Washington DC
2014 - HCMC - Hennepin County Medical Center Risk Assessment for Demolition
2013 - South Nassau Community Hospital, Oceanside NY
2013-2014 Stanford Medical Center Hospital Construction Annual Consultant, Palo Alto
2013 - Stanford Medical Center Hospital Construction, Palo Alto California
2013 - Riverwood Healthcare Center OR's
2013 - Regina Medical Center OR's
2013 - Regency Hospital Golden Valley
2013 - Fairview Southdale Medical Center
2012 - Regina Medical Center Grace Unit
2012 - Regina Medical Center Material Management Room
2012-2015 Oppenheimer Law Firm Project Consultant
2011 - Riverwood Healthcare Center Addition
2011 - Riverwood Healthcare Center MRI
2010 - Avera Regional Medical Center OR's
2010 - Avera Regional Medical Center OR's, Recovery, and Endoscopy
2010 - Southdale Medical Center
2009 - St. Joes Hospital, St. Paul, MN
2009 - Avera Regional Medical Center OR's
2008 - Jewish Medical Center, Louisville Kentucky
2007 - Avera Regional Medical Center OR's
2007 - Children's National BMT, Washington DC
2007 - Rush Memorial Chicago
2007 - Modesto Hospital Trials Ventilation Study with Mazetti and EH Price
2006 - Northeast Georgia Medical Center Women's and Children's Pavilion
2006 - Northeast Georgia Medical Center ICU
2006 - Northeast Georgia Medical Center Outpatient Services Building
2006 - Northeast Georgia Medical Center School of Nursing
2006 - Natchez Regional Hospital
2004 - Pitt County Memorial Hospital Emergency Department
2004-2006 - Pitt County Memorial Hospital NICU Assessment and Remediation Consultant
2004-2006 - Pitt County Memorial Hospital NICU Assessment and Remediation
2003 - MD Anderson Cancer Center Research Facility Construction
2003 - Pitt Count Memorial Hospital
2003 - Pitt Count Memorial Hospital Community Services Building
2003 - Pitt Count Memorial Hospital Emergency Department

Publications

- APIC 2015 Infection Prevention Manual for Construction and Renovation Author Chapter 5: Air Monitoring for Quality Evaluation in Healthcare
- Published 2010: Displacement Ventilation as a Viable Air Solution for Hospital Patient Rooms

Conference Presentations

2016 APIC Pittsburgh, Water Damage Management in Healthcare Facilities
2016 APIC Minnesota, Water Damage Management in Healthcare Facilities
2014 Construction Management in Healthcare Facilities, Winnipeg, Manitoba Canada Webcast to Provincial Healthcare Board
2010 Healthcare Occupational and Environmental Safety Workshop, Evaluation Methods and Exposure Monitoring of Anesthetic Gases
2008 ERTK, University of Minnesota Duluth
2005 OSHA Respiratory Protection Program Lakes and Plains Regional Training Center
2004 MultiData Corporation: Mold investigations
2004 Construction Management in Healthcare Facilities, University of Minnesota
2003 Construction Management in Healthcare Facilities, University of Minnesota
2003 Mold Management in Healthcare Facilities, University of Minnesota
2003 Mold Management in Healthcare Facilities, University of Minnesota
2003 Mold Investigations, Omaha Regional Conference of Air Conditioning Heating and Refrigeration Professionals

TRAINING – Current Certifications:

Asbestos Contractor Supervisor Training	NIOSH 582 – Asbestos Air Analysis
Recognition of Indoor Air Quality Issues	Building Inspector Hazardous Materials
Introduction to Food and Air-Borne Fungi	Asbestos Abatement Site Supervisor
Applied Thermographer using Infrared Technology	

TRAINING – Past Certifications:

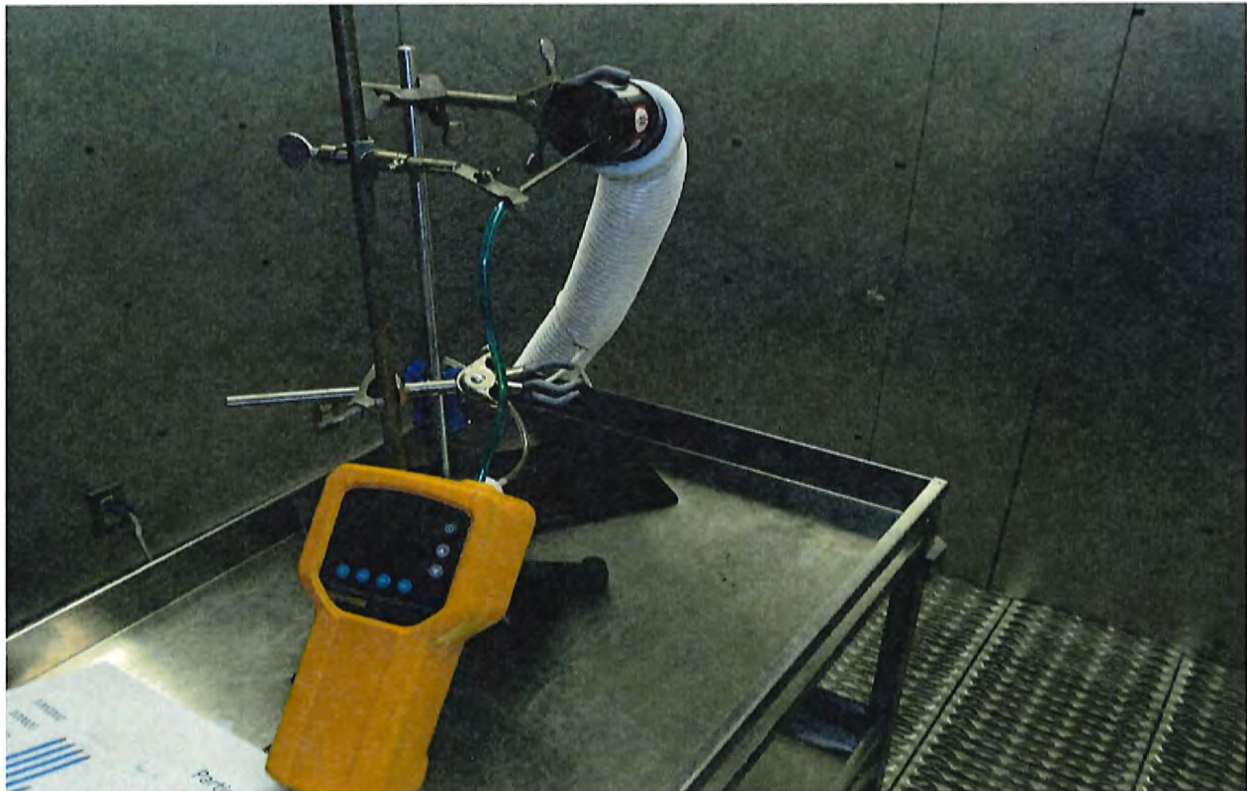
OSHA 501 Certified Trainer
Asbestos Project Designer
Lead Risk Assessor
Lead Inspector

**EXHIBIT B –
GRAPHS AND PHOTOS OF
EXPERIMENTS**

Bair Hugger 1st Set of Tests

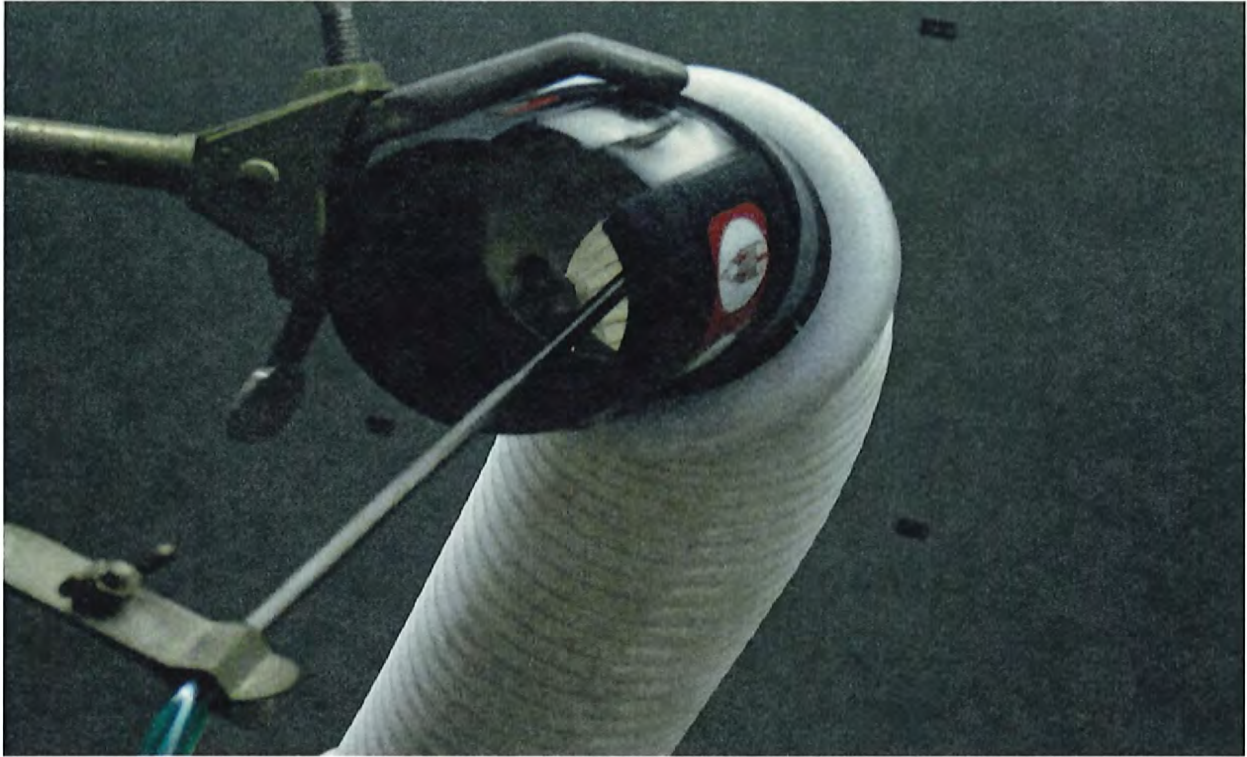


Picture #1 – Bair Hugger in Clean room

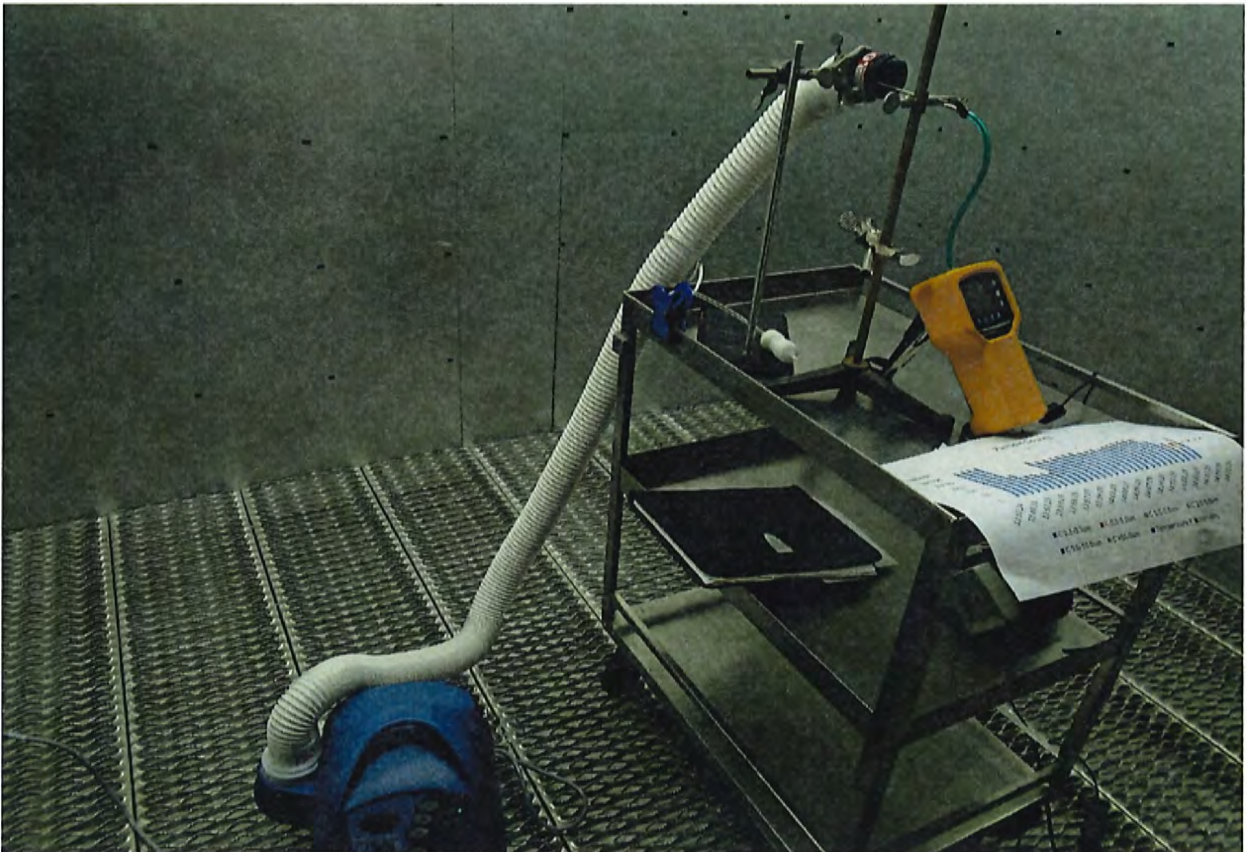


Picture #2 – Bair Hugger in Clean Room with particle counter in center of hose

Bair Hugger 1st Set of Tests



Picture #3 – Bair Hugger in Clean Room particle counter probe sampling Bair Hugger air output



Picture #4 – Bair Hugger in Clean Room

Bair Hugger 2nd Set of Tests



Picture #1 – Bair Hugger in Clean Room with blanket attached to supply air output hose in container



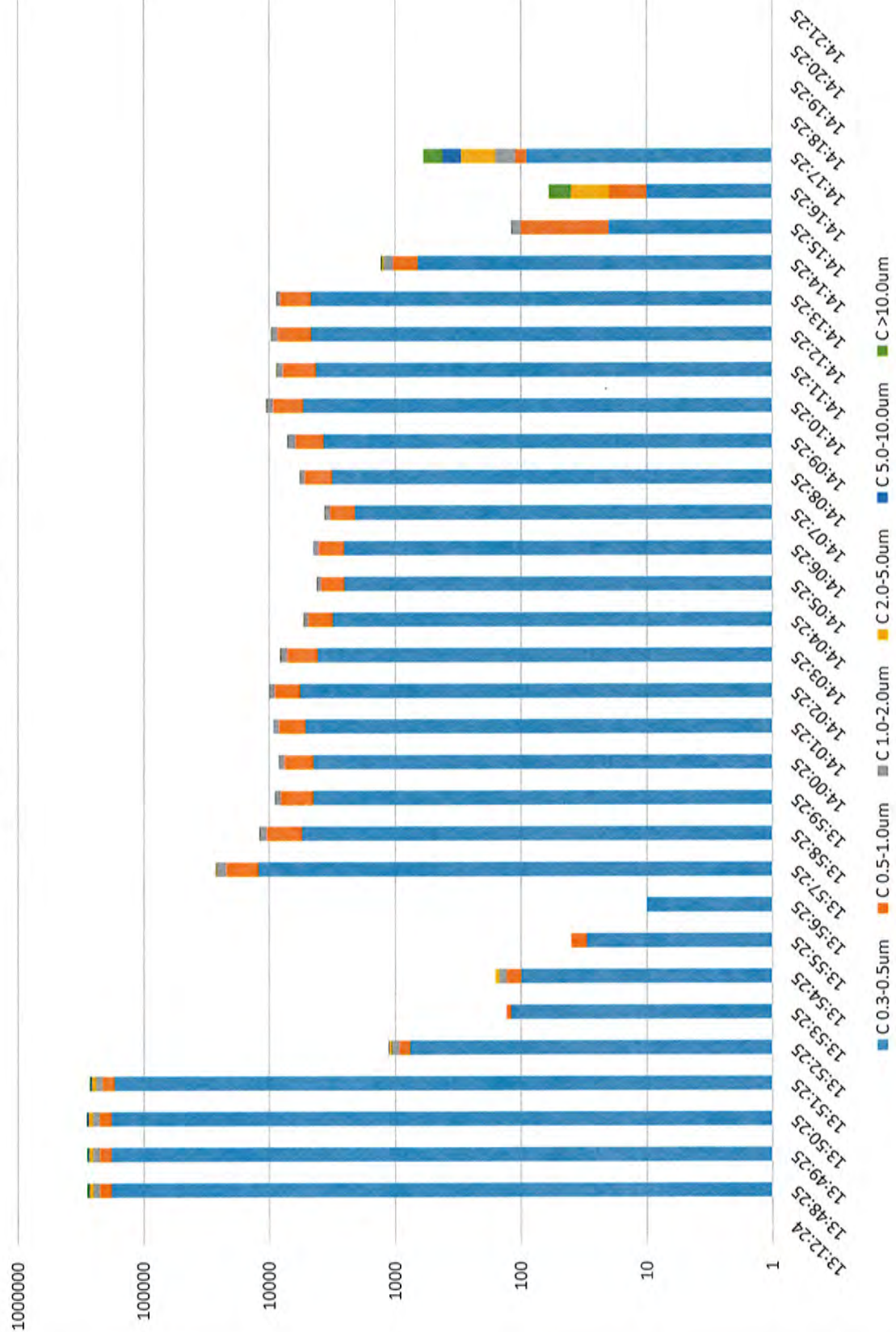
Picture #2 – Bair Hugger in Clean Room with blanket attached to supply air output hose in container

Bair Hugger 2nd Set of Tests

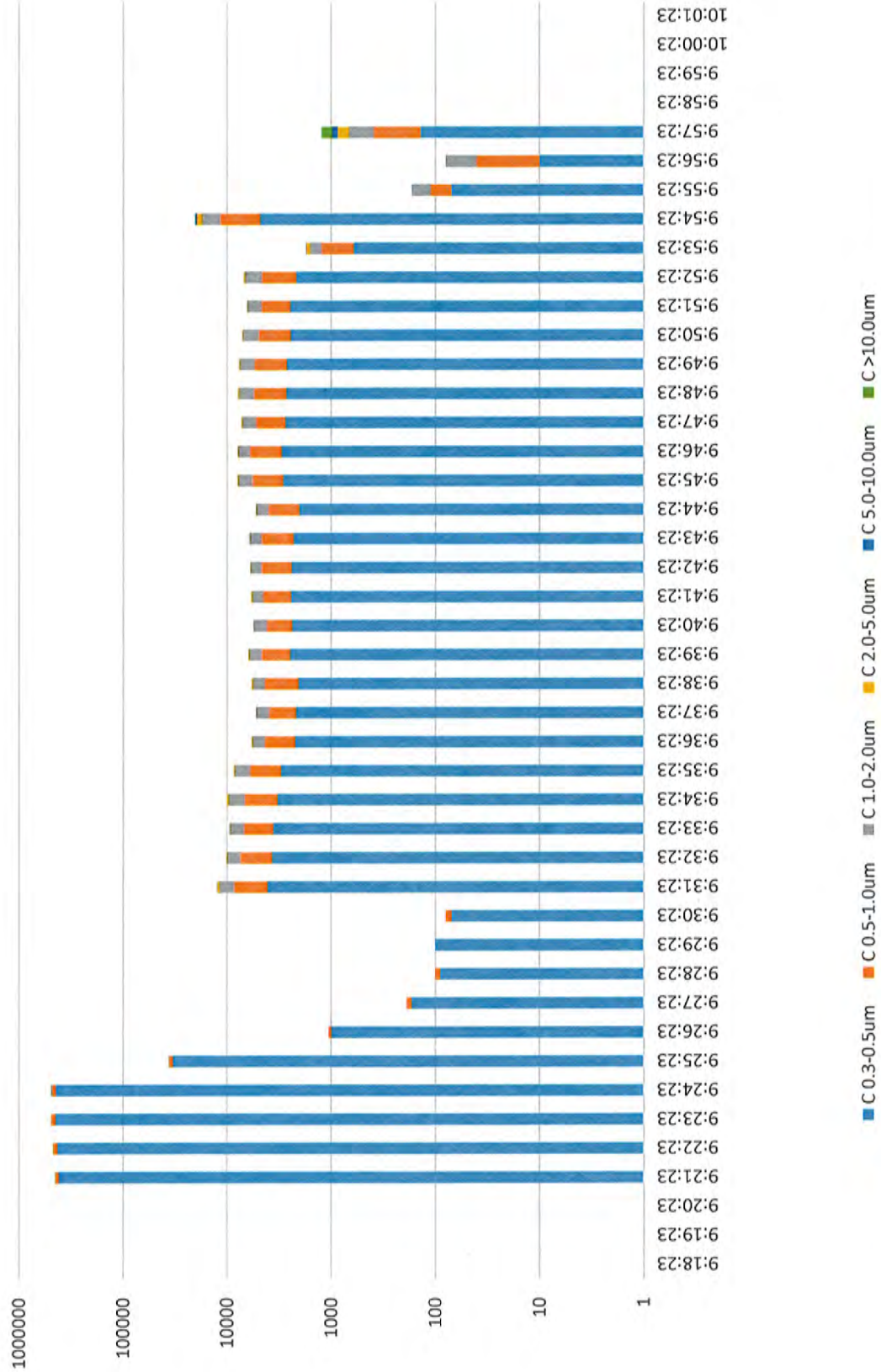


Picture #3 – Bair Hugger in Clean Room particle counter

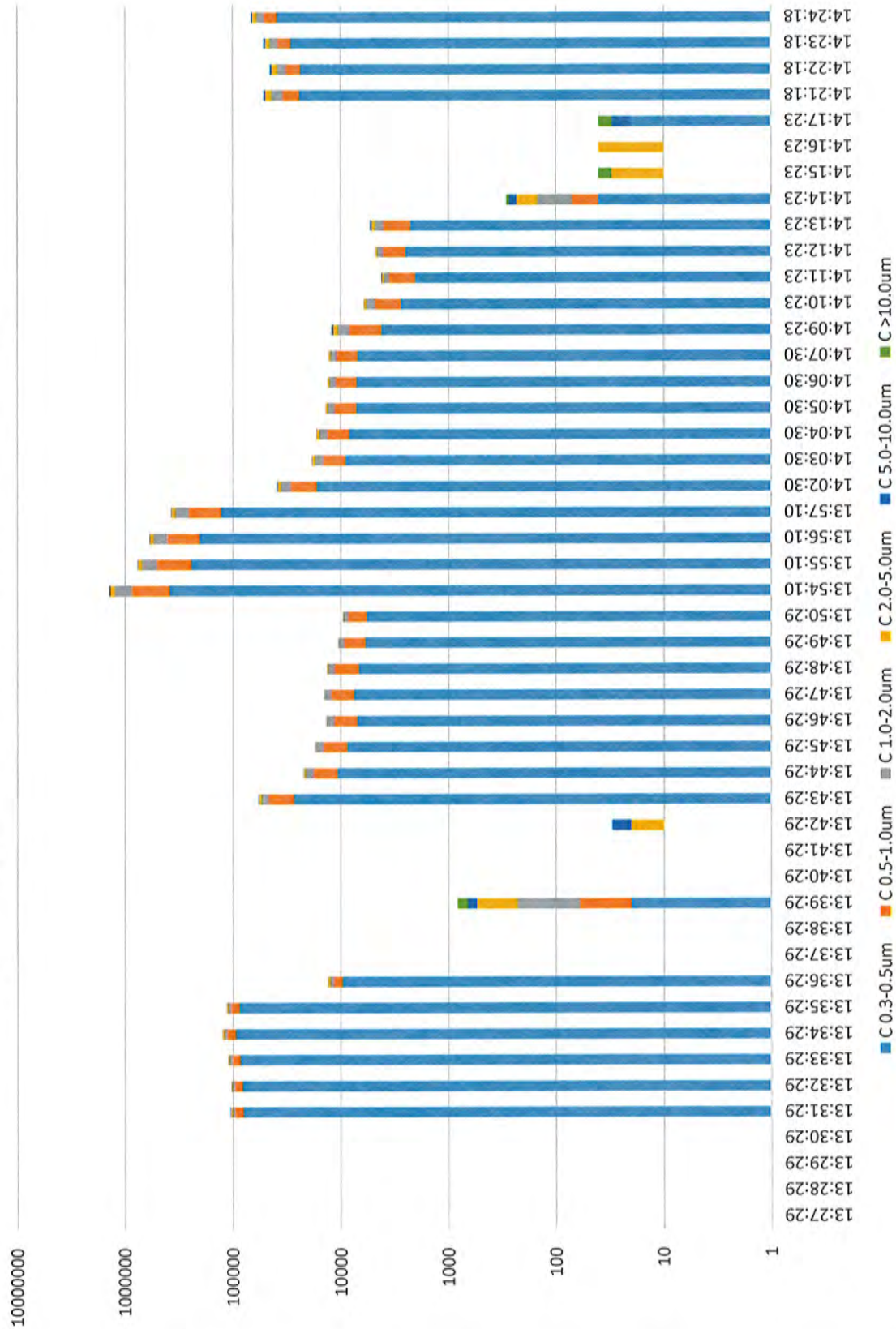
Old Bair Hugger Inside Clean Room

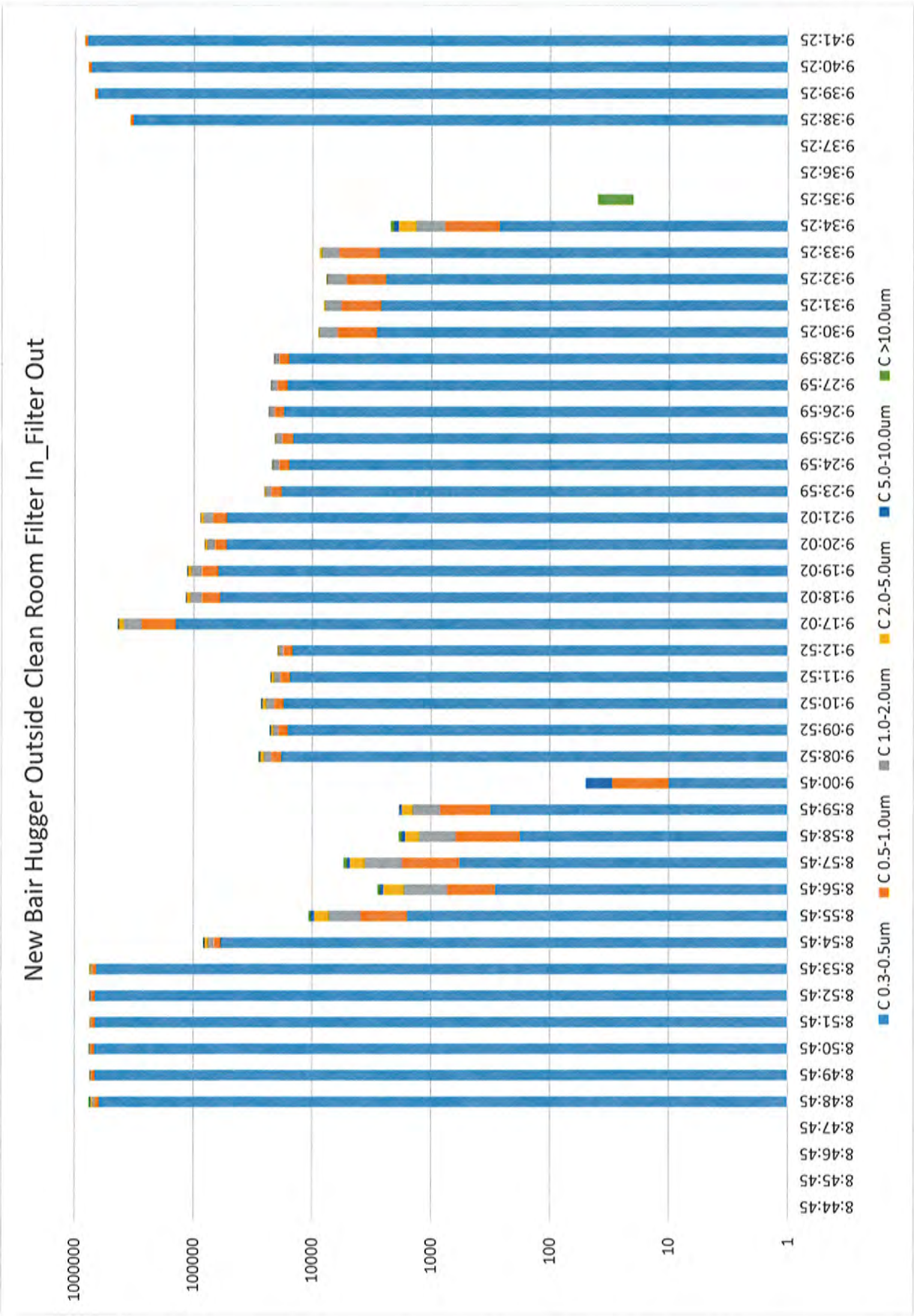


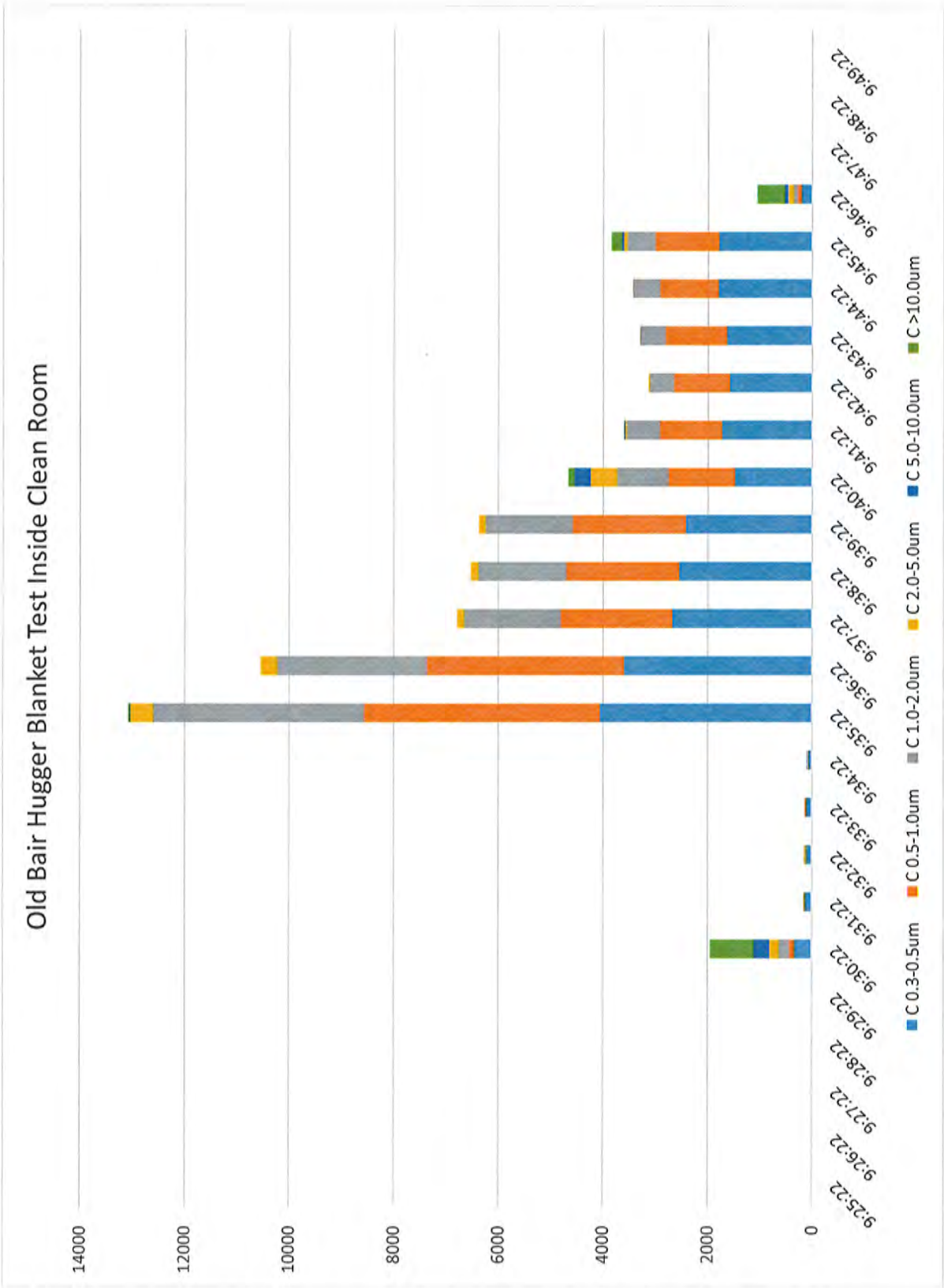
New Bair Hugger Inside Clean Room



Old Bair Hugger Outside Clean Room Filter In/Filter Out







New Bair Hugger Blanket Test Inside Clean Room

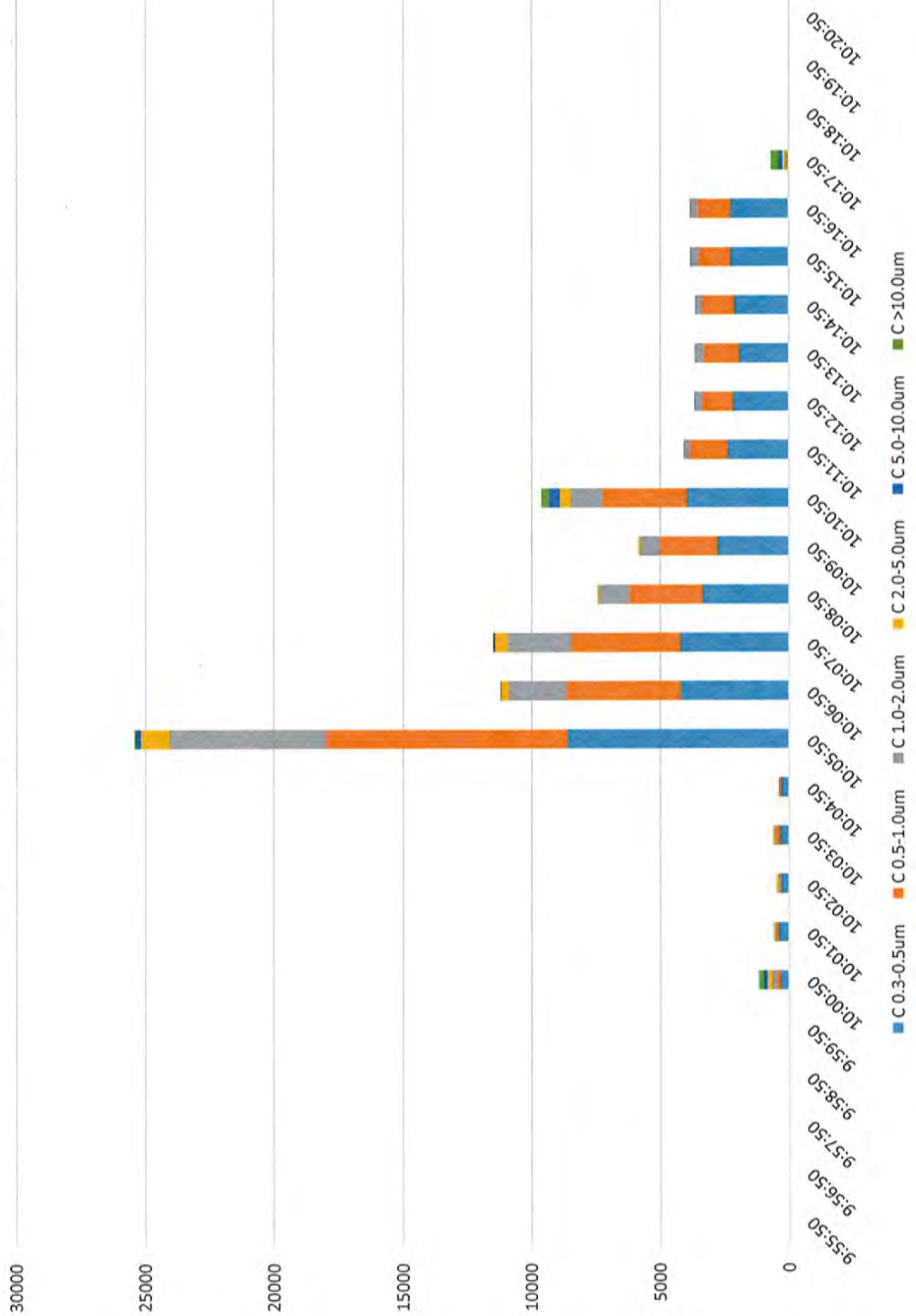


**EXHIBIT C –
REFERENCES & DOCUMENTS
CONSIDERED**

Materials Considered – Michael W. Buck

3MBH00001336 - 37	3MBH00024640	3MBH00105516 - 64
3MBH00001579	3MBH00024728	3MBH00105804
3MBH00001581	3MBH00025638 - 40	3MBH00105834 - 37
3MBH00001582	3MBH00025739	3MBH00105839 - 40
3MBH00001583 - 87	3MBH00030403	3MBH00105841 - 42
3MBH00002412 - 13	3MBH00030796	3MBH00105843
3MBH00002430	3MBH00030875 - 907	3MBH00105845 - 47
3MBH00002433	3MBH00031134 - 58	3MBH00106405 - 06
3MBH00002508	3MBH00031184 - 86	3MBH00107694 - 96
3MBH00002513 - 17	3MBH00031212	3MBH00107719 - 20
3MBH00002556 - 68	3MBH00031537 - 55	3MBH00107862 - 72
3MBH00002619 - 20	3MBH00039330 - 35	3MBH00107972
3MBH00002621	3MBH00039987	3MBH00108243 - 48
3MBH00002899	3MBH00041131	3MBH00110295
3MBH00003006 - 07	3MBH00041415 - 16	3MBH00118356 - 60
3MBH00003027 - 32	3MBH00041418	3MBH00118380 - 87
3MBH00005719	3MBH00042133 - 34	3MBH00118525
3MBH00005721	3MBH00042155 - 57	3MBH00122752
3MBH00005722 - 23	3MBH00042697 - 99	3MBH00124801
3MBH00005724	3MBH00042820	3MBH00124864
3MBH00005725	3MBH00046575	3MBH00125235 - 37
3MBH00005733	3MBH00046822 - 903	3MBH00125255
3MBH00006840	3MBH00046971 - 72	3MBH00125259
3MBH00007503	3MBH00047063	3MBH00130429 - 32
3MBH00007579	3MBH00047382 - 83	3MBH00130834 - 35
3MBH00008195	3MBH00047858 - 81	3MBH00130837
3MBH00008489	3MBH00048072	3MBH00130843
3MBH00008521	3MBH00048121 - 26	3MBH00132832 - 34
3MBH00012764 - 66	3MBH00049086	3MBH00133476 - 80
3MBH00015498 - 81	3MBH00050524 - 26	3MBH00134040
3MBH00015884	3MBH00050714 - 16	3MBH00144053
3MBH00017861 - 62	3MBH00051610	3MBH00161475 - 76
3MBH00018164 - 65	3MBH00051736 - 38	3MBH00165529 - 48
3MBH00018242	3MBH00052704	3MBH00195273 - 77
3MBH00018311 - 13	3MBH00052987	3MBH00214650 - 56
3MBH00018314 - 15	3MBH00053009	3MBH00227269 - 75
3MBH00022391 - 92	3MBH00053467 - 72	3MBH00377676 - 77
3MBH00022442 - 43	3MBH00053493 - 94	3MBH00447003 - 14
3MBH00022590 - 93	3MBH00053497 - 98	3MBH00511865
3MBH00022737 - 61	3MBH00053511 - 16	3MBH00519748 - 56
3MBH00022870	3MBH00054336 - 37	3MBH00519827 - 32
3MBH00022872	3MBH00083780	3MBH00520624
3MBH00024479	3MBH00083781	3MBH00521234 - 35
3MBH00024524 - 25	3MBH00105376 - 78	3MBH00540117 - 18

Materials Considered – Michael W. Buck

3MBH00544754 - 55
 3MBH00548021 - 49
 3MBH00565305 - 07
 3MBH00587265 - 67
 3MBH00046186 – 46309
 3MBH00046310 – 46818
 3MBH00112410 – 112442
 3MBH00112467 – 112503
 3MBH00127752 – 128189
 3MBH00128190 – 129010
 3MBH00497102 – 497359
 3MBH00498164 – 498341
 Augustine_00125751 – 12964

Literature

Albrecht et al. 2011: Albrecht M, Gauthier RL, Belani K, Litchy M, Leaper D. Forced-air warming blowers: an evaluation of filtration adequacy and airborne contamination emissions in the operating room. *Am J Infect Control* 2011;39:321-328.

Albrecht et al. 0009 → see Leaper et al. 2009

Avidan et al. 1997: Avidan MS, Jones N, Ing R, Khoosal M, Lundgren C, Morrell DF. Convection warmers - not just hot air. *Anaesthesia* 1997;52:1073-1076.

Beavers & Thoroughman 2007: Beavers S and Thoroughman D. Acinetobacter Infections among Hospitalized Patients in Kentucky - 2006. *Kentucky Epidemiologic Notes and Reports* 2007;42(2):1-5.

Belani et al. 2013: Belani KG, Albrecht M, McGovern PD, Reed M, Nachtsheim C. Patient warming excess heat: the effects on orthopedic operating room ventilation performance. *Anesth Analg* 2013;117:406-411.

Bernards et al. 2004: Bernards AT, Harinck HI, Dijkshoorn L, van der Reijden TJ, van den Broeck PJ. Persistent *Acinetobacter baumannii*? Look inside your medical equipment. *Infect Control Hosp Epidemiol* 2004;25:1002-1004.

Bischoff et al. 2007: Bischoff WE, Tucker BK, Wallis ML, Reboussin BA, Pfaller MA, Hayden FG, Sherertz RJ. Preventing the airborne spread of *Staphylococcus aureus* by persons with the common cold: effect of surgical scrubs, gowns, and masks. *Infect Control Hosp Epidemiol* 2007;28(10):1148-1154.

Brandt et al. 2010: Brandt S, Oguz R, Huttner H, et al. Resistive-polymer versus forced-air warming: comparable efficacy in orthopedic patients. *Anesth Analg* 2010;110:834-838.

Brohus et al. 2006: Brohus H, Balling KD, Jeppesen D. Influence of movements on contaminant transport in an operating room. *Indoor Air* 2006;16:356-372.

Materials Considered – Michael W. Buck

Cristina et al. 2012: Cristina ML, Spagnolo AM, Sartini M, Panatto D, Gasparini R, Orlando P, Ottria G, Perdelli F. Can particulate air sampling predict microbial load in operating theatres for arthroplasty? *PLOS One* 2012;7(12):e52809.

Dasari et al. 2012: Dasari KB, Albrecht M, Harper M. Effect of forced air warming on the performance of operating theatre laminar flow ventilation. *Anesthesia* 2012;67:224-2249.

Dirkes & Minton 1994: Dirkes WE, Minton WA. Convection warming in the operating room: evaluation of bacterial spread with three filtration levels. *Anesthesiology* 1994;81.3A

Ford & Phillips 2015: Ford J, Phillips P. Systematic Review: Forced air warming versus circulating warm water for the prevention of hypothermia in surgical patients. *Medidex* April 21 2015.

Gjolaj et al. 2009: Gjolaj MP, Ahlbrand S, Yamout IM, Armstrong D, Brock-Utne JG. Don't forget to change the Bair Hugger filter. *ASA Abstracts* 2009;A1168.

Hall & Teenier 1991: Hall AC, Teenier T. Poster Presentation: Bair Hugger warmer does not increase microbial contamination in the operating room. *Department of Anesthesiology, University of Texas Southwestern Medical Center* December 9, 1991.

Haller et al. 2016: Haller S, Holler C, Jacobshagen A, Hamouda O, Abu Sin M, Monnet DL, Plachouras D, Eckmans T. Contamination during production of heater-cooler units by *Mycobacterium chimaera* potential cause for invasive cardiovascular infections: results of an outbreak investigation in Germany, April 2015 to February 2016. *Euro Surveill* 2016;21(17):pii=30215.

Jaekel et al. 2014: Jaekel DJ, Ong KL, Lau EC, Watson HN, Kurtz SM. Epidemiology of Total Hip and Knee Arthroplasty Infection. *Periprosthetic Joint Infection of the Hip and Knee* 2014:1-14.

Kimberger et al. 2008: Kimberger O, Held C, Stadelmann K, et al. Resistive polymer versus forced-air warming: comparable heat transfer and core rewarming rates in volunteers. *Anesth Analg* 2008;107:1621-1626.

Kohler et al. 2015: Kohler P, Kuster SP, Bloemberg G, Schulthess B, Frank M, Tanner FC, Rossle M, Boni C, Falk V, Wilhelm MJ, Sommerstein R, Achermann Y, ten Oever J, Debast SB, Wolfhagen MJHM, Bruinsma GJBB, Vos MC, Bogers A, Serr A, Beyersdorf F, Sax H, Bottger EC, Weber R, van Ingen J, Wagner D, Hasse B. Healthcare-associated prosthetic heart valve, aortic vascular graft, and disseminated *Mycobacterium chimaera* infections subsequent to open heart surgery. *Eur Heart J* 2015;36:2745-2753.

Kowalski & Bahnfleth 1998: Kowalski WJ, Bahnfleth W. Airborne respiratory diseases and mechanical systems for control of microbes. *HPAC* July 1998:34-48.

Kurtz et al. 2008: Kurtz SM, Lau E, Schmier J, Ong KL, Zhao K, Parvizi J. Infection burden for hip and knee arthroplasty in the United States. *J Arthroplasty* 2008;23(7):984-991.

Kurtz et al. 2012: Kurtz SM, Lau E, Watson H, Schmier JK, Parvizi J. Economic burden of periprosthetic joint infection in the United States. *J Arthroplasty* 2012;27(8):61-65.e1.

Materials Considered – Michael W. Buck

Leaper et al. 2009: Leaper D, Albrecht M, Gauthier R. Forced-air warming: a source of airborne contamination in the operating room? *Orthop Rev* 2009;1:e28.

Legg et al. 2012: Legg AJ, Cannon T, Hamer AJ. Do forced air patient-warming devices disrupt unidirectional downward airflow? *J Bone Joint Surg (Br)* 2012;94:254-256.

Legg & Hamer 2013: Legg AJ, Hamer AJ. Forced-air patient warming blankets disrupt unidirectional airflow. *Bone Joint J* 2013;95-B:407-410.

Lehtinen et al. 2010: Lehtinen SJ, Onicescu G, Kuhn KM, Cole DJ, Esnaola NF. Normothermia to prevent surgical site infections after gastrointestinal surgery: Holy Grail or False Idol? *Ann Surg* 2010;252:696-704.

Mangram et al. 1999: Mangram AJ, Horan TC, Pearson ML, Silver LC, Jarvis WR. Guideline for Prevention of Surgical Site Infection. *Infection Control and Hospital Epidemiology* 1999;20(4):247-278.

Matsuzaki et al. 2003: Matsuzaki Y, Matsukawa T, Ohki K, et al. Warming by resistive heating maintains perioperative normothermia as well as forced air heating. *Br J Anaesth* 2003;90:689-691.

McGovern et al. 2011: McGovern PD, Albrecht M, Belani KG, et al. Forced-air warming and ultra-clean ventilation do not mix: an investigation of theatre ventilation, patient warming and joint replacement infection in orthopaedics. *J Bone Joint Surg (Br)* 2011;93:1537-1544.

Memarzadeh (Unpublished): Memarzadeh F. A novel approach to assess the effect of a forced-air patient warming system on increasing the risk of nosocomial infections at the surgical wound site.

Miyazaki et al. 2007: Miyazaki H, Sato M, Okazaki K. Forced-Air Warmer did not increase the risk of contamination caused by interference of clean airflow. *ASA Abstracts* 2007;A1594.

Moretti et al. 2009: Moretti B, Larocca AM, Napoli C, et al. Active warming systems to maintain perioperative normothermia in hip replacement surgery: a therapeutic aid or a vector of infection? *J Hosp Infect* 2009;73:58-63.

Nagpal et al. 2014 ABSTRACT: Nagpal A, Wentink JE, Berbari EF, Aronhalt KC, Wright AJ, Krageschmidt DA, Wengenack NL, Thompson RL, Tosh PK. A cluster of *Mycobacterium wolinskyi* surgical site infections at an academic medical center. *Infect Control Hosp Epidemiol* 2014;35(9):1169-1175.

Namba et al. 2013: Namba RS, Inacio MCS, Paxton EW. Risk factors associated with deep surgical site infections after primary total knee arthroplasty. *J Bone Joint Surg Am.* 2013;95:775-782.

Negishi et al. 2003: Negishi C, Hasegawa K, Mukai S, et al. Resistive-heating and forced-air warming are comparably effective. *Anesth Analg* 2003;96:1683-1687.

Ng et al. 2006: Ng V, Lai A, Ho V. Comparison of forced-air warming and electric heating pad for maintenance of body temperature during total knee replacement. *Anaesthesia* 2006;61:1100-1104.

Materials Considered – Michael W. Buck

Occhipinti et al. 2013: Occhipinti LL, Hauptman JG, Greco JJ, Mehler SJ. Evaluation of bacterial contamination on surgical drapes following use of the Bair Hugger forced air warming system. *Can Vet J* 2013;54:1157-1159.

Parvizi & Karam. Parvizi J, Karam JA. Do Forced-Air Warming Blankets Increase Surgical Site Infections? *3M Publication*.

Reed et al. 2013: Reed M, Kimberger O, McGovern PD, Albrecht MC. Forced-air warming design: evaluation of intake filtration, internal microbial buildup, and airborne-contamination emissions. *Am Assoc Nurse Anesth J* 2013;81:275-280.

Sandiford & Skinner 2009: Sandiford NA, Skinner J. (ii) The prevention of infection in total hip arthroplasty. *Orthopaedics and trauma* 2009;23(1):8-16.

Sax et al. 2015: Sax H, Bloemberg G, Hasse B, Sommerstein R, Kohler P, Achermann Y, Rossle M, Falk V, Kuster SP, Bottger EC, Weber R. Prolonged outbreak of *Mycobacterium chimaera* infection after open-chest heart surgery. *Clinical Infectious Diseases* 2015;61(1):67-75.

Scott et al. 2015: Scott AV, Stonemetz JL, Wasey JO, Johnson DJ, Rivers RJ, Koch CG, Frank SM. Compliance with surgical care improvement project for body temperature management (SCIP Inf-10) is associated with improved clinical outcomes. *Anesthesiology* 2015;123:116-125.

Sessler et al. 2011: Sessler DI, Olmsted RN, Kuelpmann R. Forced air warming does not worsen air quality in laminar flow operating rooms. *Anesth Analg* 2011;113:1416-1421.

Sharp et al. 2002: Sharp RJ, Chesworth T, Fern ED. Do warming blankets increase bacterial counts in the operating field in a laminar-flow theatre? *J Bone Joint Surg Br* 2002;84:486-488.

Shaw et al. 1996: Shaw JA, Bordner MA, Hamory BH. Efficacy of the steri-shield filtered exhaust helmet in limiting bacterial counts in the operating room during total joint arthroplasty. *J Arthroplasty* 1996;11(4):469-473.

Shiomori et al. 2001: Shiomori T, Miyamoto H, Makishima K. Significance of airborne transmission of methicillin-resistant *Staphylococcus aureus* in an otolaryngology-head and neck surgery unit. *Arch Otolaryngol Head Neck Surg* 2001;127:644-648.

Sigg et al. 1999: Sigg DC, Houlton AJ, Iazzo PA. The potential for increased risk of infection due to the reuse of convective air-warming/cooling coverlets. *Acta Anaesthesiol Scand* 1999;43:173-176.

Sikka & Prielipp 2014: Sikka RS, Prielipp RC. Forced air warming devices in orthopaedics: a focused review of the literature. *J Bone Joint Surg Am* 2014;96:e200(1-7).

Singh et al. 2011: Singh VK, Hussain S, Javed S, Singh I, Mulla R, Kalairajah Y. Sterile surgical helmet system in elective total hip and knee arthroplasty. *Journal of Orthopaedic Surgery* 2011;19(2):234-237.

Sommerstein et al. 2016: Sommerstein R, Ruegg C, Kohler P, Bloemberg G, Kuster SP, Sax H. Transmission of *Mycobacterium chimaera* from Heater-Cooler Units during Cardiac Surgery despite an Ultraclean Air Ventilation System. *Emerg Infect Dis*. 2016 Jun

Materials Considered – Michael W. Buck

Suzuki et al. 1984: Suzuki A, Namba Y, Matsuura M, Horisawa A. Airborne contamination in an operating suite: report of a five-year survey. *J. Hyg., Camb.* 1984;93:567-573.

Tan et al. 2016: Tan N, Sampath R, Abu Saleh OM, Tweet MS, Jevremovic D, Alniemi S, Wengenack NL, Sampathkumar P, Badley AD. Disseminated Mycobacterium chimaera infection after cardiothoracic surgery. *OFID* 2016;Brief Report:1-3.

Tande & Patel 2014: Tande AJ, Patel R. Prosthetic Joint Infection. *Clin. Microbiol. Rev.* 2014;27(2):302-345.

Tumia & Ashcroft 2002: Tumia N, Ashcroft GP. Convection warmers - a possible source of contamination in laminar flow theatre? *J Hosp Infect* 2002;52:171-174.

Wagner et al. 2014: Wagner JA, Schreiber KJ, Cohen R. Using Cleanroom Technology: Improving operating room contamination control. *ASHRAE Journal* Feb 2014:18-27.

Whyte et al. 1976: Whyte W, Vesley D, Hodgson R. Bacterial dispersion in relation to operating room clothing. *J. Hyg. Camb.* 1976;76:367-377.

Whyte 1988: Whyte W. The role of clothing and drapes in the operating room. *J Hosp Infect* 1988;11©:2-17.

Wood et al. 2014: Wood AM, et al. Infection control hazards associated with the use of forced-air warming in operating theatres. *J Hosp Infect* 2014;xxx:1-9.

Zink & Iazzo 1993: Zink RS, Iazzo PA. Convection warming therapy does not increase the risk of wound contamination in the operating room. *Anesth Analg* 1993;76:50-53.

ASHRAE Addenda 2008: ASHRAE Addenda 2008 Supplement: Method of Testing General Ventilation Air-Cleaning Devices for Removal Efficiency by Particle Size.

CDC 10/27/2015: Non-tuberculous Mycobacterium (NTM) Infections and Heater-Cooler Devices: Interim Practical Guidance. *CDC* October 27, 2015.

FDA 10/15/2015: Nontuberculous Mycobacterium Infections Associated with Heater-Cooler Devices: FDA Safety Communication. *FDA* October 15, 2015.

FDA Executive Summary 2016: FDA Executive Summary: Nontuberculous Mycobacterium (NTM) Infections Associated with Heater-Cooler Devices (HCD) during Cardiothoracic Surgery. 2016.

HUNTAIR Article: Advancing aerobiological quality standards for hospital operating rooms (ORs). *HUNTAIR: a Nortek Air Solutions Brand* 2015 White Paper.

EXHIBIT DX38

TO DECLARATION OF PETER J. GOSS IN
SUPPORT OF DEFENDANTS' MOTION TO
EXCLUDE PLAINTIFFS' ENGINEERING
EXPERTS



DUKE INFECTION CONTROL OUTREACH NETWORK (DICON)

Infection Prevention News

Volume 10, Number 11, November 2015

HotDogs, Bair Huggers, and Lawsuits, Oh My! A brief review of the controversy surrounding perioperative warming methods.

Maintenance of Perioperative Normothermia: Background and Rationale

A 2-degree Celsius decrease in body temperature in patients undergoing general anesthesia can triple the rate of a postoperative wound infection. The benefits of maintaining normothermia in surgical patients have been extensively studied. These benefits include: 1) reduction of risk of surgical site infection, 2) better coagulation, and 3) faster discharge from the post-anaesthesia care unit. (1, 2)

Maintenance of normothermia is now a standard of care and a key component of the Surgical Care Improvement Project (SCIP). Also, adherence to normothermia protocol is a current requirement for receipt of full reimbursement from CMS. (3)

Most operating rooms, including ours, rely on forced air warming (FAW) devices, such as the Bair Hugger, to ensure normothermia during surgery. FAW warming devices circulate warmed air in a hose connected to a disposable and inflatable blanket. All clinical trials that documented the benefit of maintaining normothermia during surgery have used FAW devices. (1,2)

Resistive Polymer Warming (RPW), FAW's competition:

RPW devices (HotDog) warm patients by passing an electric current through a resistive polymer which in turn is encased in a reusable blanket. In contrast to FAW devices, RPW devices require direct contact with a patient's skin. The warming capacity of RPW devices was compared to that of FAW devices in a 2011 study by Kimberger et al. This study showed that RPW warmed anaesthetized ENT patients at a slower rate. (4)

Current controversies:

Most operating rooms typically utilize "ultraclean air ventilation" during joint replacement procedures. "Ultraclean air ventilation" relies on constant and unidirectional filtered air flow, known as laminar flow, to protect the surgical site from airborne contamination.

A few investigators have speculated that use of FAW devices disrupts laminar flow thus potentially increasing the risk of contamination of the operative site. (5-7) Most studies that reached these conclusions were funded by the manufacturer of a single RPW device. This same company currently

sponsors “informative websites” that emphasize their claims of an increased risk of developing a surgical site infection due to the use of FAW warming devices while simultaneously promoting their alternative RPW product.

A single study done by McGovern et al is the primary source and most commonly quoted evidence for the claim that FAW warming devices are unsafe. (8) These authors evaluated ventilation airflow patterns using a machine that emitted “neutrally buoyant detergent bubbles” during a simulated hip arthroplasty and a lumbar spinal surgical procedure done on mannequins in order determine if laminar airflow was differentially and adversely disrupted by the use of a FAW warming device compared to the use of a RPW warming device. Photographs were used to provide data on “bubble counts” over the operative site during these mock surgical procedures. Bubble counts on operative site over mannequins were higher when FAW devices were used. No actual microbiologic data was collected during this portion of the experiment. (8)

McGovern et al also examined rates of surgical site infection (SSI) after use of either a FAW or RPW warming device in a total of 1,437 patients undergoing knee and hip replacements over a 2.5-year period. They concluded that the risk developing a SSI was higher in patients undergoing arthroplasty procedures when FAW warming devices were used than when RPW warming devices were used (OR 3.8, 95% CI (1.2-12.5), $p=0.024$). Curiously the risk of developing a SSI was remarkably higher in patients undergoing hip replacement procedures with the use of FAW warming devices than in patients undergoing knee replacements warmed with the same FAW devices (OR 4.1, 95% CI (1.9-8.6), $p < 0.001$). (8)

We and others (3) believe that the preceding widely quoted study by McGovern et al has significant limitations: 1) infection control practices and perioperative antibiotics were not standardized in the two study groups, and 2) the authors did not adjust their outcomes for age or other important patient-related comorbidities. Moreover, the authors failed to discuss what these important details: 1) no mention was made of whether the FAW devices used in this study had proper maintenance including appropriately timed changing of filters in their tubing (see table); 2) they did not provide sufficient supporting data to document that the use of “neutrally buoyant detergent bubbles” are a valid proxy for bacterial contamination, and 3) they did not discuss or explain why patients undergoing hip arthroplasty procedures had such high rates of SSI in their study.

Our take:

The body of evidence describing the link between FAW and increased operative site infections is weak. To the best of our knowledge, no adequately powered, properly controlled, statistically significant, reproducible study has been published that demonstrates an increased risk of SSI due to the use of FAW warming devices. We do not believe that experimental studies using machines that emit bubbles in mock surgical procedures is a proven or standardized method to assess the risk of operative site contamination. Finally, we believe it is important and notable that no studies performed by independent investigators have been published that confirm the findings of the study by McGovern et al. Until such data are published, we believe that it is reasonable and appropriate to continue the use of FAW warming devices in patients. Indeed, our data and that collected by the NHSN suggest that

approximately 99% of patients undergoing joint replacement procedures do not develop a SSI despite the fact that FAW warming devices continue to be widely and appropriately used.

Conclusions:

- We continue to believe that it is reasonable and appropriate to use FAW warming devices to maintain normothermia as these devices are the only devices proven to decrease the risk of developing a post-operative infection.
- FAW warming devices have a >20-year track record of safety in >200 million surgical patients.
- FAW devices should be regularly undergo maintenance as outlined by manufacturer's guidelines, see attached table for recommendations.

References:

1. Kurz A, Sessler DI, Lenhardt R. Perioperative normothermia to reduce the incidence of surgical-wound infection and shorten hospitalization. Study of Wound Infection and Temperature Group. N Engl J Med. 1996 May 9;334(19):1209-15.
2. Melling AC, Ali B, Scott EM, Leaper DJ. Effects of preoperative warming on the incidence of wound infection after clean surgery: a randomised controlled trial. Lancet. 2001 Sep 15;358(9285):876-80.
3. Sikka R, Prielipp R. Forced Air Warming Devices in Orthopaedics: A Focused Review of the Literature. J Bone Joint Surg Am. 2014; 96:e200(1-7).
4. Kimberger O, Held C, Stadelmann K, Mayer N, Hunkeler C, Sessler DI, Kurz A. Resistive polymer versus forced-air warming: comparable heat transfer and core rewarming rates in volunteers. Anesth Analg. 2008 Nov;107(5):1621-6.
5. Albrecht M, Gauthier RL, Belani K, Litchy M, Leaper D. Forced-air warming blowers: An evaluation of filtration adequacy and airborne contamination emissions in the operating room. Am J Infect Control. 2011 May;39(4):321-8.
6. Albrecht M, Gauthier R, Leaper D. Forced-air warming: a source of airborne contamination in the operating room? Orthop Rev (Pavia). 2009 Oct 10;1(2):e28.
7. Legg AJ, Hamer AJ. Forced-air patient warming blankets disrupt unidirectional airflow. Bone Joint J. 2013 Mar;95-B(3):407-10.
8. McGovern PD, Albrecht M, Belani KG, Nachtsheim C, Partington PF, Carluke I, Reed MR. Forced-air warming and ultra-clean ventilation do not mix: an investigation of theatre ventilation, patient warming and joint replacement infection in orthopaedics. J Bone Joint Surg Br. 2011 Nov;93(11):1537-44.

Warming Unit Information and Table

“The repair, calibration, and servicing of the warming unit requires the skill of a qualified medical equipment service technician who is familiar with good practice for medical device repair” —3M Bair Hugger Manual (<http://multimedia.3m.com/mws/media/798399O/service-manual-english.pdf>)

Refer to your model manual for exact specifications. The table below is a general guide, and should not replace model specific guidelines.

TABLE I

Proper Maintenance and Use of Forced Air Warmers

Recommendations
1. The filter should be changed every 6 months or 500 hours. A counter is available on some devices (e.g., Bair Hugger 700 series) to indicate the total hours of use.
2. Calibration testing should occur every six months by biomedical engineering staff at the user’s institution. The manufacturer should check or replace devices that fail calibration testing.
3. Do not warm patients with the warming unit’s hose alone, as severe thermal injury may occur. Always connect the hose to a new, manufacturer-approved warming gown for each patient.
4. Do not continue warming if the red over-temperature indicator light illuminates or an audible alarm sounds, as thermal injury may result. Turn the warming unit off immediately and check the patient’s skin.
5. Do not use a forced air warming device over transdermal medications; increased drug delivery and patient death or injury may result.
6. Do not allow the patient to lie on the warming unit hose or allow the hose to contact the patient’s skin during patient warming.
7. Equipment is not suitable for use in the presence of a flammable anesthetic mixture (e.g., containing air, oxygen, or nitrous oxide).
8. Do not place the non-perforated side of the blanket on the patient. Thermal injury may result. Always place the perforated side (the side with small holes) toward the patient.

Recommendations
9. The warming device should be disconnected from the power source before cleaning. Between patients, the outside of the hose should be cleaned with a damp, soft cloth and a mild detergent or antimicrobial spray and then dried with a separate cloth.
10. If a fault occurs in the unit, unplug the temperature management unit and wait for five minutes. Reconnect the temperature management unit to a grounded power source. The unit will perform the normal power-on-reset sequence and then enter the standby mode. If the unit does not return to normal operation, contact a service technician.
11. Temperature and calibration testing should be performed every 6 months or 500 hours of use.

Taken from Sikka, RS *J Bone Joint Surg Am*, 2014 Dec 17; 96 (24): e200 .
<http://dx.doi.org/10.2106/JBJS.N.00054>

EXHIBIT DX39

TO DECLARATION OF PETER J. GOSS IN
SUPPORT OF DEFENDANTS' MOTION TO
EXCLUDE PLAINTIFFS' ENGINEERING
EXPERTS

1 KOENIGSHOFER

2 UNITED STATES DISTRICT COURT

3 DISTRICT OF MINNESOTA

4 -----
5 In Re:

6 Bair Hugger Forced Air Warming

7 Products Liability Litigation

8 This Document Relates To:

9 All Actions MDL No. 15-2666 (JNE/FLN)

10 -----
11 VIDEOTAPED DEPOSITION DANIEL KOENIGSHOFER, P.E.

12 Chapel Hill, North Carolina

13 June 13, 2017

14
15
16
17
18
19
20
21
22
23
24 Randi J. Garcia, RPR

25 Job no. 124784

Page 54

KOENIGSHOFER

Q. And it says, "But most agree about 90 percent of HAIs are transmitted by direct contact with about 10 percent resulting from airborne transmission."

Do you agree with that statement?

A. Yes. I've seen publications anywhere from five to 20, but those are about 10.

Q. Going back to the question I asked earlier about endogenous and exogenous sources of surgical site infections, would the same percentage apply to infections from exogenous sources versus endogenous, meaning -- that's a bad question.

A. Yes.

Q. Would you say that approximately --

MS. ZIMMERMAN: I'm going to object --

MR. GOSS: Go ahead.

MS. ZIMMERMAN: I'll let you finish.

Then I'll jump in and then you can jump in.

BY MR. GOSS:

Q. Would you say that approximately 90 percent of hospital-acquired infections or

Page 55

KOENIGSHOFER

associated infections result from endogenous sources?

MS. ZIMMERMAN: Object to the form of the question. Foundation. And misstates the prior testimony.

THE WITNESS: I couldn't answer that question anyway. I don't know the answer.

BY MR. GOSS:

Q. So are you saying there's a difference between infections transmitted by direct contact and infections from endogenous sources?

MS. ZIMMERMAN: Objection to form.

BY MR. GOSS:

Q. Or can you answer that?

A. I can't answer that question.

Q. Would you need microbiological expertise to answer that question?

MS. ZIMMERMAN: Object to form.

THE WITNESS: I would, yes.

BY MR. GOSS:

Q. And fair to say you're not a microbiologist?

A. Correct.

Page 56

KOENIGSHOFER

Q. Any other publications on Exhibit 6 that relate to surgical site infections?

A. No.

Q. Have you written any articles on the potential for medical equipment to interfere with operating room airflow?

A. No.

Q. Have you written any articles specific to patient warming devices?

A. No.

Q. Let's go back to your resume, please. Exhibit A to the report. Let's see. The fourth paragraph talks about your hands-on engineering experience. And the last sentence says, "He has personally designed every discipline in healthcare engineering, including med gas, fire alarm, electrical, mechanical, sprinklers, HVAC, emergency power, et cetera."

And my question is: Have you ever designed a medical device?

A. No.

Q. The paragraph right above that mentions your previous role as an expert witness. And the case involved an infection

Page 57

KOENIGSHOFER

from surgery; is that right?

A. Yes.

Q. What type of surgery was it?

A. Open-heart.

Q. What type of infection?

A. Fungal infection on the outside of the heart.

Q. And what field work did you do in that case?

A. I looked inside the air handler that served the space, and I looked in the ductwork that served the particular OR where the infection occurred. And then I looked inside the OR and inside the laminar diffuser.

Q. And when you say you looked inside, were you taking samples of anything?

A. Well, I was -- I was -- I didn't do any instrumentation at all other than temperature and humidity, well, and a Kleenex for pressurization. But when a piece of black insulation fell out of the diffuser when I opened it, I guess you could say that I took a sample.

Q. Okay. So did you send the insulation

1 KOENIGSHOFER

2 only testify for plaintiffs or were you open to
3 testifying for defendants?

4 A. B.

5 Q. So both?

6 A. Yes.

7 Q. Since you put this listing up, have
8 you gotten any calls, any potential referrals?

9 A. I got a call from a guy whose air
10 conditioner burned up in his house. And a call
11 from a lady who had, I don't know, mold in her
12 crawl space or something. And I turned them
13 both down.

14 Q. Have you been approached ever by any
15 manufacturers of HVAC equipment to serve as an
16 expert witness in their cases?

17 A. No.

18 Q. Have you ever had any conversations
19 with any manufacturers of HVAC equipment about
20 litigation that they were involved in? That
21 you can recall.

22 A. No.

23 Q. So are you currently employed by
24 Dewberry?

25 A. I work for them about 20 hours a

1 KOENIGSHOFER

2 week.

3 Q. Are you still an employee or do you
4 have an independent contract relationship with
5 them? How would you characterize it?

6 A. It's complicated. Basically, I can't
7 really answer that question, not because I
8 won't, but I can't. I do get -- I can work
9 however many hours I want and I get paid
10 hourly. And I get a paycheck from them,
11 which -- from which they do withholding. But I
12 don't get any benefits.

13 Q. Do your expert fees for your work on
14 this case go to Dewberry?

15 A. No.

16 Q. And did you need to ask Dewberry for
17 permission to participate as an expert in this
18 case?

19 A. No. I mean, you know, again, the
20 agreement is I'm not going to do anything that,
21 basically that Dewberry has anything to do
22 with.

23 Q. Have you talked to anyone at Dewberry
24 about the fact that you were retained as an
25 expert witness in this case?

1 KOENIGSHOFER

2 A. Yes.

3 Q. Who have you spoken to about that?

4 A. Shepherd Hockaday.

5 Q. And who is that?

6 A. He's sort of my boss.

7 Q. Did you talk to Mr. Hockaday about
8 the deposition today?

9 A. Probably not. Probably not.

10 Q. What was the nature of your
11 conversation with Mr. Hockaday about your
12 participation as an expert in this case?

13 A. It was just casual conversation.
14 What are you up to these days? What are you
15 doing with all your time besides playing golf?

16 Q. Did you talk to Mr. Hockaday about
17 your opinions in this case?

18 A. No.

19 Q. We covered Mr. Hockaday.

20 Have you talked to anyone outside
21 from counsel at this table in preparation for
22 your deposition today?

23 A. No.

24 Q. Can you tell me what you did to
25 prepare for the deposition today?

1 KOENIGSHOFER

2 A. Well, as you know, I didn't get a
3 whole lot of warning about it. So I carefully
4 reviewed my report. Then I reviewed the
5 reports that I cited in my report and gathered
6 a few others, but I didn't really get around to
7 reading much of anything else.

8 Q. So you reviewed your report. Did you
9 have occasion to revisit any of your opinions?

10 A. No. I mean, I marked it up a little
11 bit for typos and things I found in it.

12 Q. Is there anything in your report that
13 you felt you needed to amend or modify?

14 A. Well, only one thing, but at some
15 point toward the end of my report, I said that
16 the Bair Hugger might put out 50 to 100 CFM.
17 Honestly, I don't know where I got the 100,
18 but...

19 Q. Okay.

20 A. It should have read "about 50."

21 Q. So this is on page 23 of the report,
22 right at the top of the page?

23 A. That's correct. That's correct.

24 Q. You say, "50 to 100 CFM are blown
25 from the blanket into or near the sterile

Page 70

1 KOENIGSHOFER
 2 field." And you're saying that that should
 3 read "about 50 CFM"; is that right?
 4 A. Yes. Yes.
 5 Q. And what is the 50 based on?
 6 A. Well, one of the -- I'm not a Bair
 7 Hugger expert. One of them puts out about 48
 8 CFM. I can't remember which one. I couldn't
 9 cite the model for you.
 10 Q. So if I told you that the
 11 specifications for the 750/775 say it will put
 12 out up to 48 CFMs, does that sound right to
 13 you?
 14 A. Yes.
 15 Q. Are you familiar with another model
 16 of Bair Hugger that's at issue in this case?
 17 A. You know, only in a very general way.
 18 I realize there's a 505 and 550 and a 700 or
 19 whatever. I did not make an effort to memorize
 20 the nuances of the different models.
 21 Q. Did you have an understanding that
 22 the airflow rate of other models might be
 23 different from the 750/775?
 24 A. Yes, I know that.
 25 Q. Do you -- do you know roughly what

Page 71

1 KOENIGSHOFER
 2 that airflow is?
 3 A. I think some of them are in the range
 4 of 35, 30 CFM, something like that.
 5 Q. So if the 505 were about 30 CFM,
 6 would you have any reason to disagree with
 7 that?
 8 A. I would have to look it up.
 9 Honestly, I don't remember which is which.
 10 Q. All right. Anything else in your
 11 report after reviewing it that you felt you
 12 needed to amend or modify?
 13 A. No. Again, other than just typos.
 14 Q. Okay. In preparation for your
 15 deposition today, did you review any documents
 16 from 3M or Arizant?
 17 A. So you're saying in the last two or
 18 three weeks since I've known I was going to be
 19 deposed?
 20 Q. Yeah. Let's start with that.
 21 A. No.
 22 Q. Before that, have you reviewed
 23 documents from 3M or Arizant?
 24 A. Yes.
 25 Q. Were you provided a copy of the

Page 72

1 KOENIGSHOFER
 2 protective order in this case that designates
 3 certain documents as confidential?
 4 A. Yes.
 5 Q. And have you signed an acknowledgment
 6 to be bound by it?
 7 A. Yes.
 8 MS. ZIMMERMAN: It's in the binder.
 9 MR. GOSS: Okay. Thanks.
 10 BY MR. GOSS:
 11 Q. In preparing for your deposition
 12 today, have you reviewed any reports from other
 13 plaintiff's experts?
 14 A. Yes.
 15 Q. Which ones did you review?
 16 A. Keen, K-E-E-N, Koehn, K-O-E-H-N, I
 17 believe.
 18 Q. I'm going start just by asking about
 19 plaintiff's experts. Experts on the
 20 plaintiff's side.
 21 A. Oh, Elghobashi.
 22 Q. Okay.
 23 A. I think that's it.
 24 Q. Did you review a report by Yadin
 25 David?

Page 73

1 KOENIGSHOFER
 2 A. No.
 3 Q. Did I get that right?
 4 MR. ASSAAD: Close enough.
 5 MR. GOSS: Is it David?
 6 MR. ASSAAD: David, yes.
 7 MR. GOSS: It is David. Okay.
 8 THE WITNESS: Never heard the name.
 9 BY MR. GOSS:
 10 Q. Did you review a report by Michael
 11 Buck?
 12 A. No.
 13 Q. Did you review a report by William
 14 Jarvis?
 15 A. No.
 16 Q. So you started out mentioning that
 17 you reviewed reports by Keen and Kuehn, which
 18 he actually pronounces it Keen too, so they're
 19 both Keens. And I'll just tell you for a
 20 shorthand, the way I keep it straight is
 21 there's an American Kuehn and a Canadian Keen.
 22 A. Yes.
 23 Q. All right. Do you know either of
 24 those gentlemen?
 25 A. I know Michael Keen, the Canadian

Page 78

KOENIGSHOFER

deposition.

Q. Van Duren?

A. Van Duren.

Q. Was that in the last two or three weeks?

A. No. I guess I'd have to look at the book again. I read some other expert's stuff and I can't remember who. Not expert, deposition.

Q. Some other depositions? And I'm really just asking for what you can remember, what stands out in your mind as significant that you reviewed to prepare for today. We've covered the Elghobashi expert report from the plaintiffs, the four expert reports from the defense. Any other documents that you spent particular -- gave particular focus or attention to prepare for today?

MS. ZIMMERMAN: In addition to his report.

BY MR. GOSS:

Q. In addition to your report. That's right.

A. Well, I mean, I looked at an exploded

Page 79

KOENIGSHOFER

view of a Bair Hugger on one of their maintenance manuals that's available online.

Q. Okay. And why did you do that?

A. See how it's built.

Q. Was that something you did in the last couple weeks to prepare for today?

A. No.

Q. Was there anything about that exploded view of the Bair Hugger that contributed to your opinions in this case?

A. Yes. Well, I mean, I looked carefully at how the filtration works.

Q. So from the exploded view of the Bair Hugger, you could tell how the filtration works in the unit?

A. Well, how it's installed, yes.

Q. Okay. Obviously, you met with counsel to prepare for the deposition today; correct?

A. Yes.

Q. And I'm not going to ask you about specific documents you reviewed with them. I just want to know how many meetings did you have with them to prepare for today?

Page 80

KOENIGSHOFER

A. One.

Q. Was that --

A. Yesterday.

Q. So the meeting you had in Minneapolis, was that more to do with your report than deposition preparation?

A. That's correct. Yes.

Q. Okay. I want to talk a little more about your experience. Do you have any medical training?

A. No.

Q. You've already indicated that you don't have expertise in microbiology?

A. Correct.

Q. Do you have expertise in infectious diseases?

A. No.

Q. Do you have any expertise in aseptic technique?

A. No.

Q. Expertise in infection control practices other than as they relate to HVAC systems?

A. No.

Page 81

KOENIGSHOFER

Q. Do you have expertise in heat transfer?

A. I understand heat transfer. I'm not a professor of heat transfer.

Q. Are you an expert in air filtration?

A. I understand filtration quite well. Relative to other people at ASHRAE who truly are experts, I do not know as much as they do.

Q. Have you ever conducted any testing to determine the efficiency of an air filter?

A. Well, if you go all the way back to my air pollution days, that was sort of what I was doing.

Q. Okay. Have you ever conducted any testing to determine the efficiency of an air filter used in a hospital?

A. No.

Q. Do you consider yourself an expert in ASHRAE Standard 52.2?

A. No.

Q. Do you have any expertise in biomedical engineering?

A. No.

Q. Before you were retained in this

Page 82

KOENIGSHOFER

case, had you ever heard of a Bair Hugger?

A. Yes.

Q. How did you -- what do you recall about Bair Huggers before you got into the litigation?

A. I'm just very interested in everything hospital. So when I would talk to friends of mine or owners who work at hospitals, we'd talk about, you know, what exactly do they do in there? How does it all work? So someplace along the way, someone mentioned a Bair Hugger.

Q. Did you ever have any conversations with anyone before you got involved in this case about any concerns they had about the Bair Hugger and whether it was affecting the OR environment at their hospital?

A. No. It was actually in the context of are we going to put a blanket warmer into this OR? "Yes" or "no"? No, because we use Bair Huggers. What's a Bair Hugger?

Q. Okay. So you mentioned a blanket warmer. What would that be? As distinguished from the Bair Hugger, what's a blanket warmer?

Page 83

KOENIGSHOFER

A. It's a large device that looks like a refrigerator. Literally heats whatever's in there, but they put blankets in there, I guess.

Q. Oh, okay. So this --

A. Wool blankets. I don't know what they are. Cotton -- I don't know what they're made of -- blankets.

Q. I gotcha. So this -- this would be some sort of a heater or heater storage for normal cotton or wool blankets; is that right?

A. That's correct.

Q. It's not like an electric blanket that you would put on an OR table?

A. That's correct. I mean, it's electric. Uses electricity. You plug it in the wall. You use electricity to make heat and it heats however many blankets you've got stacked in this cabinet.

Q. But the blankets themselves aren't something that you --

A. Regular old blankets.

Q. It's not something you plug in?

A. No.

Q. Okay. I think you mentioned earlier

Page 84

KOENIGSHOFER

with respect to patient-warming devices other than the Bair Hugger, you did some research on the Mistral device?

A. Yes.

Q. What did you look into with the Mistral?

A. I simply was Googling around and came upon them as a, I guess, competitor. So I went to their website and looked at what they sell, what they do, their points of view.

Q. What did you learn from your research into Mistral? What stood out in your mind as relevant to your opinions in this case?

MS. ZIMMERMAN: Object to form.

THE WITNESS: I would need to look at -- you know, it's been -- this was back when I first started on this case, a year or more ago. It seems to me I recall the fact that they used a true HEPA filter in their device.

BY MR. GOSS:

Q. Anything about -- anything else about the Mistral that stood out to you as noteworthy?

Page 85

KOENIGSHOFER

A. No. I spent a lot of time on their website reading about nosocomial -- normothermia.

Q. Okay. On the Mistral website?

A. Yeah. They just had an article about it.

Q. Other than your reading of the Mistral article about normothermia, did you do any other research into normothermia?

A. No. I can't think that I read anything else about it.

Q. Do you have an understanding of the technical definition of normothermia versus hypothermia?

A. No.

Q. Have you reviewed any literature that talked about the benefits of normothermia to the patient?

A. Yes. Some of these articles that are truly about Bair Huggers or whatever, they kind of start out with "why do Bair Huggers exist." And they'll have a paragraph about normothermia.

Q. What's your understanding of the

Page 86

1 KOENIGSHOFER
 2 benefits to the patient of normothermia?
 3 A. Well --
 4 MS. ZIMMERMAN: Object to form. You
 5 can go ahead.
 6 THE WITNESS: I understand that
 7 anesthesia, patients get cold, and for the
 8 most part, anesthesiologists don't like
 9 for the patients to get cold, and so it's
 10 beneficial to the patient to be kept warm.
 11 BY MR. GOSS:
 12 Q. To your understanding, are there any
 13 benefits to the patient of normothermia, beyond
 14 comfort?
 15 A. I believe that I have read that, you
 16 know, the outcomes are improved by not letting
 17 the body get too cold.
 18 Q. But at any rate, you're not an expert
 19 in temperature regulation of the human body?
 20 A. I am not a biological expert.
 21 Q. Have you ever participated in an
 22 investigation of an infectious outbreak at a
 23 hospital?
 24 A. Well, that expert witness case that I
 25 was on. I guess you could say it was. It

Page 87

1 KOENIGSHOFER
 2 wasn't really an outbreak.
 3 Q. Okay. It was one patient; right?
 4 A. Yes.
 5 Q. Have you ever worked with a hospital
 6 that was investigating an outbreak or cluster
 7 of infections?
 8 A. No.
 9 Q. Do you have any expertise in the
 10 cleaning chemicals that are used to clean
 11 operating rooms?
 12 A. No.
 13 Q. Do you have any expertise in hospital
 14 sanitation and hygiene practices other than
 15 HVAC?
 16 A. About this much (indicating).
 17 Q. What can you tell me that you know
 18 about that?
 19 A. Well, I understand that there's
 20 something called a terminal clean, which is, in
 21 my limited understanding, is a super-deduper
 22 cleaning, which is different than -- I didn't
 23 even know the name of a nonterminal clean.
 24 That's kind of everything I know about it.
 25 Q. You've designed HVAC systems for

Page 88

1 KOENIGSHOFER
 2 operating rooms; correct?
 3 A. Yes.
 4 Q. About how many would you say you've
 5 done?
 6 A. Well, from scratch, maybe 20.
 7 Q. Were any of those ORs dedicated to
 8 orthopedic surgery?
 9 A. You know, my mind goes fuzzy between
 10 things that I designed and places that I worked
 11 to try to improve conditions.
 12 Q. Okay. Well, let's include both in
 13 your answer.
 14 A. Okay. Then yes.
 15 Q. How many orthopedic ORs have you
 16 either designed or worked to improve in some
 17 way?
 18 A. Let's just say 15.
 19 Q. Is there a difference in your
 20 approach to the HVAC system for a general
 21 surgery OR versus an orthopedic OR?
 22 A. No.
 23 Q. So your approach is the same. Is
 24 there anything different in the execution of
 25 the design of an orthopedic OR versus a general

Page 89

1 KOENIGSHOFER
 2 surgery OR?
 3 A. Some clients insist on using HEPA
 4 filtration, although it's not required. One of
 5 the studies I did was on, the surgeons wanted
 6 to put curtains around the diffuser array. And
 7 they asked me to give them a little study of
 8 pros and cons of that. It was an orthopedic
 9 surgery -- orthopedic OR.
 10 Q. The curtain, was it an air curtain or
 11 a fabric curtain? What kind of curtain was it?
 12 A. Plexiglass.
 13 Q. Okay. So it was a Plexiglass curtain
 14 around --
 15 A. More of a barrier.
 16 Q. A barrier around the diffusers and
 17 the ceiling of the OR?
 18 A. Yes.
 19 Q. And was this an orthopedic group that
 20 wanted to do this?
 21 A. It was a hospital that -- but it was
 22 an orthopedic surgery unit. It wasn't a
 23 private orthopedic group was the distinction
 24 I'm making there.
 25 Q. So it was for a hospital, but the

1 KOENIGSHOFER

2 room was going to be for their orthopedic unit?

3 A. Yeah. Well, it already was, but they
4 wanted to add the Plexiglass barrier.

5 Q. Was there a particular manufacturer
6 of the Plexiglass barrier or was it part of an
7 integrated system with diffusers?

8 A. Yes. And I don't remember the name
9 of the manufacturer.

10 Q. What was your advice to the hospital
11 of the use of this Plexiglass barrier?

12 A. I recommended that it was not cost
13 effective.

14 Q. What was the rationale behind the
15 Plexiglass barrier? What it was supposed to
16 do?

17 A. Well, it was supposed to improve the
18 laminar flow of the air as it comes from the
19 diffuser. Keep it as straight as you can as
20 long as you can. So they would stick down, I
21 don't know, maybe 18, 24 inches, something like
22 that.

23 Q. So let me ask you some questions
24 about that statement. When we say "laminar
25 flow," what are we really talking about?

1 KOENIGSHOFER

2 MS. ZIMMERMAN: Object to form.

3 BY MR. GOSS:

4 Q. In the context of a hospital and air
5 supply from the ceiling.

6 A. Well, in the context of a hospital,
7 we put in diffusers, which literally in the
8 industry are called "laminar flow diffusers."
9 It is a type of a diffuser, which consists of
10 big metal covers with a bunch of small holes in
11 them, and the air gently flows down in kind of
12 a rainfall pattern.

13 Q. So what makes it laminar?

14 MS. ZIMMERMAN: Object to form.

15 THE WITNESS: Well, it is released in
16 a strictly vertical manner and at a speed
17 that, as I say, you -- 35 feet a minute
18 makes basically a maximum velocity at the
19 diffuser. And so you hope that it just
20 stays together as a laminar flow.

21 BY MR. GOSS:

22 Q. Okay. Do the -- do the holes in the
23 diffuser outflow, does that have something to
24 do with what makes it laminar?

25 MS. ZIMMERMAN: Object to form.

1 KOENIGSHOFER

2 Foundation.

3 THE WITNESS: Well, yeah. You've got
4 to give it a little kick in the butt to
5 get the air moving.

6 BY MR. GOSS:

7 Q. Would it be fair to say that you're
8 not an expert in laminar flow?

9 A. Yeah. Yes.

10 Q. I think there was a comment in your
11 report and a footnote on page 13. So there's a
12 sentence in the first paragraph. It says, "As
13 shown in the following figure, clean air is
14 directed into the room through so-called
15 laminar diffusers." And then there's a
16 footnote; right?

17 A. Yes.

18 Q. The footnote says, "This intentional
19 airflow is frequently called laminar, though
20 the airflow is not truly laminar from a physics
21 perspective." What did you mean by your
22 statement in the footnote?

23 A. Well, to be honest, I'm just
24 repeating what true laminar flow experts have
25 said to me, guys who are, you know, Ph.D Penn

1 KOENIGSHOFER

2 State gurus in this kind of stuff. And they
3 say it's not really laminar flow. And I say,
4 okay, okay, okay. But we engineers call it
5 that.

6 Q. All right. So do you know the names
7 of any of the -- can you remember the names of
8 any of the laminar flow gurus that you've
9 spoken to about this?

10 A. No, not really. This is a long time
11 ago. There was a guy from Penn State, but I
12 can't remember.

13 Q. It wasn't Gary Settles?

14 A. No, no, no. It was not Gary Settles.
15 He probably would -- he could probably answer
16 this question.

17 Q. Let's see. All right. So we started
18 on this tangent about laminar flow when we were
19 talking about this system that you were asked
20 to advise the hospital on that had these
21 Plexiglass barriers; right?

22 A. Uh-huh.

23 Q. Okay. And your advice to the
24 hospital was that the system was not cost
25 effective; is that right?

1 KOENIGSHOFER
 2 BY MR. GOSS:
 3 Q. I just want to know his answer to the
 4 question. Would you be able to answer that
 5 question?
 6 A. Yes.
 7 Q. And how would you answer that
 8 question?
 9 A. I would probably get a piece of paper
 10 and indicate air moving unidirectionally as
 11 opposed to turbulently.
 12 Q. Okay. And what about systems that
 13 deliver laminar flow versus turbulent flow? Do
 14 you have any expertise in the difference
 15 between those types of systems?
 16 A. Well, yes. I mean, I could design
 17 this room, and this diffuser right here works
 18 on the basis of turbulence. That's what it
 19 depends upon.
 20 Q. But in terms of operating room air
 21 supply, do you have expertise in the difference
 22 between a turbulent diffuser versus a laminar
 23 one?
 24 MS. ZIMMERMAN: Object to form.
 25 THE WITNESS: Ask me the question

1 KOENIGSHOFER
 2 again.
 3 BY MR. GOSS:
 4 Q. Sure. How would you describe or can
 5 you answer the question, what the difference is
 6 between a turbulent supply system in an
 7 operating room and a laminar supply system?
 8 A. Yes. And that's -- that was my -- my
 9 hand drawings.
 10 MS. ZIMMERMAN: And if we could just
 11 clarify for the record and the court
 12 reporter that the witness is gesturing
 13 with his hands.
 14 THE WITNESS: Vertical airflow fairly
 15 tight.
 16 BY MR. GOSS:
 17 Q. Okay. You've never calculated a
 18 Reynolds number; is that true?
 19 A. I have in college.
 20 Q. Is calculating a Reynolds number part
 21 of what you do in your engineering practice
 22 when working with hospitals?
 23 A. No.
 24 Q. Have you tried to calculate a
 25 Reynolds number for any of your work in this

1 KOENIGSHOFER
 2 case?
 3 A. No.
 4 Q. What are the issues that you've been
 5 asked to address in this case?
 6 A. I guess just the overall use of the
 7 Bair Hugger in an operating room.
 8 Q. Have you done any experiments to
 9 address that question?
 10 A. No.
 11 Q. Have you taken any measurements of
 12 air temperature or velocity coming out of a
 13 Bair Hugger blanket?
 14 A. No.
 15 Q. Have you done any experiments to
 16 determine the efficiency of Bair Hugger
 17 filters?
 18 A. No.
 19 Q. Have you done any testing
 20 measurements or experimentation of any kind on
 21 a Bair Hugger unit?
 22 A. No.
 23 Q. Have you seen a Bair Hugger unit in
 24 person?
 25 A. Yes.

1 KOENIGSHOFER
 2 Q. When was that?
 3 A. In March.
 4 Q. Was that during the meeting with
 5 counsel?
 6 A. Yes.
 7 Q. Outside of that meeting, have you
 8 seen a Bair Hugger unit in person?
 9 A. I'm sure I've seen them when I've
 10 been in operating rooms.
 11 Q. But fair to say you didn't examine
 12 them closely in that setting?
 13 A. Correct.
 14 Q. When you saw the Bair Hugger unit in
 15 March, how was it set up?
 16 A. Just sitting on the floor.
 17 Q. Was it connected to a blanket?
 18 A. No.
 19 Q. Did you do anything with the Bair
 20 Hugger unit when you saw it?
 21 A. I took the cover off so I could see
 22 inside.
 23 Q. Did you turn it on?
 24 A. I don't think so.
 25 Q. And you said it was not connected to

Page 102

KOENIGSHOFER

a perforated blanket; is that right?

A. That's correct.

Q. Have you ever felt the flow of air from a Bair Hugger blanket?

A. No.

Q. Have you ever felt the flow of air from a Bair Hugger hose that's not connected to a blanket?

A. No.

Q. So when you say you took the cover off of the Bair Hugger, what was your goal in doing that?

A. See the insides.

Q. Was there anything that stuck out in your mind as significant from your looking on the inside of a Bair Hugger unit?

MS. ZIMMERMAN: Object to form.
BY MR. GOSS:

Q. What did you take away from that, is what I'm asking.

A. It looked just like my wife's hair dryer that I tried to fix recently.

Q. So it had a heating coil in it; correct?

Page 103

KOENIGSHOFER

A. Uh-huh.

Q. And a fan?

A. And a fan.

Q. Does your wife's hair dryer have a filter?

A. No.

Q. So that would be one difference?

A. Sure.

Q. So the Bair Hugger that you examined was -- that wasn't in an OR at the time; right?

A. Correct.

Q. And if you didn't turn it on, is it fair to say that you didn't evaluate whether the air from the Bair Hugger was doing anything to the air in the room?

A. That's correct.

Q. Do you remember what model of Bair Hugger it was?

A. I think it was early in the 500 series, I believe.

Q. Do you remember if it was white or kind of blue/purple?

A. I think it was white.

Q. Did you take the filter out of that

Page 104

KOENIGSHOFER

Bair Hugger?

A. I don't remember.

Q. Do you remember what the filter looked like, like what shape it was?

A. Yeah. I think it was one of the flat rectangular ones.

Q. Did you take the filter out and examine it?

A. Honestly, I don't remember whether I did or did not.

Q. You mentioned this filter was a flat rectangular one. Are you familiar with other shapes or sizes of Bair Hugger filters?

A. Oh, again, I've seen on the exploded views that they have cylindrical ones.

Q. Other than the shape of the filter being different between the cylindrical and the rectangular, do you have any understanding as to whether the filter media in those two filters is different as of today?

A. Is different between a rectangular versus the cylindrical?

Q. Yes, sir.

A. I don't know.

Page 105

KOENIGSHOFER

Q. Do you have any understanding as to whether the filter media in the cylindrical and the rectangular filters was different at some time in the past, that they differed from each other?

A. You know, it seems like in the Van Duren or something, there was conversations about this, but sitting here right this minute, I don't remember. We could look at Van Duren. I believe it was Van Duren that said something about that I think there were some changes along the way.

Q. Do you intend to testify at trial about changes in the filter media in the Bair Hugger units?

A. I don't know.

Q. Do you -- do you have any opinions today about changes in the filter media in the Bair Hugger filters?

A. No.

Q. So you've seen a Bair Hugger unit. Have you ever seen a Mistral unit in person?

A. No.

KOENIGSHOFER

Q. Have you ever seen any other patient-warming devices in person?

A. No.

Q. Are you familiar with a device called the HotDog?

A. Only from the materials that I read in relation to this case.

Q. What's your understanding of what the HotDog is and how it works, if you have one?

A. It appears to me it's an electric blanket.

Q. Have you done any research for this case on the HotDog warming system?

A. I've looked at their website. I would not call it research.

Q. For your work on this case, have you done any research on standards or regulations that apply to patient warming devices?

MS. ZIMMERMAN: Object to form.

THE WITNESS: Can you ask me the question again.

BY MR. GOSS:

Q. Sure. Are you aware of any standards or regulations that apply to patient-warming

KOENIGSHOFER

devices?

MS. ZIMMERMAN: Object to form.

THE WITNESS: I am not aware of any.

BY MR. GOSS:

Q. Are you aware of any requirements or any regulations or standards that require the use of filtration in hospital equipment, other than the HVAC system?

MS. ZIMMERMAN: Object to the form of the question.

THE WITNESS: I'm not aware of any.

BY MR. GOSS:

Q. So for -- strike that.

Are you familiar with the types of infections that the -- no, back up.

Are you familiar with the types of surgeries that the plaintiffs in this litigation have undergone?

A. Well, in a general way, yes. My father-in-law just had a knee replacement. And I've looked at the -- a YouTube of a hip replacement.

Q. And when you say the YouTube hip replacement, are you referring to a particular

KOENIGSHOFER

video?

A. I wouldn't know. I mean, it was one of those days where you're just fishing all around the internet and you find something. It was not one put out by -- it was more of a training for medical people.

Q. Did it relate to the Bair Hugger at all?

A. No.

Q. All right. So do you have an understanding that the majority of the plaintiffs in this litigation have undergone either a hip replacement or a knee replacement?

A. Yes, I know that.

Q. And have you requested any information about the types of infections that these plaintiffs have developed as a result of those procedures?

A. No.

Q. In association with those procedures?

A. No.

Q. Do you -- for your work on this case, did you do any research into the rate of infection for hip and knee replacements in this

KOENIGSHOFER

country?

A. Somewhat, yes. But then you're going to ask me for the numbers.

Q. Yes, sir. What's your understanding of the current infection rate for hip procedures in this country?

A. I would really have to look at my booklet here.

MS. ZIMMERMAN: You can look at your notes.

THE WITNESS: If he wants me to do that, I'll do that.

MR. ASSAAD: Do it if you want to.

BY MR. GOSS:

Q. Do you have a general understanding of the infection rate for hip and knee replacements? Do you remember a figure?

A. I think it's generally in the range of 1 to 3 percent.

Q. Do you have an understanding as to whether that rate has increased, decreased or stayed the same over the last 10 years?

A. I believe -- well, I read a lot of articles and one guy says one thing and the

Page 126

KOENIGSHOFER

to some of the addenda that have come out more recently. I don't know how many addenda you have on this thing right here. They come out every month, every other month.

Q. What -- what addenda do you recall contributing to? What was the subject matter of the addenda?

A. The subject -- well, of addenda that have been adopted? I would really have to refer back to my notes on that one to remember which one, to which it applied.

Q. Is it your testimony that ASHRAE 170, Standard 170 has nothing to do with the best practices for HVAC design in healthcare facilities?

MS. ZIMMERMAN: Object to form. Misstates his testimony.

THE WITNESS: I would not make that statement.

BY MR. GOSS:

Q. Okay. So it does have something to do with best practices in the ventilation of healthcare facilities; is that right?

MS. ZIMMERMAN: Object to form.

Page 127

KOENIGSHOFER

THE WITNESS: Yes.

BY MR. GOSS:

Q. And that's something that a hospital looking to comply with Standard 170 is going to be interested in as best practices for ventilation of healthcare facilities; correct?

MS. ZIMMERMAN: Object to form. Foundation.

THE WITNESS: Again, you asked me about hospitals. I can't speak. There are 10,000 people that work at a hospital.

BY MR. GOSS:

Q. Well, you've worked with a lot of hospitals over the years, have you not?

A. I have.

Q. And those hospitals are interested in your expertise on best practices; correct?

MS. ZIMMERMAN: Object to form.

BY MR. GOSS:

Q. In HVAC design for the ventilation of healthcare facilities; true?

A. Yes.

Q. All right. 170 covers a wide range of topics, but one of the topics that's

Page 128

KOENIGSHOFER

covered, of course, is filtration; correct?

A. Yes.

Q. All right. And if you look at table 6.4, it discusses minimum filter efficiencies?

A. Yes.

Q. On page 5; correct?

A. Yes.

Q. It says, "Operating rooms for Class B and C surgery require, in filter bank number 1, a MERV 7 filter and in filter bank 2, a MERV 14 filter; is that correct?"

A. Correct.

Q. All right. First of all, let's explain what MERV is. What does that stand for?

A. Well, it's something like minimum efficiency -- always forget exactly what MERV stands for. It has something to do with minimum efficiency rating value or something like that.

Q. And do you know how MERV --

A. Minimum Efficiency Reporting Value.

Q. Okay. Do you know how MERV ratings are calculated for air filters?

Page 129

KOENIGSHOFER

A. I know something about it, yes.

Q. Are you familiar with the ASHRAE standard for calculating MERV ratings for air filters?

A. In a general way. I'm not on Standard 52.

Q. But it's Standard 52.2; correct?

A. 52.2, I believe that's the latest.

Q. All right. So coming back to this table 6.4, is it fair to say that filter bank number 2 in this table, is that the terminal filtration? In other words, the last filter before the air goes to the room?

A. It's the last filter in the system.

Q. In the system. And this provides for a MERV minimum of 14; correct?

A. Correct.

Q. Have you ever taken a position in any committee meetings for 170 that that value should be higher?

A. I've certainly been involved in a lot of discussions about it.

Q. Have you personally recommended to the committee that the final filter in the

Page 130

KOENIGSHOFER

system for an operating room -- for -- should be higher than 14?

A. Not for a general operating room.

Q. What about other than for a general operating room?

A. I have suggested that maybe we should start requiring it for orthopedic operating rooms.

Q. And you suggested this during a committee meeting of -- of the 170 Committee?

A. Yes.

Q. Did you make that recommendation -- when do you recall making that recommendation?

A. As Jim said, I've been going to these meetings for 14 years, two or three a year for 14 years. I honestly can't remember at what point.

Q. Was it in the last two years?

A. I would say probably before that.

Q. Has it been your experience that orthopedic rooms sometimes do incorporate HEPA filters?

A. Yes.

Q. And nothing in this table would

Page 131

KOENIGSHOFER

prevent an orthopedic room from doing that; correct?

A. That's correct.

Q. In your -- in the various meetings you've attended for Standard 170, do you have any understanding as to whether the committee intends to increase the minimum filter requirements for Class B and Class C surgery?

MS. ZIMMERMAN: Object to form.

THE WITNESS: Among the addenda on the table at this time, that is not one of them.

BY MR. GOSS:

Q. Where it says "Class B and Class C surgery," am I correct that orthopedic surgery would be encompassed within one of those classes?

A. Yes.

Q. Which one is it?

A. It's probably the Class C, I would assume.

Q. And the only space designation on this table 6.4 that calls for HEPA is a protective environment room; correct?

Page 132

KOENIGSHOFER

A. That's correct.

Q. And this protective environment room, is that where you put someone who is contagious with a respiratory illness, for example?

A. No, just the opposite.

Q. It's where you put somebody who's susceptible that you need to protect?

A. Correct.

Q. Okay. Are the HEPA filters in protective environment rooms, are they on the inflow to the room or the outflow from the room?

A. Inflow.

Q. If you'll turn with me to page 14, section 7.4 talks about surgery rooms. And if you look at point A, it says, "The airflow shall be unidirectional downwards and average velocity of the diffuser shall be 25 to 35 cubic feet per minute per square foot."

Are you familiar with that requirement for the face velocity or volume metric flow out of the diffusers?

A. Yes.

Q. And it says here, "For further

Page 133

KOENIGSHOFER

information, see Memarzadeh and Manning 2002, and Memarzadeh and Jeong in informative appendix B." Are you familiar with the Memarzadeh and Manning paper on this subject?

A. Yes.

Q. So what is -- what is the reason that Memarzadeh and Manning gave for setting the airflow volume and velocity at 25 to 35 CFMs per square foot?

A. Well, it was to get adequate air changes, 20 per square foot -- I'm sorry, 20 air changes per hour. And given the size the laminar diffuser is going to be, roughly the size of the table plus a foot or two on each side, you have to have a certain amount of airflow to get those air changes.

Q. Okay. But is there something about this particular velocity that's important, the 25 to 35 CFMs?

A. Memarzadeh hypothesized about a wound plume.

Q. Tell me about that. What does he mean by "wound plume"?

MS. ZIMMERMAN: Object to form.

Page 210

1 KOENIGSHOFER
 2 THE WITNESS: I wouldn't say that.
 3 BY MR. GOSS:
 4 Q. All right. How would you say it?
 5 A. If the number of particles is low,
 6 the probability is that the number of
 7 colony-forming units is also low.
 8 Q. And now, are you saying conversely,
 9 that if the particle count is high that there
 10 is a correlation of some sort to airborne
 11 bioburden?
 12 A. I believe there is, yes.
 13 MS. ZIMMERMAN: Objection.
 14 Q. How would you show that
 15 scientifically?
 16 A. Some correlation.
 17 Q. Okay.
 18 A. Well, I mean, the efforts that these
 19 different people are making. I mean, they
 20 didn't say there was no correlation.
 21 Q. No statistically significant
 22 correlation; correct?
 23 A. Within the size ranges that they're
 24 discussing.
 25 MS. ZIMMERMAN: Object to form.

Page 212

1 KOENIGSHOFER
 2 A. I think that some number of particles
 3 in the air are going to have bacteria on them.
 4 Q. No dispute there.
 5 But the correlation between the
 6 number of particles and the number of bacteria,
 7 what do you rely on in terms of your role as an
 8 expert witness in this case to make that
 9 correlation?
 10 A. For example, in the standard USP 797,
 11 they talk about CFUs per particles.
 12 Q. Okay. And that's US Pharmacopeia?
 13 A. Yes.
 14 Q. For a pharmacy?
 15 A. Yes.
 16 Q. Are you aware --
 17 A. I've seen other articles on it.
 18 Again, I can find it here. I think I have one
 19 here.
 20 Q. But as of right now, you can't point
 21 me to anything that correlates particles to
 22 bioburden in an operating room?
 23 MS. ZIMMERMAN: Objection to form.
 24 Misstates his testimony.
 25

Page 211

1 KOENIGSHOFER
 2 BY MR. GOSS:
 3 Q. Well, the results did not reveal any
 4 statistically significant correlation between
 5 microbial loads and particle counts for either
 6 of the particle diameters considered; correct?
 7 A. That's what it says, yes.
 8 Q. All right. And the Landrin article
 9 also found that no particle count value could
 10 be predictive of a microbial count higher than
 11 5 CFUs per metered cube; correct?
 12 A. Predictive. In other words, you
 13 would have trouble drawing a -- a line on a
 14 graph.
 15 Q. What --
 16 A. Does more equal more? He didn't
 17 exclude that as a possibility.
 18 Q. As a possibility, but what would you
 19 rely on to make a correlation? What research
 20 or article would you rely on to make
 21 a correlation that particle count is an
 22 appropriate surrogate for bioburden?
 23 A. Well, first of all, I'd rely on
 24 common sense.
 25 Q. Okay.

Page 213

1 KOENIGSHOFER
 2 BY MR. GOSS:
 3 Q. Is that fair?
 4 MR. GOSS: I'm not asking his
 5 testimony. I'm asking him a question.
 6 BY MR. GOSS:
 7 Q. Can you tell me right now of any
 8 study that correlates airborne particles to
 9 actual bioburden in an operating room?
 10 MS. ZIMMERMAN: Well, respectfully,
 11 counsel, he's not required to have every
 12 study memorized that he's looked at.
 13 MR. GOSS: I understand that. I'm
 14 just asking him if he knows it or he
 15 doesn't.
 16 BY MR. GOSS:
 17 Q. I'm not saying no such studies exist.
 18 A. I believe that I have seen such
 19 statement in some of these studies that are in
 20 this binder right here.
 21 Q. Would it be fair to say that the
 22 literature regarding the correlation between
 23 particle counts and airborne bioburden is mixed
 24 in terms of some find correlation and some
 25 don't?

1 KOENIGSHOFER
 2 earlier, if so I apologize.
 3 Have you tested a Bair Hugger unit
 4 for leaks around the filter?
 5 A. No.
 6 Q. Page 13. It discusses the role of
 7 site in the infection equation. And the third
 8 sentence is, "Deep wounds are generally
 9 understood to be more susceptible than shallow
 10 wounds."
 11 What's that comment based on?
 12 A. Oh, I guess it is based on, you know,
 13 the reading that I've done. And again, common
 14 sense and the fact that, I mean, I know of
 15 people -- well, I've read of people who will
 16 get wounds -- I mean, infections in hip and
 17 knee replacements, and it lasts for years and
 18 years and years.
 19 Q. Yeah.
 20 A. It's obviously very, very serious.
 21 Q. Do you have any understanding of the
 22 rate of superficial surgical site infections,
 23 meaning around the skin and the incision?
 24 A. You know, I don't know the breakdown
 25 of those percentages of hospital-acquired

1 KOENIGSHOFER
 2 infections. So when I say it's 5 to 15 -- if
 3 you dug into the CDC data it may show you.
 4 Whether some are shallow, some are deep, I
 5 don't really know.
 6 Q. So your statement here is based more
 7 just on your experience?
 8 A. Yes.
 9 Q. The last sentence in that paragraph
 10 you're talking about the space below the OR
 11 diffusers. The area directly below the
 12 diffuser is referred to as the sterile field;
 13 correct?
 14 A. It is referred to by us design
 15 engineers as the sterile field, yes.
 16 Q. I want to make sure I understand why
 17 it's referred to as the sterile field. Is it a
 18 sterile field because the air coming down is
 19 sterile, or is it because the surgical site has
 20 been prepared using cleansers and --
 21 A. I'm speaking as a design engineer,
 22 and it's the air coming down. Is it
 23 100 percent sterile? No.
 24 Q. And then you say, "Anything that
 25 disrupts this waterfall of sterile air reduces

1 KOENIGSHOFER
 2 its effectiveness. Disruptions, turbulence are
 3 caused by surgeons and staff, objects, light
 4 booms, tables, thermal plumes, markedly hot or
 5 cold air, and air currents caused by devices,
 6 personnel and doors;" correct?
 7 A. Yes.
 8 Q. And all of those things can be
 9 present in an operating room with or without
 10 the Bair Hugger; correct?
 11 A. That's correct.
 12 Q. Page 14 you talk about the element of
 13 time in the infection equation.
 14 A. Yes.
 15 Q. And this is where you discuss the
 16 20 ACH requirement from Standard 170. And you
 17 say, "In most ORs this is a flow rate of 2000
 18 to 3000 CFMs; correct?
 19 A. Yes.
 20 Q. And I think you mentioned earlier
 21 that some hospitals may want a flow rate that's
 22 higher or lower than that; correct?
 23 MS. ZIMMERMAN: Object to form.
 24 BY MR. GOSS:
 25 Q. Or is that true?

1 KOENIGSHOFER
 2 A. Well, I have had clients who want
 3 more and there are probably clients who want
 4 less. But we never do less because that's what
 5 the code is.
 6 Q. So is it fair to say that 2000 to
 7 3000 CFMs is fairly typical for operating rooms
 8 in the U.S., based on your experience?
 9 A. Yeah. I mean, it depends on the size
 10 of the operating room -- the size of the
 11 operating room, the volume.
 12 BY MR. GOSS:
 13 Q. Okay.
 14 A. That's what you're doing. You're
 15 changing out the volume of the operating room
 16 20 times per hour. So flow rate in is
 17 determined by what's the volume of the
 18 operating room.
 19 Q. And the flow rate out of the Bair
 20 Hugger blankets, what is that figure?
 21 A. About 50.
 22 Q. About 50 for the 750, 775 and
 23 something lower than that for the 505; correct?
 24 A. That's correct.
 25 Q. Page 15 you have the -- the top

Page 238

1 KOENIGSHOFER
2 surgical site, would actually lead to an
3 increased risk of surgical site infection."
4 Based on your review of this data, do
5 you agree with their conclusion?
6 MS. ZIMMERMAN: Object to the form of
7 the question. The article speaks for
8 itself.
9 BY MR. GOSS:
10 Q. What's your opinion of the data
11 and -- and their conclusion? Do you disagree
12 with -- how they interpret it?
13 MS. ZIMMERMAN: I will object to the
14 form to the extent that it suggests that
15 the witness has been provided the actual
16 data, but you can answer the question
17 about the author's interpretation.
18 BY MR. GOSS:
19 Q. And just limited to what's in the
20 paper.
21 A. He's simply saying he can't make a
22 conclusion.
23 Q. Right. And looking at this data, do
24 you think that you can make a conclusion that
25 he didn't?

Page 240

1 KOENIGSHOFER
2 mark an exhibit.
3 (Thereupon, Exhibit 20 was marked for
4 identification.)
5 BY MR. GOSS:
6 Q. Is the copy -- is Exhibit 20 the same
7 as the copy you have in your notebook?
8 A. Yes.
9 Q. It's the same study anyway.
10 A. Yes. Mine is printed better than
11 yours. It's easier to read.
12 Q. That's fair. That's fair.
13 MS. ZIMMERMAN: Bigger font; right?
14 THE WITNESS: So Avidan did both. He
15 did the agar test as well as swabbing the
16 hoses.
17 BY MR. GOSS:
18 Q. All right. And with respect to the
19 agar plates, if you go to page 1074, the second
20 page says at the top, "Experiment 1: Are
21 microbes present in the airstream of warmers?"
22 It says, "Each warmer was placed
23 sequentially on a standard place on the floor.
24 The nozzle of the hose was suspended from an
25 infusion stand 40 centimeters above two agar

Page 239

1 KOENIGSHOFER
2 MS. ZIMMERMAN: Object to form.
3 THE WITNESS: I certainly could not,
4 with the data that is in front of me.
5 BY MR. GOSS:
6 Q. Okay. Do you recall encountering a
7 study in your review of the literature that
8 showed bacteria detected -- sorry, let me try
9 again.
10 Do you recall seeing a study that
11 found bacteria emitted from the Bair Hugger
12 blanket?
13 A. I saw one that had Bair Hugger --
14 bacteria from Bair Hugger hose.
15 Q. Okay. Was that Avidan?
16 A. Well, there's this one, and there's
17 also a guy -- is this the one where he did the
18 swabs? Because there's also one where a guy
19 swabbed the hoses too.
20 Q. Let's take a look.
21 A. This is agar plate, so I guess he was
22 just blowing air.
23 Q. Are you looking at Avidan?
24 A. This is Avidan.
25 MR. GOSS: Okay. Let me go ahead and

Page 241

1 KOENIGSHOFER
2 plates," correct?
3 A. Um-hmm, yes.
4 Q. And then the machine was turned on to
5 blow air at 43 degrees c over the plates for
6 five minutes.
7 40 centimeters, how -- roughly how
8 high is that? Is it --
9 A. Well, two and a half centimeters is
10 an inch, so it's, what, 12 inches or something.
11 Q. Okay. All right.
12 A. Fourteen.
13 Q. Okay. So a little more than a foot
14 off of the agar plates?
15 A. Uh-huh.
16 Q. Okay. With that setup would it be
17 possible for room air to be entrained in the
18 flow from the hose?
19 MS. ZIMMERMAN: Object to the form of
20 the question. Foundation.
21 THE WITNESS: You know, anything is
22 possible. I have not calculated what the
23 velocity of the air is from a Bair Hugger
24 hose.
25

Page 242

1 KOENIGSHOFER
 2 BY MR. GOSS:
 3 Q. Okay.
 4 A. As I think about it, 40 centimeters,
 5 that's -- that's a half a meter almost, so it's
 6 probably more like 18 inches. But anyway --
 7 Q. Okay.
 8 A. That order of magnitude.
 9 Q. Okay. In other words, the hose
 10 wasn't blowing directly on to the plate. It
 11 was --
 12 A. Yeah.
 13 Q. -- half a meter roughly from -- from
 14 the plates; correct?
 15 A. Yes.
 16 Q. All right. And they detected
 17 bacteria in some of the plates when they did
 18 that experiment; correct?
 19 A. They did.
 20 Q. But then they did a different
 21 experiment with agar plates under the Bair
 22 Hugger blanket; correct?
 23 A. Blankets were elevated over the agar
 24 plates. Doesn't say what the distance was
 25 there. I mean, in general, yes, what she said

Page 243

1 KOENIGSHOFER
 2 is true. I don't see in my --
 3 Q. The distance?
 4 A. -- in my 10 seconds of reading here
 5 that it says what the distance was between the
 6 plate and the blanket.
 7 Q. Okay. I don't think it does say, but
 8 you're welcome to look.
 9 But at any rate, as you observed in
 10 your report, when they had the blanket attached
 11 to the hose, they did not detect CFUs on the
 12 agar plates; correct?
 13 A. That is what they did in their
 14 report -- reported from their report, yes.
 15 Q. Okay. And that's .5b in your report,
 16 correct, on page 17?
 17 A. Yes.
 18 Q. If you turn to page point F, 5F,
 19 about Avidan, you mention that, "Recommend
 20 always use perforated blankets and microbial
 21 filter on hose, ensure hoses are sterilized
 22 regularly."
 23 With respect to perforated blankets,
 24 is it your understanding that -- or do you have
 25 an understanding as to whether 3M instructs

Page 244

1 KOENIGSHOFER
 2 users to always have the hose attached to a
 3 blanket during use?
 4 MS. ZIMMERMAN: Object to form. And
 5 foundation.
 6 BY MR. GOSS:
 7 Q. Did you review the operator's manual
 8 during your work in this case?
 9 A. Yes, I did. And yes, it does.
 10 Q. Okay. So that's Avidan.
 11 Do you recall -- and Avidan did not
 12 find bacteria emitted from the blanket;
 13 correct?
 14 A. Correct.
 15 Q. Did you find any studies that found
 16 bacteria emitted from the blanket?
 17 A. I found a study where soot was
 18 ejected from a blanket.
 19 Q. Okay. Is soot the same as bacteria?
 20 A. It is not.
 21 Q. In that paper where was the soot
 22 coming from?
 23 A. From the Bair Hugger.
 24 Q. What part of the Bair Hugger?
 25 A. From the -- well, the box, the black

Page 245

1 KOENIGSHOFER
 2 box.
 3 Q. Okay.
 4 A. Presumably from the heating elements,
 5 I don't know where within, but...
 6 Q. Was it -- was the source past the
 7 intake filter?
 8 A. It was.
 9 Q. Okay. So in other words, the soot
 10 was generated inside the machine post filter;
 11 correct?
 12 MS. ZIMMERMAN: Object to form. And
 13 foundation.
 14 BY MR. GOSS:
 15 Q. If you know. If you remember.
 16 A. I would have to make that assumption
 17 because there's almost nothing before the
 18 filter. All the mechanisms are after the
 19 filter.
 20 Q. Right. Right. Do you have an
 21 understanding -- or let me ask you this. Have
 22 you tried to measure the size of the pinholes
 23 perforations in the Bair Hugger blanket?
 24 A. I have not.
 25 Q. Do you have an understanding of how

Page 254

KOENIGSHOFER

A. Yes.

(Thereupon, Exhibit 22 was marked for identification.)

BY MR. GOSS:

Q. All right. Is this the same Kowalski paper that you discussed?

A. Yes.

Q. Okay. And what you say about it is, "Table 3 confirms estimates of CFU per cubic meter to match" -- is it Galson or Galson and Goddard?

A. No, it's Galson. It's a typo.

Q. Okay.

A. Should be G-A-L.

Q. So table 3 confirms estimates of CFU per cubic meter to match Galson and Goddard as cited in figure 7 of this report?

A. Yes.

Q. All right. So let's go to figure 7 of your report.

A. All right.

Q. And it's a little difficult to read.

A. It is.

Q. But it's a slide based on --

Page 255

KOENIGSHOFER

A. What page is it?

Q. Twenty-two.

Okay. Do you have a copy of Galson and Goddard, the paper itself? I tried to find it online and it wasn't available.

MS. ZIMMERMAN: 1968?

THE WITNESS: Yeah. I think that I do. I think I've read this thing.

BY MR. GOSS:

Q. Okay. And I --

A. A buddy of mine gave it to me.

Q. Okay. I looked in here and I didn't see it.

So if you have a copy, I would greatly appreciate one. But...

A. You went into the ASHRAE archives?

Q. You know, I haven't -- I haven't done that.

A. They are very good. I would expect it's --

Q. Okay. I might try that.

A. 1968 ASHRAE journal. I imagine it's in there.

Q. But what this figure is based on is

Page 256

KOENIGSHOFER

Galson and Goddard's, I guess, measurements of CFUs --

A. Yes.

Q. -- and an article caused Hospital Air Conditioning and Sepsis Control.

A. That's right.

Q. All right.

A. This was real data, real hospitals in Atlanta.

Q. Okay. From 1968?

A. Yes, sir.

Q. Now, if we go to table 3 in Kowalski. This refers -- are you there? Page 40. Bottom of page 40.

A. Oh, okay.

Q. All right. This refers to microbial levels in indoor and outdoor air. I don't see a reference to Galson and Goddard, and I don't see any indication that these measurements relate to hospital air, do you?

A. I don't see that particular reference here.

Q. And the next page, it talks about table 3. It says, "Table 3 lists the results

Page 257

KOENIGSHOFER

of various studies that include measurements of outdoor spore levels and typical average or representative indoor levels."

A. Okay.

Q. "These levels do not necessarily pose a health threat."

But I don't see a reference to Galson and Goddard in the references for the bibliography. So what I'm trying to understand is the connection between table 3 of Kowalski '98 and your figure 7.

A. All I'm simply saying, within the order of magnitude he's reporting, you know, 50 colony-forming units per cubic meter.

Q. Okay.

A. And Galson, he's got 10. And they need to make this comparison. One is in cubic meters and one is in cubic feet.

Q. Would you say with respect to particles and bacteria, if you're within the same order of magnitude, you're essentially saying it's -- the difference is nonsignificant?

A. Order of magnitude, I'm not sure I'd

Page 286

1 KOENIGSHOFER
 2 than July 2016?
 3 A. I haven't.
 4 Q. Okay.
 5 A. But I do have that.
 6 Q. Okay.
 7 A. Again, I'm saying that I -- that's --
 8 again, I read this thing two months ago, three
 9 months ago. I recall him saying that.
 10 Q. Number 12 you say that -- you're
 11 referring to a filter test by Camfil Farr. And
 12 that's a big filter company; correct?
 13 A. Yes, it is.
 14 Q. You describe, "Flat filter efficiency
 15 measured at 72 percent at 0.4 micron. MERV 14
 16 is 75 to 85 percent at 0.3 to 1 micron. So the
 17 filter 3M uses is MERV 13, at best."
 18 Did I read that correctly?
 19 A. Yes.
 20 (Thereupon, Exhibit 26 was marked for
 21 identification.)
 22 BY MR. GOSS:
 23 Q. Is Exhibit 26 the document that you
 24 were referring to?
 25 A. Yes.

Page 288

1 KOENIGSHOFER
 2 A. Yes. Right.
 3 Q. So you agree with me that this does
 4 not appear to have been conducted according to
 5 52.2?
 6 MS. ZIMMERMAN: Object to form of the
 7 question. Foundation.
 8 THE WITNESS: This piece of paper
 9 does not give all the information that one
 10 would expect for the particle sizes in the
 11 MERV 14 test.
 12 Q. Okay. All right.
 13 A. I don't know what 52.2 even had when
 14 this test was done.
 15 Q. So you were saying about Exhibit 26
 16 that --
 17 A. I was just reading the top. I
 18 thought the top thing says test and then I
 19 thought that was a date. I'm sorry.
 20 Q. Okay. Well, there is a date on the
 21 next page. It says, "25 August '06."
 22 Do you see that?
 23 A. Yeah.
 24 Q. And so what's the relevance of the
 25 date to the document for you?

Page 287

1 KOENIGSHOFER
 2 Q. And can you tell from this document
 3 whether this test was performed according to
 4 ASHRAE 52.2?
 5 A. I -- I don't know the ASHRAE 52.2
 6 test methodology.
 7 Q. Okay. Have you ever seen a test
 8 report for a filter that is put through a 52.2
 9 test?
 10 A. Well, only in the sense if I'm
 11 looking to recommend a filter, and I'm looking
 12 at Camfil's website or American Air Filter's
 13 website or whoever, they probably will say that
 14 they -- according to 52.2 we did this test and
 15 here's the results.
 16 Q. Okay. We spoke earlier about the
 17 particle size ranges the 55.2 tests; correct?
 18 A. Yes.
 19 Q. There's .3 to 1 micron, 1 to
 20 3 microns, and then 3 to 10 microns; correct?
 21 A. I believe that's what we said. Yeah.
 22 Q. All right. So if you look at this
 23 graph below, the units are hard to read, but it
 24 looks like the highest it goes is about
 25 .9 microns; correct?

Page 289

1 KOENIGSHOFER
 2 A. I don't know what version of 52 we
 3 had at that point. And honestly, I don't know
 4 if even 52 had even been published at that
 5 point.
 6 Q. Okay. So you don't know whether
 7 there was a 52 --
 8 A. There might not have been a 52 at
 9 that point.
 10 Q. In 2006?
 11 A. 2006.
 12 Q. Okay.
 13 A. I'm simply saying I don't know that
 14 there was.
 15 (Thereupon, Exhibit 27 was marked for
 16 identification.)
 17 (Thereupon, Exhibit 28 was marked for
 18 identification.)
 19 BY MR. GOSS:
 20 Q. All right. If you look at Exhibits
 21 27 and 28, have you ever seen test reports like
 22 these for a filter?
 23 A. No.
 24 Q. If you look at 27, it says, at the
 25 top, "Test Report ASHRAE Test Standard 5.22

Page 290

KOENIGSHOFER

2012 New Classification;" correct?

A. Uh-huh. Yes.

Q. And then below that it says, "Bair Hugger filter model 505;" correct?

A. Yes.

Q. And in the test results, first it indicates the test airflow rate and CFMs and then the velocity and feet per minute; correct?

A. Yeah.

Q. So that's 48 CFMs was the flow rate and the velocity was 118 feet per minute?

A. Uh-huh. Yes.

Q. And then it lists an initial resistance in WG and a final resistance in WG; correct?

A. Yes.

Q. All right. And "WG" stands for water gauge; correct?

A. The whole thing stands for inches of water gauge, yes.

Q. Okay. What is your understanding of the difference between initial resistance and final resistance?

A. Well, "initial" is one brand-new out

Page 291

KOENIGSHOFER

of the box. And "final" would be after it has been run. That would be, in my experience, a very high number to run a filter to.

Typically when you buy a filter, you buy something from Camfil, and it will say "replace at" -- usually like 1.5 inches. I don't recall ever seeing one that would say, run it up to 2.5 inches.

Q. All right. And then it says, "The minimum efficiency rating value is MERV 14 at 48 CMF;" correct?

A. Uh-huh. Yeah.

Q. And then it breaks down the minimum average efficiency at the three different particle ranges; correct?

A. Yes.

Q. Does this appear to you to be a test report that's consistent with requirements of 52.2?

MS. ZIMMERMAN: Object to form. Foundation.

THE WITNESS: I would guess that it matches 52 because they state that it does. But that is the test of a filter in

Page 292

KOENIGSHOFER

a laboratory.

BY MR. GOSS:

Q. Okay. If you'll turn to the second page -- by the way, you're -- so you're distinguishing between a test of a filter in a laboratory and a test of a filter in the field, is that what you're suggesting?

A. I've had this only -- for only one or two minutes here. But I expect that this is all they did is to test the filter in their laboratory in their setup.

Q. Okay.

A. It was not in a Bair Hugger.

Q. Right.

A. So --

Q. Did you ask --

A. -- it was in a perfectly beautiful sealed-in device.

Q. Okay.

A. Perfectly. We've got quarter-inch stainless steel ends on this thing and wonderful perfect gaskets installed by a Ph.D technician in the laboratory.

Q. Do you know that these people are

Page 293

KOENIGSHOFER

Ph.D technicians?

A. No, I don't know. I'm just making this shit up.

Q. I think I understand.

A. Hey, you know what, it does. Yes. In fact, I do know.

Q. Okay.

A. That says it right there.

Q. All right. There you go.

A. Dr. Kwak.

Q. All right. So you're distinguishing from that situation and the performance of a filter in the Bair Hugger in the field; correct?

A. Yes, sir.

Q. But you yourself did not attempt to determine the filter efficiency or performance of the filter of a Bair Hugger unit in the field; correct?

A. That's correct.

Q. So on the second page there are different fractional efficiency results listed for the different delta Ps, which is the change in pressure; correct?

Page 294

KOENIGSHOFER

A. Right.

Q. And if you look at the initial resistance of .508 inches those are all the lowest values that are recorded at the far end of the table; correct?

A. I'm sorry?

Q. Do you follow?

A. Say that -- well, no, I don't. Say that again.

Q. Okay. Sorry.

What I want to compare is the initial resistance of .508 inches of water.

A. Got it.

Q. And the final resistance of 2.5 inches of water; correct?

A. Okay.

Q. All right. And the fractional efficiency at the final resistance begins at 99.1 and goes up to 100; correct?

A. Yes.

Q. Starting with the .3 to .4 micron size range; correct?

A. Yes.

In the 2.5 column you're talking

Page 295

KOENIGSHOFER

about?

Q. Yes, sir.

A. .7 to 1.0 size range.

Q. That's where it goes to 100 percent; correct?

A. I thought that was your question.

Q. No. I'm sorry.

It starts -- it starts at 99.1 and .3 to .4; correct?

A. Yes.

Q. All right. And then it increases --

A. Yes.

Q. -- from there?

A. Uh-huh.

Q. All right. Exhibit 28 is a similar report on the rectangular filter; correct?

A. Yes.

Q. And this too would appear to be a test report or claims to be a test report per 52.2; correct?

A. Yes. That's their statement.

Q. And it reports a MERV value of MERV 14; correct?

A. Yes.

Page 296

KOENIGSHOFER

Q. After you saw this Camfil document in Exhibit 26, did you ask counsel if there was other efficiency testing that they could provide you on the Bair Hugger filters?

MS. ZIMMERMAN: Object to -- pardon me. Object to form and to the extent it calls for attorney-client -- pardon me -- attorney work product, I'm going to instruct the witness not to answer.

BY MR. GOSS:

Q. Did you want to see other efficiency data if it existed?

A. I have wanted to see other tests.

Q. You reviewed a deposition of Dr. Robert Crowder. Do you recall reading his testimony that his understanding was that both of the filter medias that Pentair supplied to 3M and Arizant would be capable of removing bacteria?

MS. ZIMMERMAN: Object to the form of the question.

THE WITNESS: It's a wonderful question. And I don't remember the answer to that.

Page 297

KOENIGSHOFER

Q. Do you have any reason to disagree with his testimony that the filters Pentair or Porous supplied to 3M or Arizant would be capable of removing bacteria?

A. Capable of removing bacteria. I'm sure that they could remove some bacteria.

Q. Do you have an opinion as to the -- strike that.

On item 14 you cite a paper by Brandt and Oguz, among others, comparing the efficacy of resistive polymer and forced-air warming.

A. Yes.

Q. And this paper is from 2010; right?

A. Yes.

Q. Have you seen a more recent paper by Oguz comparing the levels of bacteria in the operating room during procedures performed with the Bair Hugger versus a resistive polymer device?

A. No. No. I have not seen that with that particle.

(Thereupon, Exhibit 29 was marked for identification.)

Page 302

KOENIGSHOFER

A. Cool.

(Thereupon, Exhibit 30 was marked for identification.)

BY MR. GOSS:

Q. Exhibit 30 is a letter to the editor in the Journal of Hospital Infection; correct?

A. Yes.

Q. You do not recall having seen this before?

A. I have not. I have heard of its existence.

Q. All I would ask you about this, since you have not had a chance to read it, obviously you have not attempted to reconcile what Memarzadeh says with what Dr. Elghobashi says; correct?

A. That is correct.

Q. If you'd just look at the last paragraph of this. It says, "This investigation validates Moretti's et al's conclusion that forced-air warming technology does not increase the risk of surgical wound infection."

Obviously that's a different

Page 303

KOENIGSHOFER

conclusion from what Dr. Elghobashi arrived at; correct?

A. Yes.

Q. On page 21 of your report you talk about the Bair Hugger filtration; correct?

A. Yes.

Q. You say, "If we assume the air near the floor of an OR is as clean as a standard hospital, which meets ASHRAE minimum standards, that is 10 CFU per cubic foot"; correct?

A. Yes.

Q. I want to look back at figure 7. That 10 CFU per cubic foot is for general hospital areas; correct?

A. Yes. I was specifically saying the air near the floor.

Q. Okay. So --

MS. ZIMMERMAN: For the record, Counsel, are you talking about his figure 7 in his report?

MR. GOSS: Yes. Exactly. On page 22.

BY MR. GOSS:

Q. The part that I can read says, 10 CFU

Page 304

KOENIGSHOFER

per cubic foot per general hospital areas. For general surgery, autopsy, isolation, the emergency it says 4 CFU per cubic foot; right?

A. Yes.

Q. But you chose 10 CFU per cubic foot because you're measuring CFUs near the floor?

A. Yes.

Q. Ten per cubic foot, if you express it in cubic meters, that would be how many?

A. Ten divided by 30, so .3 -- no, no, the other way around. I'm sorry. 300 -- 350.

Q. 350 CFUs per cubic foot.

A. Per cubic meter.

Q. Per cubic meter. Sorry. Thank you.

Would you agree with me that that would be an extraordinarily high number of CFUs to have in an operating room?

A. I don't -- I don't have a number for that. Other than what Galson says, you've got 2 to 4.

Q. We looked at some studies --

A. Why are we confusing ourselves by converting all of this to cubic meters when they're already cubic feet?

Page 305

KOENIGSHOFER

Q. Well, we looked at some other studies that provided airborne CFUs and CFUs per cubic meter; correct?

A. I'm sure we have sometime today, yes.

Q. Some of them were under 5, some were under 10; correct? I think one of them was 35.

A. Was that per meter or per foot? At this point, I honestly can't remember.

MS. ZIMMERMAN: If you want to refer him to something, I'm sure he will be happy to look at it.

MR. GOSS: Sure.

BY MR. GOSS:

Q. Exhibit 18 was the Der Tavitian paper.

A. I just got there too. Colonies per cubic meter. Tavitian from -- I don't know -- 6 to 12 or something, 14.

Q. CFUs per cubic meter?

A. Yeah. On the second -- third page.

Q. So Cristina paper, 17. In the abstract of it says, "Considering the total number of surgical operations the mean value is 35 CFU per cubic meter"; correct?

Page 306

KOENIGSHOFER

A. Yes. That is what she reports her -- anyway, yeah.

Q. And for your hypothetical calculation you're assuming a level of CFUs in the OR about 10 times that; correct?

A. Yes, sir.

Q. And your calculation is based on an assumption that the filter is 90 percent effective; is that right?

A. Yes. That is what I had said.

Q. Do you intend to revisit your calculation now that you have been provided some other data surrounding the Bair Hugger filters?

A. No. Because you have not yet supplied me any data for how it works inside a Bair Hugger.

Q. And you haven't conducted any testing of your own to determine that?

A. I have not.

Q. Moving on to your summary of opinions on page 22. Your first opinion, "The Bair Hugger operating in an OR will create turbulence at the floor stirring settled

Page 307

KOENIGSHOFER

particles."

Opinion number 2, "The Bair Hugger draws particles off the floor into the unit. It functions much like a household vacuum cleaner."

What is your basis for that second statement?

A. Because it sucks particles off the floor. The legs of the Bair Hugger, the one that I looked at, the ones that sit on the floor, it's actually about a half an inch. So actually my calculation, when I did it, I assumed 1 inch.

Q. Okay.

A. With the little rubber feeder on it about a half an inch, so that the velocity was actually even higher.

Q. So what size particles did you measure it sucking up from the surface?

A. I didn't --

MS. ZIMMERMAN: Object to the form of the question.

Q. Or did you?

A. I did not measure. I've already

Page 308

KOENIGSHOFER

answered that question numerous times.

Q. You're saying it functions much like a household vacuum cleaner.

A. Hmm-mmm.

Q. Is that based just on your calculation of the velocity?

A. Yes, it is.

Q. Have you done any calculations of the velocity required to dislodge a 10-micron particle from the surface?

A. I have not.

Q. Have you refinished a piece of furniture?

A. I have.

Q. I have too. I suspect Genevieve has. Have you ever sanded a surface and then vacuumed it?

A. Of floors, yes. Yeah. Sure.

Q. And then in my experience, I have wiped that surface after vacuuming it and been surprised to see particles.

A. What size were the particles that were left?

Q. I don't know. All I know is that the

Page 309

KOENIGSHOFER

particles --

A. I don't know either.

Q. -- the particles weren't vacuumed by the vacuum; correct?

A. Right.

Q. Did you make any attempt to determine whether the Bair Hugger actually functioned like a household vacuum cleaner in this case?

MS. ZIMMERMAN: Objection to the form of the question. I think it's argumentative and it has been asked and answered.

BY MR. GOSS:

Q. You can answer.

A. I've already said I didn't do any testing on this.

Q. Got it.

"The performance of the filter assembly is not appropriately or correctly documented." I think we've established that you, before today, hadn't seen all the documentation relating to the Bair Hugger filters; correct?

MS. ZIMMERMAN: Object to the form of

Page 310

1 KOENIGSHOFER
2 the question. There are documents he
3 still hasn't seen relating to the --

4 THE WITNESS: I mean, this is based
5 on the exploded view of the one that I
6 looked at.

7 Q. Okay. What documentation were you
8 expecting to see?

9 A. It says nothing about the type of
10 gasket that it has. The thickness of the
11 gasket. The adhesiveness of the gasket. If
12 there is a gasket.

13 Q. Do you know whether there is a gasket
14 on the Bair Hugger filter?

15 A. I don't know.

16 Q. Did you ever ask counsel to provide
17 you exemplar filters?

18 A. No. I've asked if I could buy a Bair
19 Hugger.

20 Q. Okay.

21 A. But I haven't done it yet.

22 Q. In your last four opinions on
23 page 23, you say number 1, "The filters in the
24 Bair Hugger are less efficient than those used
25 in the HVAC system serving an OR." Is that

Page 311

1 KOENIGSHOFER

2 based on the Camfil document that you reviewed?

3 A. It is based on the Camfil document
4 that I reviewed. It is based on, especially
5 the units that have got the flat filter. Flat
6 filters are notorious for warping like this.
7 And lacking better information that I had, it's
8 not unreasonable to assume that at certain
9 times that filter might go wonky and you get
10 leakage past it. (indicating)

11 MS. ZIMMERMAN: Just for the record,
12 the witness is gesturing with a piece of
13 paper to mimic a flexion in a rectangular
14 box.

15 BY MR. GOSS:

16 Q. The filter goes out a square and tips
17 somehow so that air can leak past it?

18 MS. ZIMMERMAN: Thank you.

19 THE WITNESS: Yes.

20 Did you get the wonky part?

21 BY MR. GOSS:

22 Q. You say, in summary, you believe that
23 the use of the Bair Hugger will adversely
24 affect the air quality in the OR and at the
25 patient, this will place the patient at

Page 312

1 KOENIGSHOFER
2 increased risk of contracting an HAI. Is that
3 your testimony?

4 A. Yes. Yes, it is.

5 Q. Do you have an opinion that the Bair
6 Hugger is capable of causing a surgical site
7 infection? Not just increased risk, but
8 actually causing.

9 MS. ZIMMERMAN: Object to form and
10 foundation.

11 THE WITNESS: I have no information
12 that there is direct causality.

13 BY MR. GOSS:

14 Q. Would you agree with me that you can
15 put the cleanest air in the world into a room,
16 but if skin particles are falling off the
17 doctors and nurses into the surgical site,
18 that's a problem that can't be solved by the
19 HVAC system?

20 MS. ZIMMERMAN: Objection to form.

21 THE WITNESS: Yes.

22 Q. And that is a problem that exists
23 whether or not you have a Bair Hugger in the
24 room; correct?

25 A. Yes.

Page 313

1 KOENIGSHOFER

2 MR. GOSS: That's all the questions I
3 have. Thank you for your patience.

4 MS. ZIMMERMAN: Should we take a real
5 short break?

6 MR. GOSS: Sure.

7 THE VIDEOGRAPHER: Off the record at
8 6:32 p.m.

9 (Thereupon, a brief recess was taken.)

10 THE VIDEOGRAPHER: Back on the record
11 at 6:40 p.m.

12 FURTHER EXAMINATION

13 BY MS. ZIMMERMAN:

14 Q. All right. Well, Mr. Koenigshofer,
15 as you know, I'm Genevieve Zimmerman. And I am
16 one of the lawyers who represents the
17 plaintiffs in a coordinated case in Minneapolis
18 called a "multi-district litigation".

19 And I'm going to have some questions
20 for you today as well. First, I just want to
21 say for the record, I appreciate your patience
22 with this process. I appreciate that it is
23 presently a quarter to 7:00 p.m. We have been
24 going all day in a very hot room, not under
25 ideal conditions.

EXHIBIT DX40

TO DECLARATION OF PETER J. GOSS IN
SUPPORT OF DEFENDANTS' MOTION TO
EXCLUDE PLAINTIFFS' ENGINEERING
EXPERTS



Contents lists available at ScienceDirect

American Journal of Infection Control

journal homepage: www.ajicjournal.org

Major article

Traffic flow in the operating room: An explorative and descriptive study on air quality during orthopedic trauma implant surgery

Annette Erichsen Andersson RN^{a,b,*}, Ingrid Bergh RN, PhD^c, Jón Karlsson MD, PhD^{d,e}, Bengt I. Eriksson MD, PhD^{d,e}, Kerstin Nilsson RN, PhD^a^a Institute of Health and Care Sciences, Sahlgrenska Academy, University of Gothenburg, Gothenburg, Sweden^b Department of Anesthesia, Surgery and Intensive Care, Sahlgrenska University Hospital, Gothenburg, Sweden^c School of Life Sciences, University of Skövde, Skövde, Sweden^d Department of Orthopedics, Sahlgrenska University Hospital, Gothenburg, Sweden^e Institute of Clinical Sciences, Sahlgrenska Academy, University of Gothenburg, Gothenburg, Sweden

Key Words:

Surgical site infection
Door opening
Air sampling
Colony-forming units

Background: Understanding the protective potential of operating room (OR) ventilation under different conditions is crucial to optimizing the surgical environment. This study investigated the air quality, expressed as colony-forming units (CFU)/m³, during orthopedic trauma surgery in a displacement-ventilated OR; explored how traffic flow and the number of persons present in the OR affects the air contamination rate in the vicinity of surgical wounds; and identified reasons for door openings in the OR. **Methods:** Data collection, consisting of active air sampling and observations, was performed during 30 orthopedic procedures.

Results: In 52 of the 91 air samples collected (57%), the CFU/m³ values exceeded the recommended level of <10 CFU/m³. In addition, the data showed a strongly positive correlation between the total CFU/m³ per operation and total traffic flow per operation ($r = 0.74$; $P = .001$; $n = 24$), after controlling for duration of surgery. A weaker, yet still positive correlation between CFU/m³ and the number of persons present in the OR ($r = 0.22$; $P = .04$; $n = 82$) was also found. Traffic flow, number of persons present, and duration of surgery explained 68% of the variance in total CFU/m³ ($P = .001$).

Conclusions: Traffic flow has a strong negative impact on the OR environment. The results of this study support interventions aimed at preventing surgical site infections by reducing traffic flow in the OR.

Copyright © 2012 by the Association for Professionals in Infection Control and Epidemiology, Inc.

Published by Elsevier Inc. All rights reserved.

The prevention of surgical site infection (SSI) after orthopedic implant surgery is a hot topic for politicians, hospital administrators, and clinicians, given the enormous amount of resources these infections consume in terms of extra costs of medications, reoperations, and extended length of hospital stays.¹⁻⁴ Adding the human perspective, a recent study indicated that afflicted patients suffer deeply, both physically and emotionally, from the consequences of a deep SSI for a prolonged period.⁵

Strategies to minimize the risk of SSI can be focused on 3 major areas: the patient, the surgical technique, and the surgical environment. Optimizing the patient preoperatively by applying current knowledge about the risks associated with smoking, malnutrition, ongoing infections and wounds, diabetes, and other underlying diseases and conditions compromising immunologic defense systems can improve postoperative outcomes significantly.⁶⁻⁹ Optimizing the surgical technique by not exceeding the estimated 75th percentile of surgery time based on the type of surgical procedure reduces the risk of SSI and also minimizes blood loss, thereby avoiding the need for (allogeneic) blood transfusions and eliminating postoperative hematomas.¹⁰⁻¹⁵

The present study focused on strategies aimed at optimizing the surgical environment, in particular the air quality in the operating room (OR). Enhancing air quality by reducing airborne contamination has been shown to be of great importance, especially in relation to implant surgery.¹⁶⁻¹⁸ It has been suggested that levels be maintained at <10 CFU/m³ during implant surgery, and that clinical

* Address correspondence to Annette Erichsen Andersson, RN, Department of Anesthesiology/Surgery, Sahlgrenska University Hospital/Östra, Smörlottsgatan 1, SE-416 85 Gothenburg, Sweden.

E-mail address: annette.erichsen@vgregion.se (A.E. Andersson).

Author contributions: A.E.A., I.B., B.E., J.K., and K.N. designed the study; A.E.A. performed data collection and coordination; A.E.A. and I.B. analyzed data; and A.E.A., I.B., B.E., J.K., and K.N. wrote the manuscript.

Conflict of interest: None to report.

benefits can be expected by reducing it to 1 CFU/m³,¹⁸ given that very low levels of clinically relevant coagulase-negative staphylococci can initiate a device-related infection.¹⁹ A landmark study found a strong linear relationship between the level of bacterial air contamination and the prevalence of deep SSI.²⁰

The most common ventilation systems in use today are turbulent, displacement, and laminar airflow (LAF) systems. Whereas turbulent and displacement ventilation systems differ primarily in the methods used to supply clean air, both are incapable of opposing heat emissions from people and lamps. Both types of systems are sensitive to movement, leading to the formation of local eddies.²¹ The most important source of airborne contamination is related to the dispersal of particles from persons present in the OR and their movements.²²⁻²⁴ Clothing OR staff in scrubs with lower air permeability compared with conventional scrubs can reduce the dispersal of microorganisms by the OR staff, thereby significantly reducing the airborne contamination.^{23,25,26} An experimental study has indicated that the protective ability of tightly woven clothing systems can deteriorate after repeated washing and sterilization.²⁷ Another study concluded that unnecessary conversation in the OR can contribute to an increased risk of airborne contamination,²⁸ and a pilot study indicated a possible association between high levels of noise during surgery and SSI.²⁹ The impact of OR door openings on air quality has been investigated in several studies,^{30,31} but clinical tests of this have proven difficult. Ritter et al³² found no significant difference in OR airborne bacterial counts between closed doors (mean, 15.2 CFU) and swinging doors (mean, 14.5 CFU). Stocks et al¹³ reached the same conclusion. Only one study to date has reported a correlation between OR door openings and elevated airborne bacterial counts³³; however, that result was based on 69 passive samples (on settle plates) and only 13 active samples (single-stage slit impact) placed outside the surgical wound area. The aims of the present study were to investigate the air quality, expressed as CFU/m³, during orthopedic trauma implant surgery in a displacement ventilated OR; to explore how traffic flow and the number of people present in the OR affect the air contamination rates in the vicinity of the surgical wound; and to identify reasons for door openings in the OR.

METHODS

Setting

The study was performed at a Swedish university hospital that performs approximately 9,000 surgical procedures annually. Data was collected in 3 parallel ORs of equal size (39 m²), each equipped with an upward air-displacement system supplying cool air (2-3°C below room temperature) above the floor in each of the 4 corners of the room. By thermal convection, the air is evacuated via 4 exhaust fans installed in the ceiling. Each OR is supposed to be maintained at positive air pressure by adjusting the inflow rate to exceed the outflow rate; however, the desired difference in pressure between the outer hall and the OR is not specified. Normally the pressure difference is ~3 kPa, and an alarm is activated if the pressure falls so that the difference is neutralized. Each OR has only a single entry point, with the door opening inward, leading directly to the outer hall. The OR teams wore conventional cotton/polyester 50/50 mix shirts and trousers, long surgical hoods tucked in, and private shoes and socks. The scrubbed team also wore reinforced disposable sterile gowns, facemasks (Rii), and double-sterile gloves. Adherence to this practice was recorded for every operation. During almost half of the operations, at least one of the air inlet supply devices was partially blocked by medical equipment.

Data were collected during 30 consecutively selected full-length orthopedic trauma operations involving different types of

closed-fracture surgery using plates and screws, intramedullary nails, or hemiarthroplasty. Sampling and data collection were done during the daytime and in most of the cases once a week, over a 7-month period from April to November 2010, with the exception of the holiday month of July.

Air sampling method

A Sartorius MD-8 air scanner (Sartorius Mechatronics, Göttingen, Germany) was used to collect airborne microorganisms. Air was sampled at a flow rate of 3 m³/hour (0.83 L/second) in 20-minute periods continuously during the operations. The instrument was placed outside the sterile zone, and a sterilized flexible hose was extended to reach the wound area, with a filter holder attached to the end. The filter holder with a gelatin filter (3 µm pore size; 80 mm diameter) was placed 20-40 cm from the wound. The filters were placed vertically (n = 60), slightly upward (n = 23), slightly downward (n = 17), or horizontally (n = 3). In those cases in which the OR nurse had problems attaching the filter holder close to the wound (n = 13), the holder was placed on the Mayo stand. Data on filter placement was absent in 4 cases. The filter was changed every 20 minutes by the scrub nurse or the assistant and given to the researcher, who immediately placed it on a nonselective Colombia agar base plate with 5% horse blood. Agar plates were incubated at 30°C for 4 days, after which the total aerobic bacterial count was measured. Microbiological results are expressed as CFU/m³. A total of 116 samples were analyzed; 4 samples were accidentally contaminated and thus excluded from the analysis. Filters and plates were handled using strict aseptic technique. To evaluate the technique, filters that had not been used for air sampling were placed on agar plates and incubated in the same way as the used filters; no bacterial growth was detected.

Observational method

Data was collected using a pretested, structured observation form. The following variables were included: date and time, OR, room temperature, type of surgery and fixation method. The period from incision time to wound closure was divided into 20-minute intervals corresponding to the ongoing air sampling. During 119 intervals (each interval corresponding to 20 minutes of air sampling), traffic flow was measured, as well as the reasons for door openings, and the current step in the surgical procedure was recorded. The number of people present in the OR, patient and researcher excluded, was recorded.

Data analysis

Primary analyses showed that CFU/m³ could not be considered a variable with a normal distribution. For this reason, the linear relationship between CFU/m³ per 20-minute interval and traffic flow per 20-minute interval was investigated using Spearman's rho. To investigate the strength and direction of the linear relationship between the total traffic flow per operation and the total CFU per operation, partial correlations were conducted, enabling the removal of duration of surgery as a potentially confounding variable and thereby giving a more accurate description of the relationship between the variables. Investigations of correlations between normally distributed variables (ie, traffic flow, duration of surgery, and number of people present) were performed using Pearson's product-moment correlation coefficient. Significance was defined as $P < .05$. All tests were 2-tailed. In relation to hierarchical multiple regression analysis, preliminary analyses were conducted to ensure no important violations of the assumptions of normality, linearity, and multicollinearity.

One-way between-group analysis of variance with post hoc tests found no significant difference in mean CFU counts among the 3 ORs. However, applying the same test on sampling device positioning indicated that these variations can lead to differences in mean CFU/m³ values. The mean difference between vertically placed filters and filters placed on the Mayo stand was significant ($P = .01$) (Table 1). In 2 operations involving tibia fractures fixed with an intramedullary nail, the sampling filters had been placed vertically on the opposite leg. During surgery, the injured leg was flexed at 90 degrees, thereby partially or completely blocking the sampling filters with the sterile drape during most of the operation. For this reason, further analysis of air quality in the vicinity of the wound area, samples obtained on the Mayo stand and during the 2 operations for tibia fracture were excluded, leaving 92 samples for analysis. Four operational phase were defined: 1, incision phase; 2, dissection phase; 3, implantation phase; and 4, wound closure phase. Content analysis was used on observational data.³⁴

Ethics

The study was approved by the University of Gothenburg's Ethics Committee (157-10). Written and oral information was provided in line with the 4 principal requirements of the Helsinki Declaration (autonomy, beneficence, nonmaleficence, and justice).³⁵ Accordingly, informed consent was obtained from all of the OR teams before observations and sampling.

RESULTS

Air sampling was performed during 30 orthopedic operations in a total of 120 air sampling intervals. The distributions of surgical procedures were 73 plates and screws (60.8%), 26 intramedullary nails (21.7%), and 21 hemiarthroplasties (17.5%). The variations in CFU/m³ values were found between operations rather than during operations ($P = .001$). In 52 of 91 samples, the CFU/m³ values exceeded the recommended level of <10 CFU/m³. In 14 of 24 operations, the mean values exceeded 10 CFU/m³; in 5 of these operations, the mean values exceeded 25 CFU/m³. The highest mean values were 37.5 and 44.3 CFU/m³. Qualitative analysis revealed high activity levels (ie, movements within the OR as well as traffic flow) during these operations, along with other potentially negative variables, such as hair hanging outside the surgical hood, the presence of a sneezing person, and more than 5 people present in the OR. In 5 operations, mean values were <5 CFU/m³, with the lowest values being 1.6 and 2.3 CFU/m³, and notes written during these operations reveal that there was no traffic flow and low activity. Basic results on air quality, expressed as CFU/m³, and related variables are provided in Table 2.

Traffic flow

The relationships between the total traffic flow rate per operation and the total CFU/m³ sampled per operation and between traffic flow rate per 20-minute interval corresponding to 20 minutes of air sampling were investigated. A positive correlation was found between CFU/m³ and traffic flow rates when measured in 20-minute intervals ($r = 0.309$; $P = .003$). The data show a strong, positive correlation between the total CFU/m³ per operation and total traffic flow rate per operation ($r = 0.74$; $P = .001$; $n = 24$ operations). Because duration of surgery correlates to the total CFU and traffic flow rates, duration of surgery was controlled for in the analysis.

A total of 529 door openings were recorded. Reasons for OR entries and exits were grouped into categories, as shown in Table 3. No reason could be identified in relation to 93 entries and exits. To

Table 1
CFU/m³ values and sampling positions

				95% confidence interval for mean	
Position	n	Mean	SD	Lower bound	Upper bound
40-20 cm from wound					
Vertically	60	15.8	13.9	12.2	19.4
Downward	17	15.2	10.2	10.0	20.5
Slightly upward	23	13.0	13.4	7.1	18.8
Horizontally	3	8.6	3.7	-0.74	18.0
Mayo stand					
Vertically	13	6.6	4.4	3.9	9.4
Total	116	13.9	12.6	11.6	16.3

n, number of samples.

Table 2
Air quality and related variables

Variables	n (missing)	Mean (SD)	95% CI for mean	Median (range)
CFU/m ³	91 (1)*	15.9 (13.4)	13.1-18.7	13 (0-55)
Total CFU/m ³ per operation	24†	60.4 (55.9)	36.8-84	33.5 (7-187)
Number of people	111 (9)‡	5.4 (1)	5.2-5.6	5 (3-10)
Traffic flow rate	119 (1)‡	4.3 (2.9)	3.8-4.8	4 (0-14)
Traffic flow rate per operation	30‡	17.4 (13.5)	12.4-22.4	14 (0-67)
Duration of surgery, minutes	29 (1)§	83.5 (39.7)	68.4-98.5	60 (20-200)

*Number of air samples.

†Number of operations.

‡Measured in 20-minute intervals.

§From incision time to end of closure in minutes.

exemplify, this could mean that a staff member would enter the OR, take a look around, and then walk out.

Traffic flow rates in relation to the previously mentioned 4 phases of the operation were analyzed by one-way analysis of variance with post hoc tests showing no significant difference in mean traffic flow rate per 20-minute intervals. In addition, no significant differences in mean CFU/m³ values were found among the different phases. No correlation was detected between the number of people present and traffic flow rates in the OR.

Number of people and the effect on air quality

A minor correlation was found between CFU/m³ and the number of people present in the OR ($r = 0.22$; $P = .04$; $n = 82$).

Duration of surgery and type of surgical procedure

No correlation was found between CFU/m³ rates measured in 20-minute intervals and duration of surgery measured in minutes. A positive correlation was found between the total CFU/m³ per operation and duration of surgery ($r = 0.62$; $P = .01$; $n = 23$). No correlation was found between traffic flow rate per 20-minute interval and duration of surgery, but a strong correlation was noted between total traffic flow rate per operation and duration of surgery ($r = 0.79$; $P = .01$; $n = 23$). Differences in mean CFU values in relation to type of surgical procedure are presented in Table 4.

Predictors of CFU

Hierarchical multiple regression was used to assess the ability of traffic flow and number of people present in the OR to predict CFU/m³ levels after controlling for duration of surgery. Duration of surgery was entered in step 1, explaining 36% (adjusted $R^2 = 0.359$)

Table 3

Reasons for traffic flow

Necessary door openings*	n	Semi-necessary door openings	n	Unnecessary door openings	n
Expert consultations (eg, help needed from senior surgeons, expert nurses, or anesthesiologists)	40	Surgical team members entering after incision or leaving before closure	76	Logistic reasons planning next or other operation	30
Instruments or other material needed	137	Lunch and coffee breaks	108	Social visits	45
				No detectable reasons	93
Total	177		184		168
					529

*The need assessed in relation to patient safety and ongoing procedure.

Table 4

Relationships among CFU, surgical procedures, and traffic flow, analysis of variance

	n	Mean	SD	95% CI	P value
Mean CFU/m ³ value in relation to surgical procedure*					.001
Plates and screws	69	18.7	13.3	15.5-21.9	
Hemiarthroplasty	11	4.73	9.87	1.1-18.6	
Intramedullary nails	11	4.73	3.1	2.6-6.8	
Mean traffic flow rates in relation to surgical procedure [†]					.004
Plates and screws	69	4.5	2.7	3.8-5.1	
Hemiarthroplasty	11	2.3	1.4	1.3-3.3	
Intramedullary nails	11	2.2	2.3	0.6-3.77	

*Number of air samplings corresponding to type of surgical procedure.

[†]Number of surgical procedures corresponding to traffic flow rate per 20-minute interval.

of the variance in total CFU/m³ per operation. After entering traffic flow and number of people present, the total variance explained by the model as a whole was 68% [$F(3,16) = 14.32$; $P = .001$]. The 2 control measurements, traffic flow and number of people, explained an additional 34% (adjusted $R^2 = 0.336$) of the variance in CFU/m³ when controlling for duration of surgery (R^2 change = 0.34; F change (2,16) = 9.91; $P = .002$). In the final model, only traffic flow was statistically significant (standardized $\beta = 0.95$; $P = .001$).

DISCUSSION

In orthopedic surgery, large-scale efforts and research activities have focused on infection control, mainly in relation to elective primary joint replacement surgery. The findings of the present study show that the recommended limit of >10 CFU/m³ was exceeded in 57% of the samples analyzed. Patients with orthopedic trauma carry an extra burden of preoperative soft tissue and skeletal damage, and have minimal opportunities to be optimized in relation to comorbidities that are known to be major risk factors in this group of patients.³⁶ Adding smoking habits and old age (the latter of which is common in patients with osteoporotic hip fracture), a picture of a highly vulnerable group of patients emerges. Reducing risk factors in the surgical environment clearly would be beneficial for this group of patients. One of the most important findings of the present study is the highly negative impact of traffic flow in the OR on bacterial contamination of the air close to the wound; that is, a high rate of door openings was associated with high rates of CFU/m³ values. This correlation is weaker when analyzing CFU/m³ per 20-minute interval compared with the total CFU/m³ per operation, which may be related to the unorganized manner in which bacterial dispersion reaches the wound area after an OR entry or exit because of turbulent air flow patterns as well as movement of people in the OR. Analysis of the factors affecting traffic flow found that only 7% of the door openings were related to the need for expert consultation. Supply issues represented the largest category (26%); improving preoperative planning and communication between the surgeon and OR nurse in charge could possibly reduce these door openings. Staff breaks accounted for 20%

of door openings; surgical team members entering or leaving the OR when the wound was open, for 14%. Reductions in all of these large categories of traffic flow are possible. Door openings for logistic reasons could all be avoided by telephone communication. Door openings related to social visits and for no detectable reasons together accounted for 27% of the traffic flow, possibly reflecting an OR culture that accepts door openings for no special reason. Although it is reasonable to think that an individual who enters an OR always has a good reason for doing so, in those cases we could find no link to the ongoing procedure. Blaming individuals for lack of discipline is not a fruitful way to address this problem, given that the cause probably extends the individual level. In addition, merely counting exits and entries while failing to analyze the reasons behind traffic flow behavior could lead to misdirected interventions.³⁷

Directing the focus of change at an organizational level, including enhanced knowledge, logistics, and perioperative planning, would give the OR staff the necessary tools to minimize door openings in the OR. This would not only minimize traffic flow, but also likely reduce the duration of wound exposure. Lynch et al³⁸ reported a mean rate of 40 door openings per hour for orthopedic total joint surgery, and Young et al³⁹ reported a mean rate of 19.2 per hour for cardiac surgery, compared with the rate of 12.9/hour in the present study. The traffic flow patterns reported in these 3 studies must be considered in light of the high correlation between door opening rate and elevated CFU levels, representing a major patient safety problem.

The large variation in CFU values among operations in the present study is in line with previous reports.^{13,20,33} This supports the perception that CFU/m³ level should not be discussed as an independent variable with a presumed normal distribution in the OR, because it is highly dependent on other variables and can be reduced to almost nondetectable levels under optimal conditions. The importance of the duration of surgery in relation to CFU/m³ levels measured at 20-minute intervals was of minor importance. However, the duration of surgery is of clinical relevance, given that the total CFU level increases with increasing duration of surgery, thereby exposing the wound to an increased total number of CFUs and increasing the risk of SSI.^{10,40} In addition, longer duration of surgery was associated with higher total OR traffic flow rates. In this sample, only very small variations in relation to the number of people present in the OR were observed; as a result, the effect of the number of people present in the OR on CFU level could not be investigated thoroughly. The differences in CFU levels related to type of surgery, with fixation with plates and screws associated with the highest levels, can be explained by the fact that these procedures were associated with 50% more door openings. The fact that in almost half of cases, at least one of the air inlet supply devices was partially blocked by medical equipment might suggest that the staff has poor knowledge of how the ventilation system works and how to deal with the reality of underdimensioned operating rooms. To investigate the consequences of blockage of air inlets, it would be necessary to control for how close the medical

equipment was placed in relation to the inlet device and also for how large an area of the inlet supply was blocked. These data were not registered in the present study, precluding analysis of the possible impact on air contamination rates. Given that our regression model explains 34% of the variance of total CFU/m³ per operation, future research should aim at developing a clinically relevant predictive model for estimating bacterial contamination under different environmental and behavioral conditions, taking into account clothing systems and activity levels in the OR.

Methodological considerations

Conducting representative air sampling in the OR in live conditions proved highly challenging, and many methodological and technical issues had to be addressed both before and during the present study. The choices of sampling velocity, time, and culture media were based on recommendations from infection control practitioners performing surveillance sampling on a regular basis. Studies have reported that the viability of microorganisms might be affected by prolonged sampling times and high airflow rates.^{41,42} Evaluation of the Sartorius air sampler demonstrated no reduction in the viability of cocci after drawing 2.6 m³ for 20 minutes, but negative effects for *Escherichia coli*.⁴³ Various cocci were the main relevant species found in the OR,²⁴ and these bacteria also are the leading cause of infections related to implanted medical devices.⁴⁴ Based on this, we believed that the sampling time was an acceptable compromise between the purpose of the study and the need to avoid being overly intrusive during the procedures. However, we consider the wide variety of sampling positions in this study a limitation, which might have led to underestimation of CFU values. The literature typically reports on the distance from the wound to the sampling device (striving to be as close as possible), sampling velocity, and time; unfortunately, methodological issues are rarely studied or discussed. Further studies addressing the positioning of sampling filters, the angle between filters and air flow, sampling velocity in relation to air flow patterns produced by different ventilation systems, and their impact on outcome data are needed. Standardizing an optimal air sampling method would produce reliable data and facilitate comparisons between studies to provide insight into the protective capacity of different ventilation systems during operations. Upward-displacement ventilation systems have been demonstrated to more effectively remove particles compared with conventional systems.^{45,46} An experimental study⁴⁷ comparing conventional ventilation and upward-displacement ventilation confirmed that the upward displacement system was more efficient in removing particles <10 µm, but found no difference between the 2 ventilation systems for particles >10 µm.⁴⁷ More importantly, the bacterial air counts were generally higher in the displacement systems than in conventional systems. Considering this in the present study, it is possible that the displacement system produced higher mean CFU/m³ values than what would have been registered under the same circumstances in a conventionally ventilated OR. However, the present study demonstrates that even in a displacement ventilated OR, very low CFU/m³ levels could be obtained by keeping the doors closed and reducing the number of people present.

Even structured observations can be susceptible to bias.⁴⁸ Human perceptual errors can affect the obtained information, as well as behavioral distortions, due to the presence of an observer. Several measures were taken to address potential bias: (1) The observational form was pretested and modified, (2) the observer had no previous connection with the ward under observation, and (3) the observer underwent self-training sessions to maximize accuracy. Concealed observations to reduce reactivity were not feasible and were considered a possible source of distrust between

the observed and the observer. To estimate the effect of the presence of an observer, the traffic flow rates at the beginning of the study period (May) were compared with rates measured after 6 months (November); no statistically significant differences in traffic flow rates were detected.

CONCLUSION

This study has clearly linked elevated airborne bacterial counts in the surgical area to door openings in conventionally ventilated ORs, thereby providing the scientific evidence needed to initiate interventions aimed at preventing SSI by reducing traffic flow in the OR. In addition, analyzing the reasons for door openings seems to be of great importance to the success of any intervention implemented.

Acknowledgment

The authors thank the OR staff and orthopedic surgeons for their participation in this study, and L.O. Persson for statistical advice.

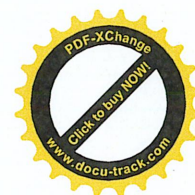
References

- Bozic KJ, Ries MD. The impact of infection after total hip arthroplasty on hospital and surgeon resource utilization. *J Bone Joint Surg Am* 2005;87:1746-51.
- Coello R, Charlett A, Wilson J, Ward V, Pearson A, Borriello P. Adverse impact of surgical site infections in English hospitals. *J Hosp Infect* 2005;60:93-103.
- de Lissovoy G, Fraeman K, Hutchins V, Murphy D, Song D, Vaughn BB. Surgical site infection: incidence and impact on hospital utilization and treatment costs. *Am J Infect Control* 2009;37:387-97.
- Monge Jodra V, Sainz de Los Terreros Soler L, Diaz-Agero Perez C, Saa Requejo CM, Plana Farras N. Excess length of stay attributable to surgical site infection following hip replacement: a nested case-control study. *Infect Control Hosp Epidemiol* 2006;27:1299-303.
- Andersson AE, Bergh I, Karlsson J, Nilsson K. Patients' experiences of acquiring a deep surgical site infection: an interview study. *Am J Infect Control* 2010;38:711-7.
- Neumayer L, Hosokawa P, Itani K, El-Tamer M, Henderson WG, Khuri SF. Multivariable predictors of postoperative surgical site infection after general and vascular surgery: results from the Patient Safety in Surgery study. *J Am Coll Surg* 2007;204:1178-87.
- Zhan C, Kaczmarek R, Loyo-Berrios N, Sangl J, Bright RA. Incidence and short-term outcomes of primary and revision hip replacement in the United States. *J Bone Joint Surg Am* 2007;89:526-33.
- Lindstrom D, Sadr Azodi O, Wladis A, Tonnesen H, Linder S, Nasell H, et al. Effects of a perioperative smoking cessation intervention on postoperative complications: a randomized trial. *Ann Surg* 2008;248:739-45.
- Thomsen T, Tonnesen H, Moller AM. Effect of preoperative smoking cessation interventions on postoperative complications and smoking cessation. *Br J Surg* 2009;96:451-61.
- Pull ter Gunne AF, Cohen DB. Incidence, prevalence, and analysis of risk factors for surgical site infection following adult spinal surgery. *Spine (Phila Pa 1976)* 2009;34:1422-8.
- Bierbaum BE, Callaghan JJ, Galante JO, Rubash HE, Tooms RE, Welch RB. An analysis of blood management in patients having a total hip or knee arthroplasty. *J Bone Joint Surg Am* 1999;81:2-10.
- Culver DH, Horan TC, Gaynes RP, Martone WJ, Jarvis WR, Emori TG, et al. Surgical wound infection rates by wound class, operative procedure, and patient risk index: National Nosocomial Infections Surveillance System. *Am J Med* 1991;91:152S-7S.
- Stocks GV, Self SD, Thompson B, Adame XA, O'Connor DP. Predicting bacterial populations based on airborne particulates: a study performed in nonlaminar flow operating rooms during joint arthroplasty surgery. *Am J Infect Control* 2010;38:199-204.
- Innerhofer P, Klingler A, Klimmer C, Fries D, Nussbaumer W. Risk for postoperative infection after transfusion of white blood cell-filtered allogeneic or autologous blood components in orthopedic patients undergoing primary arthroplasty. *Transfusion* 2005;45:103-10.
- Willis-Owen CA, Konyves A, Martin DK. Factors affecting the incidence of infection in hip and knee replacement: an analysis of 5277 cases. *J Bone Joint Surg Br* 2010;92:1128-33.
- Gruenberg MF, Campaner GL, Sola CA, Ortolan EG. Ultraclean air for prevention of postoperative infection after posterior spinal fusion with instrumentation: a comparison between surgeries performed with and without a vertical exponential filtered air-flow system. *Spine (Phila Pa 1976)* 2004;29:2330-4.
- Hansen D, Krabs C, Benner D, Brauksiepe A, Popp W. Laminar air flow provides high air quality in the operating field even during real operating conditions,

- but personal protection seems to be necessary in operations with tissue combustion. *Int J Hygiene Environ Health* 2005;208:455-60.
18. Lidwell OM, Lowbury EJJ, Whyte W. Effect of ultraclean air in operating rooms on deep sepsis in the joint after total hip or knee replacement: a randomised study. *BMJ* 1982;285:10-4.
 19. McCann MT, Gilmore BF, Gorman SP. *Staphylococcus epidermidis* device-related infections: pathogenesis and clinical management. *J Pharm Pharmacol* 2008; 60:1551-71.
 20. Lidwell OM, Lowbury EJJ, Whyte W. Airborne contamination of wounds in joint replacement operations: the relationship to sepsis rates. *J Hosp Infect* 1983;4:111-31.
 21. Chow TT, Yang XY. Ventilation performance in operating theatres against airborne infection: review of research activities and practical guidance. *J Hosp Infect* 2004;56:85-92.
 22. Whyte W, Hodgson R, Tinkler J. The importance of airborne bacterial contamination of wounds. *J Hosp Infect* 1982;3:123-35.
 23. Tammelin A, Domicel P, Hambraeus A, Ståhle E. Dispersal of methicillin-resistant *Staphylococcus epidermidis* by staff in an operating suite for thoracic and cardiovascular surgery: relation to skin carriage and clothing. *J Hosp Infect* 2000;44:119-26.
 24. Edmiston JCE, Seabrook GR, Cambria RA, Brown KR, Lewis BD, Sommers JR, et al. Molecular epidemiology of microbial contamination in the operating room environment: is there a risk for infection? *Surgery* 2005;138:573-82.
 25. Tammelin A, Hambraeus A, Ståhle E. Source and route of methicillin-resistant *Staphylococcus epidermidis* transmitted to the surgical wound during cardiothoracic surgery: possibility of preventing wound contamination by use of special scrub suits. *J Hosp Infect* 2001;47:266-76.
 26. Whyte W. The role of clothing and drapes in the operating room. *J Hosp Infect* 1988;11(Suppl C):2-17.
 27. Ljungqvist B, Reinmüller B. Aseptic production, gowning systems, and airborne contaminants. *Pharm Technol* 2005;29(5 Suppl):S30-4.
 28. Letts RM, Doermer E. Conversation in the operating theater as a cause of airborne bacterial contamination. *J Bone Joint Surg Am* 1983;65:357-62.
 29. Kurmann A, Peter M, Tschann F, Mühlemann K, Candinas D, Beldi G. Adverse effect of noise in the operating theatre on surgical-site infection. *Br J Surg* 2011;98:1021-5.
 30. Shaw BH, Whyte W. Air movement through doorways: the influence of temperature and its control by forced airflow. *Build Serv Eng* 1974;42:210-8.
 31. Wilson DJ, Kiel DE. Gravity-driven counterflow through an open door in a sealed room. *Build Environ* 1990;25:379-88.
 32. Ritter MA, Eitzen H, French ML, Hart JB. The operating room environment as affected by people and the surgical face mask. *Clin Orthop Relat Res* 1975;111: 147-50.
 33. Scaltriti S, Cencetti S, Rovesti S, Marchesi I, Bargellini A, Borella P. Risk factors for particulate and microbial contamination of air in operating theatres. *J Hosp Infect* 2007;66:320-6.
 34. Silverman D. Interpreting qualitative data: methods for analysing talk, text and interaction. London: Sage; 2001.
 35. World Medical Association. Declaration of Helsinki: ethical principles for medical research involving human subjects. *J Postgrad Med* 2002;48: 206-8.
 36. Bachoura A, Guitton TG, Smith RM, Vrahas MS, Zurakowski D, Ring D. Infirmary and injury complexity are risk factors for surgical-site infection after operative fracture care. *Clin Orthop Relat Res* 2011;469:2621-30.
 37. Parikh SN, Grice SS, Schnell BM, Salisbury SR. Operating room traffic: is there any role of monitoring it? *J Pediatr Orthop* 2010;30:617-23.
 38. Lynch RJ, Englesbe MJ, Sturm L, Bitar A, Budhiraj K, Kolla S, et al. Measurement of foot traffic in the operating room: implications for infection control. *Am J Med Qual* 2009;24:45-52.
 39. Young RS, O'Regan DJ. Cardiac surgical theatre traffic: time for traffic-calming measures? *Interact Cardiovasc Thorac Surg* 2010;10:526-9.
 40. Campbell DA Jr, Henderson WG, Englesbe MJ, Hall BL, O'Reilly M, Bratzler D, et al. Surgical site infection prevention: the importance of operative duration and blood transfusion. Results of the first American College of Surgeons National Surgical Quality Improvement Program Best Practices Initiative. *J Am Coll Surg* 2008;207:810-20.
 41. Whyte W, Niven L. Airborne bacteria sampling: the effect of dehydration and sampling time. *J Parenter Sci Technol* 1986;40:182-8.
 42. Godish DR, Godish TJ. Relationship between sampling duration and concentration of culturable airborne mould and bacteria on selected culture media. *J Appl Microbiol* 2007;102:1479-84.
 43. Parks SR. An assessment of the Sartorius MD8 microbiological air sampler. *J Appl Bacteriol* 1996;80:529-34.
 44. Rupp ME, Archer GL. Coagulase-negative staphylococci: pathogens associated with medical progress. *Clin Infect Dis* 1994;19:231-45.
 45. Memarzadeh F, Manning AP. Comparison of operating room ventilation systems in the protection of the surgical site. *ASHRAE Trans* 2002; 108(Part 2):3-15.
 46. Breum NO. Air-exchange efficiency of displacement ventilation in printing plant. *Ann Occup Hyg* 1988;32:481-8.
 47. Friberg BF, Burman S, Lundholm LG, Österlind R. Inefficiency of upward-displacement operating theatre ventilation. *J Hosp Infect* 1996;33: 263-72.
 48. Polit DF, Beck TC. Nursing research: principles and methods. 7th ed. Philadelphia [PA]: Lippincott Williams & Wilkins; 2004.

EXHIBIT DX41

TO DECLARATION OF PETER J. GOSS IN
SUPPORT OF DEFENDANTS' MOTION TO
EXCLUDE PLAINTIFFS' ENGINEERING
EXPERTS



Equipment	Gives off heat	amount	airflow
1 OR Table	no		
2 Head Light	yes		
3 Electrocautery	yes		yes
4 Defibrillator	yes		yes
5 Forced Air Warmer	yes		yes
6 Heat Pump	yes		yes
7 Slush Machine	yes		yes?
8 Back Table	no		
9 Gown	no		
10 Prep Table	no		
11 Overhead Table	no		
12 Transesophageal Echo Machine	yes		yes
13 Heater/cooler (perfusion)	yes		yes
14 Metal Bucket	no		
15 IV Pole	no		
16 Computer	yes		yes
17 Chair	no		
18 Lifts	maybe		
19 Anesthesia Machine	yes		yes
20 Anesthesia Cart	no		
21 Vacuum Canisters	yes		yes
22 Trash Hamper	no		
23 Laundry Hamper	no		
24 Case Cart	no		
25 Med Cart	no		
26 Ring Stand	no		
27 Shamp Trash	no		
HUMAN FACTOR	YES		yes

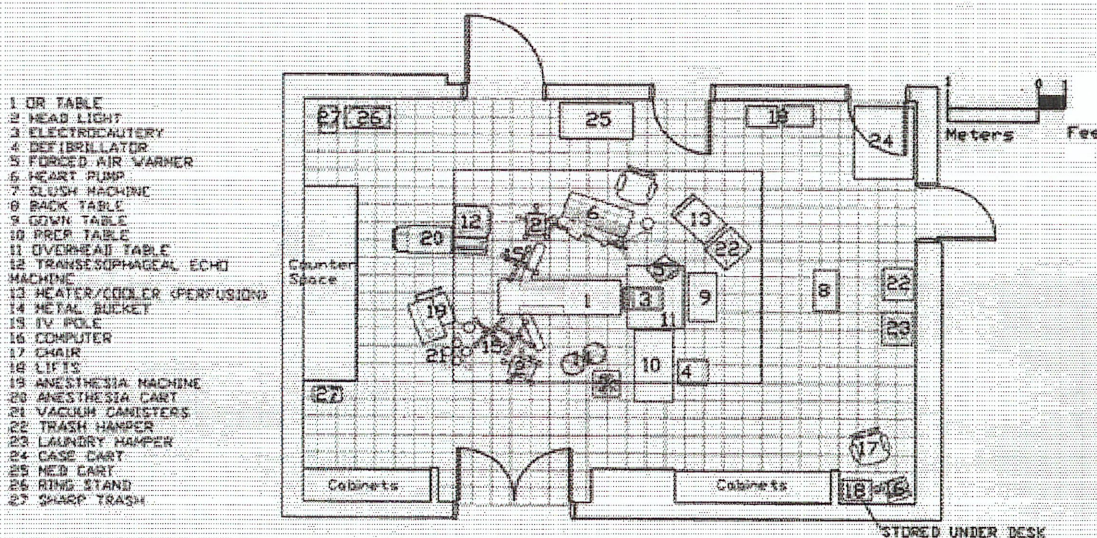
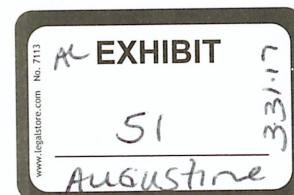




EXHIBIT DX42

TO DECLARATION OF PETER J. GOSS IN
SUPPORT OF DEFENDANTS' MOTION TO
EXCLUDE PLAINTIFFS' ENGINEERING
EXPERTS

Temperature Influence in Different Orthopaedic Saw Blades

Søren Toksvig-Larsen, MD, Leif Ryd, MD, and Anders Lindstrand, MD

Abstract: Laboratory tests were carried out on ox bone to evaluate the thermal effect of eight different saw blades while cutting cortical bone. These saw blades represented the usual clinical blades as well as saw blades specially manufactured in an attempt to decrease the temperature. Temperatures between 34°C and 450°C were registered in the saw blades. Only three measurements (of 219 tests) were below 44°–47°C, which is a critical limit for heat-induced bone necrosis. This test indicates that altering saw blade design is not a way to control the temperature elevation during cutting of bone in orthopaedic procedures. **Key words:** saw blades, bone cutting, temperatures, heat.

Earlier investigations have shown that significant temperature elevations, which cause bone necrosis, may occur when preparing bone with power tools (3, 9, 12, 13, 22, 23). This temperature response could be a factor in the formation of a fibrous tissue membrane and impaired bony ingrowth into porous prostheses (5, 18, 19). It is also conceivable that the heat trauma could have adverse effects on bone healing in general (e.g., delayed healing of osteotomies and ring sequestrum after insertion of pins for external fixation) (14, 16). Attempts to control excessive heat generation in clinical practice by external squirting of saline has been shown to be insufficient during knee surgery (23).

It was our intent to delineate the temperature response while cutting bone with different commercially available saw blades and to investigate whether changes in saw blade design and cutting edge geometry could lower the temperature.

Methods

Temperature measurements were carried out on ox diaphyseal bone. For practical purposes the bone

temperatures were about 0°C in most of the tests. Tests with fully thawed bone (18°C–20°C) were done for validation. The bone was cut transversally. Each bone was cut with each saw blade. The size, configuration, and cortical thickness of the different bones used were the same or showed only minor differences.

The saw blades tested were the 3M Maxi Driver L122 oscillating, 3M Maxi Driver p512 coarse reciproc, Hall P5002-272 oscillating, and two oscillating blades specially made by Sandvik AB to decrease the temperature generation. These latter blades had chamfer angles (Fig. 1) of 10° and 30° (compared to the ordinary 3M blade chamfer angle of 0°). This should in theory lower the heat energy produced. To evaluate the role of saw blade wear, test series were also made with used 3M Maxi Driver L122 saw blades where teeth were worn, so that one blade had teeth of approximately half the ordinary length and the other was without any real teeth. A saw blade made from two 3M Maxi Driver L122 oscillating saw blades was tested to evaluate the effect of increasing thickness of the blade (Fig. 2).

Exacon CN 7 copper-constantan-type thermocouples (Exacon scientific instruments Aps, Roskilde, Denmark) were embedded in the saw blades, so that the measuring point was within 2 mm of the cutting edge. The thermocouples were connected to a BBC

From the Department of Orthopedics, University Hospital in Lund, S-221 85 Lund, Sweden.

Reprint requests: Søren Toksvig-Larsen, MD, Department of Orthopedics, University Hospital in Lund, S-221 85 Lund, Sweden.

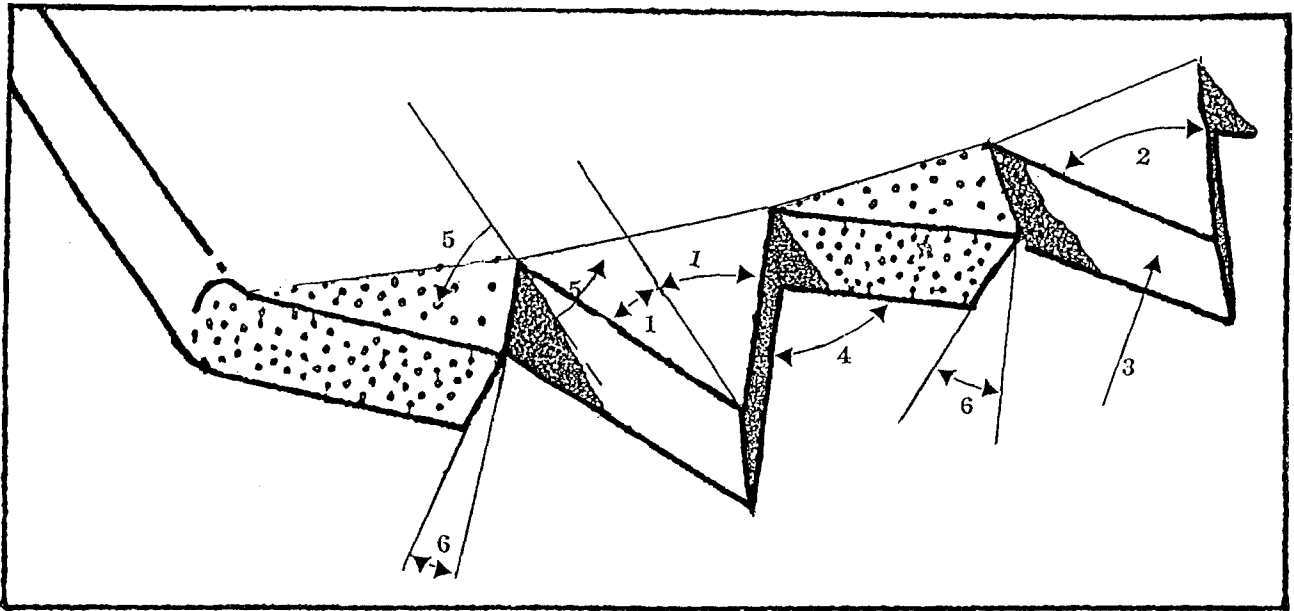


Fig. 1. Saw blade geometry. 1. Rake angle. 2. Wedge angle. 3. Rake plane. 4. Clearance angle. 5. Setting angle. 6. Chamfer angle.

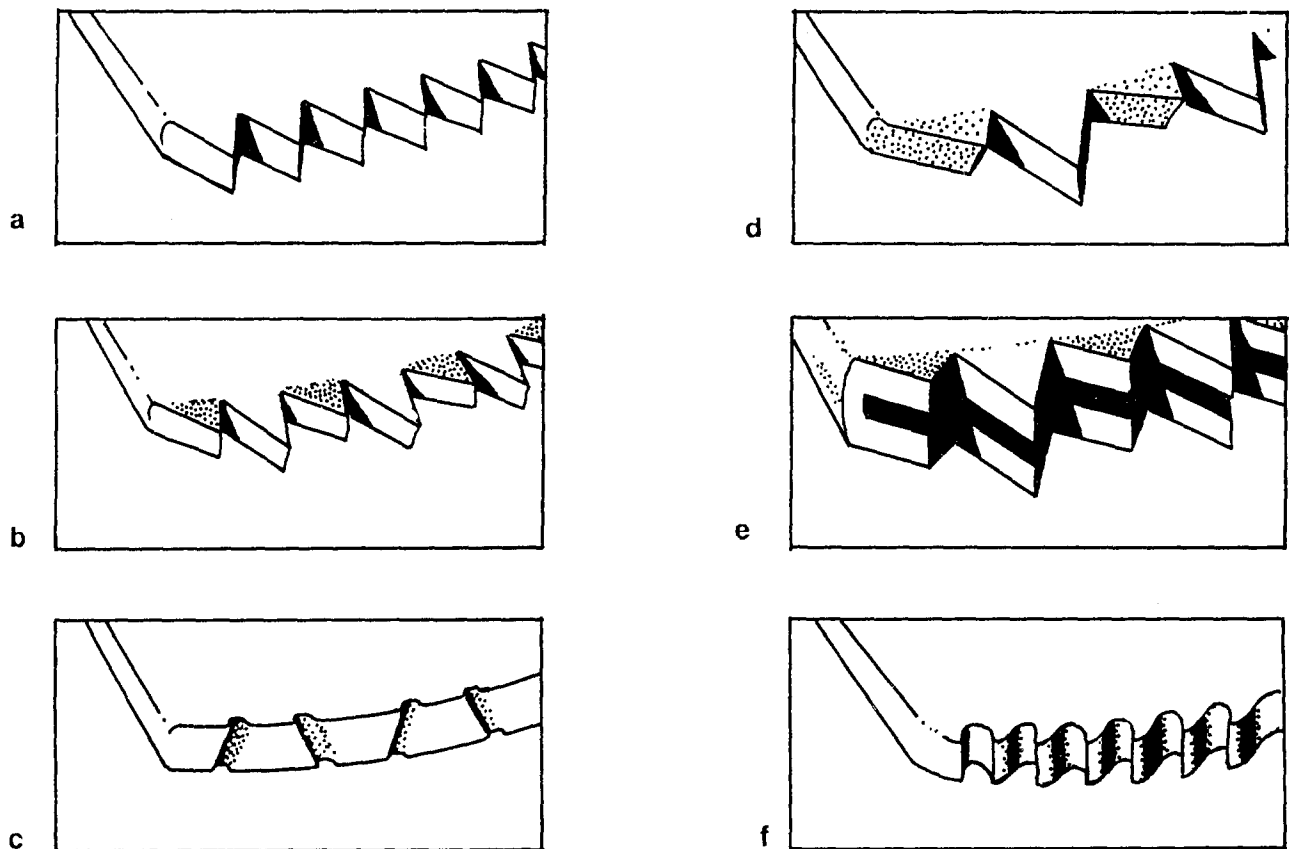


Fig. 2. Saw blade design. (A) 3 M p 512 reciproc. (B) 3 M L122. (C) 3 M L122 modification "half" teeth. (D) 3 M L122 Sandvik modification chamfer angle of 30°. (E) Double saw blade. (F) Hall saw blade.

Table 1. Maximal Temperature of Diaphyseal Ox Bone Cut with Different Saw Blades

Blade	No. Tests	Temperature (°C)	
		Average	Range
3M L122	61	101 ± 36	34–184
1/2 teeth	17	196 ± 61	88–290
0 teeth	10	188 ± 110	78–450
Sandvik 10°C	29	93 ± 37	41–194
Sandvik 30°C	18	116 ± 48	53–187
Hall	12	153 ± 38	100–200
3M reciproc	19	103 ± 37	40–200
Double	19	91 ± 19	49–112
Bone 20°C	34	108 ± 23	72–171
3M L122			

SE 460 pen recorder (Brown Boveri Goerz Metrawatt, Wien, Austria) having an accuracy of $\pm 1^\circ\text{C}$.

An ordinary air-powered 3M Maxi Driver tool (Orthopedic Products Division 3M, St. Paul, MN) connected to the hospital's main air power system was used as the driving equipment. Measured with a stroboscope (Movistrob, Ministrob type 2000) at 6–7 atm pressure, the speed was 15,000–16,000 rpm with the oscillating saw blades and about 3,800 rpm with the reciprocating saw blade. All tests were performed by the same person, who was blinded during the cutting process. All tests were done manually using the speed and pressure used in clinical practice.

The Student's *t*-test (two tail) was used in statistical methods to compare the results. The number of tests for each blade is given in Table 1.

Results

For the commercial 3M Maxi Driver L122 and 3M reciprocating saw blades and the specially made Sandvik saw blades the median maximal test temperature was between 93°C and 116°C , and there was no statistical difference. The Hall saw blade yielded higher temperatures, with a median maximal temperature of 153°C ($P < .001$), while the double-thickness saw blade produced a corresponding temperature of 91°C ($P > .05$). The used saw blades yielded higher temperatures than the new 3M L122 blades, with median maximal temperatures of 196°C and 188°C ($P < .001$).

When the tests were done on thawed bone (20°C) the median maximal temperature using the 3M Maxi Driver™ L122 saw blade was raised from 101°C to 108°C ($P > .05$). Three out of 219 tests resulted in temperatures below 44°C – 47°C .

The results are shown in Table 1.

Discussion

The problem of heat generation in orthopaedic surgery has been acknowledged previously, espe-

cially in the context of curing of cement in joint arthroplasty (6, 7, 10, 11, 15, 17, 20). The temperature while cutting bone has received less attention, although a number of investigators have reported significant temperature elevation (1, 4, 5, 9, 12, 22, 23).

Eriksson (2) has shown that bone tissue is more sensitive to heat than previously postulated. He showed that heating to 44°C – 47°C in 1 minute severely impaired bone formation.

In clinical bone cutting procedures most chips accumulate because the bone is surrounded by soft tissue and also because the saw teeth tend to push the bone chips into the uncut bone at the front of the teeth. In our studies we had a lesser accumulation of chips because the bone was free from soft tissue. The temperature in the saw blades in our study was approximately 30% higher than the temperature during in vivo bone cutting in knee arthroplasty (69°C) (23) using the same saw equipment. We believe this increase is an overall indication of the differences between the two models (i.e., human metaphyseal bone in vivo versus ox cortical diaphyseal bone in vitro). The temperatures are lower than those reported by Krause et al. (9), who used different tools and test set-up. Tests on thawed bone gave only a small but consistent increase in temperature. In conclusion, we believe that this in vitro test is valid, especially for comparison between different saw blades.

Alteration of the sawing geometry did not lower the temperature significantly below the critical level as shown by the alternate design patterns studied. This is in agreement with Krause et al. (9) who showed that the temperature could only be lowered from 259°C to 170°C by using different rake angles in a laboratory cutting test with reciprocating saws and constant bone feeding. Ludwig (12) did not find any significant differences in the temperature development when he tested three different saw blades in animal experiments.

The chip formation during the machining of bone occurs by a series of discrete fractures (25). A great deal of heat is produced during sawing when the chips are formed and the heat is carried away by the cleaning of the chips. In metal-cutting operations the heat contained in the chips comprises 60 to 70% of the total heat (21). One explanation for the small differences in our series is that the kerf of the saw blades is not cleared, and the chips accumulate and are pushed into the bone at the front of the teeth in a milling process. This may be the reason why the Hall blade yielded higher temperatures. The Hall blade has no offset of the teeth, producing a cut that is exactly as wide as the thickness of the blade. Thus no escape route is provided for the chips, which can only be impacted in the cutting area.

This investigation showed that there was a rise in temperature with saw wear. Because saw blades in clinical practice are frequently used more than once and in conjunction with a metal template employed as a cutting guide, the potential for blade damage and the production of suboptimal bone surface is high, and a suboptimal cutting process and higher temperatures should be expected. Wevers et al. (24) found that half of the saw blades taken from the operating room were severely damaged. They found that the thrust force was increased when cortical bone was cut with these worn blades. This is in accordance with Matthews and Hirsch (13), who investigated drilling in human cortical femoral bone in vitro and found worn drills to cause much greater temperature changes than new drills, also in accordance with our results.

We did not find any beneficial effects from use of a thick saw blade, in opposition to Klip (8), who, in a small test series, found that the saw blade could not be made too thick. One reason for our findings could be the heat sink phenomenon, which in prosthetic surgery is known to lower the temperature (7).

Orthopaedic surgery involves a great many occasions when bone, after being cut, is expected to heal with another bone surface (e.g., in osteotomies or with prosthetic devices, [i.e., porous, noncemented hip and knee prostheses]). Viable bone is desirable in these instances. It seems reasonable to conclude that alternating saw blade design in the patterns studied here does not appear to be a way to decrease the temperature to less than 44°C. Further development of cutting devices is indicated in order to control the temperature problem.

Supported by Alfred Österlunds Stiftelse, Lund Hospital Foundation, Lund University Medical Faculty, Greta and Johan Kocks Stiftelse, Malmöhus Läns Landsting, Stiftelsen för bistånd åt Vanföra i Skåne, Konung Gustaf V:s 80-årsfond, and the Swedish Medical Research Council (09509).

References

1. Bruun C, Andersen E: Heat generation during drilling in cancellous bone. *Acta Orthop Scand* 58:705, 1987
2. Eriksson AR: Heat induced bone tissue injury. Thesis, Göteborg, 1984
3. Eriksson AR, Albrektsson T, Albrektsson B: Heat caused by drilling cortical bone. *Acta Orthop Scand* 55:629, 1984
4. Fonden A: Sågning i ben. Report no. 7. Department of Orthopaedic Surgery and the Institute of Technology, Linköping, Sweden, 1977
5. Haddad RJ, Cook SD, Thomas KA: Biological fixation of porous-coated implants. *J Bone Joint Surg* 69A:1459, 1987
6. Holm NJ: The formation of stress by acrylic bone cements during fixation of the acetabular prosthesis. *Acta Orthop Scand* 51:719, 1980
7. Huiskes R: Some fundamental aspects of human joint replacement: analyses of stresses and heat conduction in bone-prosthesis structures. *Acta Orthop Scand Suppl* 51:185, 1980
8. Klip EJ: Sawing in bone. Report no. 1. Department of Orthopaedic Surgery and the Institute of Technology, Linköping, Sweden, 1976
9. Krause W, Bradbury DW, Kelly JE, Lunceford EM: Temperature elevation in orthopaedic cutting operations. *J Biomech* 15:267, 1982
10. Labitzke R, Paulus M: Intraoperative temperaturmessungen in der hüftchirurgie während der polymerisation des knochenementes Palacos. *Arch Orthop Unfall-Chir* 79:341, 1974
11. Lidgren L, Bodelin B, Möller J: Bone cement improved by vacuum mixing and chilling. *Acta Orthop Scand* 57:27, 1987
12. Ludewig R: Temperaturmessungen Beim Knochen-sägen. Dissertation der Medizinischen fakultet der Justus Liebig, Universität Giessen, 1971
13. Matthews LS, Hirsch C: Temperature measured in human cortical bone when drilling. *J Bone Joint Surg* 54A:297, 1972
14. Matthews LS, Green CA, Goldstein SA: The thermal effects of skeletal fixation-pin insertion in bone. *J Bone Joint Surg* 66A:1077, 1984
15. Mjöberg B: Loosening of the cemented hip prosthesis: the importance of heat injury. *Acta Orthop Scand Suppl* 57:221, 1986
16. Pallan FG: Histological changes in bone after insertion of skeletal fixation pins. *J Oral Surg Anesth Hosp D Serv* 18:400, 1960
17. Reckling FW, Dillon WL: The bone-cement interface temperature during total joint replacement. *J Bone Joint Surg* 59A:80, 1977
18. Ryd L: Micromotion in knee arthroplasty: a roentgen stereophotogrammetric analysis of tibial component fixation. *Acta Orthop Scand Suppl* 220, 1986
19. Ryd L, Lindstrand A, Stenström A, Selvik G: Porous coated anatomic tricompartmental tibial component fixation: relation between prosthetic position and micromotion. *Clin Orthop* 251:189, 1990
20. Seidel H, Eggert A, Pietsch H: Intraoperative Temperaturmessungen und der Zementknochengrenze bei TEP-Implantation. *Arch Orthop Unfall-Chir* 90:251, 1977
21. Schmidt AO: Heat in metal cutting. p. 218. In *Machining-theory and practice*. American Society for Metals, Cleveland, 1950
22. Tetsch P: Development of raised temperature after osteotomies. *J Oral Maxillofac Surg* 2:141, 1974
23. Toksvig-Larsen S, Ryd L: Temperature elevation during knee arthroplasty. *Acta Orthop Scand* 60:439, 1989
24. Wevers HW, Espin E, Cooke TDV: Orthopedic saw-blades: a case study. *J Arthroplasty* 2:43, 1989
25. Wiggins KL, Malkin S: Orthogonal machining of bone: ASME. 100:122, 1989

EXHIBIT DX43

TO DECLARATION OF PETER J. GOSS IN
SUPPORT OF DEFENDANTS' MOTION TO
EXCLUDE PLAINTIFFS' ENGINEERING
EXPERTS



STANDARD

ANSI/ASHRAE Standard 52.2-2017

(Supersedes ANSI/ASHRAE Standard 52.2-2012)

Includes ANSI/ASHRAE addenda listed in Appendix H

Method of Testing General Ventilation Air-Cleaning Devices for Removal Efficiency by Particle Size

See Informative Appendix H for approval dates by the ASHRAE Standards Committee, the ASHRAE Technology Committee, and the American National Standards Institute.

This Standard is under continuous maintenance by a Standing Standard Project Committee (SSPC) for which the Standards Committee has established a documented program for regular publication of addenda or revisions, including procedures for timely, documented, consensus action on requests for change to any part of the Standard. The change submittal form, instructions, and deadlines may be obtained in electronic form from the ASHRAE website (www.ashrae.org) or in paper form from the Senior Manager of Standards. The latest edition of an ASHRAE Standard may be purchased from the ASHRAE website (www.ashrae.org) or from ASHRAE Customer Service, 1791 Tullie Circle, NE, Atlanta, GA 30329-2305. E-mail: orders@ashrae.org. Fax: 678-539-2129. Telephone: 404-636-8400 (worldwide), or toll free 1-800-527-4723 (for orders in US and Canada). For reprint permission, go to www.ashrae.org/permissions.

© 2017 ASHRAE

ISSN 1041-2336



Special licensed to Peter Ross on 2017-05-28 for licensee's use only. All rights reserved. No further reproduction or distribution is permitted. Distributed by Techstreet for ASHRAE, www.techstreet.com

ASHRAE Standing Standard Project Committee 52.2
Cognizant TC: 2.4, Particulate Air Contaminants and Particulate Removal Equipment
SPLS Liaison: Rita M. Harrold

Michael D. Corbat*, *Chair*
 Kathleen Owen*, *Vice-Chair*
 Todd A. McGrath*, *Secretary*
 Robert B. Burkhead*
 Richard K. Chesson, Jr.*
 Kyung-Ju Choi*

David B. Christopher*
 Jeron Downing*
 Dara Marina Feddersen*
 Chris Fischer*
 Sanjeev K. Hingorani*
 David Matier*

Phil Maybee*
 Stephen W. Nicholas*
 Christine Q. Sun*
 Paolo M. Tronville*

* Denotes members of voting status when the document was approved for publication

ASHRAE STANDARDS COMMITTEE 2016–2017

Rita M. Harrold, *Chair*
 Steven J. Emmerich, *Vice-Chair*
 James D. Aswegan
 Niels Bidstrup
 Donald M. Brundage
 Drury B. Crawley
 John F. Dunlap,
 James W. Earley, Jr.
 Keith I. Emerson
 Julie M. Ferguson

Michael W. Gallagher
 Walter T. Grondzik
 Vinod P. Gupta
 Susanna S. Hanson
 Roger L. Hedrick
 Rick M. Heiden
 Srinivas Katipamula
 Cesar L. Lim
 Arsen K. Melikov
 R. Lee Millies, Jr.

Cyrus H. Nasser
 David Robin
 Peter Simmonds
 Dennis A. Stanke
 Wayne H. Stoppelmoor, Jr.
 Jack H. Zarour
 William F. Walter, *BOD ExO*
 Patricia Graef, *CO*

Stephanie C. Reiniche, *Senior Manager of Standards*

SPECIAL NOTE

This American National Standard (ANS) is a national voluntary consensus Standard developed under the auspices of ASHRAE. *Consensus* is defined by the American National Standards Institute (ANSI), of which ASHRAE is a member and which has approved this Standard as an ANS, as "substantial agreement reached by directly and materially affected interest categories. This signifies the concurrence of more than a simple majority, but not necessarily unanimity. Consensus requires that all views and objections be considered, and that an effort be made toward their resolution." Compliance with this Standard is voluntary until and unless a legal jurisdiction makes compliance mandatory through legislation.

ASHRAE obtains consensus through participation of its national and international members, associated societies, and public review.

ASHRAE Standards are prepared by a Project Committee appointed specifically for the purpose of writing the Standard. The Project Committee Chair and Vice-Chair must be members of ASHRAE; while other committee members may or may not be ASHRAE members, all must be technically qualified in the subject area of the Standard. Every effort is made to balance the concerned interests on all Project Committees.

The Senior Manager of Standards of ASHRAE should be contacted for

- interpretation of the contents of this Standard,
- participation in the next review of the Standard,
- offering constructive criticism for improving the Standard, or
- permission to reprint portions of the Standard.

DISCLAIMER

ASHRAE uses its best efforts to promulgate Standards and Guidelines for the benefit of the public in light of available information and accepted industry practices. However, ASHRAE does not guarantee, certify, or assure the safety or performance of any products, components, or systems tested, installed, or operated in accordance with ASHRAE's Standards or Guidelines or that any tests conducted under its Standards or Guidelines will be nonhazardous or free from risk.

ASHRAE INDUSTRIAL ADVERTISING POLICY ON STANDARDS

ASHRAE Standards and Guidelines are established to assist industry and the public by offering a uniform method of testing for rating purposes, by suggesting safe practices in designing and installing equipment, by providing proper definitions of this equipment, and by providing other information that may serve to guide the industry. The creation of ASHRAE Standards and Guidelines is determined by the need for them, and conformance to them is completely voluntary.

In referring to this Standard or Guideline and in marking of equipment and in advertising, no claim shall be made, either stated or implied, that the product has been approved by ASHRAE.

CONTENTS

**ANSI/ASHRAE Standard 52.2-2017,
Method of Testing General Ventilation Air-Cleaning Devices
for Removal Efficiency by Particle Size**

SECTION	PAGE
Foreword	2
1 Purpose	3
2 Scope	3
3 Definitions and Acronyms	3
4 Test Apparatus	4
5 Apparatus Qualification Testing	9
6 Test Materials	16
7 Selection and Preparation of the Test Device	17
8 Test Procedures	18
9 Measurement of Resistance versus Airflow	19
10 Determination of Particle Size Efficiency	19
11 Reporting Results	25
12 Minimum Efficiency Reporting Value (MERV) for Air Cleaners	26
13 Normative References	26
Informative Appendix A: Commentary	30
Informative Appendix B: Test Procedure Suggestions and Examples	32
Informative Appendix C: How to Read a Test Report	38
Informative Appendix D: Minimum Efficiency Reporting Guidance	42
Informative Appendix E: Cross-Reference and Application Guidelines	44
Informative Appendix F: Acronyms and Conversion Formulae	46
Informative Appendix G: Informative References	47
Informative Appendix H: Addenda Description Information	48
Informative Appendix I: (Intentionally Left Blank)	49
Informative Appendix J: Optional Method of Conditioning a Filter Using Fine KCl Particles to Demonstrate Efficiency Loss That Might Be Realized in Field Applications	50
Informative Appendix K: Optional Method of Testing Two Air Filters Arranged in Series in a System to Evaluate Particle Removal, Dust Loading, and Pressure Drop Increase That Might Be Realized in Field Applications	55

NOTE

Approved addenda, errata, or interpretations for this standard can be downloaded free of charge from the ASHRAE website at www.ashrae.org/technology.

© 2017 ASHRAE

1791 Tullie Circle NE · Atlanta, GA 30329 · www.ashrae.org · All rights reserved.

ASHRAE is a registered trademark of the American Society of Heating, Refrigerating and Air-Conditioning Engineers, Inc.
ANSI is a registered trademark of the American National Standards Institute.

(This foreword is not part of this standard. It is merely informative and does not contain requirements necessary for conformance to the standard. It has not been processed according to the ANSI requirements for a standard and may contain material that has not been subject to public review or a consensus process. Unresolved objections on informative material are not offered the right to appeal at ASHRAE or ANSI.)

FOREWORD

ANSI/ASHRAE Standard 52.2-2017 incorporates addenda to the 2012 edition. The goal of the committee was to improve the end-user experience by standardizing reporting or improving the robustness of the test method to reduce variability. The committee's intentions were to provide the best possible information for the end user to select the best air-cleaning devices to protect people and equipment.

Historically, standards for testing air cleaners have been developed in response to the needs of the times. Protection of machinery and coils came first, then reduction of soiling. Now concerns about indoor air quality and respirable particles, protection of products during manufacturing, and protection of HVAC equipment have prompted development of this test standard based on particle size.

Standards Project Committee (SPC) 52.2 was first organized in 1987 to develop a particle size test procedure but was disbanded in 1990 after it became evident that basic research was needed. In 1991, a research contract (ASHRAE Research Project 671, Informative Appendix A, Reference A2) was awarded to review test methodology and recommend approaches for obtaining particle size efficiency data. After the research project was completed and accepted in 1993, SPC 52.2 was reactivated with members representing a broad range of interests. The standard was then formally published in 1999. Changes to the method have been made over the years to improve it and to make it more relevant. The 2017 edition continues that tradition. Appendix H includes a full list of changes by addendum:

- a. Modifications were made to the MERV table to adjust the threshold for specific MERVs and allow for the 16 graduations to be more observable in testing.
- b. To address user concerns about reproducibility and reliability of the test method, ASHRAE commissioned Research Project RP-1088, a comprehensive round robin of multiple labs, including multiple levels of filtration performance. The changes in the 2017 edition of the standard are based on direct recommendations of the research project.
- c. Changes were made with the intent of making the data on reports more mandatory. The goal of the committee was to improve user experience by ensuring that reports being provided by labs and manufacturers would share the same data, allowing for a simpler evaluation of products.
- d. New Informative Appendix K uses the base methodology to test across sequenced filters. This allows users a method of testing their system in a controlled lab environment.

Description of Standard

This standard addresses two air-cleaner performance characteristics of importance to users: the ability of the device to

remove particles from the airstream and its resistance to air-flow. Air-cleaner testing is conducted at airflow rates not less than $0.22 \text{ m}^3/\text{s}$ (472 cfm) nor greater than $1.4 \text{ m}^3/\text{s}$ (3000 cfm).

A sample of air from a general ventilation system contains particles with a broad range of sizes having varied effects, sometimes dependent on particle size. Coarse particles, for example, cause energy waste when they cover heat transfer surfaces. Fine particles cause soiling and discoloration of interior surfaces and furnishings as well as possible health effects when inhaled by occupants of the space. When air cleaners are tested and reported for efficiency in accordance with this standard, there is a basis for comparison and selection for specific tasks.

The test procedure uses laboratory-generated KCl particles dispersed into the airstream as the test aerosol. A particle counter measures and counts the particles in 12 size ranges, both upstream and downstream, for the efficiency determinations.

This standard also delineates a method of loading the air cleaner with synthetic dust to simulate field conditions. A set of particle size removal efficiency (PSE) performance curves at incremental dust loading is developed and, together with an initial clean performance curve, is the basis of a composite curve representing the minimum performance in each size range. Points on the composite curve are averaged and the averages are then used to determine the minimum efficiency reporting value (MERV) of the air cleaner.

Coarse air cleaners may be tested for particle size removal efficiency when they are clean, with results reported in the prescribed format. (An example of a coarse air cleaner is the so-called "furnace" filter, a flat panel with a cardboard frame and spun glass fiber media.) However, the standard also provides the basis for evaluation using the loading dust efficiency by weight, or "arrestance," as well as an estimate of predicted life called "dust holding capacity."

Electronic Air Cleaners

Some air cleaners, such as externally powered electrostatic precipitators (also known as electronic air cleaners), may not be compatible with the loading dust used in this test method. The dust contains very conductive carbon that may cause electrical shorting, thus reducing or eliminating the effectiveness of these devices and negatively affecting their MERVs. In actual applications, the efficiency of these devices may decline over time, and their service life is dependent on the conductivity and the amount of dust collected.

Passive Electrostatic Fibrous Media Air Filters

Some fibrous media air filters have electrostatic charges that may be either natural or imposed on the media during manufacturing. Such filters may demonstrate high efficiency when clean and a drop in efficiency during their actual use cycle. The initial conditioning step of the dust-loading procedure described in this standard may affect the efficiency of the filter but not as much as would be observed in actual service. Therefore, the minimum efficiency observed during testing may be higher than that achieved during actual use.

Not an Application Standard

Users should not misinterpret the intent of this standard. This is a test method standard, and its results are to be used to directly compare air cleaners on a standardized basis irrespective of their applications. Results are also used to give the design engineer an easy-to-use basis for specifying an air cleaner. It is entirely possible that an industry organization may use this test method as the basis for an application standard with, for example, different final resistances.

Footnotes are used throughout this standard to provide nonmandatory guidance for the user in addition to the nonmandatory guidance found in the informative appendices. Footnotes are for information only and are not part of the standard.

Acknowledgments

SSPC 52.2 wishes to acknowledge with thanks the contributions of many people outside the voting membership, including European filtration authorities who made suggestions through the committee's international member. We are also indebted to the many media/filter manufacturers and third-party companies that have supported the committee by providing access to skilled and informed volunteers.

1. PURPOSE

This standard establishes a test procedure for evaluating the performance of air-cleaning devices as a function of particle size.

2. SCOPE

2.1 This standard describes a method of laboratory testing to measure the performance of general ventilation air-cleaning devices.

2.2 The method of testing measures the performance of air-cleaning devices in removing particles of specific diameters as the devices become loaded by standardized loading dust fed at intervals to simulate accumulation of particles during service life. The standard defines procedures for generating the aerosols required for conducting the test. The standard also provides a method for counting airborne particles of 0.30 to 10 μm in diameter upstream and downstream of the air-cleaning device in order to calculate removal efficiency by particle size.

2.3 This standard also establishes performance specifications for the equipment required to conduct the tests, defines methods of calculating and reporting the results obtained from the test data, and establishes a minimum efficiency reporting system that can be applied to air-cleaning devices covered by this standard.

3. DEFINITIONS AND ACRONYMS

3.1 Definitions. Some terms are defined below for the purposes of this standard. When definitions are not provided, common usage shall apply (see Informative Appendix G, Reference 1).

aerosol particle counter (OPC): an instrument that samples, counts, and sizes aerosol particles. While several different technologies exist for aerosol particle counters (e.g., optical,

aerodynamic, electrostatic mobility), only optical aerosol particle counters based on light scattering are used in this standard. Optical aerosol particle counters are often referred to as "OPCs" and, when the particles are sized into a number of sizing channels, are also sometimes referred to as "aerosol spectrometers."

airflow rate: the actual volume of test air passing through the device per unit of time, expressed in m^3/s (ft^3/min [cfm]), to three significant figures.

arrestance (A): a measure of the ability of an air-cleaning device with efficiencies less than 20% in the size range of 3.0 to 10.0 μm to remove loading dust from test air. Measurements are made of the weight of loading dust fed and the weight of dust passing the device during each loading step. The difference between the weight of dust fed and the weight of dust passing the device is calculated as the dust captured by the device. Arrestance is then calculated as the percentage of the dust fed that was captured by the device.

average arrestance (A_{avg}): for an air-cleaning device with efficiencies less than 20% in the size range of 3.0 to 10.0 μm , the average value of the arrestances made on the device during the loading test, weighted by the amounts of dust fed to the device during each incremental dust loading step.

charge neutralizer: a device that brings the charge distribution of the aerosol to a Boltzman charge distribution. This represents the charge distribution of the ambient aerosol.

coefficient of variation (CV): standard deviation of a group of measurements divided by the mean.

correlation ratio data acceptance criteria: criteria used to determine the adequacy of the correlation data, further defined in Section 10.6.2.

correlation ratio (R): the ratio of downstream to upstream particle counts without the test service installed in the test duct. It is determined from the average of at least three samples. This ratio is used to correct for any bias between upstream and downstream sampling and counting systems, and its calculation is described in Section 10.3.

device: throughout this standard the word *device* refers to air-cleaning equipment used in general ventilation for the removal of particles—specifically, the air cleaner being tested.

disposable air filters: filters that are designed to operate through a specified performance range and then be discarded and replaced.

dust holding capacity (DHC): the total weight of the synthetic loading dust captured by the air-cleaning device over all of the incremental dust loading steps.

dust increment: the amount of dust fed during a definite part of the loading procedure.

face area: the gross area of the device exposed to airflow. This area is measured in a plane perpendicular to the axis of the test duct or the specified direction of airflow approaching the device. All internal flanges are a part of this area, but items such as mounting hardware and electrical raceways normally mounted out of the airstream are not included. Face area is measured in m^2 (ft^2) to three significant figures.

face velocity: the rate of air movement at the face of the device (airflow rate divided by face area), expressed in m/s (fpm) to three significant figures.

final filter: a filter used to collect the loading dust that has passed through a device during the test procedure.

final resistance: the resistance to airflow of the air-cleaning device at which the test is terminated and results calculated, expressed in Pa (in. of water).

general ventilation: the process of moving air into or about a space or removing it from the space. The source of ventilation air is either air from outside the space, recirculated air, or a combination of these.

initial resistance: the pressure loss of the device operating at a specified airflow rate with no dust load, expressed in Pa (in. of water).

isokinetic sampling: sampling in which the flow in the sampler inlet is moving at the same velocity and direction as the flow being sampled.

loading dust: a compounded synthetic dust used for air-cleaner loading. Specifications for this dust are given in Section 6.2.

media: for a fibrous-type air cleaner, media is that part of the device that is the actual dust-removing agent. Webs of spun fiberglass and papers are examples of air-filter media.

media velocity: the rate of air movement through the filter media (airflow rate divided by net effective filtering area). The term is not applicable to plate-type electronic air cleaners. Media velocity is measured in m/s (fpm) to three significant figures.

net effective filtering area: the total area in the device on which dust collects. For devices using fibrous media, it is the net upstream area of the media exposed to airflow, measured in the plane or general surface of the media. Net effective area excludes the area blocked by sealants, flanges, or supports. In electronic air cleaners, it is the total exposed surface of those electrodes available for dust precipitation, including the ionizing section but excluding supports, holes, and insulators. Net effective filtering area is measured in m^2 (ft^2) to three significant figures.

particle size: the polystyrene latex (PSL) light-scattering equivalent size expressed as a diameter in micrometers (μm , 10^{-6} m).

penetration: the fraction (percentage) of particles that pass through the air cleaner as described in Section 10.4.

penetration data acceptance criteria: criteria used to determine the adequacy of the penetration data, further defined in Section 10.6.4.

polydisperse: a characteristic of an aerosol for which the width of its number distribution shows a geometric standard deviation of $\delta_g > 1.5$.

rated airflow: the airflow rate in m^3/s (cfm) at which the device is tested. In this standard it is specified by the manufacturer in accordance with Section 8.1.

rated final resistance: the operating pressure loss at the airflow rate at which a device should be replaced or renewed, as recommended by the manufacturer, expressed in Pa (in. of water).

reference filters: dry-media-type filters that are carefully measured for resistance and initial efficiency immediately after a test system is qualified. These filters serve as references to ensure that the test system continues to operate as it did when it was qualified. See Section 5.16.1.

release rate: the particles shedding from a filter after a dust load in particles of a given size released per sample volume.

resistance: the loss of static pressure caused by the device operating at a stated airflow rate, expressed in Pa (in. of water) to an accuracy of $\pm 2.5\%$.

test aerosol: polydisperse solid-phase (i.e., dry) potassium chloride (KCl) particles generated from an aqueous solution, used in this standard to determine the particle size efficiency of the device under test. Generation of the test aerosol is described in Section 5.3.

test rig: the total assembly consisting of the test duct, the aerosol generator, the loading dust feeder, the particle counters and associated accessories, the instrumentation, and the monitoring equipment.

3.2 Acronyms

ASME	American Society of Mechanical Engineers
ASTM	American Society for Testing and Materials
CV	coefficient of variation
DHC	dust holding capacity
HEPA	high-efficiency particulate air
MERV	minimum efficiency reporting value
OPC	optical particle counter
PSE	particle size removal efficiency
PSL	polystyrene latex, referring to commercially available particles of various specific sizes
SAE	Society of Automotive Engineers
ULPA	ultra-low penetration air

4. TEST APPARATUS

4.1 Mandatory and Discretionary Requirements. Critical dimensions and arrangements of the test apparatus are shown in the figures of this section and in Section 5. All dimensions shown are mandatory unless otherwise indicated. Tolerances are given on each drawing, and either SI or I-P dimensions are acceptable for any element of the system. Units shown are in mm (in.) unless otherwise indicated. The design of equipment not specified, including but not limited to blowers, valves, and external piping, is discretionary, but the equipment must have adequate capacity to meet the requirements of this standard.

4.2 Test Duct

4.2.1 The test duct is defined in Figures 4-1, 4-2, and 4-3 and is primarily of square cross section, 610×610 mm (24×24 in.). The duct material must be electrically conductive and electrically grounded, have a smooth interior finish, and be sufficiently rigid to maintain its shape at the operating pressures. The inlet filter bank must contain high-efficiency particulate air (HEPA) filters. Increasing the cross section of the

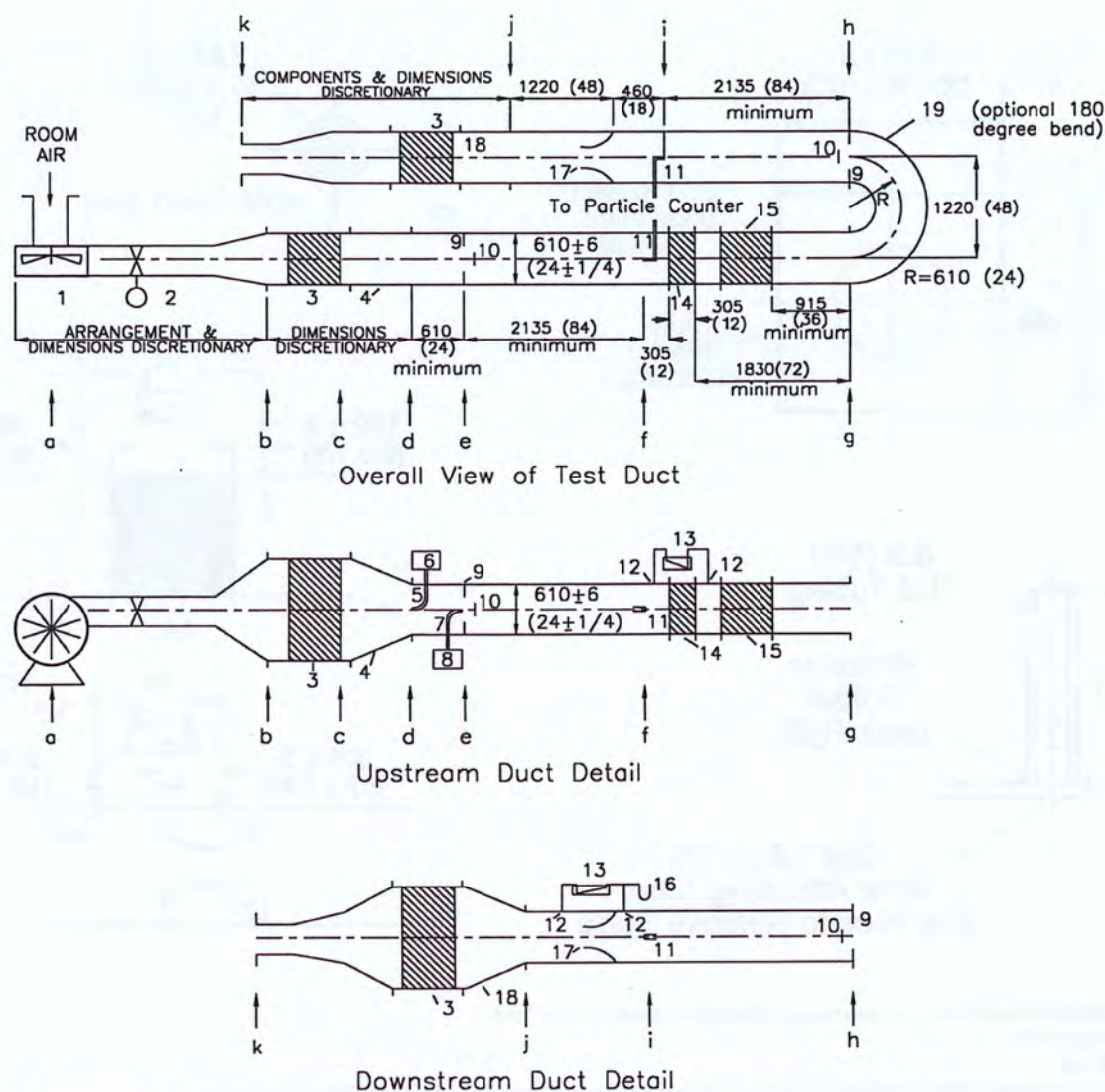


Figure 4-1 Schematic of the test duct (notes and legend are below). Dimensions are in mm (in.).

Notes for Figure 4-1:

1. Duct segments "d" through "j" shall have a cross section of 610 × 610 mm (24 × 24 in.), excluding the device section that has transitions as shown in Figures 4-3a, 4-3b, and 4-3c.
2. Segments "b" through "g" shall be in centerline alignment.
3. Segments "h" through "j" shall be in centerline alignment.
4. Upstream airflow and aerosol traverse measurements in accordance with Section 5 shall be performed at "f."
5. Aerosol injection shall occur between "c" and "e"; design discretionary in accordance with Section 4.2.4.
6. Side-by-side or over-and-under arrangements of the upstream and downstream sections of the test duct are allowed.

LEGEND FOR FIGURES 4-1 and 4-2d

- | | |
|---|---|
| 1. Blower | 10. Perforated diffusion plate |
| 2. Flow control valve | 11. Location of sample probe |
| 3. HEPA filter bank | 12. Static tap |
| 4. Transition, if any, from filter bank to 610 × 610 mm (24 × 24 in.) ducting. Maximum transition half angle = 45°. | 13. Manometer |
| 5. Aerosol injection tube | 14. Air-cleaning device and transitions (if any) |
| 6. Aerosol generator | 15. Final filter (installed only during dust loading) |
| 7. Dust feed pipe | 16. Vertical manometer |
| 8. Dust feeder | 17. Main flow measurement nozzle |
| 9. Mixing orifice | 18. Transition, if needed |
| | 19. Bend, optional |

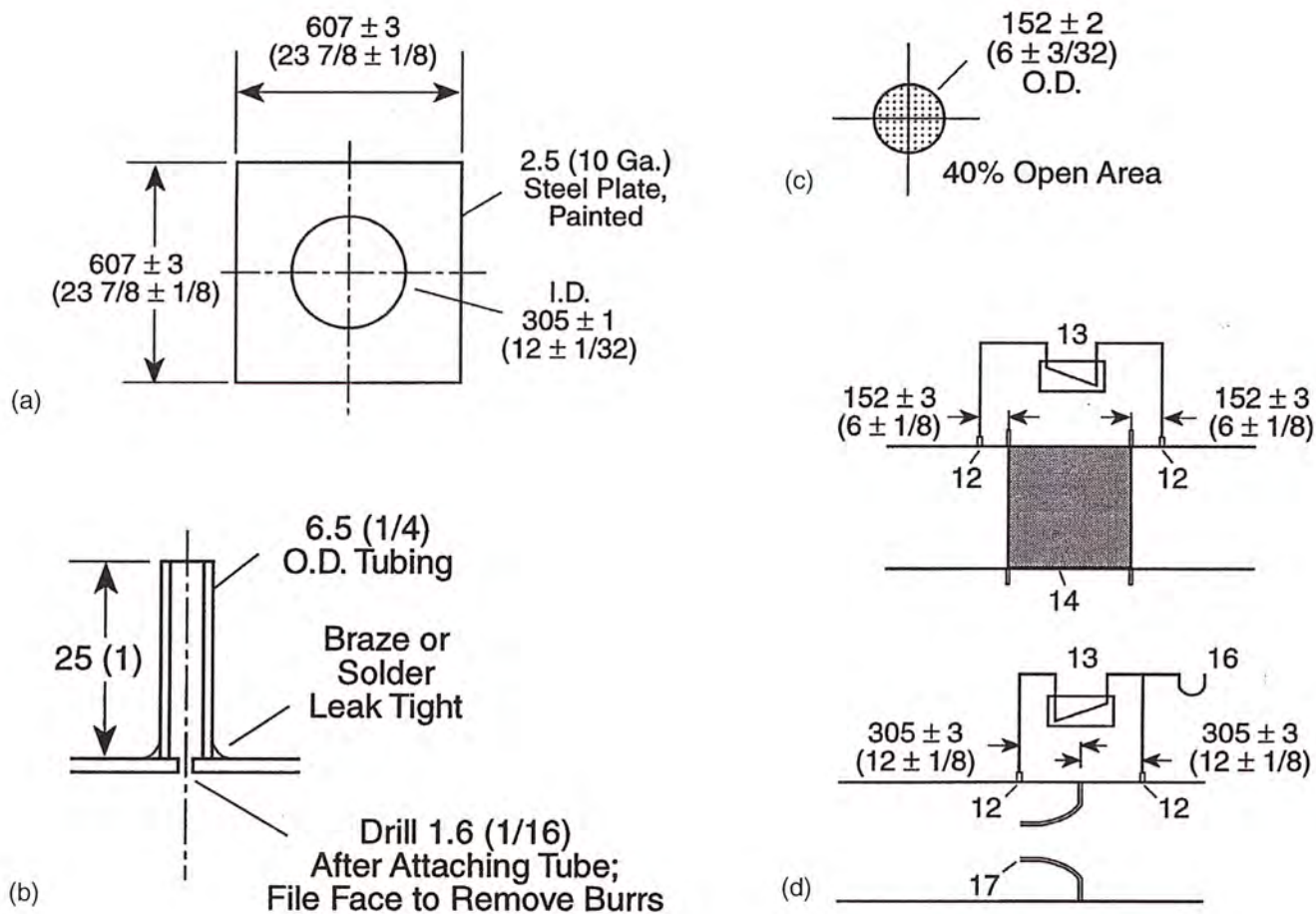


Figure 4-2 Details of test duct components. Dimensions are in mm (in.).

- (a) Mixing orifice.
- (b) Static tap.
- (c) Perforated plate with a sufficient number of equally spaced holes to provide 40% open area.
- (d) Static tap locations.

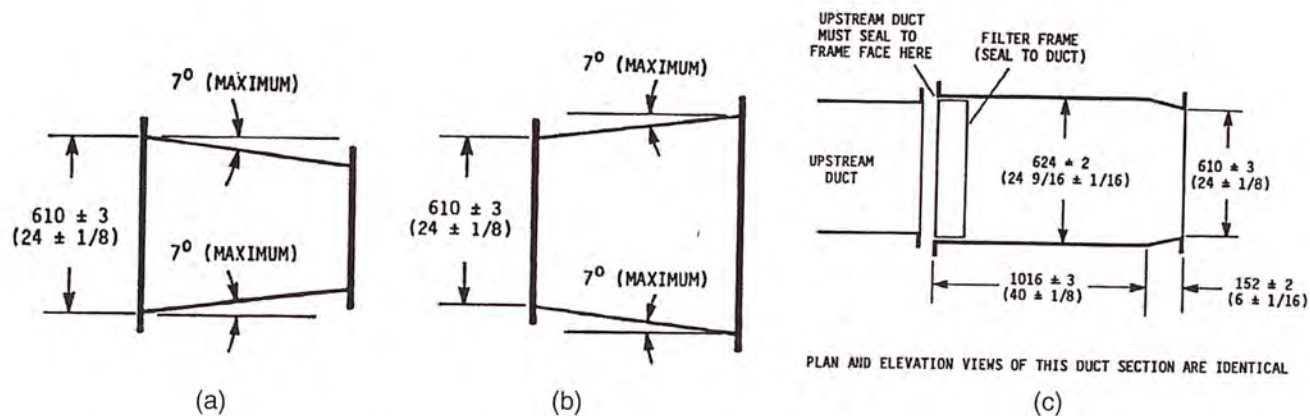


Figure 4-3 Dimensions are in mm (in.).

- (a) Transition: test air-cleaner dimensions smaller than test duct (asymmetrical dimensions are allowed).
- (b) Transition: test air-cleaner dimensions larger than test duct (asymmetrical dimensions are allowed).
- (c) Allowable special duct section for nonrigid air cleaners (must be symmetrical).

duct at the inlet filter bank to accommodate more than one 610 × 610 mm (24 × 24 in.) HEPA filter to minimize pressure drop is allowed. The inlet filter bank must discharge along the centerline of the upstream mixing orifice. System airflow is measured with an American Society of Mechanical Engineers (ASME) flow orifice (Reference 2). The duct must be operated at positive pressure, i.e., the blower discharges into the duct upstream of the test device.

4.2.2 The bend (Figure 4-1, #19) in the duct is optional, thereby allowing both a straight duct and a U-shaped duct configuration. Except for the bend itself, all dimensions and components (including the downstream mixing orifice and baffle) are the same for the straight and U-shaped configurations.

4.2.3 Room air or recirculated air shall be used as the test air source. The temperature of the air at the test device shall be between 10°C and 38°C (50°F and 100°F) with a relative humidity of 45% ± 10%¹. Exhaust flow shall be discharged outdoors or indoors or recirculated².

4.2.4 An orifice plate and a mixing baffle shall be located downstream of the aerosol injection point. An identical orifice plate/mixing baffle shall be located downstream of the test device³. The perforated diffusion plate should be located 152 ± 3 mm (6 ± 1/8 in.) downstream of the mixing orifice and mounted so that the centerline is in line with the hole in the mixing orifice.

4.2.5 The test aerosol shall be injected into the duct between the inlet filter bank and the upstream mixing orifice. The aerosol injection system shall produce an upstream challenge that meets the qualification criteria of Section 5.3. The injection system design is discretionary so long as it fulfills this requirement.

4.2.6 The test duct shall be isolated from vibration caused by the blower or other sources of vibration.

4.2.7 The test apparatus shown in Figure 4-1 is designed for test devices with nominal face dimensions of 610 × 610 mm (24 × 24 in.). Transitions in accordance with Figures 4-3a and 4-3b shall be used for test devices with face areas from 60% to 150% of the normal test duct cross section area of 0.37 m² (4 ft²). It is permitted to test a bank of several devices if the face area of an individual device is less than 60% of the duct area. It is also permitted to test specially sized air cleaners duplicating the structure of standard units if the size requirement cannot otherwise be met.

4.3 Aerosol Generator. Other than the requirements of the following subsections, design features of the aerosol generator are discretionary. Refer to Informative Appendix B of this standard for guidance.

1. A slight temperature increase with a corresponding decrease in relative humidity will occur as the room air passes through the blower.
2. HEPA filtration of the exhaust flow is recommended when discharging indoors because test aerosol and loading dust may be present.
3. The downstream orifice serves two purposes. It straightens out the flow after going around the bend and it mixes any aerosol that penetrated the test device. Mixing the penetrating aerosol with the airstream is necessary in order to obtain a representative downstream aerosol measurement.

4.3.1 The test aerosol shall be polydisperse solid-phase (dry) potassium chloride (KCl) particles generated from an aqueous solution. The aerosol generator shall provide a stable test aerosol of sufficient concentration over the 0.30 to 10 µm diameter size range to meet the requirements of Section 10 without overloading the aerosol particle counter⁴. Refer to Section 5.6.

4.3.2 The aerosol generator shall be designed to ensure that the KCl particles are dry prior to being introduced into the test duct. The relative humidity of the airflow with the particles shall be less than 50%.

4.3.3 After drying, the aerosol shall be brought to a Boltzman electrostatic charge distribution by a beta or gamma radiation generator with an activity of at least 185 MBq (5 mCi) or a corona discharge ionizer⁵. The corona discharge ionizer shall have a minimum corona current of 3 µA and shall be balanced to provide equal amounts of positive and negative ions.

4.4 Aerosol Sampling System. Other than the requirements of the following subsections, the design features of the sampling system are discretionary. Refer to Informative Appendix B of this standard for guidance.

4.4.1 The design criterion for the sampling system shall be to provide a particle transport of >50% for 10 µm diameter KCl particles from the sample probe inlet within the test duct to the inlet of the particle counter. This shall be verified by experimental measurement or by numerical calculation of particle transport based on the geometry of the sampling system⁶, the sampling flow rate, and particle deposition associated with diffusion, sedimentation, turbulent flow, and inertial forces⁷.

4.4.2 The use of a primary and secondary sampling system is allowed to optimize particle transport from the inlet probe to the particle counter⁸. The primary/secondary sampling system shall meet the following criteria:

- a. The portion of the primary sampling line in the duct shall block less than 10% of the duct cross-sectional area.
- b. Isokinetic sampling (to within 10%) shall be maintained on both primary and secondary probes.
4. Air-atomizing spray nozzles in which an aqueous KCl solution is nebulized with compressed air and then dried are a suitable means of aerosol generation.
5. Electrostatic charging is an unavoidable consequence of most aerosol generation methods.
6. For example, tube diameter, the number of bends, lengths of horizontal and vertical sections.
7. A numerical model of aerosol transport has been developed. See Informative Appendix G, Reference 3.
8. The primary lines (one from the upstream duct, one from the downstream duct) draw the samples from the duct and transport them to the vicinity of the particle counters. The primary system uses an auxiliary pump and flowmetering system to operate at a higher airflow rate than would be provided by the particle counters alone. The higher airflow rate combined with larger diameter sampling lines improves particle transport. The particle counters then draws a lower flow rate sample from the primary line. The sample lines from the particle counters to the primary sample lines are termed the *secondary sample lines*.

- c. Flow through the primary sampling system shall be measured to within 5% with volumetric devices (e.g., orifice plates and rotometers).
- d. Combined particle losses in the primary and secondary system shall be <50% for 10 μm diameter KCl particles, based on particle transport modeling.
- e. The upstream and downstream primary sampling systems shall be of equal length and equivalent geometry.
- f. The upstream and downstream secondary sampling systems shall be of equal length and equivalent geometry.
- g. The airflow rate of the upstream primary system shall be <2% of the system airflow rate.
- h. The airflow rate of the downstream primary system shall be <2% of the system airflow rate. The extracted airflow rate shall be added to the measured duct airflow rate to obtain the test airflow rate.
- i. The auxiliary pump and associated flow control and flow measurement devices of the primary sampling lines must be downstream of secondary probes.

4.4.3 Diluters, if used, shall provide equal dilution of both the upstream and downstream samples. Dilution of only the upstream samples is disallowed.

4.4.4 The upstream and downstream sample lines (both primary and secondary, if used) shall be made of rigid electrically grounded metallic tubing having a smooth inside surface, and they must be rigidly secured to prevent movement during testing. The upstream and downstream sample lines are to be nominally identical in geometry. The use of a short length (50 mm [2 in.] maximum) of straight, flexible, electrically dissipative tubing to make the final connection to the aerosol particle counter is acceptable⁹.

4.4.5 The inlet nozzles of upstream and downstream sample probes shall be sharp edged and of appropriate entrance diameter to maintain isokinetic sampling within 10% at the test airflow rate.

4.5 Device Flow Measurement. Flow measurement shall be made by means of ASME long-radius flow nozzles (see Figure 9-1) with static taps as in Figure 4-2b located as shown in Figure 4-2d. The temperature, absolute pressure, and relative humidity of the test airflow shall be measured in the duct immediately upstream of the flow-measuring orifice. These values shall be used for calculation of airflow rate.

4.6 Particle Counters. The particle counter specifications consist of the following:

- a. Measurement technology
- b. Size range
- c. Counting efficiency
- d. Resolution of particle size measurement
- e. Number of sizing channels and their boundaries
- f. Degree of monotonic response required
- g. Calibration methods
- h. Sampling flow rate stability
- i. Zero-count specification
- j. Requirements when dual counters are used
- k. Sample flow rate measurement and recording

9. This often relieves stress that would be placed on the instrument's inlet.

Table 4-1 Particle Counters Size Range Boundaries

Size Range	Size Range Boundaries		Geometric Mean Particle Size, μm
	Lower Limit, μm	Upper Limit, μm	
1	0.30	0.40	0.35
2	0.40	0.55	0.47
3	0.55	0.70	0.62
4	0.70	1.00	0.84
5	1.00	1.30	1.14
6	1.30	1.60	1.44
7	1.60	2.20	1.88
8	2.20	3.00	2.57
9	3.00	4.00	3.46
10	4.00	5.50	4.69
11	5.50	7.00	6.20
12	7.00	10.00	8.37

4.6.1 The aerosol particle counter shall be based on optical particle sizing and counting (i.e., light scattering). These instruments are commonly known as "optical particle counters" and also as "optical aerosol spectrometers."

4.6.2 The particle counters shall count and size aerosol particles in the 0.30 to 10 μm diameter size range.

4.6.3 The counting efficiency shall be at least 50% for 0.3 μm NIST-traceable polystyrene latex (PSL) particles.

4.6.4 The sizing resolution of the particle counter shall be $\leq 10\%$ (standard deviation/mean) and shall be measured in accordance with ISO 21501-1, ISO 21501-4, IEST-RP-CC014.1, or equivalent. The resolution shall be measured at a particle size in the range of 0.5 to 0.7 μm .

4.6.5 The particle counters shall group measured particles into 12 size ranges. The range boundaries (based on PSL calibration) shall conform to Table 4-1.

4.6.6 The particle counter's correlation of measured response¹⁰ to physical particle size shall be monotonic for PSL particles from 0.30 to 10 μm , such that only one size range shall be indicated for any measured response (i.e., any lack on monotonic response must be such that the associated ambiguity in particle size is contained within one channel of the particle counter).

4.6.7 Particle counter calibration shall conform to the following:

- a. The OPC shall be calibrated in accordance with ISO 21501-4.
- b. The calibration shall be performed with monodisperse NIST-traceable PSL.
- c. The calibration shall include at least one particle diameter in each of the ranges of 0.3 to 0.4 μm , 9 to 11 μm , and 4 other sizes in between.

10. Voltage, for example.

- d. The size calibration of the particle counter shall be performed at least annually.

4.6.8 The inlet volume flow rate shall not change more than 2% with a 1000 Pa (4.0 in. of water) change in the pressure of the sampled air.

4.6.9 The total measured particle count rate shall be less than 10 particles per minute when the particle counter is sampling air with a high-efficiency filter on its intake.

4.6.10 Dual particle counters, if used, shall be identical models such that they are closely matched in design and sampling flow rate.

4.6.11 The viewed sample flow rate of the particle counter shall be recorded for each data sample.

Informative Note: Some particle counters incorporate measurement of the viewed sample flow rate within the instrument and provide that measurement as part of the data stream associated with each sample. If the particle counter does not provide this output, provisions need to be made to capture this information for each sample (such as adding a mass flowmeter on the outlet stream from the particle counter's sensor). For some particle counters, viewed sample flow rate can be significantly affected by duct pressure, which can change with flow rate; the resistance of the test filter (clean and with dust loading); and test duct setup (such as the diameter of the ASME flow nozzle and pressure drop of the outlet HEPA filter bank). Changes in flow rate through the particle counter sensor will directly change the particle count rate and lead to errors when computing the particle filtration efficiency values. Changes in flow rate may also influence the particle counter calibration.

In some cases, the influence of duct pressure can be significantly reduced by routing the exhaust of the particle counter back to the duct to equalize (or reduce) the differential pressure across the particle counter, by using a mass flow controller downstream of the particle counter's sensor, or by adding a controlled restriction in the exhaust line of the particle counter.

The viewed sample flow rate is that part of the sample stream that passes through the particle counter's sensor. In many particle counters, 100% of the sample flow flows through the sensor; in some counters and/or sampling systems, the viewed sample flow is a fraction of the total sampled flow (to allow isokinetic sampling, reduced residence time in sample line, etc.).

4.7 Test Apparatus for Dust Loading

4.7.1 The test apparatus and materials required by the dust loading procedure shall include the following:

- Dust feeder
- Dust injection tube
- Backup filter
- Backup filter duct section
- Loading dust
- Seals for the particle counter sampling probes
- Dust feeder venturi calibrator

4.7.2 The dust-feed tube leading from the dust feeder to the center of the dust mixing orifice shall discharge along the centerline of the mixing orifice that is located on the centerline of the test duct.

4.7.3 The general design of the dust feeder and its critical dimensions shall conform to Figures 4-4 and 4-5. Backflow through the pickup tube from the positive-pressure duct shall be prevented when the feeder is not in use¹¹.

4.7.4 The aspirator venturi dimensions shall be monitored periodically in accordance with Table 5-2 to ensure that the tolerances shown in Figure 4-5 are met¹².

4.7.5 The gage pressure on the air line to the venturi corresponding to an airflow rate out of the dust-feeder pipe of $6.8 \pm 0.2 \text{ dm}^3/\text{s}$ ($14.5 \pm 0.5 \text{ cfm}$) shall be measured periodically in accordance with Table 5-1. The required gage pressure on the ejector tube supply line necessary to provide this airflow at discharge duct pressures of 0, 500, 1000, 1500, 2000, and 2500 Pa (0, 2, 4, 6, 8, and 10 in. of water) above ambient pressure shall be determined using the test device shown in Figure 4-6. The compressed air supply shall be fitted with a filter-dryer system to provide clean, oil-free air with a dew point no higher than 1.7°C (35°F).

5. APPARATUS QUALIFICATION TESTING

5.1 Apparatus qualification tests shall verify quantitatively that the test rig and sampling procedures are capable of providing reliable particle size efficiency measurements. The tests shall be performed in accordance with Table 5-1.

Qualification tests shall be performed for the following:

- Air velocity uniformity in the test duct
- Aerosol uniformity in the test duct
- Downstream mixing of aerosol
- Overload tests of the particle counter
- 100% efficiency test
- Correlation ratio test
- Aerosol generator response time
- Duct leakage test
- Particle counter zero
- Particle counter sizing accuracy
- Radioactivity of the aerosol neutralizer
- Dust feeder airflow rate
- Final filter efficiency
- OPC documentation
- OPC flow-rate stability test

5.2 Velocity Uniformity in the Test Duct

5.2.1 The uniformity of the challenge air velocity across the duct cross section shall be determined by a nine-point traverse (Figure 5-1) in the $610 \times 610 \text{ mm}$ ($24 \times 24 \text{ in.}$) duct immediately upstream of the device section. The velocity

- This can be achieved by installing a full-port ball valve in the duct feed pipe between the venturi and the test duct.
- The thoroughness of dust dispersion by the feeder is dependent on the characteristics of the compressed air, the geometry of the aspirator assembly, and the rate of airflow through the aspirator. The aspirator venturi is subject to wear from the aspirated dust and will become enlarged with use.

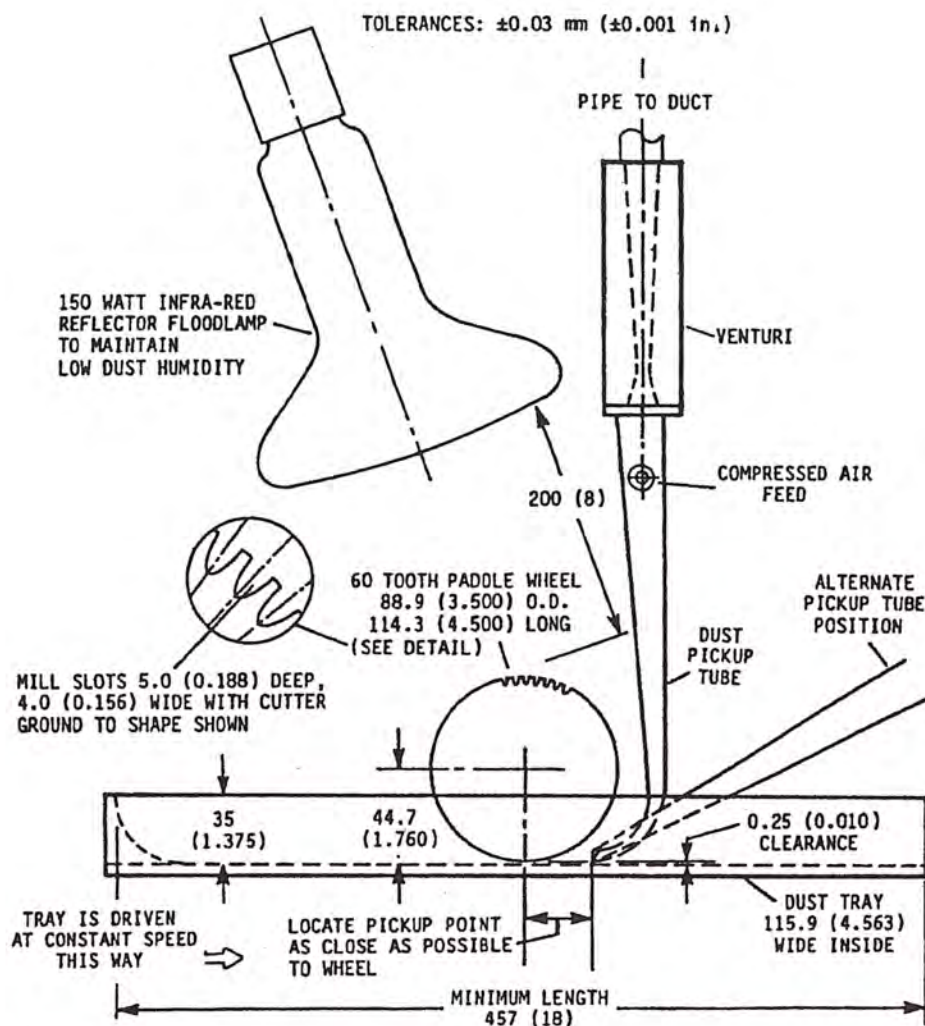


Figure 4-4 Critical dimensions of dust feeder assembly. Dimensions are in mm (in.).

measurements shall be made with an instrument having an accuracy of 10% with 0.05 m/s (approximately 10 fpm) resolution. The uniformity test shall be performed at airflow rates of 0.22, 0.93, and 1.4 m³/s (472, 1970, and 2990 cfm).

5.2.2 A one-minute average velocity shall be recorded at each grid point. The average must be based on at least ten readings taken at equal intervals during the one-minute period. The traverse shall then be repeated two more times to provide triplicate one-minute averages at each point for the given airflow rate. The average of the triplicate readings at each point shall be computed.

5.2.3 The CV (where CV is the coefficient of variation, computed as the standard deviation/mean) of the nine corresponding grid point air velocity values shall be less than 10% at each airflow rate¹³.

13. If the required degree of velocity uniformity is not achieved, confirm that the blower is providing a constant airflow rate by repeating sampling at the center-of-duct location and confirm that the upstream mixing orifice and baffle are properly centered. Changes may be required to the discretionary ductwork upstream of the upstream mixing orifice.

5.3 Aerosol Concentration Uniformity in the Test Duct

5.3.1 The uniformity of the challenge aerosol concentration across the duct cross section shall be determined by a nine-point traverse in the 610 × 610 mm (24 × 24 in.) duct immediately upstream of the device section (i.e., at the location of the upstream sample probe) using the grid points as shown in Figure 5-1. The traverse shall be made by either (a) installing nine sample probes of identical curvature, diameter, and inlet nozzle diameter but of variable vertical length or (b) repositioning a single probe. The inlet nozzle of the sample probes shall be sharp-edged and of appropriate entrance diameter to maintain isokinetic sampling within 10% at 0.93 m³/s (1970 cfm). The same inlet nozzle diameter shall be used at all airflow rates.

5.3.2 The aerosol concentration measurements shall be made with the particle counter meeting the specifications of Section 4.6. A one-minute sample shall be taken at each grid point with the aerosol generator operating. After sampling all nine points, the traverse shall be repeated four more times to provide a total of five samples from each point. The five values for each point shall then be averaged for each of the 12 particle

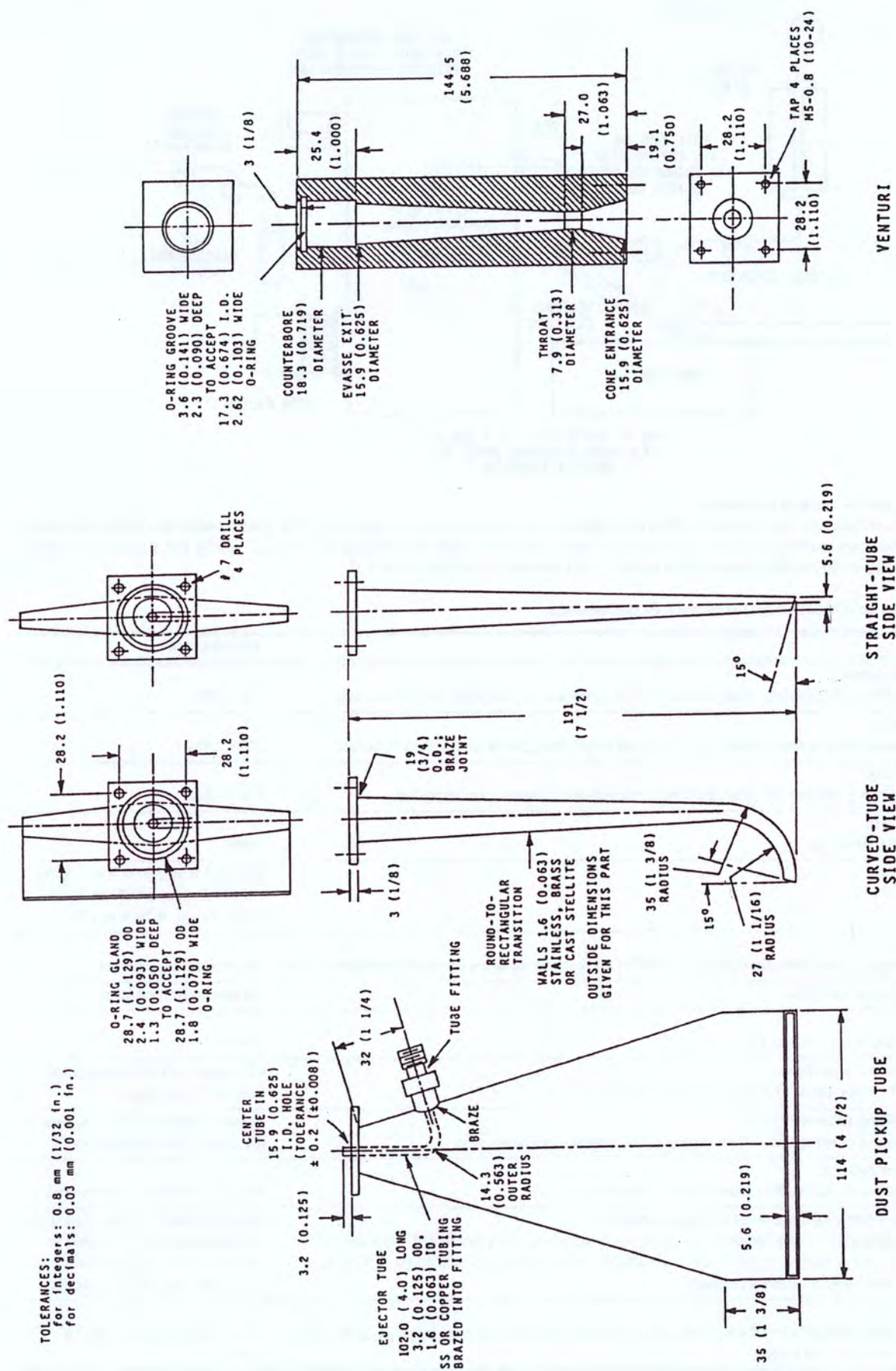


Figure 4-5 Dust feeder ejector/venturi and pickup tube details. Dimensions are in mm (in.).

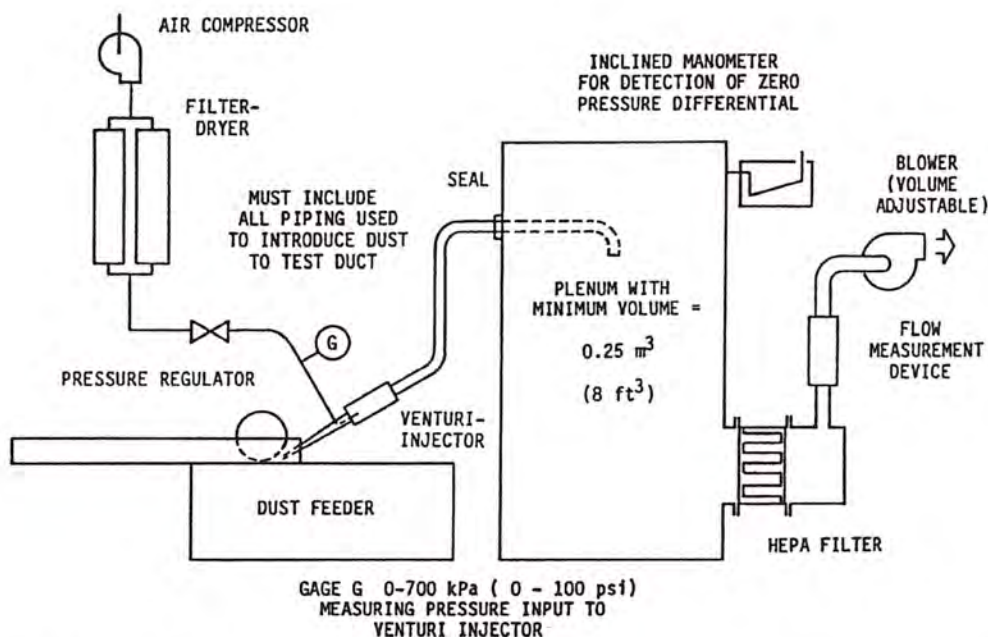


Figure 4-6 Dust feeder venturi calibrator.

Note: Gage G shall measure the pressure of the air supplied to the ejector tube supply line. This venturi calibrator shall be used to determine the pressure reading required to achieve air output from the dust feeder pipe of $6.8 \pm 0.2 \text{ dm}^3/\text{s}$ ($14.5 \pm 0.5 \text{ cfm}$) when there is zero pressure differential between the plenum and ambient. See Section 4.7.5.

Table 5-1 System Qualification Measurement Requirements

Parameter	Requirement
Air velocity uniformity: Based on traverse measurements made over a 9-point equal-area grid at each test airflow rate.	CV < 10%
Aerosol uniformity: Based on traverse measurements made over a 9-point equal-area grid at each test airflow rate.	CV < 15%
Downstream mixing: Based on a 9-point perimeter injection grid and center-of-duct downstream sampling.	CV < 10%
100% efficiency test: Based on HEPA filter test.	>99%
Correlation ratio test	0.30 to 1.0 μm : 0.90% to 1.10% 1.0 to 3.0 μm : 0.80% to 1.20% 3.0 to 10 μm : 0.70% to 1.30%
Upper concentration limit: Based on limiting the concentration to below the level corresponding to the onset of coincidence error.	No predetermined level.
Aerosol generator response time	No predetermined level.
Duct leakage: Ratio of leak rate to test airflow rate.	<1.0%
Particle counter zero count check: Based on HEPA filter attached to the instrument's inlet.	<10 counts per minute over the 0.30 to 10 μm range
Particle counter sizing accuracy check: Based on sampling of aerosolized monodisperse PSL spheres of known size.	Relative maximum must appear in the appropriate sizing channel.
Aerosol neutralizer activity: Based on detection of radioactive source within neutralizer.	Radioactivity must be detected.
Dust feeder airflow rate as a function of discharge pressure: Based on determination of gage pressure on ejector tube supply line to provide $6.8 \pm 0.2 \text{ dm}^3/\text{s}$ ($14.5 \pm 0.5 \text{ cfm}$) for discharge pressures of 0, 500, 1000, 1500, 2000, and 2500 Pa (0, 2, 4, 6, 8, and 10 in. of water) above ambient pressure.	No predetermined gage pressures. Gage pressures are recorded in order to set the proper flow rate during the dust feeder operation.
Final filter efficiency: Based on the difference between the quantity of dust injected and the quantity captured on the final filter with no test device in place.	$100 \pm 2 \text{ g}$ captured for 100 g injected.

Table 5-2 Apparatus Maintenance Schedule

Maintenance Item (Section Reference)	Incorporated Into Each Test	Monthly	Biannually	After Change that May Alter Performance	Comment
Correlation ratio measurement (5.8)	×				
Pressure drop across empty test section (5.16.2)	×				
Background particle count (10.3)	×				
Particle counter zero check (5.10)	×				
Particle counters accuracy check (5.11)	×				
Reference filter check (5.16.1)					Every two weeks
100% efficiency measurement (5.7)		×			
Particle counters primary calibration using PSL					Note 1
Air velocity uniformity (5.2)			×	×	
Aerosol uniformity (5.3)			×	×	
Downstream mixing (5.4)			×	×	
Generator response time (5.5)			×	×	
Overloading test of particle counters (5.6)			×	×	
Duct leak test (5.9)			×	×	
Confirmation of neutralizer radioactivity (5.12)			×	×	Note 5
Dust feeder airflow rate as a function of discharge pressure (5.13)			×	×	
Measurement of venturi dimensions for compliance with Figure 4-5				×	Every 500 hours of operation
Flow rates, pressure drops, temperature, relative humidity, etc.		Note 3			Note 2
Cleaning of test duct and components					Note 4

Notes:

1. Calibration performed annually.
2. In accordance with manufacturer's recommendations but at least annually.
3. Monthly visual inspection for proper installation and operation.
4. Cleaning intervals of the test duct, aerosol generator system, aerosol sampling lines, and other test components is discretionary.
5. Wash the inside of radioactive neutralizer every 100 hours of use. Check balance of the corona discharge ionizer monthly, per manufacturer's instructions.

counter size ranges. The traverse measurements shall be performed at airflow rates of 0.22, 0.93, and 1.4 m³/s (472, 1970, and 2990 cfm).

5.3.3 The CV of the corresponding nine grid point particle concentrations shall be less than 15% for each airflow rate in each of the 12 particle counter size ranges ¹⁴.

5.4 Downstream Mixing of Aerosol

5.4.1 A mixing test shall be performed to ensure that all aerosol that penetrates the air cleaner (media or frame) is detectable by the downstream sampler ¹⁵. The mixing test

14. If the required degree of aerosol uniformity is not achieved, confirm that the aerosol generator is providing a constant aerosol challenge by repeating sampling at the center-of-duct location. The aerosol injection tube may need to be repositioned and/or additional mixing baffles added to the discretionary ductwork upstream of the upstream mixing orifice.

shall be performed at airflow rates of 0.22, 0.93, and 1.4 m³/s (472, 1970, and 2990 cfm). The point of aerosol injection immediately downstream of the device section shall be traversed and the downstream sampling probe shall remain stationary in its normal center-of-duct sampling location.

5.4.2 A HEPA filter with face dimensions of 610 × 610 mm (24 × 24 in.) shall be installed to obtain smooth airflow at the outlet of the device section ¹⁶. An aerosol nebulizer shall nebulize a KCl/water solution (prepared using a ratio of 300 g of KCl to 1000 mL water) into an aerosol of primarily submicrometer sizes ¹⁷. A rigid extension tube with a length sufficient to reach each of the injection points shall be affixed to

15. For example, when testing a high-efficiency extended surface filter, it is important to know that the downstream probe will detect a leak in a corner of one of the pockets.
16. This represents a worst-case condition for aerosol mixing.

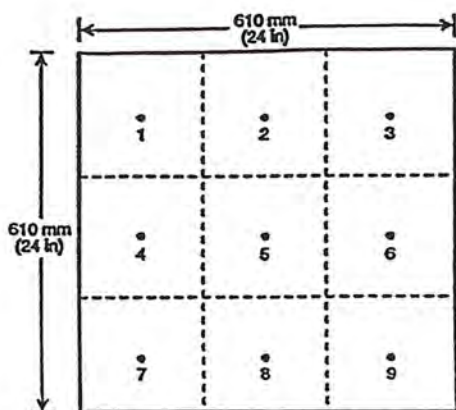


Figure 5-1 Sampling grid with nine equal-area points for measuring the uniformity of air velocity and aerosol dispersion.

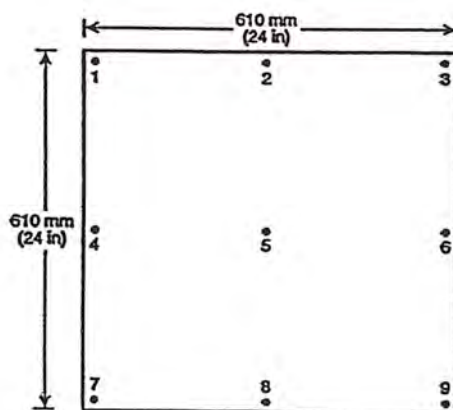


Figure 5-2 Injection grid with nine points to assess downstream mixing. Perimeter points are 25 mm (1 in.) from duct wall.

the nebulizer outlet. A 90 degree bend shall be placed at the outlet of the tube to allow injection of the aerosol in the direction of the airflow. The injection probe shall point downstream. The aerosol shall be injected immediately downstream (within 250 mm [10 in.]) of the HEPA filter at preselected points located around the perimeter of the test duct and at the center of the duct as indicated in Figure 5-2. The flow rate through the nebulizer and the diameter of the injection tube outlet shall be adjusted to provide an injection air velocity within $\pm 50\%$ of the mean duct velocity.

5.4.3 Sampling Sequence. A one-minute sample from the downstream probe shall be acquired with the nebulizer operating and the injection tube positioned at the first injection grid point. The injection point shall then be moved to the next grid-point location. A new one-minute sample shall be obtained after waiting at least 30 seconds. The procedure shall be repeated until all nine grid points have been sampled.

5.4.4 The aerosol injection traverse shall be repeated two more times to provide triplicate measurements at each grid point.

5.4.5 The downstream aerosol concentration shall be measured as total aerosol concentration $> 0.30 \mu\text{m}$ ¹⁸. The CV of the corresponding nine downstream grid-point particle concentrations shall be less than 10% for each airflow rate¹⁹.

5.5 Aerosol Generator Response Time

5.5.1 Measure the time interval for the aerosol concentration to go from background level to steady test level²⁰. The test shall be performed at an airflow rate of $0.93 \text{ m}^3/\text{s}$ (1970 cfm)

17. The nebulizer can be of any kind that produces a stable submicrometer aerosol. This nebulizer may be separate from the aerosol generator used to generate the 0.30 to $10 \mu\text{m}$ challenge aerosol for the efficiency test. A small hand-held nebulizer facilitates the traversing process.
18. The combination of (a) evaluating the downstream concentration as the total concentration $> 0.30 \mu\text{m}$ and (b) the use of a portable nebulizer greatly simplify and speed up the conduct of the test while maintaining the utility to detect inadequate downstream mixing.

with the particle counter sampling from the upstream probe. Similarly, measure the time interval for the aerosol to return to background level after turning off the generator.

5.5.2 Measure the time interval for the aerosol concentration to return to the background level after turning off the generator. These time intervals shall be used as the minimum waiting time between (a) activating the aerosol generator and beginning the particle counter sampling sequence and (b) deactivating the aerosol generator and beginning the particle counter sampling sequence for determination of background aerosol concentrations.

5.6 Concentration Limit of the Particle Counter²¹

5.6.1 A series of initial efficiency tests shall be performed over a range of challenge aerosol concentrations to determine a total concentration level for the PSE tests that does not overload the particle counters. The lowest total concentration level shall be less than 1% of the instrument's stated total concentration limit. The tests shall be performed following the procedures of Sections 10.1 through 10.6 on a media-type air cleaner using a range of upstream aerosol concentrations. The tests shall be performed at $0.93 \text{ m}^3/\text{s}$ (1970 cfm). The filters selected for this test shall have an initial efficiency in the range of 30% to 70% as measured by the 0.30 to $0.40 \mu\text{m}$ diameter size range and $> 90\%$ efficiency for the 7.0 to $10 \mu\text{m}$ diameter size range.

19. If the required degree of downstream aerosol mixing is not achieved, verify that the downstream mixing orifice and baffle are properly designed and centered. Confirm that the aerosol nebulizer is providing a stable output by injecting the aerosol at the center of the duct location while repeatedly sampling downstream. Improve the stability of the aerosol nebulizer if needed and repeat the downstream mixing test.
20. This is to ensure that sufficient time is allowed for the aerosol concentration to stabilize prior to beginning the upstream/downstream sampling sequence during the PSE tests.
21. Particle counters may underestimate particle concentrations if the concentration exceeds a certain level. Typically, errors due to overloading result in a lower air-cleaner efficiency due to underestimation of the challenge level because of coincidence error.

5.6.2 The aerosol for these tests shall be generated using the same system and procedures as specified in Section 10 for PSE tests.

5.6.3 The tests shall be performed over a sufficient range of total challenge concentrations to demonstrate that the particle counters are not overloaded at the intended test concentration²².

5.7 100% Efficiency Test and Development of Purge Time

5.7.1 An initial efficiency test shall be performed using a HEPA or ULPA filter as the test device to ensure that the test duct and sampling system are capable of providing a >99% efficiency measurement. The test procedures for determination of PSE given in Section 10 shall be followed, and the test shall be performed at an airflow rate of 0.93 m³/s (1970 cfm).

5.7.2 The computed PSE values shall be greater than 99% for all particle sizes²³.

5.7.3 One parameter affecting the efficiency during the 100% efficiency test is the purge time. The purge time is too short if, after switching from the upstream to the downstream line, residual particles from the upstream sample are counted during the downstream sampling and yield an efficiency of <99%. In this case, the purge time shall be increased and the 100% efficiency test repeated²⁴.

5.8 Correlation Test

5.8.1 A test shall be performed without a test device in place to check the adequacy of the overall duct, sampling, measurement, and aerosol generator.

5.8.2 The test procedures for determination of the correlation ratio given in Section 10.3 shall be followed²⁵.

5.8.3 The correlation ratio for each particle size shall meet the requirements specified in Table 5-1²⁶.

5.9 Test Duct Air Leakage Test

5.9.1 Air leakage from the test duct shall not exceed 1% of the total airflow rate.

5.9.2 The leak rate of the test duct shall be evaluated by a method similar to that delineated in ANSI/ASME Standard N510 (Reference 4). The test duct shall be sealed immediately upstream of the aerosol injection location and immedi-

ately upstream of the exhaust filter bank by bolting a gasketed solid plate to the duct opening or other appropriate means. Carefully meter air into the test duct until the lowest test pressure is achieved. The airflow rate required to maintain the pressure constant shall be measured and recorded as the leak rate, and the test shall then be repeated for the other two test pressures. The measured leak rates shall not exceed 1.0% of the corresponding test airflow rate.

5.9.3 To establish the pressure for the leak test, the pressure at the aerosol injection location shall be measured with the duct operating at airflow rates of 0.22, 0.93, and 1.4 m³/s (472, 1970, and 2990 cfm) without a test device installed. To determine the test pressures, add 250 Pa (1 in. of water) to the measured pressures to account for the added resistance of an air cleaner.

5.9.4 The highest pressure anticipated by this standard is 3200 Pa (13 in. of water). The user shall exercise caution and shall not pressurize the duct beyond its design limit for personal safety.

5.10 Particle Counters Zero. The zero count of the particle counters shall be verified to be <10 total counts per sample time used during testing in the 0.30 to 10 µm size range when operating with a HEPA filter attached directly to the instrument's inlet.

5.11 Particle Counters Sizing Accuracy. The sizing accuracy of the particle counters shall be checked by sampling an aerosol containing monodisperse polystyrene spheres of known size²⁷. A relative maximum particle count shall appear in the particle counter sizing channel that encompasses the PSL diameter.

5.12 Confirmation of the Activity of the Aerosol Neutralizer

5.12.1 The activity of the radiation source within the aerosol neutralizer shall be confirmed by use of an appropriate radiation detection device. The measurement may be relative (as opposed to absolute) but shall be adequate to indicate the presence of an active source and shall be capable of being performed in a repeatable manner.

5.12.2 The measurement shall be repeated annually and compared to prior measurements to determine if a substantial decrease in activity has occurred. Replace neutralizers showing a lack of activity in accordance with the manufacturer's recommendations²⁸.

5.12.3 The corona discharge level must be high enough to meet the same neutralizing level as from the radioactive source described in Section 4.3.2²⁹.

22. The measured filtration efficiencies should be equal over the concentration range where overloading is not significant. The measured filtration efficiency in the 0.30 to 0.40 µm diameter size range will often decrease as the concentration begins to overload the particle counter.
23. This test will assess the adequacy of the purge time interval provided between the sequential upstream-downstream concentration measurements. If the purge time is insufficient, residual particles from the relatively high concentration upstream sample will appear in the downstream sample.
24. Note that it is not necessary to define the absolute minimum purge time but rather to simply define a purge time that yields acceptable 100% efficiency tests.
25. A perfect system will yield correlation ratios of 1 at all particle sizes. Deviations from 1 can occur due to particle losses in the duct, differences in the degree of aerosol uniformity (i.e., mixing) at the upstream and downstream probes, and differences in particle transport efficiency in the upstream and downstream sample lines.

26. If the correlation ratio falls outside of the required specification at the smaller particle sizes (<1.0 µm), suspect incomplete mixing at the upstream probe location; the aerosol injection tube may need to be realigned or additional mixing provided in the discretionary ductwork upstream of the upstream orifice. If the small particles are within required limits but the larger particles are not, suspect unequal sample line losses. For dual particle-counter systems, also suspect that one of the counters may be out of calibration.

27. This is not a calibration but simply a calibration check of the particle counter.

28. For example, after one half life.

5.13 Dust Feeder Airflow Rate. Determine and record the gage pressure on the compressed air line to the venturi necessary to provide an airflow rate of $6.8 \pm 0.2 \text{ dm}^3/\text{s}$ ($14.5 \pm 0.5 \text{ cfm}$) for discharge pressures of 0, 500, 1000, 1500, 2000, and 2500 Pa (0, 2, 4, 6, 8, and 10 in. of water) above ambient pressure³⁰.

5.14 Final Filter Efficiency. Weigh the final filter to the nearest 0.1 g and install it in the test duct without the test device installed. The method specified in Section 10.7.3 shall be used to challenge the filter with 100 g of loading dust. Remove and weigh the filter. Its weight increase shall be within 2 g of 100 g.

5.15 OPC Documentation. Secure documentation from the particle counter manufacturer (or other source) that verifies that each specific particle counter requirement of Section 4.6 is being met.

5.16 OPC Flow Rate Stability Check

5.16.1 Install a flow restriction (such as an air filter or flow nozzle) in the test section of the test duct that will provide at least a 1000 Pa (4 in. of water) duct pressure difference between the upstream OPC sampling location and the downstream OPC sampling location when the duct is operated at a flow rate between 500 and 2000 cfm.

5.16.2 Operate the test duct at a flow rate that yields a 1000 Pa $\pm 10\%$ (4.0 in. of water $\pm 10\%$) pressure differential between the upstream and downstream OPC sample locations.

5.16.3 Measure the sampled flow rate of the OPC when sampling upstream and when sampling downstream. If dual counters are used, measure the flow rate of each OPC.

5.16.4 The particle counter's viewed sample flow rate must be the instrument's specified flow rate $\pm 5\%$.

5.16.5 The difference between the upstream and downstream viewed sample flow rates must not exceed 2%.

Informative Note to Sections 5.16.4 and 5.16.5: Corrective action, if needed, may be to route the exhaust of the particle counter back to the duct to equalize the differential pressure across the particle counter; using a mass flow controller downstream of the particle counter's sensor; or adding a controlled restriction in the exhaust line of the particle counter.

5.17 Summary of Qualification Test Requirements. Qualification test criteria shall conform to Table 5-1.

5.18 Apparatus Maintenance. Maintenance items and schedules shall conform to Table 5-2.

5.18.1 Reference Filter Check

5.18.1.1 For each test duct, a minimum of three identical reference filters shall be maintained by the testing facility solely for initial efficiency testing on a biweekly basis and shall not be exposed to dust loading. The three filters shall be labeled as "primary," "secondary," and "reserve." The primary filter shall be checked every two weeks. If the filtration effi-

ciency values shift by >5 percentage points for any of the 12 particle sizing channels, the secondary filter shall be tested³¹. If both the primary and secondary filters show shifts >5 percentage points for any of the 12 particle sizing channels, the particle counter shall be recalibrated or other system maintenance performed as needed (e.g., clean sample lines) to restore the reference filter efficiency test to a <5 percentage point shift. The reserve filter shall be used if either the primary or secondary filter becomes unusable (e.g., damaged).

5.18.1.2 The measured pressure drop across the reference filter shall be within 10% of the reference value. If the pressure drop deviates by more than 10%, system maintenance shall be performed to restore the pressure drop to within 10% of the reference value³².

5.18.1.3 The reference filter tests shall be performed at $0.93 \text{ m}^3/\text{s}$ (1970 cfm).

5.18.1.4 The filtration efficiency of the reference filters shall pass through 50% efficiency in the particle diameter range of 0.7 to 3.0 μm and be $<30\%$ efficiency at 0.30 to 0.40 μm and $>70\%$ efficiency in the 7.0 to 10.0 μm range³³.

5.18.1.5 Immediately after recalibration of the particle counters, retest each of the reference filters (or a new set of reference filters) to establish new filtration efficiency and pressure drop reference values.

5.18.1.6 When either the primary or secondary filter shows shifts >5 percentage points for any of the 12 particle size ranges and the secondary or reserve filter does not, the primary and/or secondary filter shall be replaced with an identical filter or filters, if available, or a new set of identical reference filters shall be obtained³⁴.

5.18.2 Pressure Drop Across Empty Test Section. The pressure drop across the empty test section shall be measured as part of each correlation test performed in accordance with Table 5-2. The measured pressure drop across the empty test section shall be less than 8 Pa (0.03 in. of water); system maintenance shall be performed until the pressure drop is below 8 Pa (0.03 in. of water).

6. TEST MATERIALS

6.1 Test Aerosol. The test aerosol shall be solid-phase potassium chloride (KCl) particles generated from an aqueous solution. The solution shall be prepared by dissolving reagent grade KCl in distilled water³⁵.

29. The neutralizing level may be checked using the reference filter test described in Section 5.16.1.

30. Gage pressures are used to set the proper flow rate during dust feeder operation.

31. *Percentage points* is not to be confused with *percent*. As an example, the difference between efficiency values of 30% and 35% is 5 percentage points, not 5%.

32. Examples of system maintenance steps that can be performed to restore the pressure drop include (but are not limited to) checking for leaks in the ducting and around the flow nozzle and checking the manometer for proper zero and level.

33. This is required because detecting shifts in the efficiency curves becomes difficult if the efficiency is either very high or very low for all particle sizes. Changes in the filtration efficiency of electret media reference filters may be due to reduced effectiveness of the neutralizer and its condition should then be checked.

34. A reference filter's efficiency may change with the collection of PSE test aerosol after repeated use.

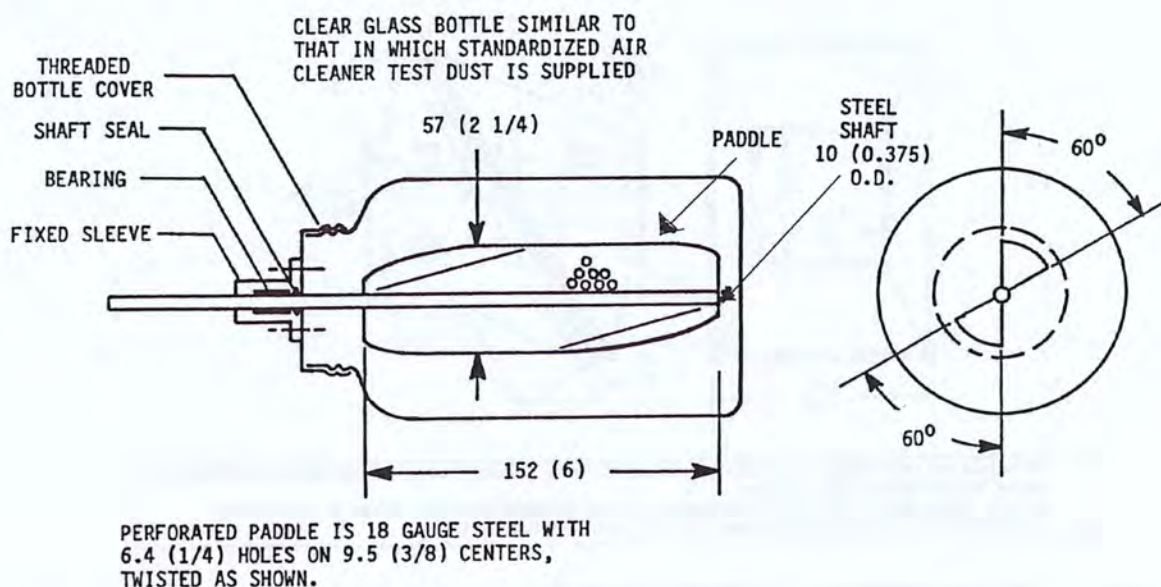


Figure 6-1 Allowable form of a loading dust blender. Dimensions are in mm (in.).

6.2 Loading Dust

6.2.1 The loading dust for testing the filtration device shall be composed, by weight, of 72% ISO 12103-1, A2 Fine Test Dust (Reference 5), 23% powdered carbon, and 5% milled cotton linters.

6.2.2 The powdered carbon shall be carbon black, with an ASTM D3765 (Reference 6) CTAB surface of $27 \pm 3 \text{ m}^2/\text{g}$, an ASTM D2414 (Reference 7) DBP adsorption of $0.68 \pm 0.7 \text{ cm}^3/\text{g}$, and an ASTM D3265 (Reference 8) tint strength of 43 ± 4 .

6.2.3 The cotton linters shall be second-cut linters removed from the cotton seed and ground in a Thomas Wiley Mill or equivalent revolving knife shearing type mill, fitted with a 4 mm screen classifier.

6.2.4 A typical 2000 g batch of test dust shall be mixed in a blender until homogeneous, as shown in Figure 6-1, or in a similar blending device as follows:

- Dry approximately 1500 g of ISO 12103-1, A2 Fine Test Dust at 104°C (220°F) for 30 minutes. Weigh $1440 \pm 1 \text{ g}$ of this dust and place in a clean blender.
- Dry approximately 600 g of the carbon powder at 104°C (220°F) for 30 minutes. Weigh $460 \pm 1 \text{ g}$ of this carbon powder and place in the blender. Mix dust and carbon powder for five minutes.
- Dry approximately 125 g of milled cotton linters in an oven at 82°C (180°F) for 30 minutes. Weigh $100 \pm 1 \text{ g}$ of these cotton linters. Sift approximately 20 g through a 14 mesh ASTM E437 (Reference 9) screen into the blender. Mix the dust-carbon powder-linter mixture for two minutes. Repeat the addition and blending of 20 g increments of linters and mixing until all 100 g of the linters and dust-powdered carbon are homogeneously blended.

35. A proportion of 300 g KCl to 1 L water is satisfactory.

6.3 Final Filter

6.3.1 Capture any test dust that passes through the test device during the dust-loading procedure in a final filter that shall be one of three different forms. In the first form, the filter shall be a flat sheet of filter media, clamped between sealing flanges and backed by a wire screen (see Figure 6-2). In the second form, the filter media shall be inserted in a holding frame in pleats that permit the use of more media than the duct cross section (see Figure 6-3). In the third form, a disposable cartridge filter shall be used (see Figure 6-4).

6.3.2 The final filter shall be capable of retaining 98% of the test dust used to load the test device. The design of the final filter and filter media shall be qualified by tests as specified in Section 5.14.

7. SELECTION AND PREPARATION OF THE TEST DEVICE

7.1 Selection Procedures

7.1.1 Devices for tests whose results reference this standard shall be selected in accordance with either Section 7.1.3 or Section 7.1.4.

7.1.2 These selection procedures shall not apply to developmental testing and the like when results are for in-house use only and not for external presentations.

7.1.3 The test sample shall be selected from a group of six or more like air cleaners taken from the manufacturer's assembly line or warehouse.

7.1.4 The test sample shall be procured on the open market by the testing laboratory.

7.2 Preparation of the Test Sample

7.2.1 The device to be tested shall be prepared in accordance with the manufacturer's recommendations.

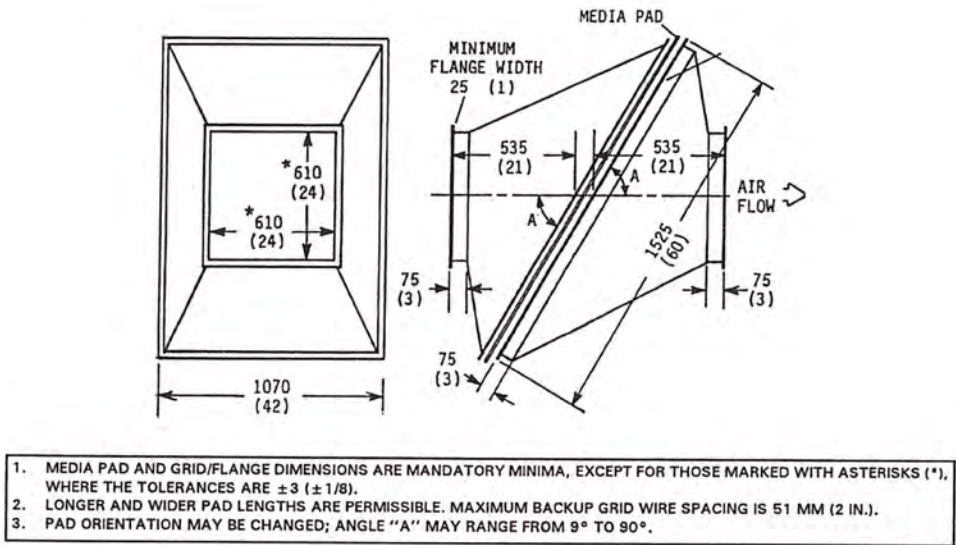


Figure 6-2 Final filter: flat sheet media form. Dimensions are in mm (in.).

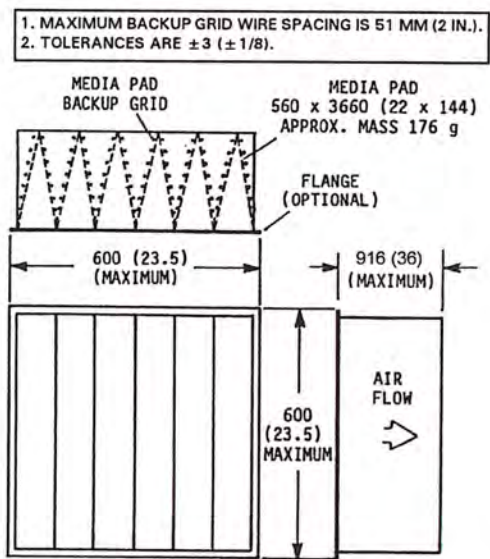


Figure 6-3 Final filter: pleated, replaceable media form. Dimensions are in mm (in.).

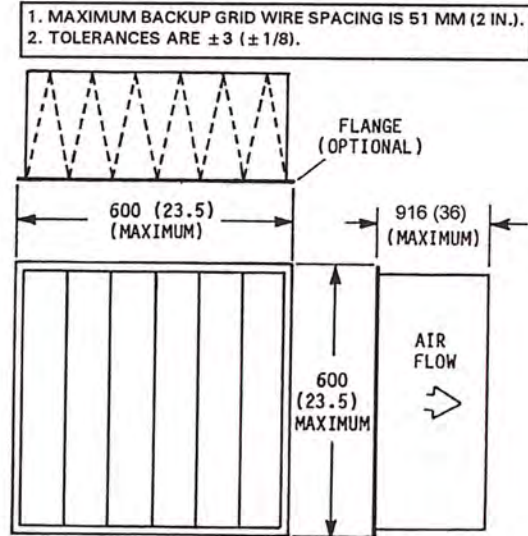


Figure 6-4 Final filter: cartridge form. Dimensions are in mm (in.).

7.2.2 The device shall be installed in the test duct so that the centerline of the airflow through the device coincides with the centerline of airflow through the duct.

7.2.3 Edge leakage and dust accumulation between the device and the test duct shall be minimized by sealing the device and its normal mounting frame to the test section on the upstream side.

8. TEST PROCEDURES

8.1 Airflow Rates for Tests. Tests shall be run and reports generated for an airflow rate as specified in either Section 8.1.1 or Section 8.1.2.

8.1.1 Airflow rates for tests conducted for MERV reporting purposes shall be at the upper limit of the test air cleaner's

application range. Also, they shall be calculated by first selecting one of the following face velocities in m/s (fpm) and then multiplying by the air cleaner's face area in m² (ft²):

0.60 (118)	2.50 (492)	1.25 (246)	3.20 (630)
1.50 (295)	3.80 (748)	1.90 (374)	

8.1.2 Test at an airflow rate corresponding to 2.50 m/s (492 fpm) if an air velocity has not been specified.

8.1.3 Test to a final resistance of 350 Pa (1.4 in. of water) if a final resistance has not been specified (otherwise test to the specified final resistance) or until the arresstance drops below 85% of the peak value, whichever comes first.

8.1.4 Adjust the airflow rate to maintain the selected face velocity when testing devices with other than 610 x 610 mm

(24 × 24 in.) face dimensions (see Section 4.2.7). Adjusted airflow rate is the product of the selected face velocity and the test device's face area.

8.2 Test Sequence. The sequence of tests on the device shall be as follows:

- Resistance vs. airflow rate of the clean device at various airflow rates as prescribed in Section 9.
- PSE of the clean device as prescribed in Section 10.
- PSE of the device when incrementally loaded with synthetic dust as prescribed in Section 10.

9. MEASUREMENT OF RESISTANCE VERSUS AIRFLOW

9.1 Install the device in the test duct.

9.2 Establish and record airflow rates measured by the flow nozzle. Refer to Figure 9-1. For the purposes of this standard, airflow rate shall be defined by the following equations³⁶:

$$Q = 1.1107 \times 10^{-6} CD^2 \{\Delta P / [\rho(1 - \beta^4)]\}^{0.5} \quad (\text{SI units})$$

$$Q = 5.9863 \times CD^2 \{\Delta P / (\rho[1 - \beta^4])\}^{0.5} \quad (\text{I-P units})$$

where

Q = test airflow rate, m³/s (cfm)

C = coefficient of discharge = $0.9975 - 6.53 \text{ Re}^{-0.5}$

D = nozzle throat diameter, mm (in.)

W = duct width, mm (in.)

β = D/W

ΔP = nozzle pressure drop, Pa (in. of water)

ρ = humid air density at nozzle inlet, kg/m³ (lb/ft³) (Refer to Figure 9-2 or calculate the value in accordance with Section 9 [Reference 11].)

μ = humid air dynamic viscosity; for the purposes of this standard, it is a constant: $1.817 \times 10^{-5} \text{ N}\cdot\text{s}/\text{m}^2$ ($1.22 \times 10^{-5} \text{ lb}_m/\text{ft}\cdot\text{s}$)

$\text{Re} = K\rho Q/\mu D = K_R \rho Q/D$, where $K_R = 5.504 \times 10^7$ (16,393)

9.3 The pressure drop across the nozzle shall be at least 100 Pa (0.4 in. of water) at the test airflow rate, and the nozzle position and static taps shall conform to Figure 4-1.

9.4 Measure and record the resistance of the device at a minimum of four airflow rates: 50%, 75%, 100%, and 125% of test airflow rate. Resistance shall be measured between the static taps.

10. DETERMINATION OF PARTICLE SIZE EFFICIENCY

This section describes the sampling sequence and data analysis procedures for sequential upstream-downstream sampling with one particle counter. For dual particle counter systems with simultaneous upstream-downstream sampling, the same procedures apply except (a) the purge times do not apply and (b) the upstream counts used in the data analysis are the observed, rather than the estimated, values. The data quality

requirements for single and dual particle counter systems are identical.

10.1 Symbols and Subscripts

10.1.1 Symbols

- U = upstream counts of each size range (or channel)
 D = downstream counts of each size range (or channel)
 R = correlation ratio
 P = penetration
 T = sampling time
 δ_g = standard deviation of a sample
 n = number of sample sets
 t = t distribution variable

10.1.2 Subscripts

- i = sample number
 o = observed
 c = correlation
 b = background
 t = testing an air cleaner
 u = upstream
 d = downstream
 e = estimated
 lcl = lower confidence limit
 ucl = upper confidence limit
 n = number of sample sets
 pc = particle counter

10.2 Test Sampling

10.2.1 The sampling pattern in Figure 10-1 illustrates one iteration of a sequential upstream-downstream sampling sequence. Sample counts in each size range shall be handled the same way, and this pattern shall be followed for all PSE tests. An initial upstream sample shall be followed by an upstream to downstream purge. Development of purge times is detailed in Section 5.7. The first downstream sampling shall be followed by a downstream to upstream purge and then shall be followed by another upstream sample. The last four time periods shall be repeated for as many sample sets as are required.

10.2.2 The calculations and data quality requirements of Sections 10.3 through 10.7 are performed separately for each of the 12 particle sizing ranges.

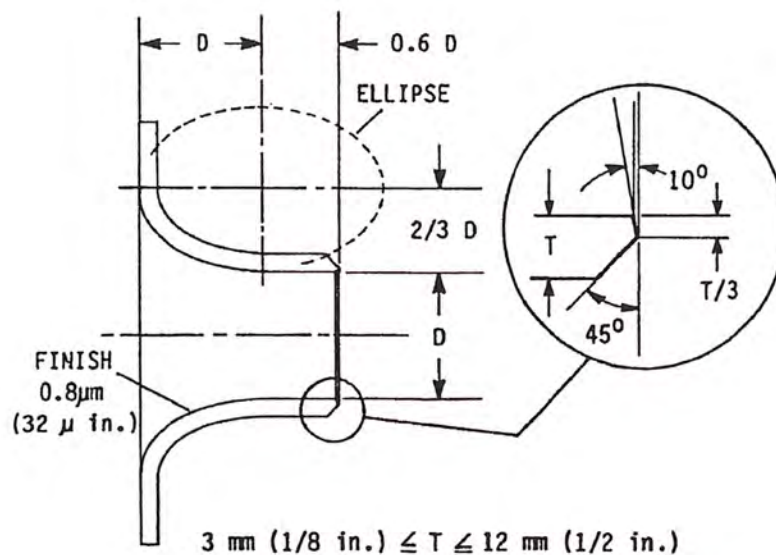
10.3 Correlation Ratio

10.3.1 The correlation ratio (R) shall be used to correct for any bias between the upstream and downstream sampling systems. The correlation ratio shall be established from the ratio of downstream to upstream particle counts without the test device installed in the test duct and before testing an air cleaner and shall be performed at the airflow rate of the air-cleaner PSE test. The general equation for the correlation ratio as used in this standard is

$$R = \frac{\text{Downstream particle concentration}}{\text{Upstream particle concentration}}$$

with the particle generator on but without a test device in place.

36. These expressions are derived from ASME Standard MFC-3M-1989 (Informative Appendix G, Reference 10).



D = Nozzle throat diameter, mm (in.)

T = Nozzle wall thickness, mm (in.)

Figure 9-1 ASME long-radius flow nozzle dimensions (Reference 6).

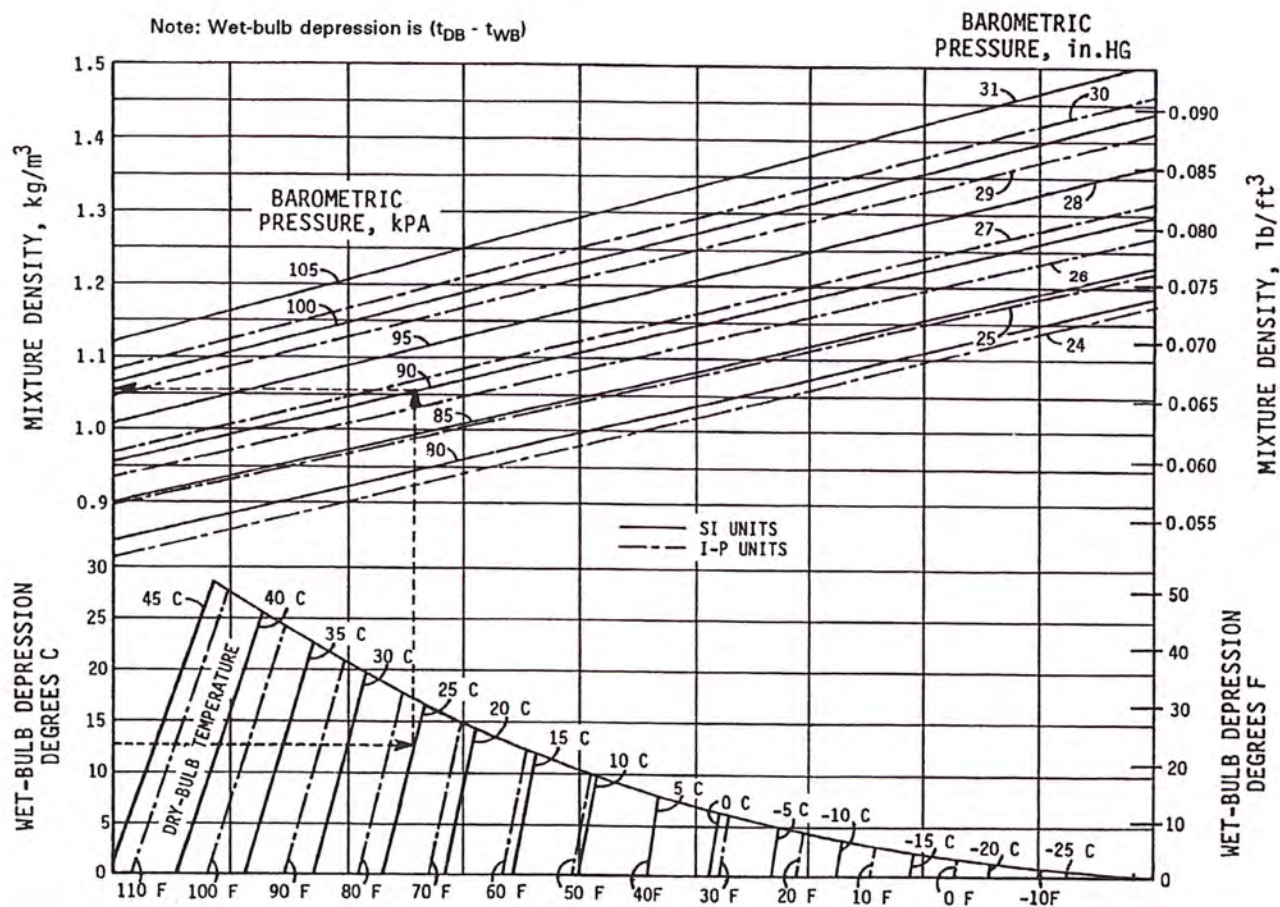


Figure 9-2 Humid air density chart. Barometric pressure as used in this chart is the absolute pressure at the nozzle inlet.

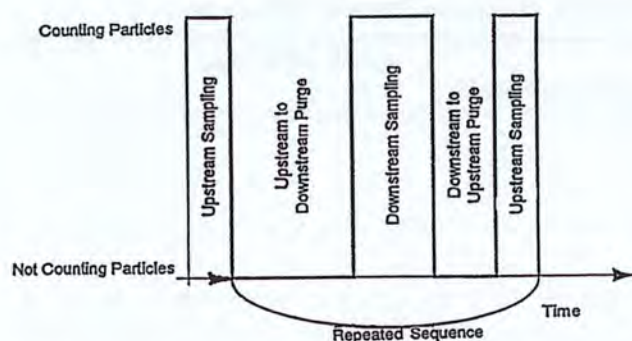


Figure 10-1 Sampling sequences.

10.3.2 Background counts shall be made before generating test aerosols. Upstream and downstream sampling shall be done sequentially, starting with an upstream sample $U_{1,o,b}$, followed by a downstream sample $D_{1,o,b}$, alternating back and forth. The total number of samples and sampling times shall be determined by the data quality requirements in Section 10.6.2, except that the final upstream sample is not needed for background sampling. Sampling times upstream and downstream shall be the same for this test.

10.3.3 Start generating aerosol when background counts are complete. Begin sampling after stabilization of the test aerosol, starting with an upstream sample $U_{1,o,c}$, followed by a downstream sample $D_{1,o,c}$. An additional upstream sample $U_{(n+1),o,c}$ shall be made following the last downstream sample $D_{n,o,c}$. The total number of samples and sampling times shall be determined by the data quality requirements in Section 10.6.2. Sampling times upstream and downstream shall be the same for this test.

10.3.4 Aerosol generation shall be turned off and background sampling shall be repeated after completion of the required correlation sampling sets.

10.3.5 The correlation ratio shall then be calculated in accordance with Section 10.6.1.

10.4 Penetration

10.4.1 The device shall be installed in the test section for determination of air-cleaner penetration. For the purposes of this standard, penetration P shall be the fraction of particles that pass through the air cleaner, and the general equation for penetration shall be

$$P = \frac{\text{Downstream particle concentration}}{\text{Upstream particle concentration}}$$

with the particle generator on and the test device in place.

10.4.2 Background counts shall be measured before generating test aerosols. Upstream and downstream sampling shall be done sequentially, starting with an upstream sample $U_{1,o,b}$, followed by a downstream sample $D_{1,o,b}$, alternating back and forth. The total number of samples and sample times shall be determined by the data quality requirements in Section 10.6.4, except that the final upstream sample is not needed for background sampling. A difference between upstream sampling time T_u and downstream sampling time T_d is allowable.

10.4.3 Start generating aerosol when background counts are complete. Start sampling with an upstream sample $U_{1,o,t}$, followed by a downstream sample $D_{1,o,t}$, after stabilization of the test aerosol. Take an additional upstream sample $U_{(n+1),o,t}$ following the last downstream sample $D_{n,o,t}$. Sampling times T_u and T_d shall be the same as those used for background sampling.

10.4.4 Aerosol generation shall be turned off and background sampling shall be repeated after completion of the required penetration sampling sets.

10.4.5 Air-cleaner penetration shall then be calculated in accordance with Section 10.6.3.

10.5 Efficiency

10.5.1 In this standard, the general equation for particle size removal efficiency³⁷ (PSE) shall be

$$\begin{aligned} \text{PSE} &= \left(1 - \frac{\text{Downstream particle concentration}}{\text{Upstream particle concentration}} \right) \times 100 \\ &= (1 - \bar{P}) \times 100 \end{aligned}$$

10.5.2 Air-cleaner efficiency shall be calculated in accordance with Section 10.6.5.

10.6 Data Reduction

10.6.1 Correlation Ratio Data Reduction

10.6.1.1 The upstream counts from two samples shall be averaged to obtain an estimate of the upstream counts that would have occurred at the same time as the downstream counts where taken³⁸.

$$U_{i,e,c} = \frac{U_{i,o,c} + U_{(i+1),o,c}}{2} \quad (10-1)$$

10.6.1.2 The background counts before and after the correlation aerosol test generation shall be simply averaged.

$$\bar{U}_b = \frac{\sum_{i=1 \rightarrow n} U_{i,o,b}}{n} \quad (10-2)$$

$$\bar{D}_b = \frac{\sum_{i=1 \rightarrow n} D_{i,o,b}}{n}$$

10.6.1.3 The correlation ratio shall be calculated for each upstream and downstream sample set using the observed downstream count, the estimated upstream count, the average downstream background count, and the average upstream background count.

$$R_i = \frac{D_{i,o,c} - \bar{D}_b}{U_{i,e,c} - \bar{U}_b} \quad (10-3)$$

37. PSE is the fraction of particles that is captured in the air cleaner.
38. For example,

$$U_{i,e,c} = \frac{U_{i,o,c} + U_{2,o,c}}{2}, \quad U_{2,e,c} = \frac{U_{2,o,c} + U_{3,o,c}}{2}$$

10.6.1.4 These correlation ratios shall be averaged to determine a final correlation ratio value.

$$\bar{R} = \frac{\sum_{i=1 \rightarrow n} R_i}{n} \quad (10-4)$$

10.6.1.5 The standard deviation of the correlation ratio shall be determined by

$$\delta_c = \sqrt{\frac{\sum_{i=1 \rightarrow n} (R_i - \bar{R})^2}{n-1}} \quad (10-5)$$

10.6.1.6 The standard deviation of the background counts shall be determined by

$$\delta_{u,b} = \sqrt{\frac{\sum_{i=1 \rightarrow n} (U_{i,o,b} - \bar{U}_b)^2}{n-1}} \quad (10-6)$$

$$\text{and } \delta_{d,b} = \sqrt{\frac{\sum_{i=1 \rightarrow n} (D_{i,o,b} - \bar{D}_b)^2}{n-1}}$$

10.6.1.7 The 95% confidence limits of the correlation value shall be determined by

$$\bar{R}_{lcl} = \bar{R} - \delta_c \times \frac{t}{\sqrt{n}} \quad (10-7)$$

$$\text{and } \bar{R}_{ucl} = \bar{R} + \delta_c \times \frac{t}{\sqrt{n}} \quad (10-8)$$

using the t distribution variable from Table 10-1 for a given n .

10.6.1.8 The 95% upper confidence limits of the background counts shall be determined by

$$\bar{U}_{b,ucl} = \bar{U}_b + \delta_{u,b} \times \frac{t}{\sqrt{n}} \quad (10-9)$$

$$\text{and } \bar{D}_{b,ucl} = \bar{D}_b + \delta_{d,b} \times \frac{t}{\sqrt{n}} \quad (10-10)$$

using the t distribution variable from Table 10-1 for a given n .

10.6.2 Correlation Ratio Data Acceptance Criteria

10.6.2.1 Correlation Ratio Error Limit. The number of correlation sample runs n shall be at least three and sufficient to satisfy the following conditions:

$$\delta_c \times \frac{t}{\sqrt{n}} \leq 0.05 \text{ for particle size ranges 1 through 8} \quad (10-11a)$$

$$\delta_c \times \frac{t}{\sqrt{n}} \leq 0.10 \text{ for particle size ranges 9 and 10} \quad (10-11b)$$

$$\delta_c \times \frac{t}{\sqrt{n}} \leq 0.15 \text{ for particle size ranges 11 and 12} \quad (10-11c)$$

This requirement shall be satisfied by calculating this expression after each sample set and halting the testing sequence when the requirement is reached for each size range,

Table 10-1 t Distribution Variable (Reference 12)

Number of Samples, n	Degrees of Freedom, $\nu = n - 1$	t
3	2	4.303
4	3	3.182
5	4	2.776
6	5	2.571
7	6	2.447
8	7	2.365
9	8	2.306
10	9	2.262
11	10	2.228
12	11	2.201
13	12	2.179
14	13	2.160
15	14	2.145
16	15	2.131
17	16	2.120
18	17	2.110
19	18	2.101
20	19	2.093
21	20	2.086
22	21	2.080
23	22	2.074
24	23	2.069
25	24	2.064
26	25	2.060
27	26	2.056
28	27	2.052
29	28	2.048
30	29	2.045
infinity	infinity	1.960

or by an acceptance criterion for a predetermined number of sample sets.

10.6.2.2 Limits on Magnitude of Correlation Ratio. The correlation ratio shall meet the requirements specified in Table 5-1.

10.6.2.3 Correlation Ratio Maximum Background Counts. The 95% upper confidence limit³⁹ of the upstream

39. This requirement establishes limits on background counts and the required number of background sample sets.

and downstream background counts shall be less than 5% of the average estimated upstream count when the particle generation is on.

$$\bar{D}_{b, ucl}, \bar{U}_{b, ucl} < \frac{\sum_{i=1 \rightarrow n} U_{i, e, c}}{n \times 20} \quad (10-12)$$

10.6.2.4 Correlation Ratio Minimum Average Upstream Counts. The sum of the estimated upstream counts shall be greater than or equal to 500. If a sufficient number of counts is not obtained, the sample time or aerosol concentration shall be increased. The aerosol concentration shall not exceed the concentration limit of the particle counters, as determined by Section 5.6.

$$\sum_{i=1 \rightarrow n} U_{i, e, c} \geq 500 \quad (10-13)$$

10.6.2.5 Viewed Sample Volume. The particle counter's viewed sample flow rate must be the instrument's specified flow rate $\pm 5\%$.

10.6.3 Penetration Data Reduction

10.6.3.1 The upstream counts from the first two samples shall be averaged to obtain an estimate of the upstream counts that would have occurred at the same time as the downstream counts where taken.

$$U_{i, e, t} = \frac{U_{i, o, t} + U_{(i+1), o, t}}{2} \quad (10-14)$$

10.6.3.2 The background counts before and after the penetration test shall be simply averaged.

$$\bar{U}_b = \frac{\sum_{i=1 \rightarrow n} U_{i, o, b}}{n}$$

$$\bar{D}_b = \frac{\sum_{i=1 \rightarrow n} D_{i, o, b}}{n} \quad (10-15)$$

where n is the number of background samples taken before and after the penetration test.

10.6.3.3 The observed penetration shall be calculated for each upstream and downstream set using the observed downstream count, the upstream count, the average downstream background count, the average upstream background count, the upstream sampling time, and the downstream sampling time.

$$P_{i, o} = \frac{D_{i, o, t} - \bar{D}_b}{U_{i, e, t} - \bar{U}_b} \times \frac{T_u}{T_d} \quad (10-16)$$

10.6.3.4 These observed penetrations shall be averaged to determine an average observed penetration value.

$$\bar{P}_o = \frac{\sum_{i=1 \rightarrow n} P_{i, o}}{n} \quad (10-17)$$

10.6.3.5 The standard deviation of the observed penetration shall be determined by

$$\delta_t = \sqrt{\frac{\sum_{i=1 \rightarrow n} (P_{i, o} - \bar{P}_o)^2}{n-1}} \quad (10-18)$$

10.6.3.6 The observed penetration shall be corrected by the correlation ratio to yield the final penetration.

$$\bar{P} = \frac{\bar{P}_o}{\bar{R}} \quad (10-19)$$

10.6.3.7 The standard deviation of the correlation ratio shall be combined with the standard deviation of the observed penetration to determine the total error by

$$\delta = \bar{P} \times \sqrt{\left(\frac{\delta_c}{\bar{R}}\right)^2 + \left(\frac{\delta_t}{\bar{P}_o}\right)^2} \quad (10-20)$$

10.6.3.8 The 95% confidence limits of the penetration shall be determined by

$$\bar{P}_{lcl} = \bar{P} - \delta \times \frac{t}{\sqrt{n}} \quad \text{and} \quad (10-21)$$

$$\bar{P}_{ucl} = \bar{P} + \delta \times \frac{t}{\sqrt{n}} \quad (10-22)$$

using the t distribution variable from Table 10-1 for a given n .

10.6.3.9 The standard deviation and 95% upper confidence limits for the background counts shall be determined using Equations 10-6, 10-9, and 10-10.

10.6.4 Penetration Data Acceptance Criteria

10.6.4.1 Penetration Error Limit. The number of sample runs n shall be at least three and sufficient to satisfy the following condition:

$$\delta \times \frac{t}{\sqrt{n}} \leq 0.07 \times \bar{P} \text{ or } \leq 0.05,$$

whichever is greater, for particle size ranges 1 through 8; (10-23a)

$$\delta \times \frac{t}{\sqrt{n}} \leq 0.15 \times \bar{P} \text{ or } \leq 0.05,$$

whichever is greater, for particle size ranges 9 and 10; (10-23b)

$$\delta \times \frac{t}{\sqrt{n}} \leq 0.20 \times \bar{P} \text{ or } \leq 0.05,$$

whichever is greater, for particle size ranges 11 and 12. (10-23c)

The requirement shall be satisfied by calculating this expression after each sample set and halting the testing sequence when the requirement is reached for each size range or by an acceptance criteria for a predetermined number of sample sets.

If the above condition cannot be met, the upper confidence limit for penetration (\bar{P}_{ucl}) shall be used to calculate efficiency for that size range.

10.6.4.2 Penetration Maximum Background Counts.

For correlation tests and tests before dust loading, the 95% upper confidence limits of the upstream and downstream background counts shall be less than 5% of the average estimated upstream count when the particle generation is ON.

$$\bar{D}_{b, ucl}, \bar{U}_{b, ucl} < \frac{\sum_{i=1 \rightarrow n} U_{i, e, t}}{n \times 20} \quad (10-24)$$

10.6.4.3 Penetration Minimum Upstream Counts. The sum of the estimated upstream counts shall be greater than or equal to 500.

$$\sum_{i=1 \rightarrow n} U_{i, e, t} \geq 500 \quad (10-25)$$

10.6.5 Efficiency. Particle size removal efficiency PSE is determined by

$$PSE = (1 - \bar{P}) \times 100 \quad (10-26)$$

10.7 Test Program for Dust-Loading and Particle Size Efficiency

10.7.1 Test Procedure

10.7.1.1 The test airflow rate shall be selected in accordance with Section 8.1. The final resistance shall be chosen equal to or greater than twice the initial resistance.

10.7.1.2 Particle size efficiency measurements shall be performed at intervals during the dust-loading procedure to establish a curve of efficiency as a function of dust loading. Efficiency curves shall be drawn for any or all of the particle size ranges of the test protocol. Efficiency measurements shall be made at the following points during the dust-loading procedure:

- Before any dust is fed to the device.
- After an initial conditioning step with a dust loading of 30 g or an increase of 10 Pa (0.04 in. of water) pressure drop across the device, whichever comes first⁴⁰.
- After the dust-loading increments have achieved an airflow resistance increase of one-quarter, one-half, and three-quarters of the difference between the beginning and the prescribed end-point limit of airflow resistance.
- After the dust increment that loads the device to its prescribed end point resistance limit.

10.7.2 Dust-Loading Procedure

10.7.2.1 Weigh the final filter to the nearest 0.1 g.

10.7.2.2 The test duct shall be in the dust-loading configuration with the final filter installed. The dust feeder shall be positioned so that the feeder nozzle is centered in the inlet mixing orifice and the nozzle tip is in the same plane as the orifice. All airflow in the particle sampling lines shall be turned off and their inlets sealed to prevent the entry of loading dust.

10.7.2.3 Weigh the quantity of dust to ± 0.1 g for one increment of loading.

10.7.2.4 Distribute the dust uniformly in the dust feeder tray. Dust shall be distributed with a depth that will provide a dust concentration in the test of 70 ± 7 mg/m³ (2.0 ± 0.2 g/1000 ft³).⁴¹

10.7.2.5 Start the test duct blower and adjust to the test airflow rate for the test device.

10.7.2.6 Turn on the dust feeder heater lamp. Adjust the air pressure regulator on the dust feeder to give the required dust feeder venturi airflow rate, 0.0068 ± 0.0002 m³/s (14.5 ± 0.5 cfm). This condition shall be maintained throughout the feed period. Start the dust feeder tray drive.

10.7.2.7 Maintain the test duct airflow rate at the test flow $\pm 2\%$. After the feeder tray motion is complete, brush dust remaining in the feeder tray into the aspirator. Vibrate or rap the dust feeder tube for 30 seconds.

10.7.2.8 Turn off the feeder tray drive and the airflow to the aspirator venturi. With the test duct airflow on, reentrain any test dust in the duct upstream of the test device by use of a compressed air jet directed obliquely away from the device. Record the airflow resistance of the test device.

10.7.2.9 If several dust increments are required to achieve one quarter of the required flow resistance increase of the device, repeat the steps of Sections 10.7.2.3 through 10.7.2.8. A complete dust increment shall be fed before running the next PSE test.

10.7.2.10 Stop the test duct airflow and remove the final filter from the test duct, taking care to avoid spilling dust from the final filter. Weigh the final filter to the nearest 0.1 g.

10.7.2.11 Collect any test dust deposited in the test duct between the test filter device and the final filter. Weigh the collected dust to the nearest 0.1 g.

10.7.2.12 Add the weight of dust collected in the procedure of Section 10.7.11 to the weight increase of the final filter to establish the amount of synthetic dust passing the device during the feed period.

10.7.2.13 For air-cleaning devices with efficiencies less than 20% in the size range of 3.0 to 10.0 μ m, calculate the arrestance A_i for dust loading increment i as follows:

$$A_i = 100(1 - W_d/W_u) \quad (10-27)$$

where

A_i = arrestance for dust loading increment i

W_d = weight of synthetic loading dust passing the device

W_u = weight of dust fed

10.7.2.14 For all devices, calculate dust holding capacity (DHC) for dust loading increment i as follows:

$$DHC_i = W_u - W_d \quad (10-28)$$

where

DHC_i = dust holding capacity for dust loading increment i

41. In cases of small dust increments or high airflows, the full length of the feeder tray may not be needed.

40. See Foreword and Informative Appendix A, Section A2.2.

W_d = weight of synthetic loading dust passing the device

W_u = weight of dust fed

10.7.3 Release Rate

10.7.3.1 Airflow shall be maintained through the device for 20 minutes. Immediately after this 20 minute period, with the airflow on and the aerosol generator OFF, use the aerosol particle counter to collect downstream particle counts over a period of ten minutes. During this time, at least three samples shall be taken. Calculate the 95% upper confidence limits of the background counts for these values using Equation 10-10.

10.7.3.2 The release rate is computed as follows:

$$\text{Release rate (\%)} = \frac{D_{b, ucl}}{\sum_{i=1-n} U_{i, o, u}} \left(\frac{T_u}{T_d} \right) 100 \quad (10-29)$$

where the release rate⁴² is expressed in #/m³, the 95% upper confidence limit is the value calculated in Section 10.7.3.1, and the V_{pc} is equal to the volumetric flow rate of the particle counter, which is multiplied by the sample time of a single count.

10.7.3.3 These values shall be reported for each dust increment and size range. If a dilutor is used in sampling, the counts must be corrected by the dilution factor to reflect the actual in-duct undiluted downstream count.

10.7.3.4 The efficiency of the air cleaner in a specific size range shall be reported as 0% if during a test run for PSE in that range the PSE is negative.

10.8 Reporting Results of Loading Tests

10.8.1 Results of loading tests shall be reported in the form of PSE curves for the test device:

- Clean
- After each incremental dust loading, a total of four curves
- At its final loading point

10.8.2 Develop a composite minimum efficiency curve by plotting the minimum PSE in each of the 12 size ranges shown on the plots of each of the six curves from Section 10.8.1.

10.8.3 The four data points from the Section 10.8.2 composite curve in each of the three size range groups from Table 10-2 shall be averaged and the resultant three average minimum PSEs E_1 , E_2 , and E_3 shall be reported.

10.8.4 For air-cleaning devices with efficiencies less than 20% in the size range of 3.0 to 10.0 μm , calculate the average arrestance A_{avg} as follows:

42. Optical particle counters are likely to be used to obtain this measure of release rate. Because of the optical properties of the shed dust particles (light absorbing and irregular shape), the sizing of the shed particles as measured by an optical particle counter may be significantly different from their actual physical size. When comparing release rate results, the best comparison will be when the same particle counter is used in all measurements.

Table 10-2 Size Range Groups

Average Minimum PSE Designator	Corresponding Size Range Group, μm
E_1	0.30 to 1.0
E_2	1.0 to 3.0
E_3	3.0 to 10

$$A_{avg} = [1/W] \sum_{i=1}^f [W_i A_i] (\text{percent}) \quad (10-30)$$

where

W = total weight of dust fed, g

W_i = weight of dust fed during loading increment i , g

A_i = arrestance measured during loading increment i , %

f = final loading increment

10.8.5 For all devices, calculate DHC as

$$\text{DHC} = \sum_{i=1}^f \text{DHC}_i \text{ (grams)} \quad (10-31)$$

where

DHC_i = dust holding capacity for loading increment i

f = final loading increment

10.8.6 Test results shall be reported in accordance with Section 11, and the air cleaner's MERV shall be determined in accordance with Section 12.

11. REPORTING RESULTS

11.1 Test results shall be reported using the test report format shown in this standard. Figures 11-1a through 11-1e comprise the complete test report and are examples of acceptable forms. Exact formats are not required, but the report shall include the items shown.

11.2 The summary section of the performance report shall include the following information:

- Name and location of the test laboratory
- Date of the test
- Test operator's names
- Brand and model number of the particle counting and sizing devices
- Air-cleaner manufacturer's name (or name of the marketing organization, if different from the manufacturer)
- How the sample was obtained
- Description of the test air cleaner, including the following:
 - Brand and model number
 - Physical description of construction (e.g., extended surface—number of pockets or number of pleats; pleated panel—number and depth of pleats)
 - Face dimensions and depth
 - For fiber media air cleaners:
 - Type and color of media
 - Effective media area
 - Type and amount of dust adhesive, if known
 - Electrostatic charge, if known
 - Any other pertinent descriptive attributes

- h. Operating data as stated by the manufacturer
 - 1. Test conditions for reporting purposes: airflow rate and final resistance
 - 2. Initial and final resistances
 - 3. Any other operating data furnished
- i. Test data
 - 1. Test air temperature and relative humidity
 - 2. Airflow rate
 - 3. Type of test aerosol
- j. Results of resistance testing
 - 1. Initial resistance
 - 2. Final resistance
- k. Performance curves
 - 1. A curve in Figure 11-1b format of air-cleaner resistance when clean vs. airflow rates from 50% to 125% of test flow
 - 2. A curve in Figure 11-1c format of PSE for the clean device and for the device at each of the five loading stages
 - 3. A minimum PSE composite curve in Figure 11-1c format whose data points are the lowest PSEs from the six measurements in each particle size range from the curves of test results (Item k[2] above)
 - 4. Resistance vs. synthetic loading dust fed (for air-cleaning devices with efficiencies less than 20% in the size range of 3.0 to 10.0 μm)
- l. Minimum efficiency reporting value (MERV)
 - 1. The average of the minimum PSE of the four size ranges from 0.30 to 1.0 μm (E_1)
 - 2. The average of the minimum PSE of the four size ranges from 1.0 to 3.0 μm (E_2)
 - 3. The average of the minimum PSE of the four size ranges from 3.0 to 10.0 μm (E_3)
 - 4. MERV for the device
- m. Release rate
 - 1. A data table including the information in Figure 11-1d shall be included
- n. Average ASHRAE dust arrestance (for air-cleaning devices with efficiencies less than 20% in the size range of 3.0 to 10.0 μm)
- o. Dust holding capacity (DHC)

11.3 Inclusion of test data in the summary report is required. The reported data shall consist of all data recorded during the six test runs and shall be formatted similarly to Figure 11-1e.

12. MINIMUM EFFICIENCY REPORTING VALUE (MERV) FOR AIR CLEANERS

12.1 The minimum efficiency reporting value (MERV) for an air cleaner shall be based on three composite average PSE points developed from tests at the manufacturer's specified airflow rate selected in accordance with Section 8.1. Dust loading shall follow the procedure outlined in Section 10.7,

and results of the tests shall be reported in accordance with Section 10.8.

12.2 The minimum final resistance for an air cleaner shall be the same as or greater than twice the initial resistance.

12.3 The minimum efficiency reporting value in the specified size ranges and final resistance for reporting purposes shall be in accordance with Table 12-1. Air cleaners with MERV1 to MERV4 (i.e., devices with efficiencies less than 20% in the size range of 3.0 to 10.0 μm) shall also be tested in accordance with the dust-loading procedure outlined in Section 10.7.2 of this standard before using this system for reporting.

12.4 The reporting designator shall be a combination of the air cleaner's MERV and the test airflow rate (e.g., MERV10 at 0.93 indicates that the air cleaner has a MERV10 when tested at 0.93 m^3/s [1970 cfm]).

12.5 The classification term "MERV" shall only be used in the performance report and product labeling if the entire procedure prescribed by the standard has been included.

13. NORMATIVE REFERENCES

1. See informative reference list in Informative Appendix G.
2. ASME. 1972. ASME PTC (Performance Test Code) 19.5-72 Application, Part II of Fluid Meters, Sixth Edition 1971, *Interim Supplement on Instruments and Apparatus*. New York: American Society of Mechanical Engineers.
3. See informative reference list in Informative Appendix G.
4. ASME. 1989. ANSI/ASME N510, *Testing of Nuclear Air Treatment Systems*. New York: American Society of Mechanical Engineers.
5. ISO. n/d. ISO 12103-1, *A2 Fine Test Dust for Filter Evaluation, Part A, Arizona Test Dust*. Geneva, Switzerland: International Standards Organization.
6. ASTM. 1995. ASTM Standard D3765, *Test Method for Carbon Black CTAB Surface Area*. Philadelphia, PA: American Society for Testing and Materials.
7. ASTM. 1996. ASTM Standard D2414, *Test Method for Carbon Black Dibutyl Phthalate Adsorption Number*. Philadelphia, PA: American Society for Testing and Materials.
8. ASTM. 1995. ASTM Standard D3265, *Test Method for Carbon Black Tint Strength*. Philadelphia, PA: American Society for Testing and Materials.
9. ASTM. 1992. ASTM Standard E437, *Industrial Wire Cloth and Screens (Square Opening Series)*. Philadelphia, PA: American Society for Testing and Materials.
10. See informative reference list in Informative Appendix G.
11. ASHRAE. 1985. ANSI/ASHRAE Standard 51 (AMCA Standard 210-85), *Laboratory Method for Testing Fans for Rating*. Atlanta: ASHRAE.
12. CRC. 1993. *CRC Handbook of Tables for Probability and Statistics*, W.H. Beyer, Ed. Cleveland, OH: CRC Press.

Page 1 of ____
ASHRAE Std. 52.2 Air Cleaner Performance Report Summary (This report applies to the tested device only)
Laboratory Data
Report No. _____ Test No. _____ Date _____
Test laboratory _____
Operator _____ Supervisor _____
Particle counter(s): Brand _____ Model _____
Device Manufacturer's Data
Manufacturer _____
Product name _____ Model _____
Test requested by _____
Sample obtained from _____
Catalog rating: Airflow rate _____ Initial press. drop _____
Specified test conditions: Airflow rate _____
Final pressure drop _____ Face velocity _____
Device Description
Dimensions: height _____ width _____ depth _____
Generic name _____ Media type _____
Effective media area _____ Media color _____
Amount and type of adhesive _____
Other attributes _____
Test Conditions
Airflow rate _____ Temperature _____ RH _____
Test aerosol type _____
Final pressure drop _____ Face velocity _____
Remarks _____
Resistance Test Results
Initial resistance _____ Final resistance _____
Minimum Efficiency Reporting Data
Composite average efficiencies E ₁ _____ E ₂ _____ E ₃ _____
Air cleaner average Arrestance per Std. 52.1 _____
Minimum efficiency reporting value (MERV) for the device: _____

Figure 11-1a Typical air-cleaner performance report summary.

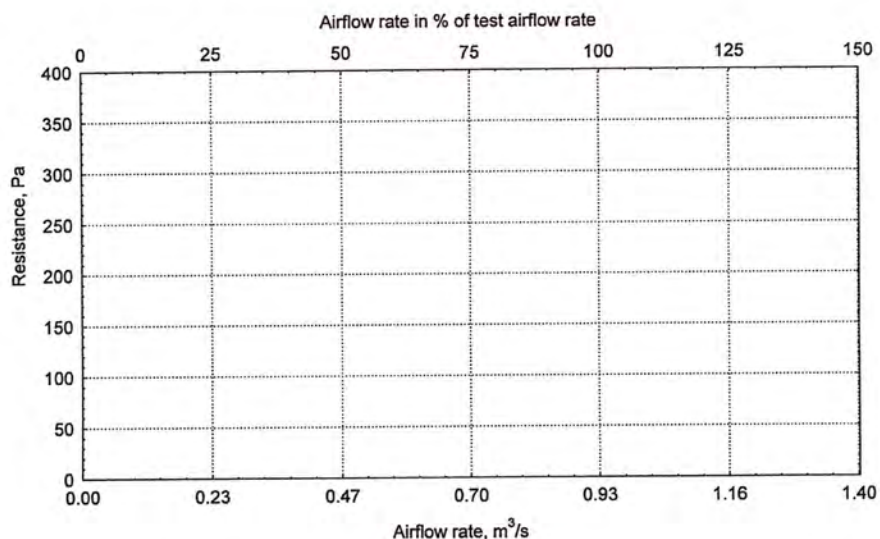


Figure 11-1b Airflow rate vs. resistance of clean device. Illustration is for an air cleaner with a test airflow rate of 0.93 m^3/s (1970 cfm).

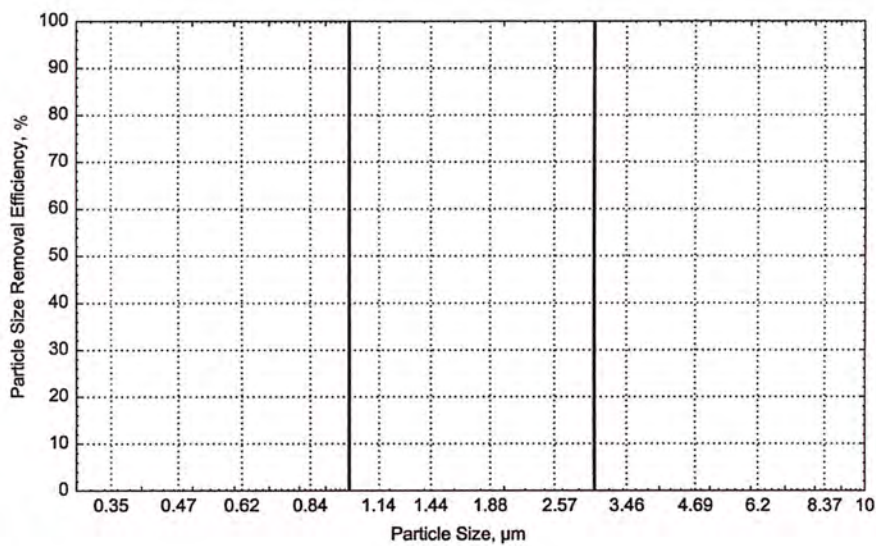


Figure 11-1c Particle size vs. efficiency.

Test Data for Release Rate						
Size Range No.	Geometric Mean of Particle Size Range, μm	Release Rate After Loading Stage 1	Release Rate After Loading Stage 2	Release Rate After Loading Stage 3	Release Rate After Loading Stage 4	Release Rate After Loading Stage 5
1	0.35					
2	0.47					
3	0.62					
4	0.84					
5	1.14					
6	1.44					
7	1.88					
8	2.57					
9	3.46					
10	4.69					
11	6.20					
12	8.37					

Figure 11-1d Release rate data report form.

Test Data for <input type="checkbox"/> Clean Device <input type="checkbox"/> Loading Stage Number _____		
Size Range No.	Geometric Mean of Particle Size Range, μm	Calculated Particle Size Efficiency, %
1	0.35	
2	0.47	
3	0.62	
4	0.84	
5	1.14	
6	1.44	
7	1.88	
8	2.57	
9	3.46	
10	4.69	
11	6.20	
12	8.37	

Figure 11-1e Test data report form.

Table 12-1 Minimum Efficiency Reporting Value (MERV) Parameters

Standard 52.2 Minimum Efficiency Reporting Value (MERV)	Composite Average Particle Size Efficiency, % in Size Range, μm			Average Arrestance, %
	Range 1 0.30 to 1.0	Range 2 1.0 to 3.0	Range 3 3.0 to 10.0	
1	N/A	N/A	$E_3 < 20$	$A_{avg} < 65$
2	N/A	N/A	$E_3 < 20$	$65 \leq A_{avg}$
3	N/A	N/A	$E_3 < 20$	$70 \leq A_{avg}$
4	N/A	N/A	$E_3 < 20$	$75 \leq A_{avg}$
5	N/A	N/A	$20 \leq E_3$	N/A
6	N/A	N/A	$35 \leq E_3$	N/A
7	N/A	N/A	$50 \leq E_3$	N/A
8	N/A	$20 \leq E_2$	$70 \leq E_3$	N/A
9	N/A	$35 \leq E_2$	$75 \leq E_3$	N/A
10	N/A	$50 \leq E_2$	$80 \leq E_3$	N/A
11	$20 \leq E_1$	$65 \leq E_2$	$85 \leq E_3$	N/A
12	$35 \leq E_1$	$80 \leq E_2$	$90 \leq E_3$	N/A
13	$50 \leq E_1$	$85 \leq E_2$	$90 \leq E_3$	N/A
14	$75 \leq E_1$	$90 \leq E_2$	$95 \leq E_3$	N/A
15	$85 \leq E_1$	$90 \leq E_2$	$95 \leq E_3$	N/A
16	$95 \leq E_1$	$95 \leq E_2$	$95 \leq E_3$	N/A

(This appendix is not part of this standard. It is merely informative and does not contain requirements necessary for conformance to the standard. It has not been processed according to the ANSI requirements for a standard and may contain material that has not been subject to public review or a consensus process. Unresolved objections on informative material are not offered the right to appeal at ASHRAE or ANSI.)

INFORMATIVE APPENDIX A COMMENTARY

This appendix includes commentary by the project committee. Comments on some of the more important questions that were posed during the writing of this standard relate to the bend in the test duct; the use of a particle's physical size, its aerodynamic size, or its white light-scattering size; dust loading and minimum efficiency reporting; the particle size range covered by the standard; the selection of the test aerosol; and round-robin testing.

A1. BEND IN THE TEST DUCT

The test duct may be constructed with a 180 degree bend downstream of the test device. The bend serves the following purposes:

- a. It brings the downstream sample location relatively close to the upstream location, allowing short sample lines to the particle counter. Because of the physical dimensions and airflow rates involved, particle losses will generally be relatively low per unit length in the test duct and relatively high in sample lines. The bend and additional duct length provide shorter sample line length, reducing overall particle loss.
- b. It reduces the overall length of the test duct, facilitating its placement within the test room.

A2. DUST LOADING AND MINIMUM EFFICIENCY REPORTING

A2.1 Final resistance from Table 12-1 and dust loading to achieve that final resistance are simply means to identify where the air cleaner's minimum efficiency occurs. They are not intended as recommendations for use or to give any indication of actual service life. Some air cleaners have their lowest efficiency when they are clean (e.g., dry media filters); others have their highest efficiency when they are clean and drop steadily as they are loaded (e.g., electronic air cleaners). Some may drop in efficiency as they begin to be loaded (e.g., electret media) and some start low and then rise in efficiency as they are loaded but may shed dust at the end (e.g., viscous impingement filters).

A2.1.1 Electrostatic Phenomenon Considerations. The test dust and loading procedure specified herein may not be representative of real-world particulate loading and may favor or disfavor air-cleaning devices that rely on electrostatic phenomenon to enhance their performance. The electrostatic phenomenon may be natural or imposed upon the media during manufacturing. As an example of an alternative method for testing electret filters, filtration authorities in the Nordic countries have developed techniques addressing charge-removal efficiencies of fibrous electret filter materials (Reference A1).

A2.2 ASHRAE Technical Committee 2.4 funded a research project (ASHRAE RP-1190) to develop a new loading test method that would more nearly represent the minimum efficiency points in actual real-world use. The results of this research were used to develop a method of conditioning that has been demonstrated in limited cases to more closely predict filter performance in field use. This method of conditioning is now included in this standard as Informative Appendix J with an optional step to help predict the efficiency loss the filter may realize in field applications.

A3. SELECTION OF THE PARTICLE SIZE RANGE

A3.1 This section presents background information and reasons for the selection of the 0.30 to 10 μm particle size range chosen for this standard. This issue was thoroughly debated, not only during the development and monitoring of ASHRAE Research Project RP-671 (Reference A2), on which this standard is based, but also during the deliberations of the committee that formulated this document.

A3.2 The upper size limit of 10 μm was chosen to address the ability of air cleaners to remove potentially irritating and nuisance particles that adversely affect human health and air-handling equipment. Particles of this size may be trapped in the nose and cause irritation and/or allergic reactions. These particles can also soil surfaces and equipment. Such contamination can provide nutrients for biological growth in ductwork or cause duct corrosion, both of which contribute to indoor air quality (IAQ) degradation. Filtration of large particles is needed to protect air-handling systems and equipment from contamination, according to ASHRAE SSPC 62, the standing committee maintaining ANSI/ASHRAE Standard 62.1, *Ventilation for Acceptable Indoor Air Quality*.

A3.2.1 We recognize that extrapolation from 3 or 5 μm efficiencies to 10 μm is common practice. However, in ASHRAE RP-671 it was demonstrated that "bounce" of 5 to 10 μm particles in low-efficiency air-cleaner media must be taken into account, thus making extrapolation a questionable practice. A Standard 52.2 test report will show particle bounce, if any, in an air cleaner. Refer to Informative Appendix C of this standard, "How to Read a Test Report," for guidance.

A3.2.2 Recirculated air in HVAC systems may contain high concentrations of large particles. Those up to 10 μm are inhalable and affect the health-related aspects of IAQ (Reference A3). Many allergens, fungi, and bioaerosols are in the 3 to 10 μm size range (Reference A4). Large particles can also be carriers of viruses and small bioaerosols.

A3.2.3 Additional factors influenced the selection of the 10 μm size limit. Particles larger than 10 μm rarely remain airborne long enough in an indoor space to be carried to the air cleaner. Also, larger particles are difficult to generate and keep in uniform suspension during air-cleaner testing due to their high settling velocities.

A3.3 The primary reason for selecting 0.30 μm as the lower limit was to permit the test facility to choose from a wide variety of commercially available off-the-shelf particle counters. For example, white-light wide-angle-scattering optical particle counters typically have good monotonic response to polydisperse aerosols, and many have an achievable lower size limit of 0.30 μm . Expensive or custom-built particle counters are not needed for the tests.

An additional consideration is the limit of the upper-to-lower size range ratio, which is about 30 for most particle counters. Thus, if 10 μm is the upper size limit, the lower should be 0.30 μm . The ratio becomes critical if the need, cost, and the additional error source of multiple instruments are to be avoided.

A4. SELECTION OF POTASSIUM CHLORIDE AS THE TEST AEROSOL

A4.1 Particulate potassium chloride (KCl) was chosen as the test aerosol for ASHRAE Research Project RP-671 by consensus among the project monitoring committee and the research contractor. The decision was later unanimously supported by the project committee.

A4.2 Nonsynthetic outdoor (ambient) air would have been preferred as the test aerosol but it could not be used for the following reasons:

- It lacks a statistically significant quantity of particles $>3 \mu\text{m}$. The particle size range of this standard includes sizes up to 10 μm .
- It is difficult to obtain reproducible test data from laboratories located in different geographical areas, or even in the same laboratory at different times, without knowing the chemical composition of the ambient aerosol and the size distribution and concentration of the aerosol and rigid control of test hardware. The project committee chose to emphasize performance parameters and relax hardware constraints.
- High particle concentrations in sizes $<3 \mu\text{m}$ could overload the particle counter, and inconsistent particle size and shape could produce measurement errors.

A4.3 Potassium chloride particles have advantages over other synthetic test aerosols because they are easy to generate, have a low cost, are commonly available, and are benign to health. Potassium chloride is also a polydisperse aerosol and has a high critical relative humidity. Commentary follows on other test aerosols that were considered.

A4.3.1 Monodisperse polystyrene latex (PSL) spheres would require a repeat of the test for each particle size of interest, significantly increasing the time to develop a 0.30 to 10 μm efficiency curve. Although monodisperse PSL aerosols are routinely used for instrument calibration and in small-scale test rigs, it is difficult to generate them in sufficient concentration for the test airflows specified in this standard.

A4.3.2 Polydisperse PSL spheres or other polydisperse particles have not been standardized or defined. One type, a latex resin, may be harder to clean up because it is not water soluble.

A4.3.3 Solid-phase aerosol particles were desired for this standard because they usually present a more severe chal-

lenge to an air cleaner. They frequently bounce off collection surfaces (e.g., fibers), increasing the chance of penetration. Particle sizes $>3 \mu\text{m}$ are most likely to bounce.

A4.3.4 Sodium chloride was also considered, but it was not chosen because the relative humidity of the air must be stringently controlled at less than 55% in order to dry droplets of its solution. KCl droplets dry to solid-phase particles at a relative humidity below $\approx 70\%$.

A5. ROUND-ROBIN TESTING

A5.1 Many people, including commenters on the first public review draft of this standard, expressed a desire for round-robin testing before issuing the standard. The committee decided against it for these reasons:

- The method is based on ASHRAE RP-671, an advantage that ANSI/ASHRAE Standard 52-68 (and its subsequent revisions) lacked.
- Extensive data quality criteria are included in the standard.
- Very recent favorable SAE experience with a round-robin on a similar method and European experience in particle size efficiency testing in the 0.20 to 0.50 μm range indicates the validity of the method.
- Even if a number of laboratories could be convinced to build the expensive test rig before the standard is accepted and published, and if they were ready to start testing immediately, a round-robin would delay the standard by at least two years.

A5.2 In 2001, ASHRAE Technical Committee 2.4 funded an interlaboratory research project to quantify the repeatability and reproducibility of the 52.2-1999 procedures (ASHRAE RP-1088).

A6. APPENDIX A REFERENCES

- NORDTEST. 1996. Development of test methods for electret filters. Technical Report 320, NORDTEST, Espoo, Finland.
- Hanley, J.T., D.D. Smith, and D.S. Ensor. 1993. Define a fractional efficiency test method that is compatible with particulate removal air cleaners used in general ventilation. ASHRAE Research Project RP-671 Final Report, Atlanta, GA.
- Suess, M. 1992. The indoor air quality program of the WHO regional office for Europe. *Proceedings of Indoor Air II*, Copenhagen, Denmark, World Health Organization.
- Foarde, K.K., et al. 1994. Investigate and identify indoor allergens and biological toxins that can be removed by filtration. ASHRAE Research Project RP-760, Final Report, Atlanta, GA.

(This appendix is not part of this standard. It is merely informative and does not contain requirements necessary for conformance to the standard. It has not been processed according to the ANSI requirements for a standard and may contain material that has not been subject to public review or a consensus process. Unresolved objections on informative material are not offered the right to appeal at ASHRAE or ANSI.)

INFORMATIVE APPENDIX B TEST PROCEDURE SUGGESTIONS AND EXAMPLES

B1. INTRODUCTION

The ability to generate, sample, and measure particles over the 0.30 to 10 μm diameter size range is critical to the successful performance of a PSE test. The design of an aerosol generation system and an aerosol sampling system believed to meet the required performance criteria of this standard is described in this appendix. These designs are based on those developed in ASHRAE Research Project RP-671. This standard has intentionally made the design of the system elements discretionary so as not to hinder the development and implementation of improved methods.

B2. PARTICLE COUNTER

B2.1 The aerosol concentrations in ASHRAE RP-671 were measured with a single optical particle counter (OPC) using a white-light illumination source and a wide collection angle for

the scattered light. The OPC's sampling rate was $0.00012 \text{ m}^3/\text{s}$ (0.25 cfm).

B2.2 The OPC output was directed to a multichannel analyzer providing the appropriate sizing channels covering the range of 0.30 to 10 μm . The multichannel analyzer was equipped with an interface board providing a contact closure at the end of each sample and a 15 second delay in particle counting after each sample. The contact closure operated electromechanical valves in the upstream and downstream sample lines. The 15 second delay allowed time for the acquisition of a new sample.

B3. AEROSOL GENERATION

B3.1 The test aerosol in ASHRAE RP-671 was solid-phase dry potassium chloride (KCl) in particulate form generated from an aqueous solution. The aerosol was generated by nebulizing an aqueous KCl solution with an external mixing air atomizing nozzle (Figure B-1). The spray nozzle was operated at a relatively low air pressure to keep the particle concentrations in the duct below the coincidence error concentration limit of the particle counter.

B3.2 The nozzle was positioned at the top of a 310 mm (12 in.) diameter, 1300 mm (51 in.) high transparent acrylic spray tower. The tall tower served two purposes: it allowed the salt droplets to dry by providing an approximately 40 second mean residence time, and it allowed larger-sized particles to fall out of the aerosol. An aerosol neutralizer reduced the charge level on the aerosol until the level was equivalent to a Boltzman charge distribution. A Boltzman charge distribution is the average charge found in the ambient air. Electrostatic charging is an

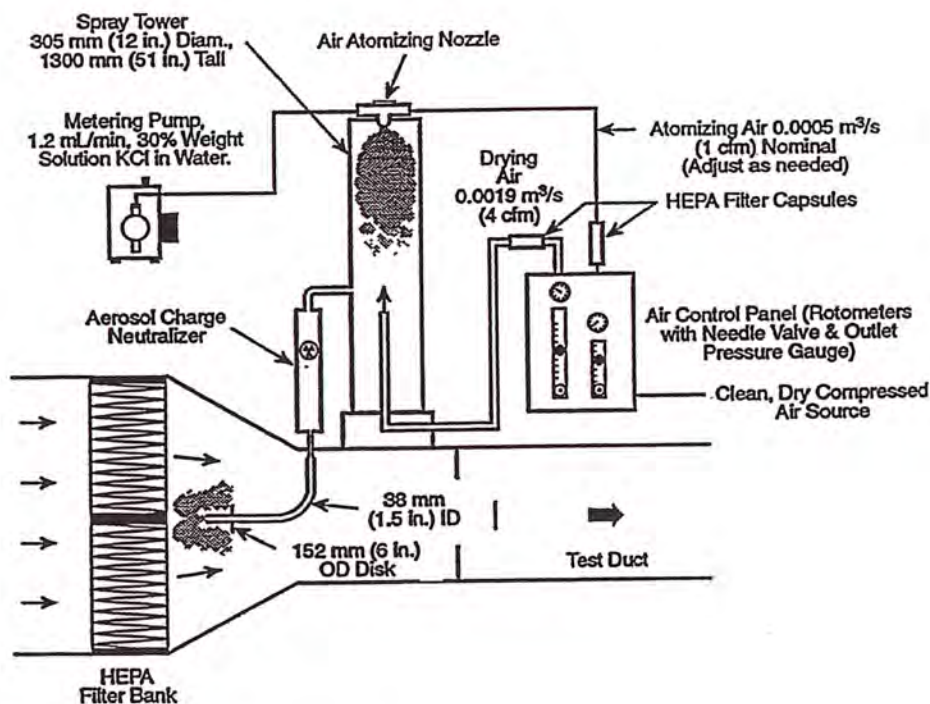


Figure B-1 Schematic of the aerosol generator system.

unavoidable consequence of most aerosol generation methods. The aerosol was injected counter to the airflow, as illustrated in Figure B-1, to improve the mixing of the aerosol with the air-stream.

B3.3 The KCl solution was prepared by combining 300 g of KCl with 1 L of distilled water. The solution was fed to the atomizing nozzle at 1.18 mL/min by a metering pump. Varying the operating air pressure of the generator allowed control of the challenge aerosol concentration.

B4. AEROSOL SAMPLING SYSTEM

B4.1 The sampling lines must be carefully designed and constructed to minimize the loss of particles. In ASHRAE RP-671, 14 mm (0.55 in.) ID stainless steel lines and gradual bends (radius of curvature = 57 mm [2.25 in.]) were used. These dimensions were chosen to minimize particle losses within the lines at the sampling rate of 0.00012 m³/s (0.25 cfm).

B4.2 The “Y” fitting connecting the upstream and downstream lines to the particle counter was custom made (Figure B-2). The two branches of the “Y” merge gradually to minimize particle loss in the intersection of the “Y” due to impaction forces.

B4.3 Electrically actuated ball valves were installed in each branch immediately above the “Y.” The opening and closing action of the valves was automatically controlled by a relay closure on the particle counter’s multichannel analyzer. The valves took approximately two seconds to open or close.

B4.4 Isokinetic sampling nozzles of the appropriate entrance diameter were placed on the ends of the sample probes to maintain isokinetic sampling for all test airflow rates.

B5. EXAMPLES OF AIR-CLEANER EFFICIENCY CALCULATIONS

B5.1 Correlation Calculations

B5.1.1 Figure B-3 shows an example correlation calculation for all particle size ranges. Here a fixed number of samples sets (nine) is used. The correlation ratios R are determined for each particle size range. The resulting correlation ratio error limits,

$$\sigma_c \times \frac{t}{\sqrt{n}}$$

are found for each particle size range and compared to the criteria in Equation 10-11 of Section 10.6.2.1. Also, the correlation ratio maximum background counts $\bar{D}_{b,uc1}$, $\bar{U}_{b,uc1}$ are calculated and compared to the criteria in Equation 10-12 of Section 10.6.2.3. Lastly, the correlation ratio minimum average upstream counts Avg. $U_{e,c}$ are calculated and compared to the criteria in Equation 10-13 of Section 10.6.2.4.

B5.1.2 Figure B-4 shows an example correlation calculation for a single particle size range. Here the correlation ratio error limit is calculated at the third measurement. The correlation ratio error limit is recalculated for each additional upstream and downstream measurement set. The test can be stopped when the correlation ratio error limit criterion of Section 10.6.2.1 is met.

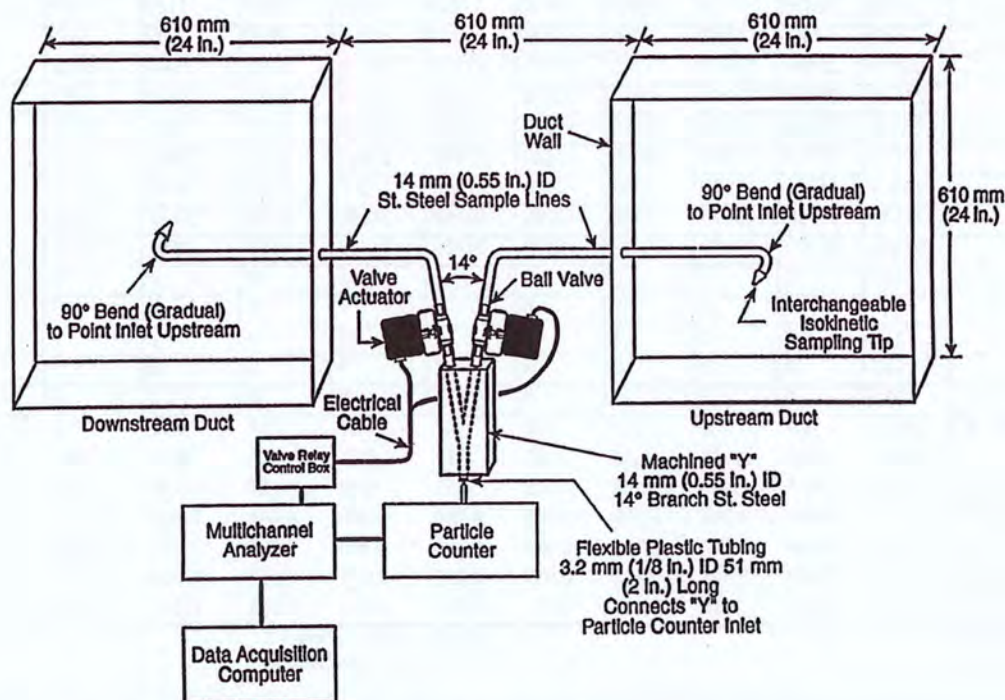


Figure B-2 Schematic of the aerosol sampling system.

OPC Channel # Geo. Mean Dia. (μm)	1 0.35	2 0.45	3 0.55	4 0.69	5 0.89	6 1.22	7 1.73	8 2.45	9 3.46	10 4.69	11 6.20	12 8.37
Upstream—Bkg	139	0	0	0	0	0	1	0	1	0	0	1
Upstream—Bkg	110	0	0	3	0	0	1	1	1	2	1	0
Upstream—Bkg	106	1	2	0	1	2	0	0	1	0	1	2
Upstream—Bkg	101	3	0	0	0	1	0	0	0	2	0	0
Upstream—Bkg	69	0	2	3	1	0	4	4	5	1	9	4
Upstream	26290	26890	20170	24870	13040	21590	26320	8967	2881	1603	697	440
Upstream	26390	27240	20410	25320	13260	21830	26310	9273	3040	1688	722	451
Upstream	26080	26560	19840	24960	13030	21640	26060	9010	2922	1697	732	446
Upstream	26240	26780	20050	25120	13140	21570	26330	9312	2927	1727	736	428
Upstream	25530	25590	19330	24360	12600	20810	25520	8724	2777	1619	659	430
Upstream	25600	26560	19780	24710	12900	21180	25460	8877	2931	1620	695	456
Upstream	24720	25410	19020	24000	12430	20680	25020	8662	2855	1551	657	412
Upstream	25550	25650	19250	24220	13070	21130	25620	8909	2857	1647	675	468
Upstream	24970	25490	19030	23780	12580	20610	25040	8468	2817	1540	612	382
Upstream	25190	25280	18960	24050	12490	20400	24770	8623	2705	1540	609	406
Upstream—Bkg	102	0	1	1	0	0	0	4	1	2	1	0
Upstream—Bkg	109	0	0	0	0	02	2	4	2	1	0	0
Upstream—Bkg	124	1	0	0	0	0	0	0	0	0	0	0
Upstream—Bkg	111	1	0	0	0	0	0	1	1	0	0	0
Upstream—Bkg	94	0	1	0	0	0	0	1	1	1	0	0
Avg. U_b	106.5	0.6	0.6	0.7	0.2	0.5	0.8	1.5	1.3	0.9	1.2	0.7
Std. Dev. U_b	18.30	0.97	0.84	1.25	0.42	0.85	1.32	1.78	1.42	0.88	2.78	1.34
$U_{b, ucl}$	119.59	1.29	1.20	1.60	0.50	1.11	1.74	2.77	2.31	1.53	3.19	1.66
Avg. U_c	25656	26145	19584	24539	12854	21144	25645	8882.5	2871.2	1623.2	679.4	431.9
$U_{b, ucl}/\text{Avg. } U_c$	0.005	0.000	0.000	0.000	0.000	0.000	0.000	0.000	0.001	0.001	0.005	0.004
Downstream—Bkg	125	12	0	1	5	3	14	11	29	16	8	10
Downstream—Bkg	112	1	0	0	0	2	3	3	5	1	3	1
Downstream—Bkg	102	1	2	3	0	2	2	3	4	2	1	2
Downstream—Bkg	74	5	0	2	2	5	15	21	11	10	9	13
Downstream—Bkg	72	5	3	5	0	1	8	14	7	6	2	9
Downstream	25470	25760	19260	24690	12710	21140	25600	8605	3002	1602	637	443
Downstream	26180	26740	20150	25330	13180	21960	26370	9030	3102	1670	675	433
Downstream	25390	26060	19660	24280	12850	21130	25550	8897	3042	1679	652	461
Downstream	25880	26580	19950	25240	13020	21580	25910	8942	2944	1632	651	450
Downstream	25110	25630	19200	23980	12710	21060	25310	8664	2985	1607	625	455
Downstream	25310	25830	19530	24110	12820	20920	25070	8655	2961	1570	632	457
Downstream	25170	25510	19030	24000	12820	20490	25060	8542	2894	1535	618	379
Downstream	25600	25720	19500	24360	12920	21160	25200	8739	2858	1568	625	439
Downstream	24570	24710	18690	23480	12200	20290	24650	8439	2724	1602	603	398
Downstream	24310	24670	18420	23250	12330	20120	24410	8380	2839	1441	610	419
Downstream—Bkg	111	0	0	0	0	1	1	0	2	1	0	0
Downstream—Bkg	129	1	0	2	0	1	0	0	0	0	0	1
Downstream—Bkg	110	3	0	1	1	0	3	0	1	1	0	0
Downstream—Bkg	105	0	0	0	0	1	0	2	0	0	0	0
Downstream—Bkg	114	1	1	0	0	1	5	0	2	0	0	0
Avg. D_b	105.4	2.9	0.6	1.4	0.8	1.7	5.1	5.4	6.1	3.7	2.3	3.6
Std. Dev. D_b	18.93	3.70	1.07	1.65	1.62	1.42	5.51	7.37	8.75	5.40	3.43	5.02
$D_{b, ucl}$	118.94	5.54	1.37	2.58	1.96	2.71	9.04	10.67	12.36	7.56	4.76	7.19
$D_{b, ucl}/\text{Avg. } U_c$	0.005	0.000	0.000	0.000	0.000	0.000	0.000	0.001	0.004	0.005	0.007	0.017
R	0.991	0.988	0.993	0.993	0.995	0.996	0.990	0.981	1.021	0.985	0.931	0.999
Std. Dev. R	0.017	0.019	0.021	0.017	0.017	0.017	0.011	0.017	0.019	0.022	0.031	0.062
Std. Dev. $R \times 1/n^{0.5}$	0.013	0.015	0.016	0.013	0.013	0.013	0.008	0.013	0.015	0.017	0.024	0.047

* For limits, see Section 10.6.2.4.

** For limits, see Section 10.6.2.3

† For limits, see Section 10.6.2.3.

†† For limits, see Section 10.6.2.1.

Figure B-3 Example correlation calculations for $n = 9$ sample sets in all particle size ranges. From run 1 of 5, 100% penetration test, ASHRAE RP-671 (Reference A1).

i	$U_{i,o,c}$	$D_{i,o,c}$	$U_{i,e,c}$	R_i	\bar{R}	δ_c	\bar{R}_{lcl}	\bar{R}_{ucl}	$\delta_c \times \frac{t}{\sqrt{i}}$
1	26290	25470	26340	0.967					
2	26390	26180	26235	0.998	0.982	0.022			
3	26080	25390	26160	0.971	0.978	0.017	0.936	1.021	0.042
4	26240	25880	25885	1.000	0.984	0.017	0.956	1.012	0.028
5	25530	25110	25565	0.982	0.983	0.015	0.965	1.002	0.019
6	25600	25310	25160	1.006	0.987	0.016	0.970	1.004	0.017
7	24720	25170	25135	1.001	0.989	0.016	0.975	1.004	0.015
8	25550	25600	25260	1.013	0.992	0.017	0.978	1.006	0.014
9	24970	24570	25080	0.980	0.991	0.016	0.978	1.004	0.013
10	25190	24310							

Figure B-4 Example correlation calculation for one particle size range with error evaluation at each step. From run 1 of 5, size range 1, 100% penetration tests, ASHRAE RP-671 (Reference A1).

B5.2 Penetration Calculations

B5.2.1 Figure B-5 shows an example penetration calculation for all particle size ranges. Here a fixed number of samples sets (nine) is used. The penetration ratios P are determined for each particle size range. The resulting penetration ratio error limits,

$$\sigma_c \times \frac{t}{\sqrt{n}}$$

are found for each particle size range and compared to the criteria in Equation 10.23 of Section 10.6.4.1. Also, the penetration ratio maximum background counts $\bar{D}_{b,ucl}$, $\bar{U}_{b,ucl}$ are calculated and compared to the criteria in Equation 10-24 of Section 10.6.4.2. Lastly, the penetration ratio minimum average upstream counts Avg. $U_{e,t}$ are calculated and compared to the criteria in Equation 10-25 of Section 10.6.4.3.

B5.2.2 Figure B-6 shows an example penetration calculation for a single particle size range. Here the penetration ratio error limit is calculated at the third measurement. The penetration ratio error limit is recalculated for each additional upstream and downstream measurement set. The test can be stopped when the penetration ratio error limit criterion of Section 10.6.4.1 is met.

B6. TEST SEQUENCE

The following tabulation of the test sequence steps may help to clarify the procedure:

Step	Air Cleaner	KCI Generator	Dust Feeder
1. Correlation ratio	None	On	Off
2. Resistance vs. airflow	In place	Off	Off
3. Initial PSE test	In place	On	Off
4. First dust loading	In place	Off	On
5. PSE test	In place	On	Off
6. Second dust loading	In place	Off	On
7. PSE test	In place	On	Off
8. Third dust loading	In place	Off	On
9. PSE test	In place	On	Off
10. Fourth dust loading	In place	Off	On
11. PSE test	In place	On	Off
12. Fifth dust loading	In place	Off	On
13. PSE test	In place	On	Off

Notes:

1. Each PSE test consists of the following:

a. Background counts	In place	Off	Off
b. Efficiency measurement	In place	On	Off
c. Background	In place	Off	Off

2. Prior to each dust loading, the duct airflow is turned off, the filter is installed, and the particle counters' inlet probes are capped. The duct airflow is then resumed.

3. After each dust loading, the duct airflow is turned off, the particle counters' inlet probes are uncapped, and the final filter is removed. The duct airflow is then resumed.

OPC Channel # Geo. Mean Dia. (µm)	1 0.35	2 0.45	3 0.55	4 0.69	5 0.89	6 1.22	7 1.73	8 2.45	9 3.46	10 4.69	11 6.20	12 8.37
Upstream—Bkg	147	2	1	2	0	0	1	1	0	0	2	1
Upstream—Bkg	308	77	7	2	0	2	0	0	0	0	0	0
Upstream—Bkg	174	0	0	0	0	0	0	0	0	0	0	0
Upstream—Bkg	184	1	0	0	0	0	0	0	0	0	0	0
Upstream—Bkg	169	0	0	0	0	0	0	0	0	0	0	0
Upstream	21850	21770	16280	19670	10280	16830	21570	7618	2505	1376	547	321
Upstream	20820	20880	15270	18580	9843	16090	20680	7189	2479	1329	470	305
Upstream	21350	21040	15600	19160	9977	16500	20980	7314	2499	1332	511	332
Upstream	22630	22460	16420	20320	10660	17400	22360	7876	2620	1395	531	314
Upstream	21560	21210	15730	19260	10030	16800	21010	7348	2393	1270	536	291
Upstream	22240	21940	16060	19780	10390	17340	21530	7565	2557	1276	552	303
Upstream	22680	22170	16430	20180	10410	17620	22490	7546	2503	1362	546	324
Upstream	22590	21990	16550	19980	10450	17620	22360	7578	2576	1325	548	297
Upstream	23300	22980	16580	20660	10650	17730	22460	7706	2574	1329	498	300
Upstream	23850	23480	17180	21150	11180	18260	23480	8175	2675	1453	516	325
Upstream—Bkg	147	5	0	2	0	4	4	5	2	1	0	0
Upstream—Bkg	159	1	2	0	0	0	1	2	2	0	0	0
Upstream—Bkg	142	0	0	0	0	1	0	2	0	1	0	0
Upstream—Bkg	135	0	0	1	0	0	1	2	0	0	0	1
Upstream—Bkg	113	0	0	0	0	0	1	0	3	2	2	0
Avg. U_b	167.8	8.6	1	0.7	0	0.8	0.9	1.2	0.7	0.4	0.4	0.2
Std. Dev. U_b	53.38	24.08	2.21	0.95	0.00	1.32	1.20	1.62	1.16	0.70	0.84	0.42
$U_{b,ucf}$	205.98	25.83	2.58	1.38	0.00	1.74	1.76	2.36	1.53	0.90	1.00	0.50
Avg. U_t	22287	21992	16210	19874	10387	17219	21892	7591.5	2538.1	1344.7	525.5	311.2
$U_{b,ucf}/\text{Avg. } U_t$	0.009	0.001	0.000	0.000	0.000	0.000	0.000	0.000	0.001	0.001	0.002	0.002
Downstream—Bkg	157	0	1	0	0	0	2	1	1	0	1	0
Downstream—Bkg	207	1	2	1	0	1	1	2	0	1	0	1
Downstream—Bkg	167	0	1	1	0	2	3	2	2	0	0	0
Downstream—Bkg	164	0	1	1	1	1	7	12	4	1	1	1
Downstream—Bkg	170	2	2	1	2	2	1	1	1	0	1	2
Downstream	17450	16070	11070	11840	4955	6220	3506	271	34	13	5	2
Downstream	17060	16080	10800	11540	4880	5969	3449	305	37	23	2	3
Downstream	17480	16480	10960	12040	5122	6288	3644	319	41	15	2	7
Downstream	18640	17170	11590	12550	5264	6379	3813	303	42	11	6	3
Downstream	17180	15760	10770	11540	4859	6053	3497	272	24	10	7	2
Downstream	18350	16740	11440	12200	5134	6251	3607	317	39	14	3	5
Downstream	18220	16780	11300	12000	5091	6239	3608	298	40	11	6	3
Downstream	18500	17190	11590	12300	5180	6442	3720	302	42	15	6	3
Downstream	18970	17780	12170	12620	5470	6745	3851	303	53	17	9	2
Downstream	19450	18030	12380	13330	5667	6940	3995	263	37	13	3	1
Downstream—Bkg	189	14	1	0	0	0	0	0	0	0	0	0
Downstream—Bkg	138	0	1	0	0	0	0	0	0	0	0	0
Downstream—Bkg	161	0	0	0	0	1	0	2	1	2	1	0
Downstream—Bkg	136	0	0	0	0	0	1	0	0	0	0	0
Downstream—Bkg	139	1	0	0	0	0	0	3	1	1	1	0
Avg. D_b	162.8	1.8	0.9	0.4	0.3	0.7	1.5	2.3	1	0.5	0.5	0.4
Std. Dev. D_b	22.72	4.34	0.74	0.52	0.67	0.82	2.17	3.56	1.25	0.71	0.53	0.70
$D_{b,ucf}$	179.05	4.91	1.43	0.77	0.78	1.29	3.05	4.85	1.89	1.01	0.88	0.90
$D_{b,ucf}/\text{Avg. } U_t$	0.008	0.000	0.000	0.000	0.000	0.000	0.000	0.001	0.001	0.001	0.002	0.003
R	0.991	0.988	0.993	0.993	0.995	0.996	0.990	0.981	1.021	0.985	0.931	0.999
Std. Dev. R	0.808	0.761	0.699	0.609	0.493	0.366	0.166	0.039	0.015	0.010	0.009	0.009
Std. Dev. $R/n^{0.5}$	0.815	0.770	0.704	0.613	0.496	0.367	0.168	0.040	0.015	0.010	0.009	0.009
Std. Dev. P_o	0.017	0.015	0.015	0.012	0.009	0.009	0.004	0.002	0.003	0.003	0.005	0.005
Std. Dev. R	0.017	0.019	0.021	0.017	0.017	0.017	0.011	0.017	0.019	0.022	0.031	0.062
Std. Dev. P	0.022	0.021	0.021	0.017	0.012	0.011	0.005	0.002	0.003	0.003	0.005	0.005
Std. Dev. $P \times t/n^{0.5} \dagger$	0.017	0.016	0.016	0.013	0.010	0.008	0.003	0.002	0.002	0.002	0.004	0.004

* For limits, see Section 10.6.4.4.

** For limits, see Section 10.6.4.2.

† For limits, see Section 10.6.4.2.

†† For limits, see Section 10.6.4.1.

Figure B-5 Example penetration calculations for $n = 9$ sample sets in all particle size ranges. From run 1 of 3, pleated paper filter tests, ASHRAE RP-671 (Reference A1).

i	$U_{i,o,t}$	$D_{i,o,t}$	$U_{i,e,t}$	$P_{i,o}$	\bar{P}_o	\bar{P}	δ_t	d	\bar{P}_{lcl}	\bar{P}_{ucl}	$\delta_c \times \frac{t}{\sqrt{n}}$
1	21850	17450	21335	0.818							
2	20820	17060	21085	0.809	0.814	0.820	0.006	0.015			
3	21350	17480	21990	0.795	0.807	0.814	0.012	0.018	0.762	0.836	0.045
4	22630	18640	22095	0.844	0.816	0.823	0.020	0.025	0.777	0.849	0.039
5	21560	17180	21900	0.784	0.810	0.816	0.023	0.027	0.777	0.838	0.033
6	22240	18350	22460	0.817	0.811	0.817	0.021	0.025	0.785	0.833	0.026
7	22680	18220	22635	0.805	0.810	0.817	0.019	0.023	0.789	0.828	0.022
8	22590	18500	22945	0.806	0.810	0.816	0.018	0.022	0.791	0.824	0.019
9	23300	18970	23575	0.805	0.809	0.816	0.017	0.022	0.793	0.822	0.017
10	23850	19450									

Figure B-6 Example penetration calculation for one particle size range with error evaluation at each step, where $\delta_o = 0.017$ and $R = 0.992$. From run 1 of 3, size range 1, pleated paper filter tests, ASHRAE RP-671 (Reference A1).

(This appendix is not part of this standard. It is merely informative and does not contain requirements necessary for conformance to the standard. It has not been processed according to the ANSI requirements for a standard and may contain material that has not been subject to public review or a consensus process. Unresolved objections on informative material are not offered the right to appeal at ASHRAE or ANSI.)

INFORMATIVE APPENDIX C HOW TO READ A TEST REPORT

This appendix is meant to provide background information about the test report and explanations in layman's terms for users (building owners, installers, and design engineers).

C1. BACKGROUND

C1.1 ASHRAE does not actually test air cleaners or determine their performance but only promulgates the test procedure used by manufacturers and independent testing laboratories.

C1.2 Air-cleaner testing in a laboratory is intended to help the user compare the performance of different types of air cleaners. Testing attempts to simulate the performance of air cleaners in real-life operation but cannot duplicate field conditions. Field conditions vary from location to location. The reporting values obtained in accordance with this standard cannot be used by themselves to predict the air cleanliness of a specific ventilated space or the service life of installed air cleaners.

C1.3 Testing accelerates the life experience of an air cleaner, and accelerated use is different from normal use. The ASHRAE test involves concentrations and compositions that are almost certain to be different from those the air cleaner will encounter when installed in a system. Also, the airflow rate, final resistance, and temperature and humidity level of the air may be different in the testing laboratory from those on the job.

C1.4 Laboratory accuracy is expected of the instrumentation used in testing to the standard. However, this does not mean that the tested filter will perform with laboratory accuracy on an installed job.

C2. READING A TEST REPORT

C2.1 The summary section of a sample performance report on a typical extended-surface media filter is shown in Figures C-1, C-2, and C-3. The circled numbers refer to the explanations that follow.

1. The test method should be in accordance with the latest edition of the ASHRAE standard.
2. These sections are helpful to trace the test laboratory, test owner, and test specimen.
3. This information is important for identification. Upon request, independent test laboratories will verify data with users and identify any tampering with the results.
4. This information is useful because different types of detecting devices may give differing readings. Good calibration is most necessary.
5. Manufacturers' catalog data are not required by the standard, but if such data are included in the test report, it will

help the user compare published data and actual performance.

6. The test airflow rate is specified by the manufacturer and generally depends on the filter size (height, width, and depth), media area, and construction. The airflow rate must be between 0.22 and 1.4 m³/s (472 and 2990 cfm) and be selected from Section 8.1.
7. Device manufacturers must specify the final resistance for testing using Table 12-1 values as minimums.
8. The physical description must match the filter being considered. This part is very important because there are many filters with the same name and a different appearance (fewer pockets, longer pockets, etc.).
9. The test airflow rate and net effective media area may be used to calculate media velocity:

$$\text{Media velocity, m/s (fpm)} = \frac{\text{Airflow rate, m}^3/\text{s (cfm)}}{\text{Effective media area, m}^2(\text{ft}^2)}$$

10. Note that the performance of a manufactured filter will usually be very different from that of a flat sheet of the media used to construct the filter.
11. The initial resistance is the resistance to airflow of the filter at the test airflow rate. Depending on the design and construction of the filter, initial resistance may or may not indicate life expectancy.
12. These minimum averages help to define the minimum performance of the device in removing particles of various sizes. They are not full averages.
13. The MERV is based on the minimum PSEs and Table 12-1. The reporting value helps the user select an air cleaner but does not reflect the total behavior of the device.
14. This curve shows the resistance of the clean filter over the prescribed range of face velocities.
15. These curves show the PSE after loading with incremental amounts of dust.
16. This curve shows the minimum values of PSE during the test. Refer to Informative Appendix D for examples of the use of this curve.
17. The dust-holding capacity presents the total weight of synthetic loading dust captured by the air-cleaning device over all of the incremental dust loading steps. This value should not be used to calculate the expected life of the device in use.
18. The average dust arrestance presents the ability of the filter to remove loading dust from test air. This is measured and reported only for air-cleaning devices with efficiencies less than 20% in the size range of 3.0 to 10.0 µm.
19. The release rate gives an indication of filter shedding.
20. This curve shows the resistance vs. synthetic loading dust fed (for air-cleaning devices with efficiencies less than 20% in the size range of 3.0 to 10.0 µm).

Page 1 of 3

ASHRAE Std. 52.2 Air Cleaner Performance Report Summary

① (This report applies to the tested device only)

Laboratory Data ③

Report No. 99-392 Test No. 99-1798 Date DEC. 12, 1999
 Test laboratory INDEPENDENT TEST LABS, INC.
 Operator T. SMITH Supervisor G. SUPER
 Particle counter(s): Brand COUNTALL Model 226/80

④ Device Manufacturer's Data ② ③

Manufacturer FILTERMAKER, INC.
 Product name FLO-RITE Model 12
 Test requested by FILTER SALES CO.
 Sample obtained from OPEN MARKET ⑤
 Catalog rating: Airflow rate 1.18 m³/s Initial press. drop 53 Pa
 Specified test conditions: Airflow rate 1.18 m³/s ⑥
 Final pressure drop 250 Pa ⑦ Face velocity 3.2 m/s

Device Description ⑧

Dimensions: height 590 mm width 590 mm depth 560 mm
 Generic name BAG FILTER Media type SPN. NONWOVEN POLYESTER
 Effective media area 3.5 m² ⑨ Media color YELLOW
 Amount and type of adhesive NONE
 Other attributes 5 POCKETS

Test Conditions

Airflow rate 1.18 m³/s Temperature 22°C RH 50%
 Test aerosol type KCl
 Final pressure drop 250 Pa Face velocity 3.2 m/s
 Remarks NONE

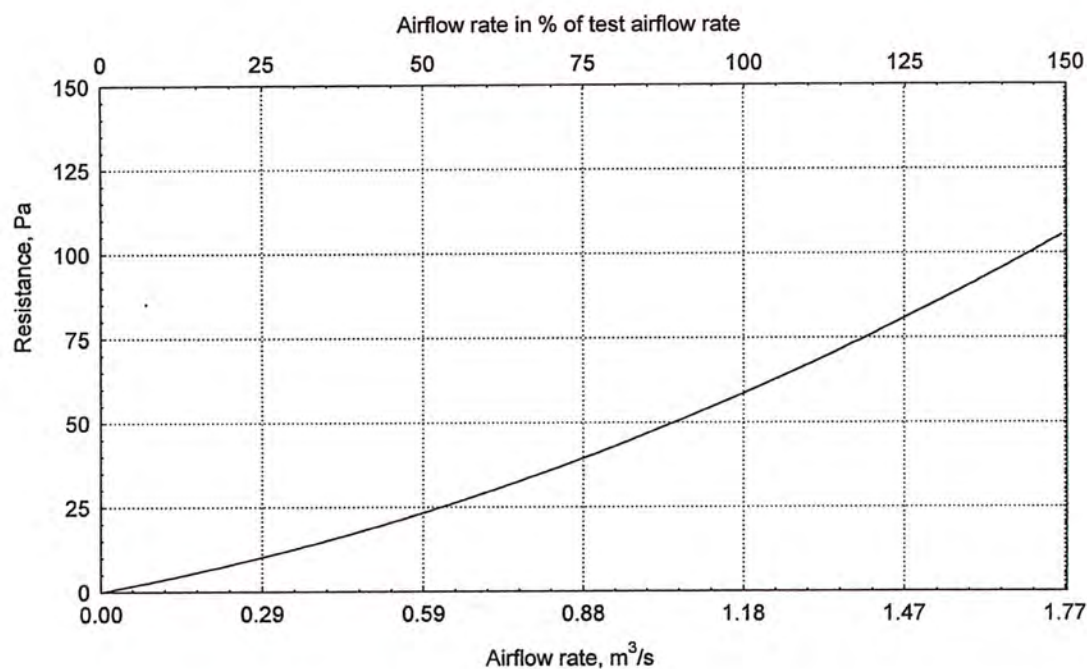
Resistance Test Results

Initial resistance 57 Pa ⑩ Final resistance 250 Pa

Minimum Efficiency Reporting Data

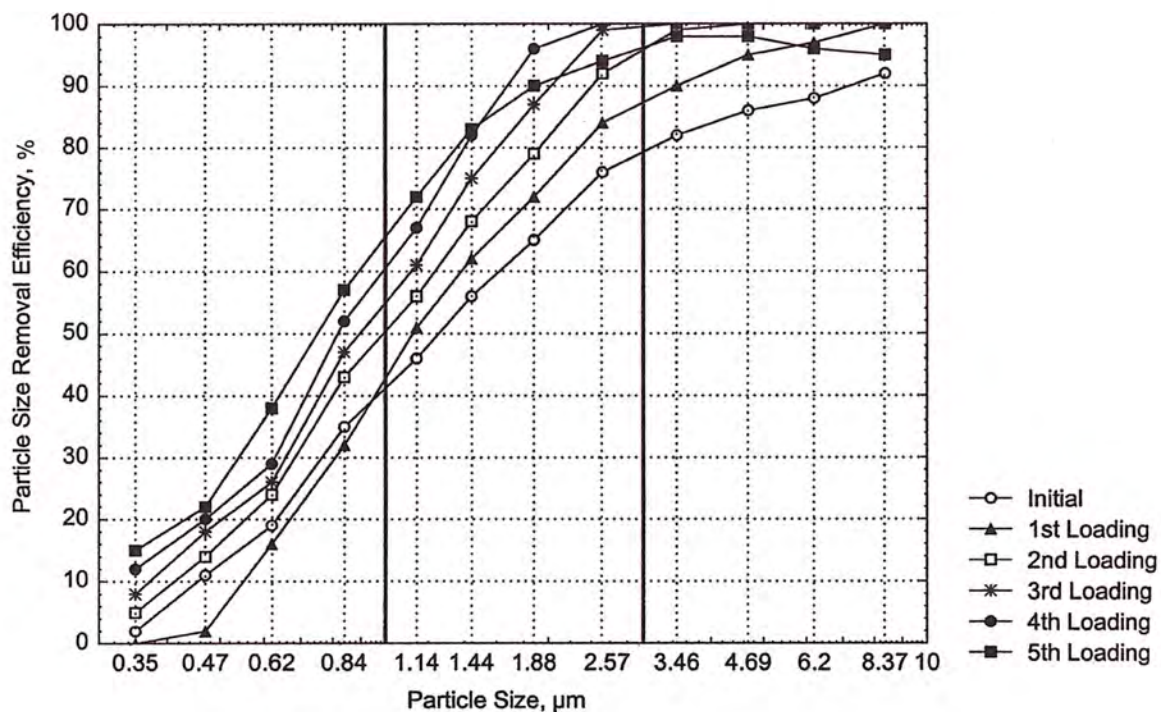
Composite average efficiencies E₁ 13% E₂ 60% E₃ 87% ⑪
 Air cleaner average Arrestance N/A ⑪
 Minimum efficiency reporting value (MERV) for the device:
 Dust Holding Capacity (g) 693 ⑫ MERV 10 @ 1.18 ⑫

Figure C-1 Sample summary air-cleaner performance report, Page 1.



(a)

13



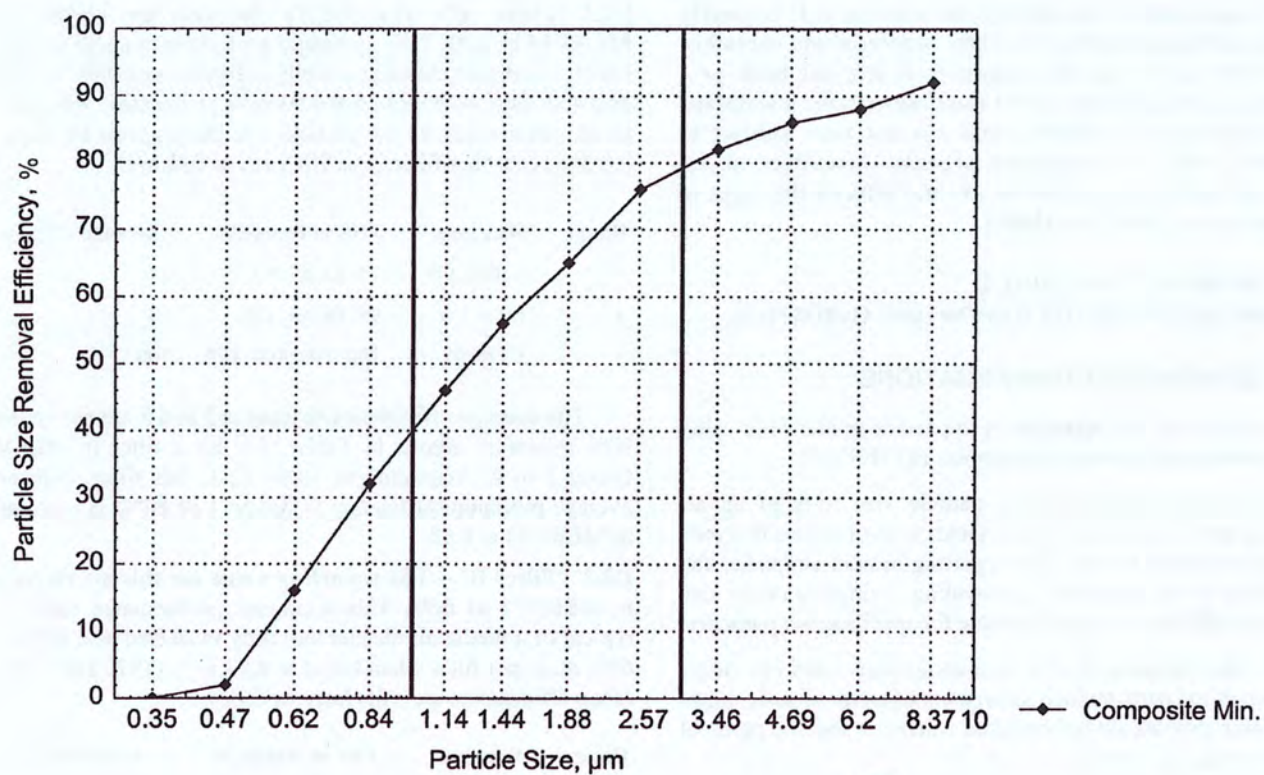
(b)

14

Figure C-2 Sample air-cleaner performance report summary, Page 2.

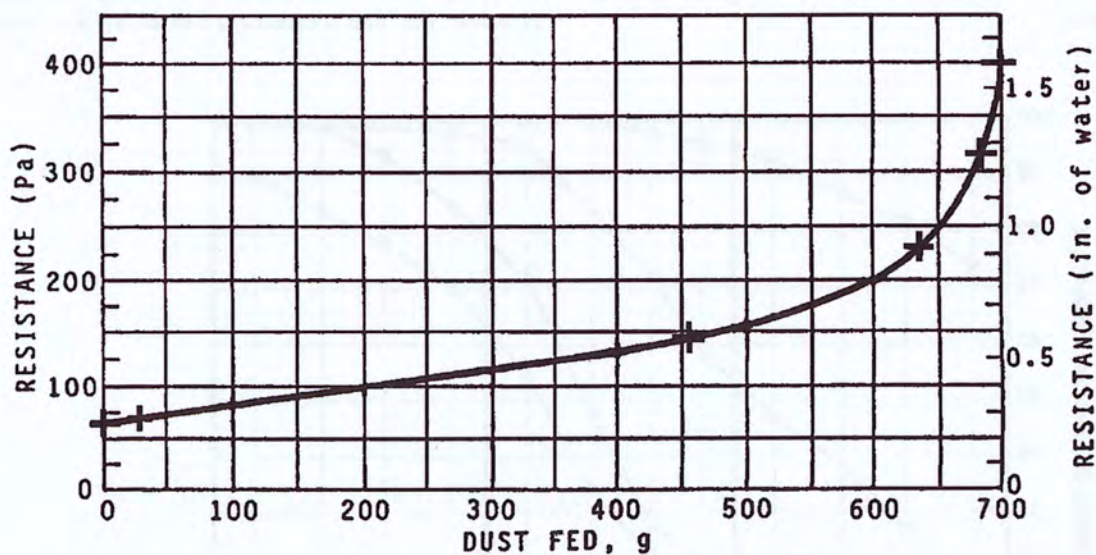
(a) Resistance of clean device vs. airflow.

(b) PSE after incremental dust loading.



(15)

Figure C-3 Sample air-cleaner performance report summary, Page 3.
—Composite minimum efficiency curve.



(18)

Figure C-4 Sample air-cleaner report summary, Page 3.
—Resistance vs. Synthetic Loading Dust Fed graph ONLY for air-cleaning devices with efficiencies less than 20% in the size range of 3.0 to 10.0 μm).

(This appendix is not part of this standard. It is merely informative and does not contain requirements necessary for conformance to the standard. It has not been processed according to the ANSI requirements for a standard and may contain material that has not been subject to public review or a consensus process. Unresolved objections on informative material are not offered the right to appeal at ASHRAE or ANSI.)

INFORMATIVE APPENDIX D
MINIMUM EFFICIENCY REPORTING GUIDANCE

D1. GENERAL RECOMMENDATIONS

The purpose of this appendix is to provide guidance in using the system and show some examples of MERVs.

D1.1 Removal efficiency vs. particle size tests of an air cleaner as it is loaded with dust yields a set of curves that may be inconvenient to use. This reporting system simplifies the selection of air cleaners by providing a single particle size removal efficiency reporting value for specification purposes.

D1.2 Any reporting system is a compromise and can never reflect all the performance parameters of an air cleaner. Manufacturer data should be consulted whenever specific removal performance is desired.

D2. EXAMPLES

Examples of typical minimum efficiency curves are shown in Figure D-1. Each curve is the minimum performance of the air cleaner from the initial test of the clean device to the test at its final loading stage. It will be helpful to have Table 12-1 readily available for reference when reviewing these curves and the method.

D2.1 “Filter A”—The MERV for this air cleaner is MERV14 at 0.93. This minimum performance curve is typical of a media air cleaner currently marketed as a 90% to 95% dust spot filter when tested at 0.93 m³/s (1970 cfm). The minimum efficiencies for the particle size ranges must be calculated to report the filter. The PSEs are as follows:

Range	Size, μm	PSE in Range, %	Average PSE, %
1	0.30 to 1.0	74, 82, 87, 92	84
2	1.0 to 3.0	96, 98, 99, 100	98
3	3.0 to 10	100, 100, 100, 100	100

The average efficiencies in Ranges 2 and 3 are above the 90% minimum shown in Table 12-1 for a filter in MERV Group 1 to 4. According to Table 12-1, this filter, with an average minimum efficiency in Range 1 of 84%, is reported as MERV14 at 0.93.

D2.2 “Filter B”—The reporting value for this air cleaner is MERV11 at 0.93. This minimum performance curve is typical of a media air cleaner currently marketed as a 60% to 65% dust spot filter when tested at 0.93 m³/s (1970 cfm). The range efficiencies are calculated as follows:

Range	Size, μm	PSE in Range, %	Average PSE, %
1	0.30 to 1.0	18, 28, 38, 47	33
2	1.0 to 3.0	58, 72, 84, 96	78
3	3.0 to 10	98, 99, 99, 99	99

The average efficiency in Range 3 is above the 85% and 90% minimums shown in Table 12-1 for the MERV Group 9 to 12 and MERV Group 13 to 16 categories, respectively. However, the filter is categorized in the MERV Group 9 to 12

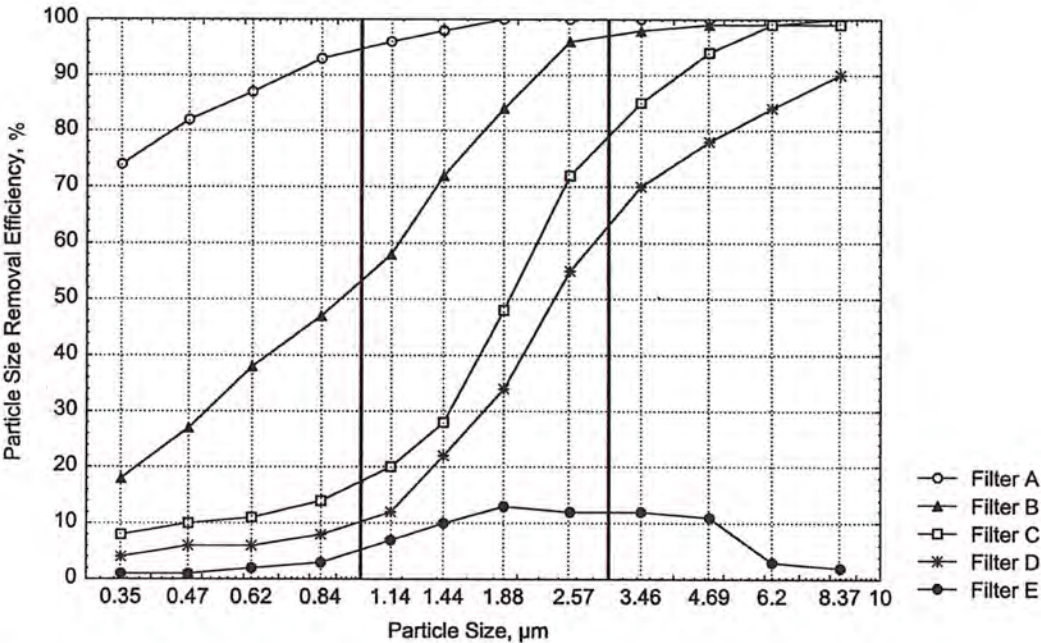


Figure D-1 Typical minimum efficiency curves.

area since the average efficiency in Range 2 is below the 90% minimum requirement for the MERV Group 13 to 16 category. The average efficiency in Range 1 is not used for reporting. Based on the average efficiency of 78% in Range 2, the filter is reported as MERV11 at 0.93.

D2.3 “Filter C”—The reporting value for this air cleaner is **MERV9 at 0.93**. This minimum performance curve is typical of a media air cleaner currently marketed as a 40% to 45% dust spot filter when tested at 0.93 m³/s (1970 cfm). As in the examples above, the range efficiencies are calculated as follows:

Range	Size	PSE in Range, %	Average PSE, %
1	0.30 to 1.0	8, 10, 11, 14	11
2	1.0 to 3.0	20, 28, 48, 72	42
3	3.0 to 10	85, 94, 98, 99	94

The average efficiency in Range 3 is above the 85% and 90% minimums shown in Table 12-1 for the MERV Group 9 to 12 and MERV Group 13 to 16 categories, respectively. The filter is categorized in the MERV Group 9 to 12 area because the average efficiency in Range 2 is below the 90% minimum requirement for the MERV Group 13 to 16 category. The average efficiency in Range 1 is not used for reporting. Based on the average efficiency of 42% in Range 2, this filter is reported as MERV9 at 0.93.

D2.4 “Filter D”—The reporting value for this air cleaner is **MERV8 at 0.93**. This minimum performance curve is typical of a media air cleaner currently marketed as a 25% to 30% dust spot filter when tested at 0.93 m³/s (1970 cfm). The range efficiencies are calculated as follows:

Range	Size	PSE in Range, %	Average PSE, %
1	0.30 to 1.0	5, 6, 6, 8	6
2	1.0 to 3.0	12, 22, 33, 55	31
3	3.0 to 10	70, 78, 84, 90	81

The average efficiency in Range 3 is in the 80% to 85% range shown in Table 12-1 for the MERV Group 10 category. However, the E2 value is above the 20% required for MERV 8 and below the 35% required for MERV 9. Thus, the MERV of this filter is reported as MERV 8 at 0.93.

D2.5 “Filter E”—The dust-loading test in this standard **cannot be used to report this air cleaner**. This minimum performance curve is typical of a media air cleaner currently marketed as a “furnace” filter. The average efficiencies are below the 20% minimum requirement shown in Table 12-1 for MERV Group 5 to 8:

Range	Size, μm	PSE in Range, %	Average PSE, %
1	0.30 to 1.0	1, 1, 2, 3	2
2	1.0 to 3.0	8, 10, 13, 12	11
3	3.0 to 10	12, 11, 4, 2	7

The filter is classified as MERV Group 1 to 4 and must be tested in accordance with the arrestance method outlined in Section 10.7 of this standard. The air cleaner can then be reported in accordance with Table 12-1 using the average arrestance value.

D3. CONCLUSIONS

In most cases, comparisons of air cleaners of similar type and material will yield good relationships between laboratory and field conditions. However, the user must be aware that the tests are made under laboratory conditions using synthetic dust for loading. The synthetic dust used to load the test air cleaner is not representative of all atmospheric particulates, and, thus, tests on some types of air cleaners may be affected favorably or otherwise.

(This appendix is not part of this standard. It is merely informative and does not contain requirements necessary for conformance to the standard. It has not been processed according to the ANSI requirements for a standard and may contain material that has not been subject to public review or a consensus process. Unresolved objections on informative material are not offered the right to appeal at ASHRAE or ANSI.)

INFORMATIVE APPENDIX E CROSS-REFERENCE AND APPLICATION GUIDELINES

E1. INTRODUCTION

E1.1 The purpose of this appendix is to provide an approximate cross reference of Standard 52.1-1992 reporting methods (arrestance and atmospheric dust-spot efficiency) to the air-cleaner minimum efficiency reporting system outlined in Section 12. A corollary purpose is to provide application guidance to the user and HVAC system designer. To do this most effectively, HEPA/ULPA filters have been added to the reporting system. HEPA/ULPA filters have been assigned MERVs based on their performance in accordance with Institute of Environmental Sciences and Technology (IEST) standards. Table E-1 combines all of the parameters into a single reference covering most general ventilation air-cleaner types and applications.

E1.2 A single performance measurement system cannot be applied precisely to all types and styles of air cleaners. Each air cleaner has unique characteristics that change during its useful life. Also, the particle size efficiency test method in this standard does not eliminate the need for dioctyl phthalate (DOP) penetration and arrestance testing. This new reporting system may, however, eventually replace the arrestance and atmospheric dust-spot and DOP efficiency reporting values as performance references.

E1.3 Typical contaminants listed in Table E-1, "Application Guidelines," appear within the general reporting group that removes the smallest known size of that particular contaminant. The order in which they are written has no significance, nor is the list complete.

E1.4 Typical applications and typical air-cleaner types listed are intended to show where and what type air cleaner is traditionally used. The order in which they are written has no significance, nor is the list complete. Traditional use may not represent the optimum choice, so using the table as a selection guide is not appropriate when a specific performance requirement is needed. Consultation with an air-cleaner specialist is then advisable, and manufacturer's performance curves should be reviewed.

E1.5 Some knowledge of how air cleaners work and common sense will also help the user achieve satisfactory results. Air-cleaner performance varies from the time it is first installed until it reaches the end of its service life. Generally, the longer a media-type filter is in service, the better it performs. The accumulation of contaminants begins to close the porous openings and, therefore, the filter is able to intercept particles of smaller size. However, there are exceptions that vary with different styles of media-type filters.

E1.6 Some air cleaners, particularly those in the lower part of the minimum efficiency reporting values, may begin to shed some of the collected contaminants after varying lengths of service life. Testing with standardized synthetic loading dust attempts to predict this occurrence, but this will rarely, if ever, duplicate performance on atmospheric dust.

E2. AIR-CLEANER EFFECTIVENESS

Three factors determine the effectiveness of an air cleaner to treat the air in an occupied space: air-cleaner efficiency, the amount of air being filtered, and the path that the clean air follows after it leaves the filter.

E2.1 As an example of the interaction of air-cleaner efficiency and airflow rate, portable self-contained (fan and filter) air-cleaner effectiveness is often measured by the clean air delivery rate (CADR), which is the combined effect of how much air actually is moved through the filter and the efficiency of the filter. A high-efficiency air filter in an air cleaner with a low airflow rate can have a lower CADR than one with a lower MERV air filter but higher airflow volume.

E2.2 An airflow path considered best would be one that would enter the space where the cleanest air is required, flow without turbulence through 100% of the space toward the point where cleanliness is least important (perhaps near the floor), and then return to the air cleaner. These ideal conditions can rarely be met, so most installations must be a compromise between what is desired and what is practical.

E2.3 Air cleaners are tested under ideal laboratory conditions where care is taken to prevent leakage of air around them. Totally leak-free hardware is unusual in HVAC equipment, so air cleaners rarely perform to the same degree of effectiveness under field conditions. Only extreme care in finding and sealing all the leak paths in the hardware and in ductwork between the filter and the fan will ensure full performance of the air cleaner.

E2.4 Table E-1, "Application Guidelines" covers particulate contamination control only, as does this standard. Gaseous contaminant control is also important in many systems but is not addressed in this guideline.

Table E-1 Application Guidelines

Std. 52.2 Minimum Efficiency Reporting Value (MERV)	Application Guidelines		
	Typical Controlled Contaminant	Typical Applications and Limitations	Typical Air Filter/Cleaner Type
16	0.30 to 1.0 μm Particle Size	Hospital inpatient care	Bag Filters
15	All bacteria	General surgery	Nonsupported (flexible) microfine fiberglass or synthetic media. 300 to 900 mm (12 to 36 in.) deep, 6 to 12 pockets.
14	Most tobacco smoke	Smoking lounges	Box Filters
13	Droplet nuclei (sneeze)	Superior commercial buildings	Rigid style cartridge filters 150 to 300 mm (6 to 12 in.) deep may use lofted (air laid) or paper (wet laid) media.
	Cooking oil		
	Most smoke		
	Insecticide dust		
	Copier toner		
	Most face powder		
	Most paint pigments		
12	1.0 to 3.0 μm Particle Size	Superior residential	Bag Filters
11	Legionella	Better commercial buildings	Nonsupported (flexible) microfine fiberglass or synthetic media. 300 to 900 mm (12 to 36 in.) deep, 6 to 12 pockets.
10	Humidifier dust	Hospital laboratories	Box Filters
9	Lead dust		Rigid style cartridge filters 150 to 300 mm (6 to 12 in.) deep may use lofted (air laid) or paper (wet laid) media.
	Milled flour		
	Coal dust		
	Auto emissions		
	Nebulizer drops		
	Welding fumes		
8	3.0 to 10.0 μm Particle Size	Commercial buildings	Pleated Filters
7	Mold	Better residential	Disposable, extended surface, 25 to 125 mm (1 to 5 in.) thick with cotton-polyester blend media, cardboard frame.
6	Spores	Industrial workplaces	Cartridge Filters
5	Hair spray	Paint booth inlet air	Graded density viscous coated cube or pocket filters, synthetic media.
	Fabric protector		Throwaway
	Dusting aids		Disposable synthetic media panel filters.
	Cement dust		
	Pudding mix		
	Snuff		
	Powdered milk		
4	>10.0 μm Particle Size	Minimum filtration	Throwaway
3	Pollen	Residential	Disposable fiberglass or synthetic panel filters
2	Spanish moss	Window air conditioners	Washable
1	Dust mites		Aluminum mesh, latex coated animal hair, or foam rubber panel filters
	Sanding dust		Electrostatic
	Spray paint dust		Self charging (passive) woven polycarbonate panel filter
	Textile fibers		
	Carpet fibers		

Note: A MERV for other than HEPA/ULPA filters also includes a test airflow rate, but it is not shown here because it has no significance for the purposes of this table.

Copyrighted material Licensed to Peter Goss on 2017-05-28 for Licensee's use only. All rights reserved. No further reproduction or distribution is permitted. Distributed by Techstreet for ASHRAE, www.techstreet.com

(This appendix is not part of this standard. It is merely informative and does not contain requirements necessary for conformance to the standard. It has not been processed according to the ANSI requirements for a standard and may contain material that has not been subject to public review or a consensus process. Unresolved objections on informative material are not offered the right to appeal at ASHRAE or ANSI.)

INFORMATIVE APPENDIX F
ACRONYMS AND CONVERSION FORMULAE

F1. ACRONYMS

CADR	Clean air delivery rate
IAQ	Indoor air quality
IENT	Institute of Environmental Sciences and Technology
OPC	Optical particle counter

For the meanings of other acronyms, refer to Section 3.2.

F2. CONVERSION FORMULAE

The following units and conversions may be useful in using this standard.

1 m	≈	3.2808 ft
1 m ²	≈	10.764 ft ²
1 m ³	≈	35.315 ft ³
1 m/s	≈	196.85 fpm
1 m ³ /s	≈	2118.9 cfm
1 m ³ /s	=	1000 L/s
1 m ³ /min	≈	35.315 cfm
1 m ³ /h	≈	0.5886 cfm
1 cm ³ /s	≈	0.00212 cfm
1 Pa	≈	0.00402 in. of water

A converted value is no more precise than the original value. The final value should be rounded off to the same number of significant figures as the original value.

(This appendix is not part of this standard. It is merely informative and does not contain requirements necessary for conformance to the standard. It has not been processed according to the ANSI requirements for a standard and may contain material that has not been subject to public review or a consensus process. Unresolved objections on informative material are not offered the right to appeal at ASHRAE or ANSI.)

INFORMATIVE APPENDIX G INFORMATIVE REFERENCES

The following references are cited for information only. Normative references are located in Section 13 of the standard.

1. ASHRAE. 1991. *ASHRAE Terminology of Heating, Ventilation, Air Conditioning, & Refrigeration*, Second Edition. Atlanta: ASHRAE.
2. See normative references in Section 13.

3. Riehl, J., V.R. Dileep, N.K. Anand, and A.R. McFarland. 1996. *DEPOSITION 4.0: An Illustrated User's Guide*. Report 8836/07/96, Aerosol Technology Laboratory, Department of Mechanical Engineering, Texas A&M University, College Station, TX.
4. See normative references in Section 13.
5. See normative references in Section 13.
6. See normative references in Section 13.
7. See normative references in Section 13.
8. See normative references in Section 13.
9. See normative references in Section 13.
10. ASME. 1989. ASME Standard MFC-3M, *Measurement of Fluid Flow in Pipes Using Orifices, Nozzles and Venturi*. New York: American Society of Mechanical Engineers.
11. See normative references in Section 13.
12. See normative references in Section 13.

(This appendix is not part of this standard. It is merely informative and does not contain requirements necessary for conformance to the standard. It has not been processed according to the ANSI requirements for a standard and may contain material that has not been subject to public review or a consensus process. Unresolved objectors on informative material are not offered the right to appeal at ASHRAE or ANSI.)

INFORMATIVE APPENDIX H

ADDENDA DESCRIPTION INFORMATION

ANSI/ASHRAE Standard 52.2-2017 incorporates ANSI/ASHRAE Standard 52.2-20012 and Addenda a, b, c, d, e, f, g, and i to ANSI/ASHRAE Standard 52.2-2012. Table H-1 lists the addendum and describes the way in which the standard is affected by the change. It also lists the ASHRAE and ANSI approval dates for the addendum.

Table H-1 Addenda to ANSI/ASHRAE Standard 52.2-2012

Addendum	Sections Affected	Description of Changes*	ASHRAE Standards Committee Approval	ASHRAE BOD Approval	ANSI Approval
a	12, Appendix D, Appendix J	Replaces Table 12-1, modifies language in D2.4 to correspond to updated Table 12-1, and replaces Table J-2.	12/30/14	12/30/14	12/31/14
b	3.1, 10.1, 10.4.2, 10.6.3.2, 10.6.3.3, 10.7.3, 11, C2.1	Adds new definition, adds symbol, modifies language in 10.4.2, clarifies equation in 10.6.3.2, replaces equation in 10.6.3.3, revises 10.7.3 and adds new section 10.7.3.3, adds language to 11.2, revises Figure 11-1d, adds language to C2.1.	6/28/14	7/2/14	7/31/14
c	3.1, 4.6, 5.1, 5.15, 5.16, 10.6.2, 10.6.4	Adds new definition, adds new language to Section 4.6, adds new Sections 5.15 and 5.16, adds new language to Section 10.6.2.5, and corrects numbering in Section 10.6.4.1.	7/1/15	NA	7/28/15
d	4.2.3, 4.3.2, Appendix J	Revises relative humidity language in 4.2.3, 4.3.2, and J10.8.	6/28/14	7/2/14	7/3/14
e	12.5	Adds new Section 12.5.	2/29/16	NA	3/1/16
f	11.3 and Figure 11-1d	Modifies language in Section 11.3 and makes changes to Figure 11-1d.	2/29/16	NA	3/1/16
g	Appendix K	Adds new Appendix K.	12/30/16	NA	12/30/16
i	13, Appendix G, 6.2	Removes a reference and adds new reference to Section 13, modifies language in Section 6.2, removes footnote 38.	12/30/16	NA	12/30/16

NOTE

Approved addenda, errata, or interpretations for this standard can be downloaded free of charge from the ASHRAE Web site at www.ashrae.org/technology.

(This appendix is not part of this standard. It is merely informative and does not contain requirements necessary for conformance to the standard. It has not been processed according to the ANSI requirements for a standard and has not been subject to public review or a consensus process. Unresolved objectors on informative material are not offered the right to appeal at ASHRAE or ANSI.)

INFORMATIVE APPENDIX I (INTENTIONALLY LEFT BLANK)

(This appendix is not part of this standard. It is merely informative and does not contain requirements necessary for conformance to the standard. It has not been processed according to the ANSI requirements for a standard and has not been subject to public review or a consensus process. Unresolved objectors on informative material are not offered the right to appeal at ASHRAE or ANSI.)

INFORMATIVE APPENDIX J

OPTIONAL METHOD OF CONDITIONING A FILTER USING FINE KCL PARTICLES TO DEMONSTRATE EFFICIENCY LOSS THAT MIGHT BE REALIZED IN FIELD APPLICATIONS

J1. PURPOSE OF OPTIONAL TEST

Appendix J presents a conditioning procedure to determine the magnitude of the efficiency loss a filter may realize in field applications. This procedure is a separate test from that described in Section 10.7.1.2(b). For any particular type or model of filter, the test described in the body of the standard must be used. If desired, both tests may be used; however, the same test filter may not be tested with both methods. When the test in Appendix J is used, the data output obtained from the efficiency test procedure after the KCl conditioning step is referred to as MERV-A, as defined in Section J2.2. The data output value is thus differentiated from the MERV value that is the data output of the test without the KCl conditioning.

The conditioning step described herein is representative of the best available knowledge of real-life filter efficiency degradation at the time of the publication of this procedure. Changes in filtration performance are environment dependent and, therefore, filters may or may not degrade to the conditioned efficiencies described in this document. For this reason, the results in this appendix may be used to compare filters as described in the foreword to Standard 52.2 (see section titled “Not an Application Standard”).

The goal of this appendix is to provide an optional conditioning method of test, gather data using this method, and validate this method to achieve consensus for possible future incorporation into the body of the standard. This procedure is being included as an option to the test method so that those concerned about a possible drop in filtration efficiency have a recognized test method to predict the magnitude of the efficiency loss. This standard is under continuous maintenance, and the committee welcomes continuous maintenance proposals addressing means to improve the method.

J2. DEFINITIONS AND ACRONYMS

J2.1 Definitions to be used in addition to those listed in Section 3 of the standard are as follows:

condensation particle counter (CPC): an instrument used to measure the concentration of submicrometer aerosol particles. Also called a *condensation nucleus counter (CNC)*.

conditioning aerosol: a submicrometer solid-phase potassium chloride aerosol used to reproduce the falloff in efficiency that electret filters may experience in real-life applications.

CT: for the conditioning aerosol, the product of the in-duct aerosol concentration C measured with the CPC and the exposure time T .

Laskin generator: a nozzle that uses a source of compressed air as part of a system to generate a polydispersed aerosol from a liquid. **Note:** A Laskin generator is shown in *NSF Standard 49: Class II (Laminar Flow) Biosafety Cabinetry*.

J2.2 Acronyms to be used in addition to those listed in Section 3 of the standard are as follows:

A_{avg} -A = average value of the arrestances made on the device during loading test when Appendix J conditioning is used.

DHC-A = the total weight of the synthetic loading dust captured when Appendix J conditioning is used.

MERV-A #-A = minimum efficiency reporting value according to Appendix J, where # represents the numeric value from Table J-2.

J3. TEST APPARATUS FOR CONDITIONING AEROSOL IN ADDITION TO THE TEST APPARATUS REQUIRED IN SECTION 4, “TEST APPARATUS”

J3.1 Condensation Particle Counter. The in-duct concentration of the conditioning aerosol shall be measured with a CPC having a minimum 50% counting efficiency at 0.02 μm . The CPC shall have a concentration limit of $\geq 500,000 \text{ cm}^{-3}$. The CPC shall not be operated above its concentration limit.

J3.2 Laskin Generator. The conditioning aerosol shall be generated using one or more Laskin generators. The aerosol output of the Laskin generators is not required to be passed through a charge neutralizer. The nozzles shall be operated at air pressures of 20 to 60 psig. The Laskin generators shall be operated with an aqueous solution of KCl in water prepared to a ratio of 1.00 g of reagent grade KCl for each 1.00 L of distilled or filtered deionized water. The compressed air line supplying the Laskin generator shall be equipped with devices for the removal of oil and water and have a high-efficiency particle filter (99.97% @ 0.3 μm or better) installed near the Laskin generators. The conditioning aerosol shall be injected between the inlet filter bank (item 3 of Figure 4-1) and the upstream mixing orifice (item 9 of Figure 4-1).

J3.3 Separate Duct for Conditioning Step. The use of a separate duct for the conditioning portion of the test is acceptable as long as the conditioning duct meets the following criteria:

- The cross-sectional dimensions of the duct are 610 \times 610 mm (24 \times 24 in.).
- The HEPA filter bank, transition, aerosol injection tube, mixing orifice, perforated diffusion plate, upstream sampling probe, and main flow measurement nozzle are designed and installed according to Section 4.2.
- The test filter does not extend beyond the length of the duct.
- Test environmental conditions meet Section 4.2.3.

The conditioning duct can be operated in a positive or a negative pressure mode.

J4. SUBSECTION TO BE USED WITH SECTION 5.1

J4.1 If a separate duct is used for the conditioning step (see Section J3.3) then velocity uniformity (see Section 5.2) shall be performed on that duct.

J5. SUBSECTION TO BE USED WITH SECTION 5, "APPARATUS QUALIFICATION TESTING"**J5.1 Uniformity of the Conditioning Aerosol Concentration**

J5.1.1 The uniformity of the conditioning aerosol concentration across the duct cross section shall be determined by a nine-point traverse in the 610 × 610 mm (24 × 24 in.) duct immediately upstream of the device section (i.e., at the location of the upstream sample probe) using the grid points shown in Figure 5-1. The traverse shall be made by either (a) installing nine sample probes of identical curvature, diameter, and inlet nozzle diameter but of variable vertical length or (b) repositioning a single probe.

J5.1.2 The conditioning aerosol generation system shall be operated in the same manner as intended for conditioning of test filters.

J5.1.3 The aerosol concentration measurements shall be made with a CPC meeting the specifications of Section J3.1. A one-minute average concentration shall be recorded at each grid point. The average shall be based on at least ten readings

taken at equal intervals during the one-minute period. After sampling all nine points, the traverse shall then be repeated four more times to provide a total of five samples from each point. These five values for each point shall then be averaged. The traverse measurements shall be performed at airflow rates of 0.22, 0.93, and 1.4 m³/s (472, 1970, and 2990 cfm).

J5.2 The CV of the corresponding nine grid point particle concentrations shall be less than 15% for each airflow rate.

J5.2.1 Ratio of Small to Large Particles in the Conditioning Aerosol. With the conditioning aerosol generator operating as it would for conditioning operation during a standard test, the in-duct aerosol concentration shall be measured with the CPC and with the particle counter used for PSE testing. The CPC sample inlet shall be located within 100 mm (4 in.) of the OPS inlet, and they can share the same inlet. The ratio of the CPC concentration to the concentration of particles >0.3 μm (measured by the PSE particle counter and consisting of all particles measured between 0.3 and 10 μm) shall be >20,000.

Note: The units of concentration must be the same to calculate the correct ratio. Typically the particle counter output is in units of particles/m³ and the CPC output is in units of particles/cm³.

J6. SUBSECTION TO BE USED WITH TABLE 5-1, SYSTEM QUALIFICATION MEASUREMENT REQUIREMENTS OF THE STANDARD

Parameter	Requirement
Ratio of the CPC concentration to the concentration of particles >0.3 μm (measured by the PSE particle counter)	Ratio > 20,000
Conditioning aerosol uniformity: based on traverse measurements made over a 9-point equal-area grid at each test airflow rate	CV < 15%
Conditioning aerosol in-duct aerosol concentration	<1 × 10 ⁶ cm ⁻³ or less than the concentration limit of the CPC, whichever is smaller

J7. SUBSECTION TO BE USED WITH TABLE 5-2, APPARATUS MAINTENANCE SCHEDULE OF THE STANDARD

Maintenance Item	Incorporated into Each Test	Monthly	Biannually	After Change that May Alter Performance	Comment
Drain, rinse, and refill the Laskin generator with fresh 0.1% KCl solution					Daily
Ratio of the CPC concentration to the concentration of particles >0.3 μm	×				
Conditioning aerosol uniformity			×	×	
Conditioning aerosol concentration	×				

J8. SUBSECTION TO BE USED WITH SECTION 6, "TEST MATERIALS"

J8.1 Conditioning Aerosol. The conditioning aerosol shall be solid-phase potassium chloride (KCl) particles generated from an aqueous solution. The solution shall be prepared by dissolving reagent-grade KCl in distilled or filtered deionized water at a proportion of 1.00 g of KCl per 1.00 L of water.

J9. SUBSECTION TO BE USED WITH SECTION 8.2, "TEST SEQUENCE"

J9.1 Test Sequence. The sequence of tests on the device shall be as follows:

- Resistance vs. airflow rate of the clean device at various airflow rates as prescribed in Section 9.
- PSE of the clean device as prescribed in Section 10.
- PSE of the device, as prescribed in Section 10, after conditioning per this appendix.
- PSE of the device, as prescribed in Section 10, when incrementally loaded with synthetic dust, with the exception of the 30 g conditioning load (see Section 10.7.1.2.b).

**J10. CONDITIONING PROCEDURE
(USE THIS PROCEDURE INSTEAD OF
SECTION 10.7.1.2.B OF THE STANDARD)**

J10.1 After the initial efficiency test is completed, the filter shall be exposed to the conditioning aerosol. The duct airflow rate used during the conditioning step will be the same as is used during the dust-loading and particle size efficiency testing. Note that all filters tested according to this standard must be exposed to the same conditioning aerosol procedure, regardless of the specific materials, construction details, or other variables.

J10.2 Prior to conditioning, all internal surfaces of the Laskin generator shall be rinsed with distilled or filtered deionized water and then filled with KCl solution, as specified in Section J8.1.

J10.3 Record the background concentration using the CPC upstream of the test device with the duct airflow rate set to the same value used during testing.

J10.4 The measured in-duct conditioning aerosol concentration shall not exceed 1.0×10^6 particles/cm³.

J10.5 Conditioning shall be performed in incremental steps with a PSE taken after each increment. The minimum incremental conditioning step shall be a CT of 6.4×10^7 particles/cm³·min. Conditioning is stopped when either (a) the current measurement shows no further significant drop in efficiency or (b) the cumulative CT exposure of the filter reaches a CT of 1.2×10^9 particles/cm³·min. A "significant drop" is a drop in efficiency of at least two percentage points in two or more adjacent particle size ranges relative to the minimum efficiencies in those ranges measured in any of the previous steps.

Note: Filters with large media area (typical of 300 mm or 12 in. filters and bag filters) may require cumulative conditioning CTs up to the maximum level of 1.2×10^9 particles/cm³·min. The test laboratory should select an incremental conditioning step size consistent with this expectation and avoid relatively

small conditioning increments that may underchallenge the filter.

J10.6 Periodically during conditioning, the in-duct concentration of the conditioning aerosol shall be measured and recorded. The measurement interval shall be such that a minimum of three measurements are obtained during each conditioning interval.

J10.7 Whenever the determined correlation ratio is (see Section 10.3), it is recommended that the ratio of the concentration of small to large particles be measured. This ratio must be evaluated a minimum of two times during the conditioning procedure, once at the beginning of the conditioning and once at the end of the conditioning. The small-particle concentration is that obtained from the CPC. The large-particle concentration is that obtained from the PSE particle counter and is the concentration of all particles $>0.3 \mu\text{m}$. The ratio of the concentrations must be $>20,000$.

J10.8 To prevent deliquescence of the KCl during conditioning, relative humidity must be maintained below 50% in the test duct at all times during the test. Also, the airflow from all particle generators must result in relative humidity $\leq 50\%$ in the air in the rig at all times after mixing has occurred. If the filter is removed from the test duct for any reason during the test, it must be stored in an environment with relative humidity less than 65%.

J11. SUBSECTION TO BE USED WITH SECTION 11.2**J11.1 Conditioning**

- The background concentration (particles/cm³)
- The average conditioning aerosol concentration (particles/cm³)
- The cumulative conditioning duration (minutes)
- The cumulative conditioning CT (particles/cm³·min)
- The PSE following each conditioning increment
- Dust holding capacity DHC-A (grams)

**J11.2 Minimum Efficiency Reporting Value (MERV-A)
According to Appendix J**

- The average of the minimum PSE of the four size ranges from 0.30 to 1.0 μm (E_1 -A)
- The average of the minimum PSE of the four size ranges from 1.0 to 3.0 μm (E_2 -A)
- The average of the minimum PSE of the four size ranges from 3.0 to 10.0 μm (E_3 -A)
- MERV-A for the device

**J11.3 Minimum Efficiency Reporting Value (MERV-A)
According to Appendix J for Air Cleaners**

J11.3.1 The minimum efficiency reporting value (MERV-A) for an air cleaner shall be based on three composite average PSE points developed from a test at a manufacturer's specified airflow rate selected in accordance with Section 8.1. Dust loading shall follow the procedure outlined in Section 10.7 except substituting Section J10 of this appendix for Section 10.7.1.2(b) of the standard. The results of the tests shall be reported in accordance with Sections 10.8.1 and 10.8.2. The four data points from the Section 10.8.2 composite curve in each of the three size range groups from

Table J-1 shall be averaged and the resultant three average minimum PSEs (E_1 -A, E_2 -A, and E_3 -A) shall be reported.

J11.3.2 With this appendix, the minimum final resistance for an air cleaner shall always be the same as or greater than twice the initial resistance.

J11.3.3 With this appendix, the minimum efficiency reporting value in the specified size ranges for reporting purposes shall be in accordance with Table J-2.

J11.3.4 The reporting designator shall be a combination of the air cleaner's MERV-A and the test airflow rate (e.g., MERV-A 10-A at 0.93 indicates that the air cleaner has a

Table J-1 Size Range Groups

Average Minimum PSE Designator	Corresponding Size Range Group, μm
E_1 -A	0.30 to 1.0
E_2 -A	1.0 to 3.0
E_3 -A	3.0 to 10

Table J-2 KCl Conditioned Per Appendix J Minimum Efficiency Reporting Value (MERV-A) Parameters

Standard 52.2 Minimum Efficiency Reporting Value (MERV-A)	Composite Average Particle Size Efficiency, % in Size Range, μm			
	Range 1 (0.30 to 1.0 μm)	Range 2 (1.0 to 3.0 μm)	Range 3 (3.0 to 10.0 μm)	Average Arrestance, %
1-A	N/A	N/A	E_3 -A < 20	$A_{avg} < 65$
2-A	N/A	N/A	E_3 -A < 20	$65 \leq A_{avg}$
3-A	N/A	N/A	E_3 -A < 20	$70 \leq A_{avg}$
4-A	N/A	N/A	E_3 -A < 20	$75 \leq A_{avg}$
5-A	N/A	N/A	$20 \leq E_3$ -A	N/A
6-A	N/A	N/A	$35 \leq E_3$ -A	N/A
7-A	N/A	N/A	$50 \leq E_3$ -A	N/A
8-A	N/A	$20 \leq E_2$ -A	$70 \leq E_3$ -A	N/A
9-A	N/A	$35 \leq E_2$ -A	$75 \leq E_3$ -A	N/A
10-A	N/A	$50 \leq E_2$ -A	$80 \leq E_3$ -A	N/A
11-A	$20 \leq E_1$ -A	$65 \leq E_2$ -A	$85 \leq E_3$ -A	N/A
12-A	$35 \leq E_1$ -A	$80 \leq E_2$ -A	$90 \leq E_3$ -A	N/A
13-A	$50 \leq E_1$ -A	$85 \leq E_2$ -A	$90 \leq E_3$ -A	N/A
14-A	$75 \leq E_1$ -A	$90 \leq E_2$ -A	$95 \leq E_3$ -A	N/A
15-A	$85 \leq E_1$ -A	$90 \leq E_2$ -A	$95 \leq E_3$ -A	N/A
16-A	$95 \leq E_1$ -A	$95 \leq E_2$ -A	$95 \leq E_3$ -A	N/A

ASHRAE Standard 52.2 Air-Cleaner Performance Report Summary with Optional Conditioning Procedure According to Appendix J

(This report applies to the tested device only)

Laboratory Data

Report number _____ Test number _____ Date _____

Test laboratory _____

Operator _____ Supervisor _____

Particle counters: Brand _____ Model _____

Device Manufacturer's Data

Manufacturer _____ Product name _____

Model _____ Test requested by _____

Sample obtained from _____

Catalog rating: Airflow rate _____ Initial pressure drop _____

Specified test conditions: Airflow _____ Final pressure drop _____

Face velocity _____

Device Description

Dimensions: Height _____ Width _____ Depth _____

Generic name _____ Media type _____

Effective media area _____ Media color _____

Amount and type of adhesive (Tackifier) _____

Other attributes _____

Test Conditions

Airflow rate _____ Temperature _____ Relative Humidity _____

Test aerosol type _____ Final pressure drop _____ Face velocity _____

Duct configuration (one or two ducts used): _____

Remarks _____

Conditioning Parameters

Background concentration (particles/cm³) _____

Average cond aerosol concentration (particles/cm³) _____

Cumulative conditioning duration (minutes) _____

Is filter continuously conditioned in the same duct? _____

Cumulative conditioning CT (particles/cm³ min) _____

PSE following each conditioning increment _____

Resistance Test Results

Initial resistance _____ Final resistance _____

KCI Conditioned Minimum Efficiency Reporting Data (According to Appendix J)

Composite average efficiencies: E_1 -A _____ E_2 -A _____ E_3 -A _____

Air-cleaner average arrestance: A_{avg} -A _____

Dust holding capacity: DHC-A _____

Minimum efficiency reporting value: MERV-A _____

(This appendix is not part of this standard. It is merely informative and does not contain requirements necessary for conformance to the standard. It has not been processed according to the ANSI requirements for a standard and has not been subject to public review or a consensus process. Unresolved objectors on informative material are not offered the right to appeal at ASHRAE or ANSI.)

INFORMATIVE APPENDIX K OPTIONAL METHOD OF TESTING TWO AIR FILTERS ARRANGED IN SERIES IN A SYSTEM TO EVALUATE PARTICLE REMOVAL, DUST LOADING, AND PRESSURE DROP INCREASE THAT MIGHT BE REALIZED IN FIELD APPLICATIONS

K1. PURPOSE OF OPTIONAL TEST

This appendix is to be used to evaluate the performance of two air-cleaning devices arranged in airflow series. In this appendix the first filter serves as a prefilter and the second filter serves as the final filter. It is possible for both filters to be the same filter. The test protocol is based on ASHRAE Standard 52.2. Equipment and procedures specified in Standard 52.2 are used to conduct this test.

This procedure measures the ability of the prefilter and final filter to remove dust as the filters become loaded with a standardized loading dust. The loading dust is fed at intervals to simulate accumulation of particles during filter service life. Resistances of the individual filters are monitored separately. The prefilter is replaced with a new prefilter whenever its preselected final resistance is reached. This process is continued until the preselected resistance of the final filter is reached. After the initial particle size efficiency (PSE) test, the resistance of the final filter is used to position the five additional PSE tests.

K2. DEFINITIONS AND ACRONYMS

K2.1 Definitions to be used in addition to those listed in Section 3 of Standard 52.2 are as follows.

dust-holding capacity final filter (DHCF): the total weight of the synthetic loading dust captured by the second-in-series air-cleaning device over the dust-loading steps until the final filter reaches its predetermined final resistance.

dust-holding capacity prefilter #1 (DHCPF1): the total weight of the synthetic loading dust captured by the first-in-series air-cleaning device over the dust-loading steps until the prefilter reaches its predetermined final resistance. Each additional prefilter designation would be the next incremental numerical digit, i.e., DHCPF2, DHCPF3.

final filter: the second filter in the two-stage system.

prefilter: the first filter in the two-stage system.

total system dust-holding capacity (TDHC): the sum total weight of the synthetic loading of all prefilters and the final filter.

K3. SUBSECTION TO BE USED WITH SECTION 7.2, "PREPARATION OF THE SAMPLES"

K3.1 The devices shall be installed in the duct with a space between the filters of 203 to 914 mm (8 to 36 in.).

K3.2 Distance between devices should be documented in the test report.

K4. SUBSECTION TO BE USED WITH SECTION 8.2, "TEST PROCEDURES"

K4.1 Test Sequence. The sequence of tests on the two-stage system shall be as follows:

- Resistance vs. airflow rate of the prefilter at various airflow rates as prescribed in Section 9.
- Resistance vs. airflow rate of the final filter at various airflow rates as prescribed in Section 9.
- PSE prescribed in Section 10.7.1.2(b) to be replaced with the following: *The prefilter after an initial conditioning step with a dust loading of 30 g or an increase of 10 Pa (0.04 in. of water) pressure drop across the prefilter, whichever comes first.*
- PSE prescribed in Section 10.7.1.2(c) to be replaced with the following: *After the dust-loading increments have achieved an airflow resistance increase of one-quarter, one-half, and three-quarters of the difference between the beginning and the prescribed end-point limit of airflow resistance for the final filter.*
- PSE prescribed in Section 10.7.1.2(d) to be replaced with the following: *After the dust increment that loads the final filter to its prescribed end point resistance limit.*

K5. SUBSECTION TO BE USED WITH SECTION 9, "MEASUREMENT OF RESISTANCE VERSUS AIRFLOW"

K5.1 Measure, record, and report the resistance of the prefilter, the final filter, and the system at a minimum of four airflow rates: 50%, 75%, 100%, and 125% of test airflow rate. Resistance shall be measured between the static taps.

K6. SUBSECTION TO BE USED WITH SECTION 10.7.2, "DUST LOADING PROCEDURES"

K6.1 When the prefilter reaches its prescribed final resistance, it shall be replaced by a clean prefilter. The replacement filter shall be identical to the one being replaced.

K6.2 Repeat the prefilter replacement process until the final filter reaches its final resistance.

K6.3 Weigh each prefilter to the nearest 0.1 g before and after use to determine dust weight gain (DWG).

K6.4 Weigh final filter to the nearest 0.1 g before and after use to determine DWG.

K7. SUBSECTION TO BE USED WITH SECTION 10.8, "REPORTING RESULTS OF LOADING TESTS"

K7.1 Results of loading tests shall be reported in the form of PSE curves for the two-stage system:

- a. clean;
- b. after each incremental dust loading of the final filter, a total of four curves; and
- c. at final filters final loading point.

K8. SUBSECTION TO BE USED WITH SECTION 11, "REPORTING RESULTS"

K8.1 The summary section of the performance report shall include the following information.

- a. Name and location of the test laboratory
- b. Date of the test
- c. Test operator's names
- d. Brand and model number of the particle counting and sizing devices
- e. Air-cleaner manufacturer's name (or name of the marketing organization if different from the manufacturer)
- f. How the sample was obtained
- g. Description of each test air cleaner, including the following:
 - 1. Brand and model number
 - 2. Physical description of construction (e.g., extended surface—number of pockets or number of pleats; pleated panel—number and depth of pleats)
 - 3. Face dimensions and depth
 - 4. For fiber media air cleaners
 - i. Type and color of media
 - ii. Effective media area
 - iii. Type and amount of dust adhesive if known
 - iv. Electrostatic charge if known
 - 5. Any other pertinent descriptive attributes
- h. Operating data as stated by the manufacturer
 - 1. Test conditions for reporting purposes: airflow rate
 - 2. Final resistances for both air cleaners

- 3. Any other operating data furnished
- i. Test data
 - 1. Test air temperature and relative humidity
 - 2. Airflow rate
 - 3. Type of test aerosol
 - 4. Distance between the two filters from back edge of prefilter to front edge of final filter
- j. Results of resistance testing
 - 1. Initial resistance of prefilter
 - 2. Initial resistance of final filter
 - 3. Initial resistance of system
 - 4. Final resistance of system
 - 5. Number of times the prefilter is changed
- k. Performance curves
 - 1. A curve in Figure 11-1b format of the prefilter, final filter, and system resistance when clean vs. airflow rates from 50% to 125% of test flow
 - 2. A curve in Figure 11-1c format of PSE for the clean system and for the system at each of the five loading stages of the final filter
 - 3. A minimum PSE composite curve in Figure 11-1c format whose data points are the lowest PSEs from the six measurements in each particle size range from the curves of test results for the system
 - 4. Resistance vs. synthetic loading dust fed during the entire test sequence for prefilter, final filter, and system
- l. Average ASHRAE dust arrestance
- m. Dust holding capacity (DHC)
 - 1. A DHC for each prefilter
 - 2. A DHC for the final filter
 - 3. A DHC for the entire test cycle

NOTICE

INSTRUCTIONS FOR SUBMITTING A PROPOSED CHANGE TO THIS STANDARD UNDER CONTINUOUS MAINTENANCE

This standard is maintained under continuous maintenance procedures by a Standing Standard Project Committee (SSPC) for which the Standards Committee has established a documented program for regular publication of addenda or revisions, including procedures for timely, documented, consensus action on requests for change to any part of the standard. SSPC consideration will be given to proposed changes within 13 months of receipt by the Senior Manager of Standards (SMOS).

Proposed changes must be submitted to the SMOS in the latest published format available from the SMOS. However, the SMOS may accept proposed changes in an earlier published format if the SMOS concludes that the differences are immaterial to the proposed change submittal. If the SMOS concludes that a current form must be utilized, the proposer may be given up to 20 additional days to resubmit the proposed changes in the current format.

ELECTRONIC PREPARATION/SUBMISSION OF FORM FOR PROPOSING CHANGES

An electronic version of each change, which must comply with the instructions in the Notice and the Form, is the preferred form of submittal to ASHRAE Headquarters at the address shown below. The electronic format facilitates both paper-based and computer-based processing. Submittal in paper form is acceptable. The following instructions apply to change proposals submitted in electronic form.

Use the appropriate file format for your word processor and save the file in either a recent version of Microsoft Word (preferred) or another commonly used word-processing program. Please save each change proposal file with a different name (for example, "prop01.doc," "prop02.doc," etc.). If supplemental background documents to support changes submitted are included, it is preferred that they also be in electronic form as word-processed or scanned documents.

For files submitted attached to an e-mail, ASHRAE will accept an electronic signature (as a picture; *.tif, or *.wpg) on the change submittal form as equivalent to the signature required on the change submittal form to convey non-exclusive copyright.

Submit an e-mail containing the change proposal files to:
change.proposal@ashrae.org

Alternatively, mail paper versions to:
ASHRAE
Senior Manager of Standards
1791 Tullie Circle, NE
Atlanta, GA 30329-2305

Or fax them to:
Attn: Senior Manager of Standards
678-539-2129

The form and instructions for electronic submittal may be obtained from the Standards section of ASHRAE's Home Page, www.ashrae.org, or by contacting a Standards Secretary via phone (404-636-8400), fax (678-539-2129), e-mail (standards.section@ashrae.org), or mail (1791 Tullie Circle, NE, Atlanta, GA 30329-2305).



FORM FOR SUBMITTAL OF PROPOSED CHANGE TO AN ASHRAE STANDARD UNDER CONTINUOUS MAINTENANCE

NOTE: Use a separate form for each comment. Submittals (Microsoft Word preferred) may be attached to e-mail (preferred), or submitted in paper by mail or fax to ASHRAE, Senior Manager of Standards, 1791 Tullie Circle, NE, Atlanta, GA 30329-2305. E-mail: change.proposal@ashrae.org. Fax: +1-678-539-2129.

1. Submitter:

Affiliation:

Address:

City:

State:

Zip:

Country:

Telephone:

Fax:

E-Mail:

I hereby grant ASHRAE the non-exclusive royalty rights, including non-exclusive rights in copyright, in my proposals. I understand that I acquire no rights in publication of the standard in which my proposals in this or other analogous form is used. I hereby attest that I have the authority and am empowered to grant this copyright release.

Submitter's signature: _____ Date: _____

All electronic submittals must have the following statement completed:

I (insert name), through this electronic signature, hereby grant ASHRAE the non-exclusive royalty rights, including non-exclusive rights in copyright, in my proposals. I understand that I acquire no rights in publication of the standard in which my proposals in this or other analogous form is used. I hereby attest that I have the authority and am empowered to grant this copyright release.

2. Number and year of standard:

3. Page number and clause (section), subclause, or paragraph number:

4. I propose to: ☐ Change to read as follows ☐ Delete and substitute as follows
(check one) ☐ Add new text as follows ☐ Delete without substitution

Use underscores to show material to be added (added) and strike through material to be deleted (~~deleted~~). Use additional pages if needed.

5. Proposed change:

6. Reason and substantiation:

7. Will the proposed change increase the cost of engineering or construction? If yes, provide a brief explanation as to why the increase is justified.

☐ Check if additional pages are attached. Number of additional pages: _____

☐ Check if attachments or referenced materials cited in this proposal accompany this proposed change. Please verify that all attachments and references are relevant, current, and clearly labeled to avoid processing and review delays. *Please list your attachments here:*

**POLICY STATEMENT DEFINING ASHRAE'S CONCERN
FOR THE ENVIRONMENTAL IMPACT OF ITS ACTIVITIES**

ASHRAE is concerned with the impact of its members' activities on both the indoor and outdoor environment. ASHRAE's members will strive to minimize any possible deleterious effect on the indoor and outdoor environment of the systems and components in their responsibility while maximizing the beneficial effects these systems provide, consistent with accepted Standards and the practical state of the art.

ASHRAE's short-range goal is to ensure that the systems and components within its scope do not impact the indoor and outdoor environment to a greater extent than specified by the Standards and Guidelines as established by itself and other responsible bodies.

As an ongoing goal, ASHRAE will, through its Standards Committee and extensive Technical Committee structure, continue to generate up-to-date Standards and Guidelines where appropriate and adopt, recommend, and promote those new and revised Standards developed by other responsible organizations.

Through its *Handbook*, appropriate chapters will contain up-to-date Standards and design considerations as the material is systematically revised.

ASHRAE will take the lead with respect to dissemination of environmental information of its primary interest and will seek out and disseminate information from other responsible organizations that is pertinent, as guides to updating Standards and Guidelines.

The effects of the design and selection of equipment and systems will be considered within the scope of the system's intended use and expected misuse. The disposal of hazardous materials, if any, will also be considered.

ASHRAE's primary concern for environmental impact will be at the site where equipment within ASHRAE's scope operates. However, energy source selection and the possible environmental impact due to the energy source and energy transportation will be considered where possible. Recommendations concerning energy source selection should be made by its members.

ASHRAE • 1791 Tullie Circle NE • Atlanta, GA 30329 • www.ashrae.org

About ASHRAE

ASHRAE, founded in 1894, is a global society advancing human well-being through sustainable technology for the built environment. The Society and its members focus on building systems, energy efficiency, indoor air quality, refrigeration, and sustainability. Through research, Standards writing, publishing, certification and continuing education, ASHRAE shapes tomorrow's built environment today.

For more information or to become a member of ASHRAE, visit www.ashrae.org.

To stay current with this and other ASHRAE Standards and Guidelines, visit www.ashrae.org/standards.

Visit the ASHRAE Bookstore

ASHRAE offers its Standards and Guidelines in print, as immediately downloadable PDFs, on CD-ROM, and via ASHRAE Digital Collections, which provides online access with automatic updates as well as historical versions of publications. Selected Standards and Guidelines are also offered in redline versions that indicate the changes made between the active Standard or Guideline and its previous version. For more information, visit the Standards and Guidelines section of the ASHRAE Bookstore at www.ashrae.org/bookstore.

IMPORTANT NOTICES ABOUT THIS STANDARD

To ensure that you have all of the approved addenda, errata, and interpretations for this Standard, visit www.ashrae.org/standards to download them free of charge.

Addenda, errata, and interpretations for ASHRAE Standards and Guidelines are no longer distributed with copies of the Standards and Guidelines. ASHRAE provides these addenda, errata, and interpretations only in electronic form to promote more sustainable use of resources.

EXHIBIT DX44

TO DECLARATION OF PETER J. GOSS IN
SUPPORT OF DEFENDANTS' MOTION TO
EXCLUDE PLAINTIFFS' ENGINEERING
EXPERTS


LMS TECHNOLOGIES, INC.

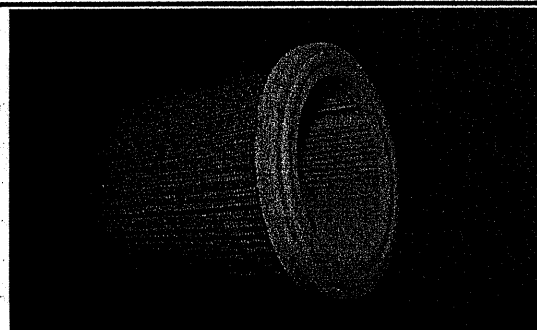
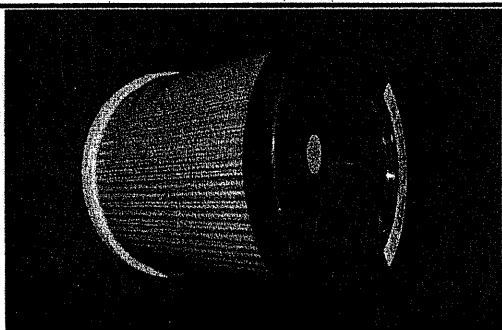
6423 Cecilia Circle
Bloomington, MN 55439
(952) 918-9060, Fax: (952) 918-9061

Test Report-ASHRAE Test Standard 52.2-2012 (New Classification)

Test Requested By: 3M
 Manufacturer: 3M
 Product Name: Bair Hugger Filter - Model 505 # 1
 Lot #: 4693367
 Part #: 78-8083-5447-2
 Dimensions: 5.5" x 5.375"
 Filter Description: Mini Pleated Cylindrical Filter with White Media
 How Filter Obtained: Provided by 3M

Report #: 3461

Test Date: 05/10/2016


Test Results

Test Air Flow Rate(CFM)/Velocity (FPM)	<u>48 cfm/118 fpm</u>
Initial Resistance (in. WG)	<u>0.508"</u>
Final Resistance (in. WG)	<u>2.500"</u>
Minimum Efficiency Rating Value (MERV)	<u>MERV 14 @ 48 cfm</u>
Minimum Average Efficiency 0.3 to 1.0 Microns (E1)	<u>81.5</u>
Minimum Average Efficiency 1.0 to 3.0 Microns (E2)	<u>98.7</u>
Minimum Average Efficiency 3.0 to 10 Microns (E3)	<u>100.0</u>
Dust Fed to Final Resistance (grams)	<u>6.1 grams</u>
Dust Holding Capacity (grams)	<u>6.0 grams</u>
Arrestance:	<u>98.4%</u>

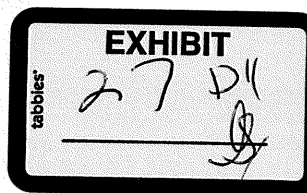
Test Description

Temp & Humidity: 71° F @ 40%
 Particle Analysis: Met One 3400
 Test Dust: ASHRAE 52.1 Dust
 Test Aerosol: KCl, Neutralized
 LMS#: 3894

Test Engineer : Emile Tadros/Kevin Kwong/Pat Best/Jose Tizcareno

Approved By: K. C. Kwok, Ph.D.

Data verified by LMS Calibration filter* Patent Pending



LMS Technologies, Inc.

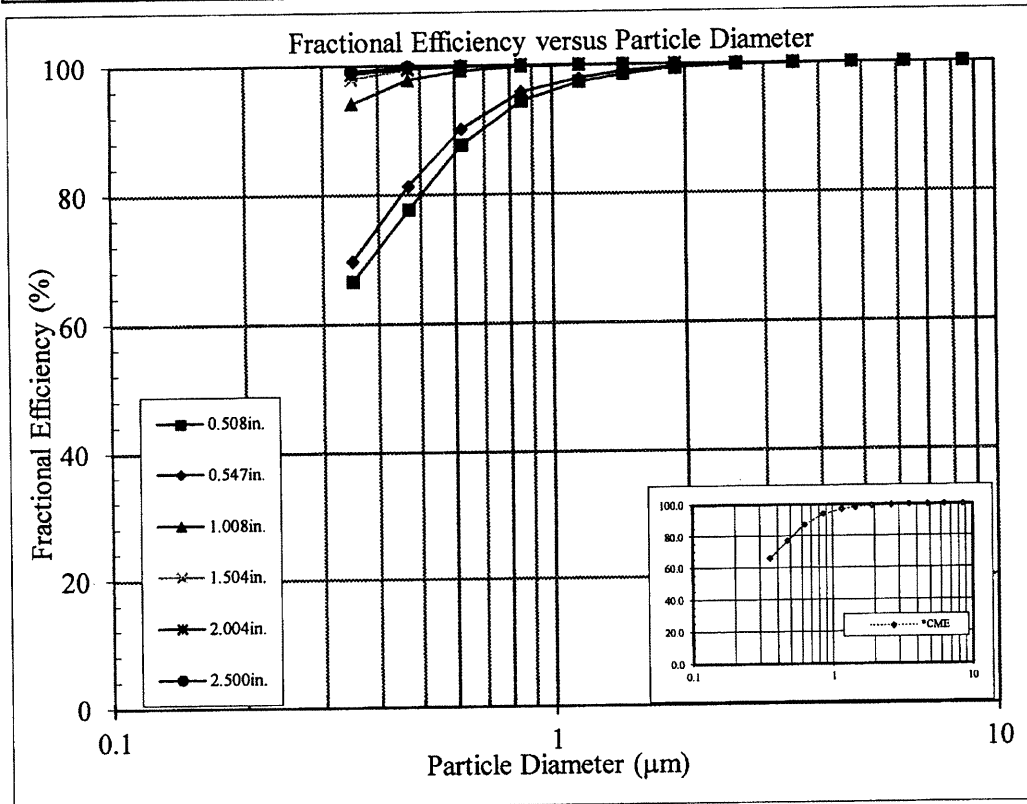
6423 Cecilia Circle

Bloomington, MN 55439

(952) 918-9060, Fax: (952) 918-9061

Date :	May 10, 2016	Requested by :
Filter ID :	Bair Hugger-Model 505 #1	3M
Test Type :	52.2-2012 REP# 3461	Manufacturer :
Test Aerosol :	KCl, Neutralized	3M

ΔP (" H ₂ O)	0.508in.	0.547in.	1.008in.	1.504in.	2.004in.	2.500in.	*CME
Size Range (μm)	Fractional Efficiency (%)						
0.3-0.4	66.5	69.7	94.1	97.9	98.7	99.1	66.5
0.4-0.55	77.6	81.3	97.7	99.3	99.5	99.8	77.6
0.55-0.7	87.6	90.1	99.1	99.7	99.8	99.9	87.6
0.7-1.0	94.3	95.8	99.7	99.9	100.0	100.0	94.3
1.0-1.3	97.2	97.8	99.9	100.0	100.0	100.0	97.2
1.3-1.6	98.4	98.9	99.9	100.0	100.0	100.0	98.4
1.6-2.2	99.3	99.5	100.0	100.0	100.0	100.0	99.3
2.2-3.0	99.7	99.8	100.0	100.0	100.0	100.0	99.7
3.0-4.0	99.9	99.9	100.0	100.0	100.0	100.0	99.9
4.0-5.5	100.0	100.0	100.0	100.0	100.0	100.0	100.0
5.5-7.0	100.0	100.0	100.0	100.0	100.0	100.0	100.0
7.0-10.0	100.0	100.0	100.0	100.0	100.0	100.0	100.0

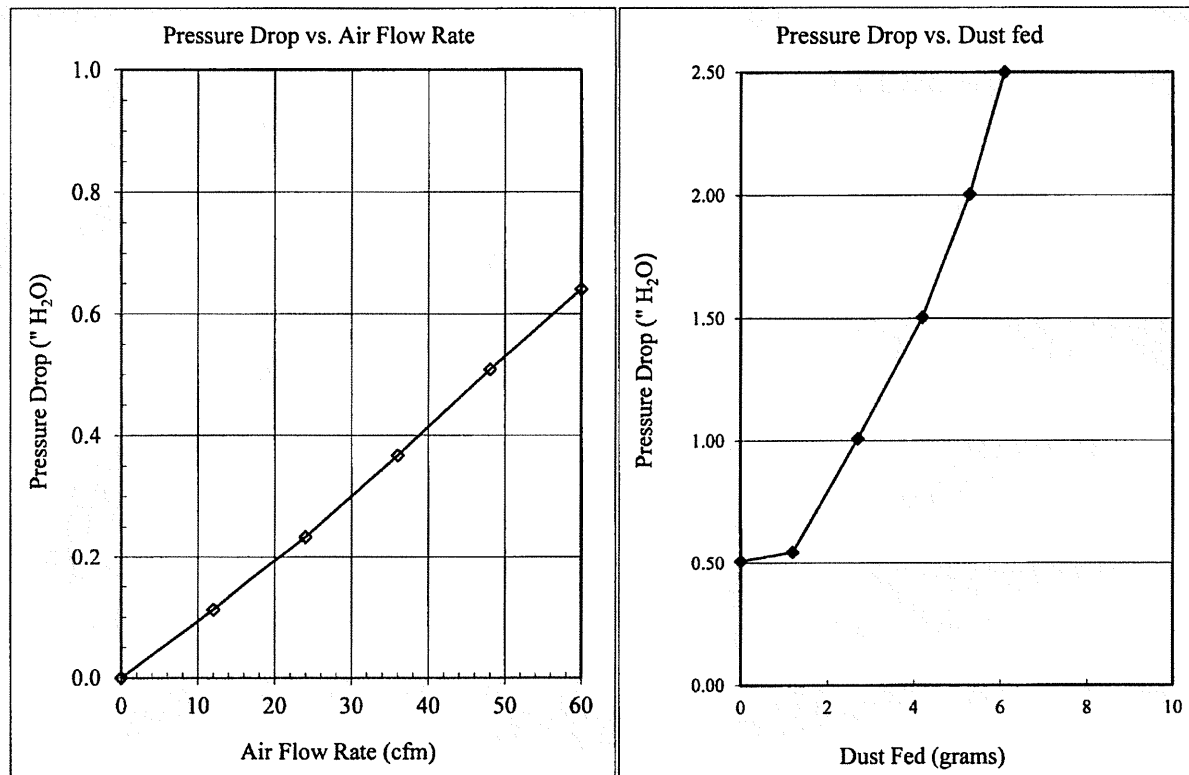


ENGINEERING APPROVAL
K.C. KWOK, PH.D. _____

LMS Technologies, Inc.
6423 Cecilia Circle, Bloomington, MN 55439
(952) 918-9060, Fax: (952) 918-9061

Date:	May 10, 2016	Test Requested by :
Filter ID :	Bair Hugger Filter-Model 505 #1	3M
Test Type :	Pressure Drop of Clean Filter	Filter Manufacturer :
	For ASHRAE 52.2-2012 REP# 3461	3M

Flow Rate CFM	Velocity FPM	dP (mm H ₂ O)	Pressure drop ("H ₂ O)	% of Rated Airflow	Dust fed	Pressure drop
0	0	0.00	0.000	0%	0.00	0.508
12	30	2.86	0.113	25%	1.20	0.547
24	59	5.95	0.234	50%	2.70	1.008
36	89	9.33	0.367	75%	4.20	1.504
48	118	12.92	0.509	100%	5.30	2.004
60	148	16.27	0.641	125%	6.10	2.500



ENGINEERING APPROVAL
K.C.KWOK PH.D. _____

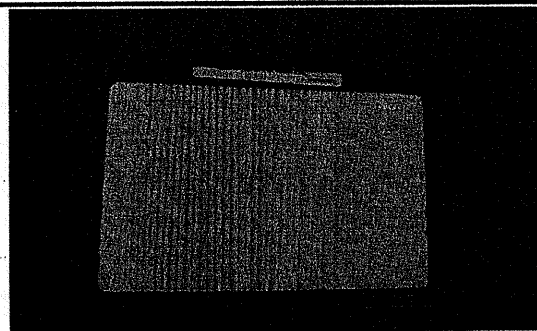
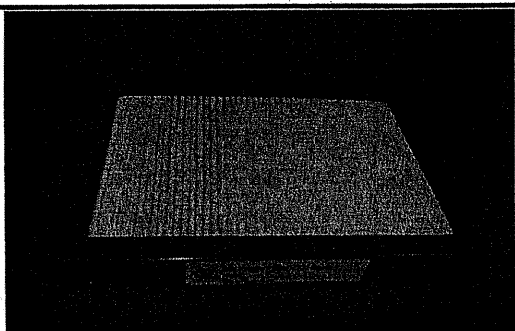
**LMS TECHNOLOGIES, INC.**

6423 Cecilia Circle
Bloomington, MN 55439
(952) 918-9060, Fax: (952) 918-9061

Test Report-ASHRAE Test Standard 52.2-2012 (New Classification)

Test Requested By: 3M
 Manufacturer: 3M
 Product Name: Bair Hugger Filter - 700 Series #1
 Lot #: 4693352
 Part #: N/A
 Dimensions: 4.75" x 6.625" x 0.75"
 Filter Description: Mini Pleated Filter with White Media
 How Filter Obtained: Provided by 3M

Report #: 3463
Test Date: 05/12/2016

**Test Results**

Test Air Flow Rate(CFM)/Velocity (FPM)	<u>48 cfm/246 fpm</u>
Initial Resistance (in. WG)	<u>1.256"</u>
Final Resistance (in. WG)	<u>2.500"</u>
Minimum Efficiency Rating Value (MERV)	<u>MERV 14 @ 48 cfm</u>
Minimum Average Efficiency 0.3 to 1.0 Microns (E1)	<u>84.1</u>
Minimum Average Efficiency 1.0 to 3.0 Microns (E2)	<u>99.4</u>
Minimum Average Efficiency 3.0 to 10 Microns (E3)	<u>100.0</u>
Dust Fed to Final Resistance (grams)	<u>1.1 grams</u>
Dust Holding Capacity (grams)	<u>1.1 grams</u>
Arrestance:	<u>100.0%</u>

Test Description

Temp & Humidity: 71° F @ 40%
 Particle Analysis: Met One 3400
 Test Dust: ASHRAE 52.1 Dust
 Test Aerosol: KCl, Neutralized
 LMS#: 3894

Test Engineer : Emile Tadros/Kevin Kwong/Pat Best/Jose Tizcareno

Approved By: K. C. Kwok, Ph.D.

Data verified by LMS Calibration filter* Patent Pending



LMS Technologies, Inc.

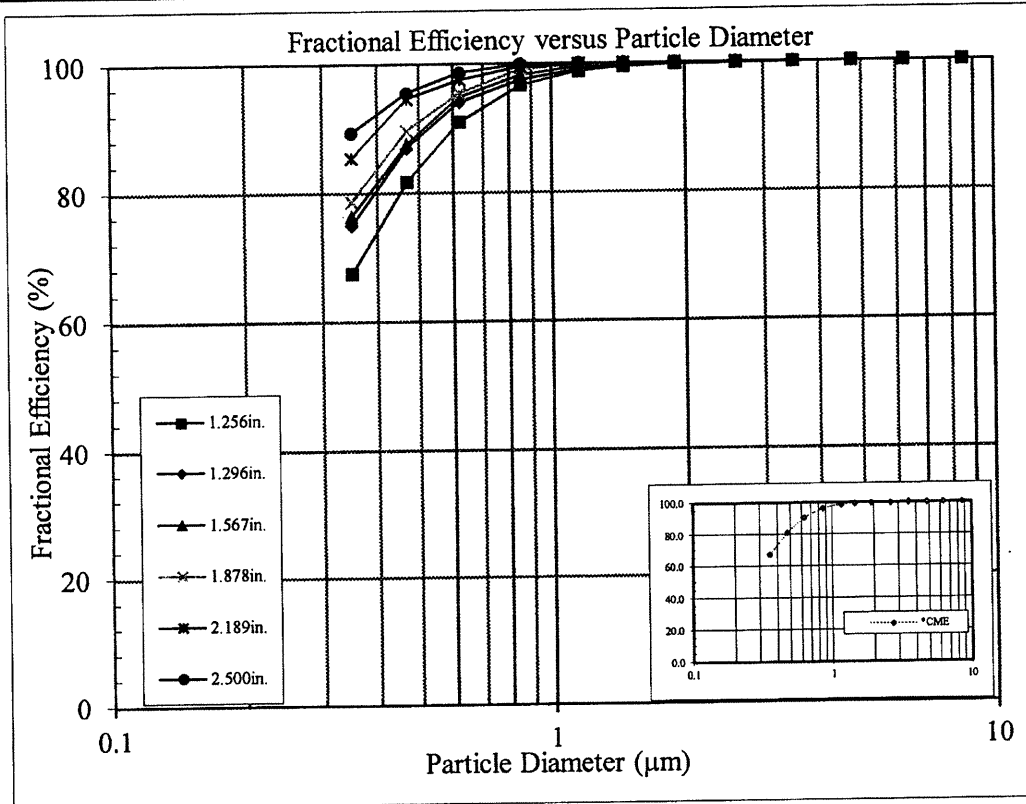
6423 Cecilia Circle

Bloomington, MN 55439

(952) 918-9060, Fax: (952) 918-9061

Date :	May 12, 2016	Requested by :
Filter ID :	Bair Hugger-700 Series #1	3M
Test Type :	52.2-2012 REP# 3463	Manufacturer :
Test Aerosol :	KCl, Neutralized	3M

ΔP (" H ₂ O)	1.256in.	1.296in.	1.567in.	1.878in.	2.189in.	2.500in.	*CME
Size Range (μm)	Fractional Efficiency (%)						
0.3-0.4	67.4	74.9	76.3	78.6	85.4	89.3	67.4
0.4-0.55	81.6	86.9	87.5	89.6	94.6	95.5	81.6
0.55-0.7	90.9	94.0	94.8	95.4	97.5	98.6	90.9
0.7-1.0	96.6	97.5	98.2	99.1	99.5	99.9	96.6
1.0-1.3	98.7	99.0	99.4	99.7	99.9	100.0	98.7
1.3-1.6	99.4	99.5	99.8	99.9	100.0	100.0	99.4
1.6-2.2	99.7	99.8	99.9	100.0	100.0	100.0	99.7
2.2-3.0	99.8	100.0	100.0	100.0	100.0	100.0	99.8
3.0-4.0	99.9	100.0	100.0	100.0	100.0	100.0	99.9
4.0-5.5	100.0	100.0	100.0	100.0	100.0	100.0	100.0
5.5-7.0	100.0	100.0	100.0	100.0	100.0	100.0	100.0
7.0-10.0	100.0	100.0	100.0	100.0	100.0	100.0	100.0



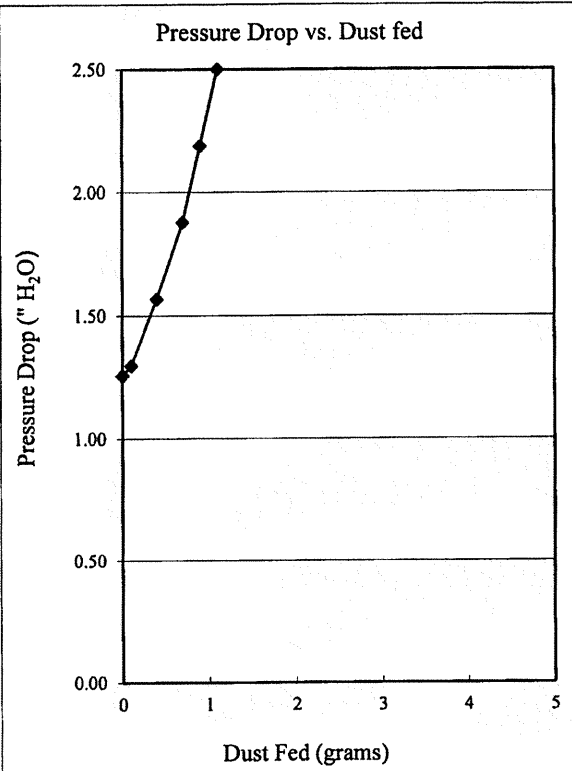
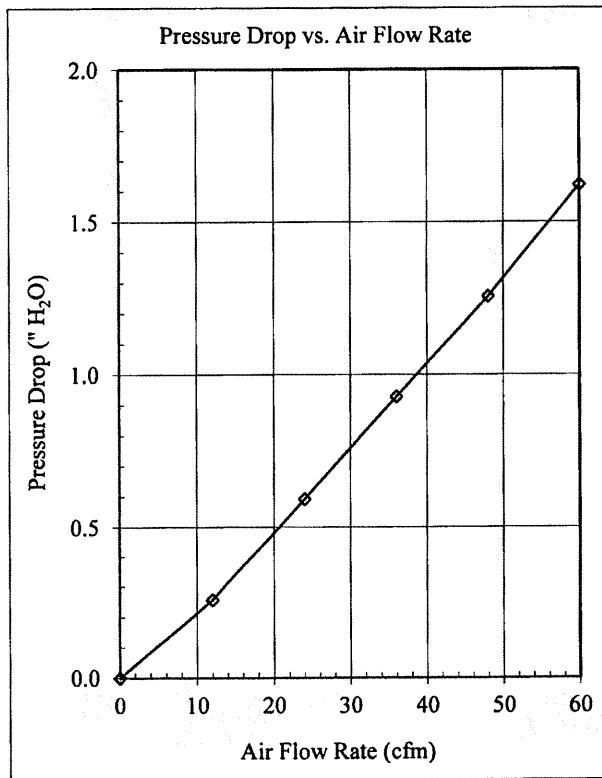
ENGINEERING APPROVAL

K.C. KWOK, PH.D. _____

LMS Technologies, Inc.
6423 Cecilia Circle, Bloomington, MN 55439
(952) 918-9060, Fax: (952) 918-9061

Date:	May 12, 2016	Test Requested by :
Filter ID :	Bair Hugger Filter-700 Series #1	3M
Test Type :	Pressure Drop of Clean Filter	Filter Manufacturer :
	For ASHRAE 52.2-2012 REP# 3463	3M

Flow Rate CFM	Velocity FPM	dP (mm H ₂ O)	Pressure drop ("H ₂ O)	% of Rated Airflow	Dust fed	Pressure drop
0	0	0.00	0.000	0%	0.00	1.256
12	62	6.52	0.257	25%	0.10	1.296
24	123	15.05	0.593	50%	0.40	1.567
36	185	23.56	0.928	75%	0.70	1.878
48	246	31.91	1.256	100%	0.90	2.189
60	308	41.15	1.620	125%	1.10	2.500



ENGINEERING APPROVAL
K.C.KWOK PH.D. _____